Functional Resistance Training During Walking: Design, Testing, and Evaluation of Passive and Semi-Passive Wearable Devices for Providing Targeted Resistance to the Leg During Gait

by

Edward Peter Washabaugh IV

A dissertation submitted in partial fulfillment
of the requirements for the degree of
Doctor of Philosophy
(Biomedical Engineering)
in the University of Michigan
2021

Doctoral Committee:

Associate Professor Chandramouli Krishnan, Chair
Dr. Edward S. Claflin
Professor R. Brent Gillespie
Professor Douglas C. Noll
Associate Professor Riann Palmieri-Smith
Associate Professor Rajiv Ranganathan, Michigan State University

Edward P. Washabaugh

epwiv@umich.edu

ORCID iD: 0000-0002-1038-0954

Dedication

For my namesakes, the original engineers in the family.

Acknowledgements

First and foremost, I would like to thank my adviser and mentor, Chandramouli Krishnan. Thank you for taking a chance on me when accepting me into your lab. Thank you for setting high expectations and encouraging me towards lofty goals. Mostly, thank you for taking the time to help me reach them.

Thank you to my committee members, who have helped me immensely over the years: providing inputs for my research, providing edits to my manuscripts, referring research participants, writing letters, and encouraging me through this process. Your help has been greatly appreciated.

I would like to thank all the members of the Neuromuscular and Rehabilitation Robotics Laboratory (NeuRRo Lab), both past and present. I have been very fortunate to be able to work alongside a great team of smart and talented individuals. I especially would like to thank Tom Augenstein, Scott Brown, and Varun Joshi, who always provided help when it was needed, or coffee and a distraction when it was also needed.

Thank you to my fiancé, Katie Burke, who has been patient and supportive throughout this entire process. We have persisted through a long-distance relationship, a pandemic, and a crazy puppy, and this isn't even our final form. I am so thankful I had you to help me complete this journey, and I look forward to our future journeys, whatever they may be.

Thank you to my family. Mom and Dad, I could not have done this without your constant support, impromptu help, and persistent calls to chat. Thank you for always being in my corner. I

would also like to thank my grandma, Mooma, who always knew I would grow up to be an engineer, even if I did not, and my grandpa, Papa, who is always looking out for me.

Lastly, thank you to the agencies and institutions that have helped fund me and my work for this dissertation, including the National Science Foundation (NSF), National Institute of Health (NIH), and the University of Michigan Rackham Graduate School. Additionally, thank you to the Michigan Medicine Department of Physical Medicine and Rehabilitation (PMR) and staff for all of the support that has been provided throughout my graduate training.

Table of Contents

List of Tables

List of Figures

List of Equations

List of Appendices

Abstract

Injuries to the neuromusculoskeletal systems often result in muscle weakness, abnormal coordination strategies, and gait impairments. Functional resistance training during walking—where a patient walks while a device increases loading on the leg—is an emerging approach to combat these symptoms. While simple passive devices (i.e., ankle weights and resistance bands) can be applied for this training, rehabilitation robots have more potential upside because they can be controlled to treat multiple gait abnormalities and can be monitored by clinicians. However, the cost of conventional robotic devices limits their use in the clinical or home setting. Hence, in this dissertation, we designed, developed, and tested passive and semi-passive wearable exoskeleton devices as low-cost solutions for providing controllable/configurable functional resistance training during walking.

We developed and tested two passive exoskeleton devices for providing resistance to walking and tested their effects on able-bodied participants and stroke survivors. First, we created a *patented* device that used a passive magnetic brake to provide a viscous (i.e., velocity-dependent) resistance to the knee. The resistive properties of the device could be placed under computer control (i.e., made semi-passive) to control resistance in real-time. Next, we created a passive exoskeleton that provided an elastic (i.e., position-dependent) resistance. While not controllable, this device was highly configurable. Meaning it could be used to provide resistance to joint flexion, extension, or to both (i.e., bidirectionally). Human subjects testing with these devices indicated they increased lower-extremity joint moments, powers, and muscle activation

during training. Training also resulted in significant aftereffects—a potential indicator of therapeutic effectiveness—once the resistance was removed. A separate experiment indicated that individuals often kinematically slack (i.e., reduce joint excursions to minimize effort) when resistance is added to the limb. We also found that providing visual feedback of joint angles during training significantly increased muscle activation and kinematic aftereffects (i.e., reduced slacking).

With passive devices, the type of passive element used largely dictates the muscle groups, types of muscle contraction, joint actions, and the phases of gait when a device is able to apply resistance. To examine this issue, we compared the training effects of viscous and elastic devices that provided bidirectional resistance to the knee during gait. Additionally, we compared training with viscous resistances at the hip and knee joints. While the resistance type and targeted joint altered moments, powers, and muscle activation patterns, these methods did not differ in their ability to produce aftereffects, alter neural excitability, or induce fatigue in the leg muscles. While this may indicate that the resistance type does not have a large effect on functional resistance training during walking, it is possible that an extended training with these devices could produce a different result.

Lastly, we used musculoskeletal modeling in OpenSim to directly compare several strategies that have been used to provide functional resistance training to gait in the clinic or laboratory setting. We found that devices differed in their ability to alter gait parameters during walking. Hence, these findings could help clinicians when selecting a resistive strategy for their patients, or engineers when designing new devices or control schemes.

Collectively, this dissertation introduces a new class of wearable devices for functional resistance training during walking and establishes the biomechanical and neurophysiological effects and the clinical potential of these devices in able-bodied and stroke survivors.

Chapter 1

Functional Resistance Training During Walking: Review of Devices and their Effects on Muscle Activation, Neural Control, and Gait Mechanics

Abstract

Objective: Injuries to the neuromusculoskeletal system often result in muscle weakness and abnormal coordination strategies, which can lead to gait impairments. Functional resistance training (FRT) during walking—where a patient walks while a device increases loading on the leg—is an emerging approach to combat these symptoms. There are many different strategies and devices that can be used to convey resistance to the patient, ranging from simple weighted cuffs to sophisticated rehabilitation robots. This review highlights the different devices used in FRT and characterizes how they alter muscle activation and gait biomechanics with acute training. *Methods:* We performed a literature search to identify studies that have performed acute FRT during walking and examined how each resistive strategy altered joint moments and muscle activation during training, kinematic and spatiotemporal aftereffects following training, and neural control of walking. We also examined the potential financial and practical trade-offs of different training strategies. *Results:* We found that muscle activation, gait biomechanics, and kinematic aftereffects varied based on the strategy used for training. There were no clear consistent effects on neural control of walking. *Conclusion:* Resistive strategies can be selected to target patient-specific strength deficits and gait impairments, but this selection should also account for affordability and ease of use of the device. *Significance:* This information can help

inform clinicians when selecting a strategy for FRT that is appropriate for their patients while remaining feasible for use in their clinic or home, as well as engineers developing new devices for this purpose.

1.1 Introduction

Walking is a motor skill that is intrinsically learned at a young age; however, this seemingly basic skill is actually carried out by a complex network of interdependent pathways in the neural and muscular systems. Hence, damage to these systems due to neurological or orthopedic conditions (e.g., stroke, spinal cord injury, cerebral palsy, osteoarthritis, etc.) often results in gait abnormalities or disability (Chen et al., 2005; Duffell et al., 2017; Perry et al., 1995; Pietrosimone et al., 2018). Unfortunately, current trends in public health—such as the increase in the ageing population—suggest that the prevalence of many of the conditions will grow (Pollock et al., 2014).

Individuals with these neurological or orthopedic conditions typically exhibit motor impairments, with the most common being muscle weakness (Harvey, 2016; Olney & Richards, 1996; Williams et al., 2014). Strength is highly correlated with functional activity performance (Bohannon, 2007; Hsu et al., 2003; Pouliot-Laforte et al., 2020), and therapists frequently prescribe resistance training with the goal of improving walking (Cramp et al., 2006; Flansbjer et al., 2008; Harvey, 2016; Teixeira-Salmela et al., 1999). While resistance training alone can improve walking function (e.g., increased walking velocity or endurance) (Cramp et al., 2006; Flansbjer et al., 2008; Lima et al., 2013; Liu & Latham, 2009; Pak & Patten, 2008), it has also been shown that resistance training has limited transfer to functional activities (Krebs et al., 2007; Sullivan et al., 2007). Rather, functional activities, such as walking, are better improved using task-specific training (e.g., training patients to walk by specifically practicing walking

overground or on a treadmill) (Carroll et al., 2001; Krebs et al., 2007; Sullivan et al., 2007). This is not surprising considering that task-specific training is a key determinant for inducing plastic changes in the nervous system (Carroll et al., 2001; Harvey, 2009; Kleim & Jones, 2008; Maier et al., 2019). Given the unique contributions that task-specific and resistive training offer for gait rehabilitation, therapeutic interventions that combine these two training types may be more effective than either training type by itself (Eng & Tang, 2007).

Functional resistance training (FRT) is essentially a fusion of resistive and task-specific training principles, and is administered by having a patient perform a task-specific training against an applied resistance. As such, it is specifically designed to improve functional ability by: 1) increasing voluntary muscle force throughout the range of motion for a task and 2) modulating force in muscle groups appropriate for the activity being trained (Cooke et al., 2010; Donaldson et al., 2009). Historically, FRT principles have been widely applied for training sport performance, such as when a sprinter trains by running with a parachute attached to their waist. By comparison, these training techniques have only recently been adapted by the rehabilitation community for gait training. In this context, FRT during walking is applied by having the patient walk with a resistance applied to their lower-extremity. Resistance can be applied to the legs using many different strategies, which vary based on the type of device used, how that device interfaces with the user, and the type of resistance that the device supplies. Notably, the characteristics of the resistance—such as the force profile, the timing relative to the gait cycle, and the muscles that are targeted—vary greatly depending on strategy that is being used. Ultimately, the resistive strategy selected for FRT during walking could greatly affect the outcomes of the training.

This introductory chapter is a literature review that highlights the types of devices that have been used to apply external loads for FRT during walking, as well as the characteristics of the unique resistances provided by each device. It also discusses potential trade-offs and the different effects that may occur due to acute training with these various resistive strategies. Specifically, it reviews how FRT has been applied during walking to alter joint moments and muscle activation, how training has elicited kinematic and spatiotemporal aftereffects once resistance is removed, and how it has altered neural control of walking. Throughout the review, attention is given to many areas where future research is required to advance our understanding of FRT.

1.2 Methods

1.2.1 Literature Search

The literature search was performed in PubMed using the following permutations of the text and keyword combinations (Figure 1.1). Relating to the functional task we searched for “gait” and “walking”, along with the type of training being “resistance”. The search was also conducted based on the variables measured, which included “electromyography”, “kinematics”, "transcranial magnetic stimulation", “spatiotemporal”, “spatial”, and “temporal” along with relevant abbreviations. The references found from this computerized search were manually inspected to identify other potential studies that fit our inclusion criteria. All databases were searched for relevant articles up until August 4, 2020.

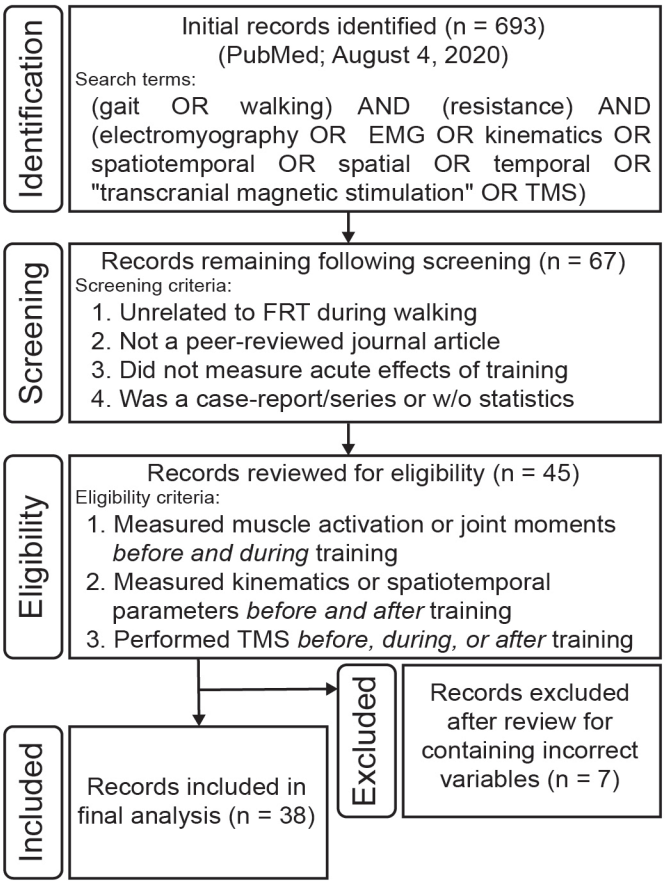

Figure 1.1 Flow diagram depicting study identification.

We found 699 articles that matched these criteria. From these articles, we selected those that met a more stringent criteria. Mainly, studies were included if they were original investigations related to FRT during walking (see Functional Resistance Training Operational Definition), published as peer-reviewed journal articles (i.e., excluding conference proceedings), and designed to measure the acute effects/adaptations (i.e., excluding clinical trials) of FRT during walking on adult human subjects (i.e., excluding trials on infants or animals). Additionally, studies were only included if they had appropriate statistical analysis (i.e., excluding case studies and series). Eligible articles were reviewed to see if they collected at least one of the following variables: muscle activation or joint moments before and during training; spatiotemporal gait parameters or kinematic variables before training and after removing the

resistance (i.e., aftereffects from washout periods or catch trials); or transcranial magnetic stimulation variables before and during training, or before and after training. Additional articles were excluded because they only measured from the unresisted leg or presented variables as asymmetries. In total, 38 articles met all of our criteria (See Appendix A).

From these articles, we extracted the population that was trained, the type of device that was used to apply resistance (i.e., whether it was a passive device or an active motorized robot), the mode that was used to apply the resistance (i.e., tethered to a point on the participant [point-based] or directly to the participant's joint [joint-based]), the resistance type (e.g., whether the resistance was inertial, elastic, viscous, etc.), and the movement that the device was resisting. For all of our variables of interest (muscle activations, joint moments, kinematics, spatiotemporal gait parameters, and transcranial magnetic stimulation), we report all of the statistically significant findings relative to baseline (i.e., normal walking) and indicate the direction of change with an arrow pointing upwards (variable increased) or downwards (variable decreased).

1.2.2 Functional Resistance Training Operational Definition

During screening, studies were excluded based on whether they performed FRT during walking. We defined this based on whether the study used a device to increase the loading experienced by the leg during walking beyond what would be experienced during normal unassisted walking. We would like to note that many abstractions of existing therapies could be viewed as FRT but were not included in this review. Examples include body-weight supported treadmill training, split-belt treadmill training, stair climbing, inclined walking, electrical stimulation, perturbation research, and prosthesis research. Lastly, we have not reviewed many studies that examined the effects of ankle-foot orthoses because these studies often aim to assist the user, report the net moments from both the user and device, and do not make comparisons to

walking without the device. Additionally, the biomechanical effects of walking with compliant ankle-foot orthoses have been reviewed elsewhere (Totah et al., 2019).

1.3 Results

1.3.1 Populations Being Researched

While FRT during walking is often motivated for use in populations with neurological injuries, a majority of this acute research has actually been performed on able-bodied individuals (29/38 studies). This is likely due to the ease of recruiting able-bodied participants, and the need to validate methods before testing on patients. The remainder of the studies were performed on individuals with neurological injuries, including spinal cord injuries (5/38 studies), strokes (4/38 studies), and cerebral palsy (3/38 studies). A single study was performed in individuals with knee osteoarthritis, an orthopedic condition.

1.3.2 Devices for Functional Resistance Training

The devices that have been applied for FRT during walking range from simple passive devices to advanced active rehabilitation robots (Figure 1.2). We refer to these devices as active or passive based on how energy flows between the device and user. Active rehabilitation robots use active actuators (e.g., motors), which add external energy to the user in order to provide resistance. Meanwhile, passive devices—including weighted cuffs/vests, elastic bands, and brakes—do not add external energy to the user. Rather, resistance is produced in passive devices when the user exerts their own internal energy on the device. In some cases, the energy put into the device can be stored and returned to the user; however, this is not external power as it was originally input by the user.

We found that most studies performed FRT during walking using passive devices (21/38 studies). This majority likely stems from the accessibility and affordability of these devices, many of which are already possessed by rehabilitation clinics (e.g., weighted cuffs and resistance bands). However, several studies have also used active robots (17/38 studies). Typically, these studies have used custom devices built for research purposes or programmed commercially available rehabilitation robots to be resistive.

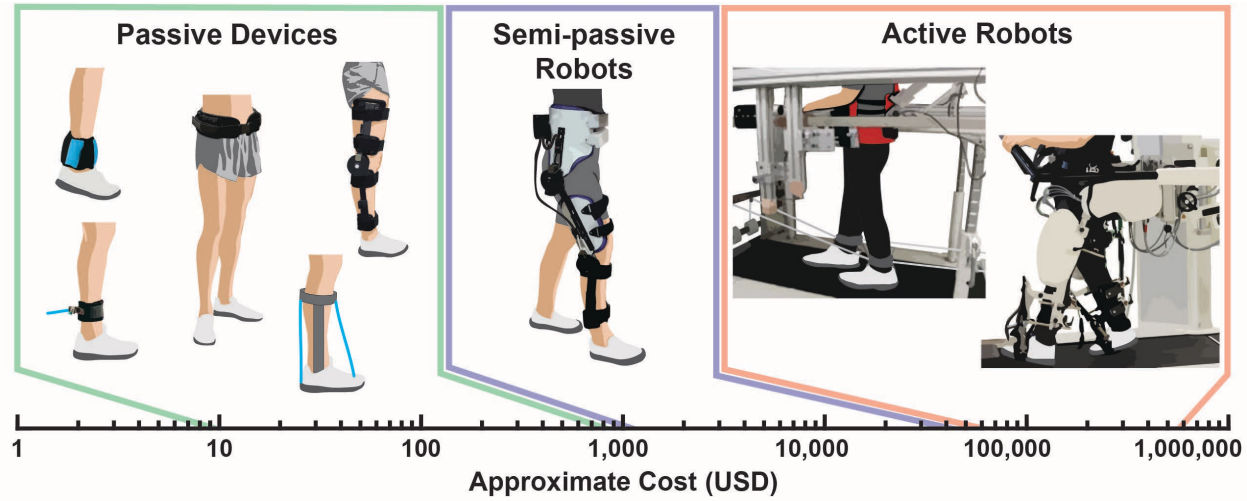

Figure 1.2 The spectrum of devices used for functional resistance training during gait and their approximate costs. Active robots provide exceptional control over the rehabilitation setting but are also the most expensive to acquire. Meanwhile, passive devices (e.g., weighted cuffs/belts, elastic bands, and passive braces) are the most cost-effective option but offer no real-time control. While not widely studied in functional resistance training, semi-passive robots utilize controllable passive elements (e.g., controllable brakes) in order to provide a limited set of controls but at a modest price.

1.3.3 Modes of Interfacing with the Limb

Within each of these classes of devices (i.e., active robots and passive devices), there are two separate modes that can be used to interface with the limb. By modes, we are referring to whether the resistance is applied at a point on the user (i.e., attached externally to a segment on the body, as is typically done with weights, resistance bands, or tethered robots; sometimes referred to as an end-effector based) or directly to the joints of the user (as is common with wearable braces or exoskeleton robots). Ultimately, the differences between these two modes can affect how a device is able to resist the user during training, as point loads make it more difficult

to target specific joints (Figure 1.3). Despite this, we found that most studies applied resistance through point loads (27/38 studies), while only 14 studies used joint loads.

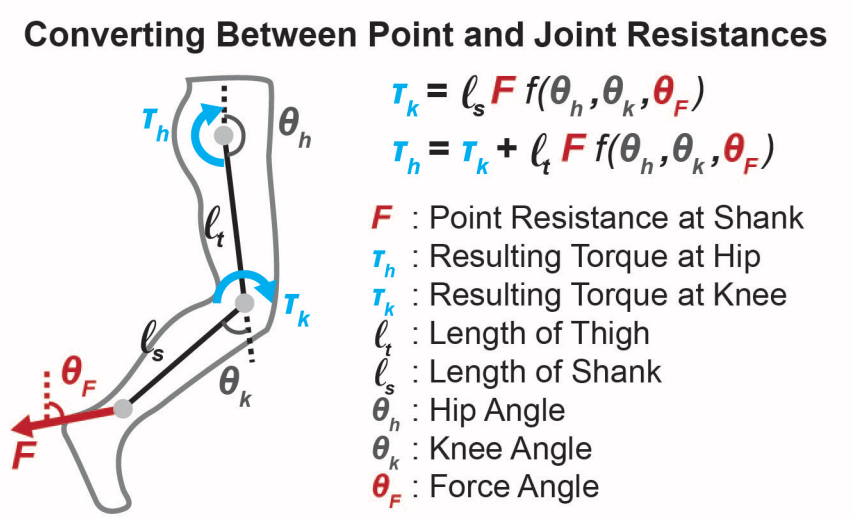

Figure 1.3 Schematic depicting how a point-based resistance applied to the shank translates to torques at the hip and knee (i.e., joint-based resistances) during the swing phase. Equations can describe the relationship between point- and joint-based resistances, and indicate that the resulting torques depend on the limb lengths and joint angles. Additionally, the torques at the hip and knee are coupled with one another. The notation f(Θ) denotes a function of Θ.

1.3.4 Types of Resistance

While the mode of applying the resistance dictates how the device is attached to the user, the type of resistance largely dictates the characteristics of the resistance. Generally, resistances can be characterized as inertial, elastic, viscous, frictional, or any combination thereof. In passive devices, the type of resistance is inherent to the type of passive element that the device uses (e.g., mass, spring, damper, etc.). In active robots, the motors can potentially be programmed to emulate any of these resistance types, or provide customized (i.e., user-defined) resistances that are not possible with passive elements. All of these resistance types will provide different resistance profiles based on the mechanics of the movement: inertial resistance depends on acceleration, elastic resistance scales based on position, viscous resistance depends on velocity, and friction provides a constant resistance (Figure 1.4A). Notably, the resistance type employed by the device will also determine the type of muscle contraction (i.e., concentric or eccentric)

that can be trained (Figure 1.4B). While most devices can engage the user's muscles concentrically, eccentric contractions can only be elicited by a device that can exert energy on the user (i.e., active robots, or inertial and elastic devices returning stored energy to the user).

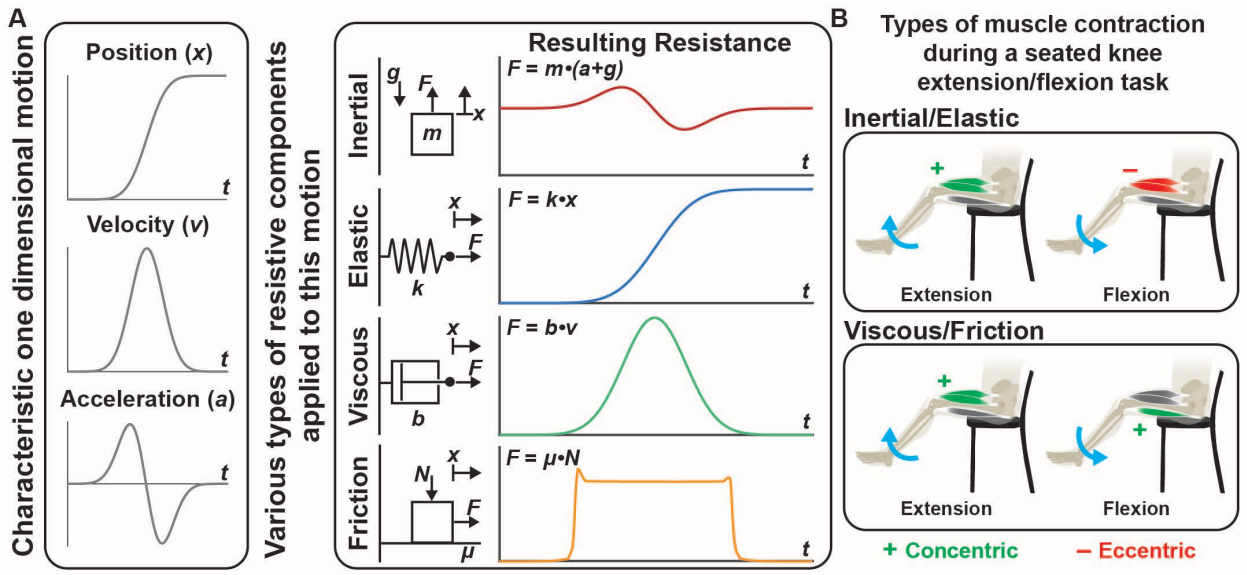

Figure 1.4 (A) Resistance types and the resulting forces when they are applied to a one-dimensional motion. The left panel characterizes this simple motion. Maintaining these characteristics, the right panel shows the force F that would be required to: lift a weight with mass m against gravity g; deform an elastic spring with stiffness k; deform a viscous damper with a damping coefficient b; or move along a surface with a coefficient of friction μ. Most passive devices will provide one of these resistance types, and active robots can emulate these components or provide customized resistances. **(B)** Resistances types differ in the types of muscle contractions (e.g., concentric and eccentric) that they can elicit. During the seated knee extension/flexion task depicted, inertial and elastic resistances elicit concentric contraction when extending the leg and eccentric contraction when flexing the leg. During the same task, viscous and friction-based resistances require concentric contraction during both extension and flexion.

We found that most of the studies we examined used inertial resistances (13/38 studies) by attaching a weight at some point on the body. In comparison, 7 studied elastic resistances and 6 studies used viscous resistances. Several studies also examined customized robotic resistances (12/38 studies). Many of these studies used the robot to emulate a system of passive devices (creating a viscoelastic resistance), while others used closed-loop control to create a constant resistance or one that was proportional to some other variable.

1.3.5 Joint Moments and Muscle Activation During Training

It is important to note that the mode and type of resistance cannot be viewed independently—every resistive device must utilize both—and the combination of these factors

determines the resistance that the patient experiences. Further, because gait is a repetitive task with stereotypical kinematics, each resistive strategy is going to be stereotypical in its ability to resist the user. Hence, the FRT strategy largely dictates the muscles groups, types of muscle contraction, joint action, and the phase of gait when a device is able to apply resistance. This section examines all of the studies that have measured muscle activation or joint moments while providing FRT (Table 1.1). In total, we found 24 studies measured muscle activation while only 7 measured joint moments.

1.3.5.1 Inertial Point Resistances

Typically, point-based inertial resistances have been administered by placing weights on the foot/shank, thigh, pelvis, or torso. When attached to the foot/shank, weighted cuffs increased hip extension and flexion moments during the stance phase, as well as hip flexion and knee flexion moments during the swing phase (Browning et al., 2007; Duclos et al., 2014; Noble & Prentice, 2006). This strategy also increased muscle activation of the quadriceps at the transition between stance and swing (Browning et al., 2007), the hamstrings during swing (Lam et al., 2008), and the triceps surae during stance (Browning et al., 2007). Weighted cuffs attached to the thigh or pelvis had no significant effects on joint moments; however, triceps surae activation increased during the stance phase (Browning et al., 2007; McGowan et al., 2008). Weights attached to the torso (e.g., using a backpack) (Chow et al., 2005; Krupenevich et al., 2015; Kubinski & Higginson, 2012; Silder et al., 2013; Simpson et al., 2011) significantly increased hip extension, knee flexion and extension, and ankle dorsi and plantarflexion moments during the stance phase (Chow et al., 2005; Krupenevich et al., 2015; Silder et al., 2013). This strategy also increased muscle activation of the quadriceps, hamstrings, and triceps surae during the stance and swing phases (Silder et al., 2013; Simpson et al., 2011). Inertial resistance pulling

backwards on the shank increased muscle activation of the quadriceps during the pre-swing phase of gait (Savin et al., 2010).

Table 1.1 Summary of how resistance during walking altered muscle activation and internal joint moments**.**

Reference	**Pop**	**Device**	**Mode**	**Type**	**Resisting**	**Significant Findings** [Variable (Phase of Gait)]
Browning et al. (2007)	AB	Passive	Point	Inertial	Foot	**MA:** RF (PSw) ↑, TA (TSw) ↑, MG (MSt–TSt) ↑, Sol (MSt–TSt) ↑ **Moment:** H Ext (MSt) ↑, H Flex (TSt–Isw, TSw) ↑, K Flex (TSw) ↑, A Dorsi (ISw) ↑
Lam et al. (2008)	SCI	Passive	Point	Inertial	Shank	**MA:** LH (Sw) ↑
Duclos et al. (2014)	Stroke	Passive	Point	Inertial	Shank	**Moment:** H Ext (LR,TSw) ↑, H Flex (TSt–PSw) ↑, K Flex (LR,TSw) ↑
Browning et al. (2007)	AB	Passive	Point	Inertial	Shank	**MA:** MG (MSt–TSt) ↑ **Moment:** No Effect
Noble & Prentice (2006)	AB	Passive	Point	Inertial	Shank	**Moment:** H Flex (ISw) ↑, H Ext (TSw) ↑, K Ext (ISw) ↑, K Flex (TSw) ↑
Savin et al. (2010)	AB	Passive	Point	Inertial	Shank Back	**MA:** RF (ISw) ↑
Browning et al. (2007)	AB	Passive	Point	Inertial	Thigh	**MA:** MG (MSt–TSt) ↑, Sol (MSt–TSt) ↑ **Moment:** No Effect
Browning et al. (2007)	AB	Passive	Point	Inertial	Pelvis	**MA:** MG (MSt–TSt) ↑, Sol (MSt–TSt) ↑ **Moment:** No Effect
McGowan et al. (2008)	AB	Passive	Point	Inertial	Pelvis	**MA:** MG (LR–PSw) ↑, Sol (LR–PSw) ↑
Kubinski & Higginson (2012)	Knee OA	Passive	Point	Inertial	Torso	**Moment:** No Effect
Chow et al. (2005)	AB	Passive	Point	Inertial	Torso	**Moment:** H Flex (PSw) ↑, H Abd (St) ↑, H Int (St) ↑, H Ext (St) ↑, K Ext (St) ↑, K Val (St) ↑, A Plant (St) ↑
Krupenvich et al. (2015)	AB	Passive	Point	Inertial	Torso	**Moment:** K Ext (St) ↑, A Plant (St) ↑
Kubinski & Higginson (2012)	AB	Passive	Point	Inertial	Torso	**Moment:** No Effect
Silder et al. (2013)	AB	Passive	Point	Inertial	Torso	**MA:** RF (St, Sw) ↑, VM (LR–MSt, TSw) ↑, VL (LR–MSt, TSw) ↑, MH (MSw–TSw) ↑, LH (LR–MSt, MSw–TSw) ↑, MG (MSt–PSw) ↑, Sol (MSt–PSw, Sw) ↑ **Moment:** H Ext (LR - MSt) ↑, K Ext (MSt) ↑, K Flex (PSw), A Dorsi (LR) ↑, A Plant (PSw) ↑
Simpson et al. (2011)	AB	Passive	Point	Inertial	Torso	**MA:** VL (LR, TSw) ↑, MG (TSt–PSw) ↑
Blanchette & Bouyer (2009)	AB	Passive	Point	Elastic	Foot Front	**MA:** LH (PSw–MSw) ↑, MH (PSw–MSw) ↑
Blanchette et al. (2012)	AB	Passive	Point	Elastic	Foot Front	**MA:** LH (PSw–MSw) ↑, MH (PSw–MSw) ↑
Gottschall & Kram (2003)	AB	Passive	Point	Elastic	Pelvis Back	**MA:** MG (TSt–PSw) ↑, Sol (TSt–PSw) ↑
Shin et al. (2014)	CP	Passive	Point	Elastic	Shank Front	**MA:** Hst (LR–MSt) ↓
Shin et al. (2014)	AB	Passive	Point	Elastic	Shank Front	**MA:** Hst (LR–MSt) ↓
Mun et al. (2017)	AB	Active	Point	Constant	Pelvis Back	**MA:** RF (St) ↑, VM (St) ↑, TA (St) ↑, GMax (St) ↑, AdL (St) ↑
Vashista et al. (2016)	AB	Active	Point	Constant	Pelvis Down	**MA:** No Effect
Tang et al. (2019)	CP	Active	Point	Viscoelastic	Shank Back	**MA:** No Effect
Yen et al. (2013)	SCI	Active	Point	Viscoelastic	Shank Back	**MA:** TA (Psw–ISw) ↑
Barthélemy et al. (2012)	AB	Passive	Joint	Elastic	Ankle Dorsi	**MA:** TA (Sw) ↑
Houldin et al. (2011)	SCI	Active	Joint	Viscous	Hip Bi	**MA:** RF (Sw) ↑
Houldin et al. (2011)	AB	Active	Joint	Viscous	Hip Bi	**MA:** RF (Sw) ↑
Houldin et al. (2012)	AB	Active	Joint	Viscous	Hip Bi	**MA:** RF (Sw) ↑, TA (Sw) ↑
Lam et al. (2008)	SCI	Active	Joint	Viscous	Hip+Knee Bi	**MA:** No Effect
Klarner et al. (2013)	AB	Active	Joint	Viscous	Hip+Knee Bi	**MA:** RF (ISw–MSw) ↑
Lam et al. (2006)	AB	Active	Joint	Viscous	Hip+Knee Bi	**MA:** RF (MSw) ↑, MH (PSw, MSw) ↑, LH (PSw) ↑, TA (MSw) ↑
Diaz et al. (1997)	AB	Active	Joint	Constant	Knee Ext	**MA:** RF ↑, VM ↑, VL ↑
Diaz et al. (1997)	AB	Active	Joint	Constant	Knee Flex	**MA:** VM ↓
Blanchette et al. (2011)	AB	Active	Joint	Custom	Ankle Dorsi	**MA:** TA (PSw–MSw) ↑
Conner et al. (2020)	CP	Active	Joint	Custom	Ankle Plantar	**MA:** TA (St) ↓, Sol (St) ↑

Population abbreviations: Pop (population), AB (able-bodied), SCI (spinal cord injury), CP (cerebral palsy), OA (osteoarthritis); muscle activation (MA) abbreviations: AdL (adductor longus), GMax (gluteus maximus), GMed (gluteus medius), Hst (hamstring), LH (lateral hamstring), MH (medial hamstring), MG (medial gastrocnemius), RF (rectus femoris), Sol (soleus), TA (tibialis anterior), VL (vastus lateralis), VM (vastus medialis); resistance and internal moment abbreviations: H (hip), K (knee), A (ankle), Flex (flexion), Ext (extension), Abd (abduction), Val (valgus), Int (internal), Plant (plantar flexion), Dorsi (dorsiflexion), Bi (Bidirectional [e.g., Flex & Ext]); gait phase abbreviations: St (stance), Sw (swing), LR (loading response), MSt (mid-stance), TSt (terminal stance), PSw (pre-swing), ISw (initial-swing), MSw (mid-swing), TSw (terminal swing). Front/Back/Down indicate the direction the device is pulling. ↑ Indicates that the variable significantly increased during training, while ↓ indicates a significant decrease. Note, many studies had additional variables that were reported but that did not show significance.

1.3.5.2 Elastic Point Resistances

Pulling forward on the foot/shank with an elastic resistance band increased muscle activation of the hamstrings during the early–mid swing phase (Blanchette & Bouyer, 2009; Blanchette et al., 2012). However, when the band was placed proximally on the shank, hamstring activation decreased during the stance phase (Shin et al., 2014). Pulling backwards on the pelvis increased muscle activation of the triceps surae muscles during the terminal stance and pre-swing phases of gait (Gottschall & Kram, 2003).

1.3.5.3 Custom Point Resistances

An active robotic cable device that pulled backwards on the shank with a viscoelastic resistance (Tang et al., 2019; Yen et al., 2013) increased muscle activation of the tibialis anterior during the swing phase (Yen et al., 2013), and it would likely increase quadriceps activation as well if tested on less impaired individuals. A robotic walker that pulled backwards on the pelvis with a constant force (Mun et al., 2017) increased muscle activation of the quadriceps, tibialis anterior, gluteus maximus, and adductor longus muscles during the stance phase of gait. Yet another motorized cable device pulled downwards on the pelvis with a constant force (Vashista et al., 2016); however, this strategy did not significantly alter muscle activation.

1.3.5.4 Elastic Joint Resistances

An ankle orthosis with elastic tubing between the heel and calf has been used to resist to ankle dorsiflexion during walking (Barthélemy et al., 2012). This strategy increased muscle

activation of the tibialis anterior muscle during pre- and initial-swing (Barthélemy et al., 2012). Future research in this area has large potential given the availability of elastic ankle-foot orthoses.

1.3.5.5 Viscous Joint Resistances

Viscous resistances have been applied to the hip and/or knee joints using active robotic exoskeletons (i.e., the Lokomat) (Houldin et al., 2012; Houldin et al., 2011; Klarner et al., 2013; Lam et al., 2006; Lam et al., 2008). In each instance, the resistance has been applied to both flexion and extension of the joint (i.e., bidirectionally). When applied to the hip, this strategy increased muscle activation of the rectus femoris and tibialis anterior during the swing phase of gait (Houldin et al., 2012; Houldin et al., 2011). Applying viscous resistance to both the hip and knee increased muscle activation of the hamstrings during pre-swing, and the rectus femoris, medial hamstring, and tibialis anterior during mid-swing (Klarner et al., 2013; Lam et al., 2006). These effects were absent when tested in individuals with spinal cord injury (Lam et al., 2008).

1.3.5.6 Custom Joint Resistances

Several active robotic exoskeletons have been programmed to provide custom resistances. One device provided a constant torque to resist either knee flexion or extension (Diaz et al., 1997). With this device, resisting extension increased activation of the quadriceps muscles and resisting flexion reduced activation of the vastus medialis (Diaz et al., 1997). An electrohydraulic ankle foot orthosis has also been programmed resist to ankle dorsiflexion during the early swing phase (Blanchette et al., 2011). This strategy increased muscle activation of the tibialis anterior muscle from pre- to mid-swing (Blanchette et al., 2011). Lastly, a wearable, soft robot has been used to resist ankle plantar flexion (Conner et al., 2020). The resistance provided by this robot was unique because the torque was proportional to the real-time ankle moment;

thus, mimicking normal joint loading. During training, this strategy increased muscle activation of the soleus while decreasing muscle activation of the tibialis anterior during the stance phase (Conner et al., 2020).

1.3.6 Aftereffects Following the Removal of Resistance

Aftereffects are typically measured when studying motor adaptation. Motor adaptation occurs when a movement (in this case, walking) is practiced in the presence of a perturbation (Bastian, 2008; Martin et al., 1996), such as the extra loading presented by a resistive device. During practice with the perturbation, one's perception of the movement gets altered and the nervous system gradually creates a new set of controls for the movement. Finally, once the perturbation is removed, some aspects of the modified movement persist, which are referred to as aftereffects. These aftereffects contain information about how the nervous system is being driven to adapt (Morton & Bastian, 2006; Shadmehr & Mussa-Ivaldi, 1994) and may indicate potential gains a particular training can produce, as aftereffects have been seen to transfer to overground walking after training (Gama et al., 2018; Reisman et al., 2009; Savin et al., 2014; Yen et al., 2012). We found that 12 studies measured kinematic aftereffects while 18 studies measured spatiotemporal aftereffects. In this section, we examine how different strategies for FRT during walking have produced kinematic and spatiotemporal aftereffects (Table 1.2).

1.3.6.1 Inertial Point Resistances

Aftereffects have been measured with inertial resistances by placing weighted cuffs on the shank (Gama et al., 2018; Lam et al., 2008; Noble & Prentice, 2006). Once resistance was removed with this strategy, individuals walked with increased knee flexion (Lam et al., 2008). Spatiotemporally, this resulted in increased overground gait speed and step length (Gama et al., 2018) and foot clearance when walking on a treadmill (Noble & Prentice, 2006). Pulling

backwards on the shank with an inertial resistance (Savin et al., 2014; Savin et al., 2010; Savin et al., 2013) increased hip flexion and reduced hip extension once the resistance was removed (Savin et al., 2010). Spatiotemporally, this strategy increased step length and single leg support time while reducing swing time (Savin et al., 2010; Savin et al., 2013). It also increased overground gait speed and stride length (Savin et al., 2014).

Table 1.2 Summary of how strategies produce spatiotemporal and kinematic aftereffects

Reference	**Population**	**Device**	**Mode**	**Type**	**Resisting**	**Significant Aftereffects** [Variable (Phase of Gait)]
Gama et al. (2018)	AB	Passive	Point	Inertial	Shank	**Spatiotemporal:** OG Gait Speed ↑, OG Step Length ↑
Noble & Prentice (2006)	AB	Passive	Point	Inertial	Shank	**Spatiotemporal:** Foot Clearance ↑ **Kinematic:** No Effect
Lam et al. (2008)	SCI	Passive	Point	Inertial	Shank	**Kinematic:** K Flex (Sw) ↑
Savin et al. (2010)	AB	Passive	Point	Inertial	Shank Back	**Spatiotemporal:** Step Length ↑, Swing Time ↓ **Kinematic:** Hip Flexion (Sw) ↑, Hip Extension (St) ↓
Savin et al. (2014)	AB	Passive	Point	Inertial	Shank Back	**Spatiotemporal:** OG Gait Speed ↑, OG Stride Length ↑
Savin et al. (2014)	Stroke	Passive	Point	Inertial	Shank Back	**Spatiotemporal:** OG Gait Speed ↑, OG Stride Length ↑
Savin et al. (2013)	Stroke	Passive	Point	Inertial	Shank Back	**Spatiotemporal:** Step Length ↑, SLS Time ↑
Blanchette & Bouyer (2009)	AB	Passive	Point	Elastic	Foot Front	**Spatiotemporal:** Foot Speed (Sw) ↓
Blanchette et al. (2012)	AB	Passive	Point	Elastic	Foot Front	**Spatiotemporal:** Foot Speed (Sw) ↓
Vashista et al. (2013)	AB	Passive	Point	Elastic	Pelvis Down	**Kinematic:** Pelvis Displacement ↑
Tang et al. (2019)	CP	Active	Point	Viscoelastic	Shank Back	**Spatiotemporal:** Step Length ↑
Yen et al. (2013)	SCI	Active	Point	Viscoelastic	Shank Back	**Spatiotemporal:** Stride Length ↑
Yen et al. (2014)	SCI	Active	Point	Viscoelastic	Shank Back	**Spatiotemporal:** Stride Length ↑
Yen et al. (2015)	Stroke	Active	Point	Viscoelastic	Shank Back	**Spatiotemporal:** Step Length ↑
Yen et al. (2012)	SCI	Actve	Point	Viscoelastic	Thigh Back	**Spatiotemporal:** OG Gait Speed ↑, OG Stride Length ↑, Stride Length ↑, Stance Time ↑
Vashista et al. (2016)	AB	Active	Point	Custom	Pelvis Down	**Spatiotemporal:** Stance Time ↑ **Kinematic:** No Effect
Barthélemy et al. (2012)	AB	Passive	Joint	Elastic	Ankle Dorsi	**Kinematic:** A Exc ↑
Houldin et al. (2011)	AB	Active	Joint	Viscous	Hip Bi	**Spatiotemporal:** Foot Clearance ↑ **Kinematic:** H Flex (Sw) ↑, K Flex (Sw) ↑
Houldin et al. (2012)	AB	Active	Joint	Viscous	Hip Bi	**Spatiotemporal:** Foot Clearance ↑ **Kinematic:** H Flex (Sw) ↑, K Flex (Sw) ↑
Houldin et al. (2011)	SCI	Active	Joint	Viscous	Hip Bi	**Spatiotemporal:** Step Length ↑ **Kinematic:** H Flex (Sw) ↑
Lam et al. (2006)	AB	Active	Joint	Viscous	Hip+Knee Bi	**Kinematic:** H Flex (Sw) ↑, K Flex (Sw) ↑
Lam et al. (2008)	SCI	Active	Joint	Viscous	Hip+Knee Bi	**Kinematic:** No Effect
Blanchette et al. (2011)	AB	Active	Joint	Custom	Ankle Dorsi	**Kinematic:** A Dorsi (MSw) ↑

Reference	Population	Device	Mode	Type	Resisting	**Significant Aftereffects** [Variable (Phase of Gait)]
Cajigas et al. (2017)	AB	Active	Joint	Custom	Shank Back	**Spatiotemporal:** Step Length ↑
Severini et al. (2020)	AB	Active	Joint	Custom	Shank Back	**Spatiotemporal:** Step Length ↑

A full list of abbreviations can be found in Table 1.1. Additional abbreviations: Exc (excursion), OG (overground), SLS (single leg support). If not specified as overground, variables were measured over a treadmill; many studies had additional variables that were reported but that did not show significance or were not variables of interest for this review.

1.3.6.2 Elastic Point Resistances

Pulling forward on the foot with an elastic resistance band decreased foot velocity once the resistance was removed (Blanchette et al., 2012). A passive device that pulled downward on the pelvis did not have an effect on sagittal plane hip, knee, or ankle kinematics (Vashista et al., 2013).

1.3.6.3 Custom Point Resistances

Several studies have provided a viscoelastic resistance using a cable robot to pull backwards on the shank (Tang et al., 2019; Yen et al., 2013, 2014; Yen et al., 2015) and thigh (Yen et al., 2012). While none of these studies have measured kinematic aftereffects, spatiotemporally, this strategy increased overground gait speed (Yen et al., 2012) and step/stride length (Tang et al., 2019; Yen et al., 2013, 2014; Yen et al., 2012; Yen et al., 2015). Another active robot has been used to pull downward on the pelvis with a custom force (Vashista et al., 2016). With this strategy, hip range of motion and cadence were unchanged once the resistance was removed; however, the stance phase duration increased.

1.3.6.4 Elastic Joint Resistances

Walking with resistance to ankle dorsiflexion during the swing phase (Barthélemy et al., 2012) resulted in an aftereffect of increased ankle range of motion.

1.3.6.5 Viscous Joint Resistances

A bidirectional viscous resistance at the hip produced a kinematic aftereffect of increased hip and knee flexion (Houldin et al., 2012; Houldin et al., 2011). Spatiotemporally, these aftereffects presented as increased stride length and foot clearance (Houldin et al., 2012; Houldin et al., 2011). When applied to the hip and knee concurrently, viscous resistances produced a kinematic aftereffect of increased hip and knee flexion (Lam et al., 2006). However, knee angle was unchanged when this strategy was applied on individuals with spinal cord injury (Lam et al., 2008).

1.3.6.6 Custom Joint Resistances

Walking with an active ankle-foot orthosis that resisted ankle dorsiflexion during the swing phase significantly increased ankle dorsiflexion angle during the mid-swing phase once the resistance was removed (Blanchette et al., 2011). Joint-based resistances that emulated pulling backwards on the shank were found to increase step length (Cajigas et al., 2017; Severini et al., 2020).

1.3.7 Neural Adaptations to Functional Resistance Training

Although neural adaptation is a motivator for providing FRT during walking, only a few studies that have directly investigated the neural effects of this training (Barthélemy et al., 2012; Bonnard et al., 2002; Chisholm et al., 2015; Zabukovec et al., 2013). A majority of these studies have analyzed neural adaptation using transcranial magnetic stimulation (TMS)—a noninvasive brain stimulation technique, where an electromagnet (referred to as a coil) is placed over the scalp to stimulate the superficial brain cortex. TMS can be used to assess neural excitability of the motor system by stimulating over a motor "hotspot" of a muscle (i.e., the area of the brain that corresponds to that muscle) then recording the output from the muscle (i.e., a motor evoked

potential [MEP]) using electromyography or dynamometry. Therefore, comparing MEPs before, during, or after training can indicate an increase or decrease in excitability in the neurons that control that muscle.

TMS has been used to evaluate neural excitability both during training (i.e., stimulating the brain as the participant walked on the treadmill) and directly after training (i.e., with the participant seated in a chair) in able-bodied participants. Bonnard et al. (Bonnard et al., 2002) measured neural excitability during training, which consisted of walking with an elastic band attached between the subject's feet and shoulders (i.e., a point-based resistance pulling upwards on the foot). They found that neural excitability (i.e., the size of the MEPs) increased in the rectus femoris and lateral hamstring during the late swing phase while training. Barthélemy et al. (Barthélemy et al., 2012) measured changes in neurological excitability both during and after training with an elastic ankle-foot orthosis (i.e., a joint-based strategy) that provided resistance to ankle dorsiflexion during the swing phase. They found that excitability increased in the tibialis anterior during the swing phase while training, but did not see any significant changes following training. Lastly, Zabukovec et al. (Zabukovec et al., 2013) applied a joint-based viscous resistance to the hip and knee joints and measured the neural excitability after training; however, they did not see any significant changes in neural excitability. Hence, these studies have typically found that excitability increases during training (Barthélemy et al., 2012; Bonnard et al., 2002), but that these effects are not present following training (Barthélemy et al., 2012; Zabukovec et al., 2013).

1.4 Discussion

FRT during walking is an emerging technique for rehabilitation following neuromusculoskeletal injury. As such, there are several different strategies that have been used to

apply resistance, which vary based on the type of device used, how the device interfaces with the user, and the type of resistance that the device supplies. Hence, we examined the different strategies that have been used to apply FRT during walking, and how the characteristics of each resistive strategy altered the acute effects of training. Specifically, we reviewed how FRT has been applied during walking to alter joint moments and muscle activation, how training has elicited kinematic and spatiotemporal aftereffects once resistance is removed, and how it has altered neural control of walking. In this section, we will discuss the significance of our findings, as well as any potential trade-offs to consider when applying this training.

1.4.1 Patient Populations that May Benefit

While the majority of acute research on FRT during walking was performed on able-bodied individuals, these studies were often motivated for individuals with neurological injuries, including spinal cord injury, stroke, and cerebral palsy. This is understandable, as FRT is largely based on principles of experience dependent neural plasticity (Carroll et al., 2001; Harvey, 2009; Kleim & Jones, 2008; Maier et al., 2019). However, we found that training strategies often had more evident effects in able-bodied participants than individuals with neurological injuries (Lam et al., 2006; Lam et al., 2008; Tang et al., 2019; Yen et al., 2013). This may have occurred because many participants with neurological injuries were too impaired to overcome the resistance. Hence, it has been suggested that patients with severe impairments following injuries could be better served with assistive training rather than FRT (Wu et al., 2012).

Notably, patients with orthopedic injuries are underrepresented in this research. We only found a single study trained individuals with osteoarthritis (Kubinski & Higginson, 2012). However, following orthopedic injury or reconstructive surgery, most patients present with muscle weakness, altered neural control, and functional impairments, which often extend to gait

(Garcia, Curran, et al., 2020; Pietrosimone et al., 2018; Rodriguez et al., 2020). Hence, we feel that individuals with orthopedic injuries could be prime beneficiaries of this training, and recommend that future studies be performed on these patient groups. Indeed, preliminary evidence from pilot clinical trials indicate that FRT during walking could have positive effects in individuals with anterior cruciate ligament (ACL) injuries (Brown et al., 2021; Rocchi et al., 2020).

1.4.2 Types of Devices for Functional Resistance Training

We found that most studies have either used active rehabilitation robots or passive devices to apply FRT during walking. While there are benefits to both types of devices, there are also several trade-offs that must be considered when selecting a device for training. In this section, we will discuss this broad spectrum of devices (Figure 1.2) and the practicality of their application for FRT during walking. Additionally, we will introduce a third type of device that has the potential to alter how this training is applied.

1.4.2.1 Active Robots

We will first consider active rehabilitation robots; we refer to this set of robots as active because they use active actuators capable of either assisting or resisting movement. There is large potential for training with active robots because the motors can be controlled to provide unique force environments to the user. Additionally, sensors on the robot allow for a therapist to track the progress of a patient throughout training and offer opportunities to provide real-time feedback to the user in the form of interactive games. Given this upside, it is not surprising that active robots have been widely applied for FRT during walking.

However, a major issue with most of these active robots is that they are not very accessible for patients or clinicians. First, a majority of these robots are custom-built, and

building such devices requires an investment and expertise. Second, commercially available robots are also very expensive, which prevents their widespread use in-home or in small clinics (Lu et al., 2011). Lastly, the commercial versions of these devices are typically used for assistive training on heavily impaired individuals, and resistance settings are not available for routine clinical use. For these reasons, clinicians are more likely to use the more cost-effective passive devices instead of active robots.

1.4.2.2 Passive Devices

A majority of the studies in this review used passive devices for training. This is likely because passive devices are very practical—they have the inherent ability to provide large resistances at a fraction of the cost of a robot (Chang et al., 2018). Moreover, they can be purchased at a local sporting goods store, which increases the feasibility of in-home use by the patient. The downside to these passive devices is that they are not controllable, so resistance must be scaled by manually adjusting the device. Further, these devices are not typically instrumented with encoders and load cells, which limits a clinician's ability to monitor the patient's compliance or recovery throughout the training process, especially if the device is being used at home. Without these capabilities, patients must be intrinsically motivated to train. Some of these issues could potentially be remedied if the devices were instrumented in order to track movement (e.g., using encoders or inertial sensors) or, as we will see in the next section, if the passive elements were made controllable.

1.4.2.3 Semi-Passive Robots

There is another class of devices that exist in the middle ground between active robots and passive devices, which we refer to as semi-passive rehabilitation robots (Chang et al., 2018). These robots draw inspiration from passive rehabilitation devices by employing passive elements

to provide resistance to the patient; however, like with active robots, the passive elements can be controlled by a computer. Thus, the resulting robotic devices are able to balance the cost and portability of passive devices, while still allowing for patient monitoring and interactive treatment. Although this will typically sacrifice the ability to assist the user during training, semi-passive robots may offer a cost-effective way to provide FRT. To date, this principle has only been applied in upper-extremity rehabilitation robots to re-train reaching (Chang et al., 2018; Haraguchi & Furusho, 2013; Stienen et al., 2007), and it has not been widely used for FRT during walking. Hence, there is great potential to develop devices in this area.

1.4.3 Differences in Modes of Interfacing with the Limb

In this review, we distinguished devices based on how they interfaced with the limb. That is, if they attached the resistive element to a point on the user (i.e., a point-based resistance), or if the resistance was applied as a torque directly at the joint (i.e., a joint-based resistance). From a mechanical viewpoint this distinction is largely semantic, as point resistances can be applied to emulate a desired joint-based resistance (i.e., torques) and vice versa (Figure 1.3). However, in practice, the differences between these two modes can have a profound effect on how a device is able to resist the user during training and how exercise using that device should be administered.

Joint-based resistances have a large upside because they can be easily applied to target patient-specific weaknesses. In the rehabilitation field, strength is typically measured at the joint level using dynamometry or graded scales such as manual muscle testing (Bohannon, 2001). Hence, with a joint-based approach, muscle weakness can be detected at a specific joint and a resistive torque can be prescribed to target the weakened muscle group. While targeted resistance is still possible with a point-based approach, it is more difficult. First, the torques experienced at the joints due to a point-based resistance are often coupled with one another. For example, the

point-based resistance applied to the ankle in Figure 1.3 produces torques at both the knee and hip joints. Hence, any distal joint cannot be targeted without also loading the more proximal joints of the leg. Second, joints located further away from the point where the resistance is applied often experience more resistance (due to a larger lever arm), which makes these joints more likely to fatigue faster. Third, the resistances experienced at the joints under a point-based resistance are more dependent on anatomy and gait kinematics, as the torque is a function of segment lengths and joint angles. Despite these limitations, devices that apply point-based resistance can still provide utility for FRT. Additionally, we found that a majority of the studies in this review actually applied point-based resistances (27/38 studies). Hence, there are other factors to be considered when distinguishing between these two modes.

Point and joint-based resistances can also differ based on their cost and ease of use. Devices that provide point-based resistances are typically lower cost and easier to set up than joint-based devices, especially if they are passive devices. This stems from how they attach to the user with a simple strap/cuff; hence, more time can be spent on training and a single device can be used on multiple patients. This is in contrast to the braces and exoskeletons, as care must be taken to fit the device to the patient, or it will not perform as intended. For these reasons, clinicians may choose to train their patients using devices that apply point- rather than joint-based resistances. Hence, while there are some differences between how training can be applied with these two modes, ultimately, the decision of which to apply may be based on pragmatic choices.

1.4.4 How the Type of Resistance Could Affect Training

While numerous types of resistive loads were identified by this review, it is difficult to make comparisons between studies due to differences in the methods and variables analyzed. As

such, it is still unclear how altering the type of resistance affects training outcomes. Undoubtedly there are differences in the resistance profiles that are generated by different types of resistive elements (Figure 1.4A), but only a single study in this review tested multiple resistance types (inertial and viscous) (Lam et al., 2008). Without a larger number of acute studies, computer-based analyses, or even randomized controlled clinical trials, the role of resistance type for FRT will remain unclear.

We do know that the type of resistance dictates the type of muscle contractions that can be elicited during training (Figure 1.4B) and how the resistance feels to the user. Inertial, elastic, and customized robotic resistances permit concentric, eccentric, and even isometric muscle contractions during training, while friction and viscous resistances only permit concentric muscle contraction. The ability to provide eccentric training may be an advantage, as eccentric training can better promote strength when compared with concentric training (Kaminski et al., 1998; Lepley et al., 2017; Lepley et al., 2015; Roig et al., 2009). However, strength also increases when training involves concentric muscle contractions (Higbie et al., 1996). It has been speculated that viscous resistances could benefit power training, as the peak force requirements when using a viscous resistance coincide with the peak velocity profile of the movement (Figure 1.4A) (Stoeckmann et al., 2009). While FRT during walking is generally regarded as safe, the same mechanism that allows for eccentric contractions also poses a potential safety risk, as the momentum of the weight, recoil of the spring, or unvalidated programming in a robot could hyperextend the user's limb during training. For this reason, viscous resistance is also seen as the safest option.

The feeling of the resistance (i.e., the haptics) also affects how widely a device will be adopted. While inertial, elastic, and viscous devices all feel different to the user, they are all said

to feel smooth because the resistance scales with the mechanics of the movement. Notably, none of the studies in this review applied friction-based resistance training during walking. This is likely because friction-based resistance feels jerky due to instability at the beginning and end of a movement (often referred to as stiction) (Figure 1.4A). Stiction occurs because the coefficient of friction (the constant that determines the magnitude of the resistance) is different when an object is at rest (where the coefficient is larger) or in motion. In order to avoid this unpleasant feeling, friction is often minimized in mechanical systems. However, the haptics of resistance types is a potential area for future research, and it is possible that all resistance types have a role to play.

1.4.5 Applying Biomechanics and Aftereffects Results

The main goal of this review was to examine different strategies that have been used to apply resistance during walking and how these strategies alter the outcomes of acute training. Generally, we found that different resistive strategies varied in their ability to alter gait biomechanics (i.e., muscle activations and moments) during training and aftereffects following the removal of the resistance. Given that muscle strength and functional deficits vary between patients, we do not believe that there is a single resistive strategy that can be applied uniformly. Instead, clinicians must select a resistive strategy that will work for their patient given their current impairments (e.g., strength deficits and kinematic abnormalities) and functional goals (e.g., to reduce fall risk or increase gait speed), while remaining feasible for use in their clinic or home. We hope the information within this review can serve as a reference to inform these decisions.

Interpreting biomechanics data is relatively straightforward. When prescribing FRT during walking, we would suggest that a strategy be applied based on patient-specific strength deficits. While strength can be measured using dynamometry or clinical metrics, it could also be

measured more functionally in a gait-lab setting (i.e., integrated kinematics and kinetics). Once strength deficits are identified, we would suggest applying a resistive strategy that has been shown to increase the joint moment of the specific action that is weakened, or in the muscles that contribute to that joint moment (Table 1.1). A similar logic can be applied to aftereffects. That is, we would suggest that any kinematic or spatiotemporal deficits be identified using either motion capture, inertial measurement units, a gait mat, etc. Once the desired outcome is identified, Table 1.2 can be used to identify a resistive strategy has produced increases in that particular outcome. When referring to the tables in this review, please note that all variables were not measured by each study. Hence, it is possible that a resistive strategy could have an effect that is not indicated simply because it has not been measured.

We must note that using aftereffects to predict the outcomes for rehabilitation is still an active area of research. As such, it is not yet certain whether the aftereffects observed after an acute training are retained in the patient's normal walking pattern following an intervention (Roemmich & Bastian, 2018). While acute aftereffects have been seen to persist in overground walking following training (Gama et al., 2018; Reisman et al., 2009; Savin et al., 2014; Yen et al., 2012), the patient typically deadapts eventually once the resistance is removed. A few clinical trials have trained adaptation paradigms over several weeks to see if the patient's normal movement strategy begins to resemble the aftereffect (Reisman et al., 2013; Rode et al., 2015; Ten Brink et al., 2017). While these trials have found that these aftereffects can persist for months following training (Reisman et al., 2013; Rode et al., 2015), it is also unclear if motor adaptation paradigms provide any benefit beyond the standard of care (Ten Brink et al., 2017). However, this information is still incomplete and researchers are still searching for ways to supplement adaptation training to produce more robust effects (Roemmich & Bastian, 2018). At

the very least, aftereffects are a surrogate variable that represents the muscles that generate the desired motion. For example, pulling backwards on the shank increased muscle activation from the rectus femoris during training, and this produced an aftereffect of increased step length (Savin et al., 2010). Hence, even if aftereffects do not represent the cumulative gains from a training, they still indicate that the muscles integral to that task are being trained.

1.4.6 Interpreting Neural Adaptations using TMS

Surprisingly, there were very few studies that have examined the effects of FRT during walking on neural excitability. Without such information, we can only discuss the methods that have been used to measure neural excitability, highlight potential problems with interpreting these data, and stress the importance of creating larger datasets to better understand the neural mechanisms of recovery.

The results from the limited number of studies suggest that neural excitability is altered during training but not following training. However, the methods that were used to measure neural excitability were very different in these two instances. During training, TMS was performed functionally (i.e., as the participant walked on the treadmill), but following the training, TMS was applied more conventionally, with the subject in a seated posture. While functional TMS is potentially a powerful technique, it is not widely used because there are several factors that must be controlled when performing TMS, and it is difficult to control for these factors during functional tasks. The finding that neural excitability remained unchanged when measured in a seated posture following training does not necessarily indicate that neural excitability is unchanged in the entire motor system; rather, there may not be a net change in excitability. TMS is a measure of the entire corticospinal tract—which includes the motor cortex, midbrain, brainstem, spinal cord, and all of the connections in between—as well as peripheral

motor neurons and muscles. Hence, it is possible that an increase in cortical excitability is being masked by a decrease somewhere else in the system. However, techniques that are more targeted within the corticospinal tract (e.g., transcranial electrical stimulation, cervicomedullary stimulation, Hoffmann's reflex) would be required to test this theory.

It is also important to mention that an increase in excitability is not necessarily a desirable outcome, while a decrease in excitability is not necessarily undesirable. For example, decreased neural excitability has been found following strength training in uninjured subjects (Carroll et al., 2002). This does not mean that strength training should be avoided, but that an adaptive change (presumably inhibitory) is happening somewhere along the corticospinal tract, which could potentially have therapeutic value. Indeed, patients with overactive spinal reflexes (i.e., hyperreflexia), as is often seen following neurological injury, could potentially benefit from a training that induces inhibitory effects (Nielsen et al., 2007). Ultimately, the desired neural outcome will need to be defined by the condition being tested. Unfortunately, it is still not well understood how specific neural changes correlate with functional outcomes.

1.4.7 Feedback during Training

Feedback has rarely been provided when performing FRT during walking, however, this may be a crucial component to induce positive outcomes after an intervention. Feedback can be used to increase the intensity or ensure the participant walks with normal kinematics. Typically, when a resistance is applied to the leg, subjects have a tendency to alter their walking in order to take “the path of least resistance”; but feedback can help to alert the subject that they are using an abnormal gait strategy. The few studies that have provided feedback have typically provided the subject with a real-time depiction of their kinematics or spatiotemporal gait parameters (Houldin et al., 2012; Klarner et al., 2013; Zabukovec et al., 2013). While these methods require

some sort of instrumentation, a similar effect could also be obtained through verbal coaching or having the patient avoid/clear an obstacle while walking (Reid & Prentice, 2001).

1.5 Summary

This review examined the strategies that have been used to apply FRT during walking, and characterized how resistive strategies altered the acute effects of training—including biomechanics during training, aftereffects once resistance was removed, and neural excitability. We found that strategies varied in their ability to alter gait biomechanics (i.e., muscle activations and moments) during training and aftereffects following the removal of the resistance. Too few studies examined neural adaptations due to FRT to determine how these can be affected by the resistance strategy. Overall, we believe that resistive strategies can be selected to target patient specific strength deficits and gait impairments. When interfacing resistance to the user, joint-based approaches (such as wearable braces/exoskeletons) permit resistance that is more targeted to patient weaknesses as measured clinically and can be used outside the clinic, while point-based approaches are often more cost effective and easier to implement in the clinic. This review also indicates that more research is needed to determine how the type of resistance (i.e., inertial, elastic, viscous, or custom) affects functional resistance training during walking. Lastly, more research is needed to characterize how this training can be used to alter gait biomechanics, aftereffects, and neural control of walking.

1.6 Organization of Thesis

This introductory review was performed to better educate our understanding of how different resistive strategies can be used to facilitate functional resistance training during walking. However, it can be difficult to make comparisons between resistive strategies because they often use different modes of interfacing with the limb, types of resistance, and resist

different joints/actions. Additionally, studies rarely measure the same variables as one another. Thus, this dissertation attempts to determine how resistive strategies can be used to facilitate FRT during walking though device design, human subjects research, and musculoskeletal modeling.

In Chapter 2 we designed and developed a passive device that provided a bidirectional joint-based viscous resistance to the knee and tested that device on able-bodied individuals. This work was previously published in the Annals of Biomedical Engineering (Washabaugh et al., 2016) In Chapter 3 we did a preliminary evaluation of the acute effects of training with this device on stroke survivors. This work was previously published in Restorative Neurology and Neuroscience (Washabaugh & Krishnan, 2018).

In our previous experiments we noted that participants often reduced their joint excursions when walking with resistance, which we believed to be a form of motor slacking. Hence, in Chapter 4 we ran an experiment to determine if participants were slacking during training, and if visual feedback could be used to augment the training and reduce any slacking behavior. This chapter also introduces a controllable semi-passive version of the viscous brace developed in chapter 2.

In Chapter 5, we designed and developed a passive device to provide joint-based elastic resistance to the knee, then tested this device on an able-bodied individual. This device was unique in that it could be configured to resist either joint flexion, extension, or both. Additionally, peak torque for each joint action could be tailored to the individual's strength. This work was published in IEEE Transactions on Biomedical Engineering (Washabaugh, Augenstein, Ebenhoeh, et al., 2020).

In Chapter 6, we compared how these viscous and elastic devices differed in their ability to alter gait biomechanics during and after training, as well as muscle fatigue and neural excitability after training. We also these variables where altered when using the viscous device to resist the knee or both the hip and knee together.

In Chapter 7, we used a biomechanical simulation-based analyses to comprehensively evaluate how several strategies for functional resistance training during walking that are commonly used in clinics and research could alter gait biomechanics and muscle activation. This work was published in Gait and Posture (Washabaugh, Augenstein, & Krishnan, 2020).

Chapter 8 is a conclusion chapter, where we summarize the many findings represented by this work and discuss future directions that could be pursued to advance research in this field.

1.7 Acknowledgement

A version of this work has been formally submitted for publication and I would like to acknowledge my co-author, Dr. Chandramouli Krishnan for his contributions. This work was supported in part by the National Institutes of Health (Grant R21 HD092614), the National Science Foundation (Grants 1804053 and DGE 1256260), and the UM-BICI Collaboratory Initiative. Any opinions, findings, and conclusions or recommendations expressed in this material are those of the authors and do not necessarily reflect the views of the funding sources.

Chapter 2

Eddy Current Braking for Functional Resistance Training During Walking

Abstract

Functional resistance training is becoming increasingly popular when rehabilitating individuals with neurological injury such as stroke or cerebral palsy. Typically, resistance during walking is provided using cable robots or weights that are secured to the distal shank of the subject. However, there are few devices that are wearable and capable of providing resistance across the joint, allowing over ground gait training. In this study, we created a lightweight and wearable device using eddy current braking to provide resistance to the knee. We then validated the device by having subjects wear it during a walking task through varying resistance levels. Electromyography and kinematics were collected to assess the biomechanical effects of the device on the wearer. We found that eddy current braking provided resistance levels suitable for functional resistance training of leg muscles in a package that is both lightweight and wearable. Applying resistive forces at the knee joint during gait resulted in significant increases in muscle activation of many of the muscles tested. A brief period of training also resulted in significant aftereffects once the resistance was removed. These results support the feasibility of the device for functional resistance training during gait. Future research is warranted to test the clinical potential of the device in an injured population.

2.1 Introduction

Many patients with stroke, cerebral palsy, and other neurological conditions have significant limitations in walking, and experience limited mobility for the rest of their life (Damiano & Abel, 1998; Duncan et al., 2007; van der Krogt et al., 2010). Lack of mobility significantly affects functional independence, and consequently results in greater physical disability (Hesse, 2001). Facilitating gait recovery, therefore, is a key goal in rehabilitation. With the growing elderly population, the prevalence of many of the neurological conditions is expected to increase worldwide, and the need for interventions to address gait dysfunction will grow (Pollock et al., 2014). Appropriately designed rehabilitation devices can assist in meeting this imminent heightened demand for care.

Task-specific training is recognized as the preferred method for gait training following neurological injury because the motor activity seen in this type of rehabilitation is known to facilitate neural plasticity and functional recovery (Dobkin, 2008; Langhorne et al., 2011; Plautz et al., 2000). However, current task-oriented gait training approaches seldom focus on improving muscle strength and impairment, which are also critical for motor recovery and plasticity (Corti et al., 2012; Nadeau et al., 2013; Platz, 2004). For example, incorporating strengthening exercises into rehabilitation interventions can counteract muscle weakness and improve function in individuals with a wide variety of neuromuscular disorders (Pak & Patten, 2008; Patten et al., 2004; Scandalis et al., 2001). Numerous studies have also demonstrated a link between the ability to produce adequate force in the muscles of lower limbs and gait speed following neurological injury (Damiano & Abel, 1998; Kim & Eng, 2003). Additionally, resistance training may result in adaptive changes in the central nervous system (Carroll et al., 2011). However, the benefits of strength training may not translate *maximally* into improvements in gait function

unless the training incorporates task-specific elements (Eng & Tang, 2007). This task-specific loading of the limbs–termed as functional resistance training–is gaining popularity when rehabilitating individuals with neurological injury (Mares et al., 2013; Yang et al., 2006).

Devices do exist to provide functional resistance training during walking. The simplest of which applies resistance by placing a weight on the lower limb. Research indicates that this intervention can increase the metabolic rate of healthy subjects (Browning et al., 2007) as well as increase power of the hip and knee and muscle activation during walking in neurologically injured populations (Duclos et al., 2014). While this method of functional resistance training is simple and practicable, it is hindered by a low torque-to-weight ratio: making large resistances unobtainable without excessively large weights. Cable driven devices, such as that created by Wu et al (2011), address this issue by locating the heavy force generating elements (actuators and cable spools) away from the patient. This device resists ankle translation during the swing phase of gait, and studies have found that it can potentially improve step length symmetry (Yen et al., 2015) and gait speed following stroke (Wu, Landry, et al., 2014). However, methods that resist the user through cables will be difficult to use in over-ground training.

The majority of the existing methods for functional resistance training apply resistance to the end effector region of the leg (i.e., foot or ankle). Because of this, the resistance may be irregularly distributed between the hip and knee joints, and compensatory strategies could be promoted as weaker muscles are not specifically targeted in the training. The magnitude of resistance applied to the leg could also change as a function of limb position. Further, the resistance in these applications is usually unidirectional, which would assist movement during certain phases of gait. Bidirectional resistance is possible, but only obtainable with supplementary equipment (additional actuators and cables) and controls that utilize gait

detection. For these reasons, providing resistance in the joint space (i.e., across the joint) may be beneficial for training and other biomechanical evaluations. However, making a device that is lightweight and wearable while still providing high bidirectional torque requires a unique approach. Therefore, the goal of this study was to develop a gait-training device that is capable of providing variable levels of resistance across the knee during walking and to test the biomechanical effects of this device on the wearer by studying muscle activation patterns and sagittal plane kinematics during treadmill walking.

2.2 Materials and Methods

This study consisted of two phases: (1) development of a lightweight wearable device that provides resistance to the leg during walking and (2) evaluation of the effects of that device in a study involving healthy human subjects.

2.2.1 Eddy Current Braking for Functional Resistnace Training

A device was created with the goal of providing resistance across the joint during concentric flexion and extension of the knee. In order to accomplish this, we created a benchtop viscous damping device in the form of an eddy current disc brake, and later adapted it for a commercially available knee brace (T Scope Premier Post-Op Knee Brace, Breg, Grand Prairie, TX). Eddy current brakes convert kinetic energy into electrical currents with the motion of a conductor through a magnetic field. Eddy currents, which are localized circular electric currents within the conductor, slow or stop a moving object by dissipating kinetic energy as heat, thus providing a non-contact dissipative force that is proportional and opposite to the velocity of the movement (Figure 2.1a). Eddy current braking has been widely used in applications such as trains, roller-coasters, and even some exercise equipment (i.e., stationary bikes); however, to the authors' knowledge, it has not been miniaturized and made wearable for rehabilitation purposes.

We selected this method of resistance because it provides a smooth, contact free, and frictionless means of generating loads applied directly to the knee that can further be engineered into a compact and lightweight device.

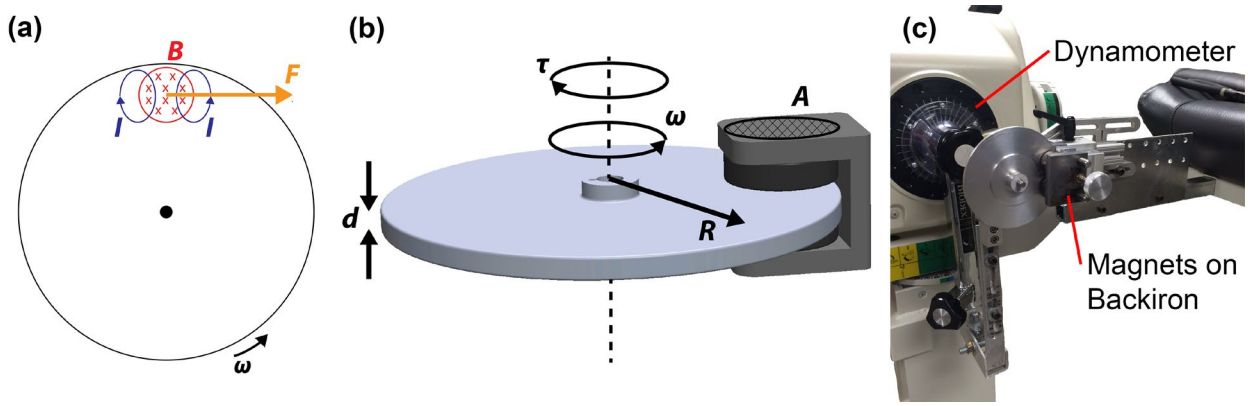

Figure 2.1 (a) Diagram showing the basis of force generation during eddy current braking. As the disc rotates through a magnetic field (*B)* with angular velocity (ω), eddy currents (*I*) form within the disc. In accordance with Lorentz force equation and the right hand rule, the resulting force always opposes the angular velocity. **(b)** Principles that affect the magnitude of the torque experienced during braking based on equation (Equation 2.1). **(c)** Experimental set-up of benchtop testing.

The most widely studied configuration of eddy current braking is that of a rotational disc. Previous research performed over the past several decades has determined many of the parameters that govern the phenomenon (Simeu & Georges, 1996; Wouterse, 1991). This work was elegantly summarized by Gosline and Hayward(Gosline & Hayward, 2008) for eddy current braking as it applies to haptic devices (Equation 2.1).

$$\tau = \sigma * A * d * B^2 * R^2 * \omega$$

Equation 2.1

In this equation, resistive torque τ depends on the conductivity of the disc material $\boldsymbol{\sigma}$, area of the disc exposed to the magnetic field A, the thickness of the disc d, the magnitude of the magnetic field strength B, the effective radius of the disc R, and the angular velocity of the disc rotation ω, as shown in Figure 2.1b. This means that simply changing the area of the aluminum disc exposed to the magnetic field can change the resistive properties of the device.

In the design of our benchtop device, two pairs of permanent magnets (DX08B-N52, KJ Magnetics, Pipersville, Pa) mounted on a ferromagnetic backiron were used to create the magnetic field. Eddy currents were induced within a non-ferrous, 10.16 cm (4 in) diameter aluminum disc (6061 aluminum alloy). Aluminum was chosen as the disc material because it is both lightweight and conductive. The disc was also interchangeable, which allowed us to test the effect of disc thickness (1 mm, 3 mm, and 5 mm) on the resistive torque generated by the device. The device was outfitted with a gearbox (227 g, 2 stage, planetary) (P60, BaneBots, Loveland, CO) with a 26:1 ratio in order to amplify angular velocity of the disc as well as the torque applied to the leg.

The benchtop device was then characterized for its resistive torque profile using an isokinetic dynamometer (System Pro 4, Biodex, Shirley, NY). A custom built jig was used to rigidly attach the device to the input arms of the dynamometer (Figure 2.1c). Care was taken to ensure that the axis of the dynamometer was aligned with the rotational center of the benchtop device. The dynamometer was then programmed to operate in the isokinetic mode, where the input arm rotates at a specified angular velocity (10, 20, 30, and 45 degrees/s), while the resistive torque was logged using the dynamometer's built-in functionality. Between trials, the area of magnetic field exposed to the disc was set to full exposure, half exposure, or no exposure to cover a range of resistive settings possible with the device. We then exchanged the disc for one of a different thickness and repeated the testing. Five trials were performed at each angular velocity and the average was used in further analysis. After characterizing the resistive properties of the device, we tuned the parameters (magnet size, number, etc.) to optimize wearability while maintaining a high resistance. The device was then fitted to an orthopedic knee brace that can fit

across a wide range of patient sizes (5’ to 6’7”).The entire assembly weighed 1.6 kg (Figure 2.2) and cost about $2100 for fabrication (including the brace).

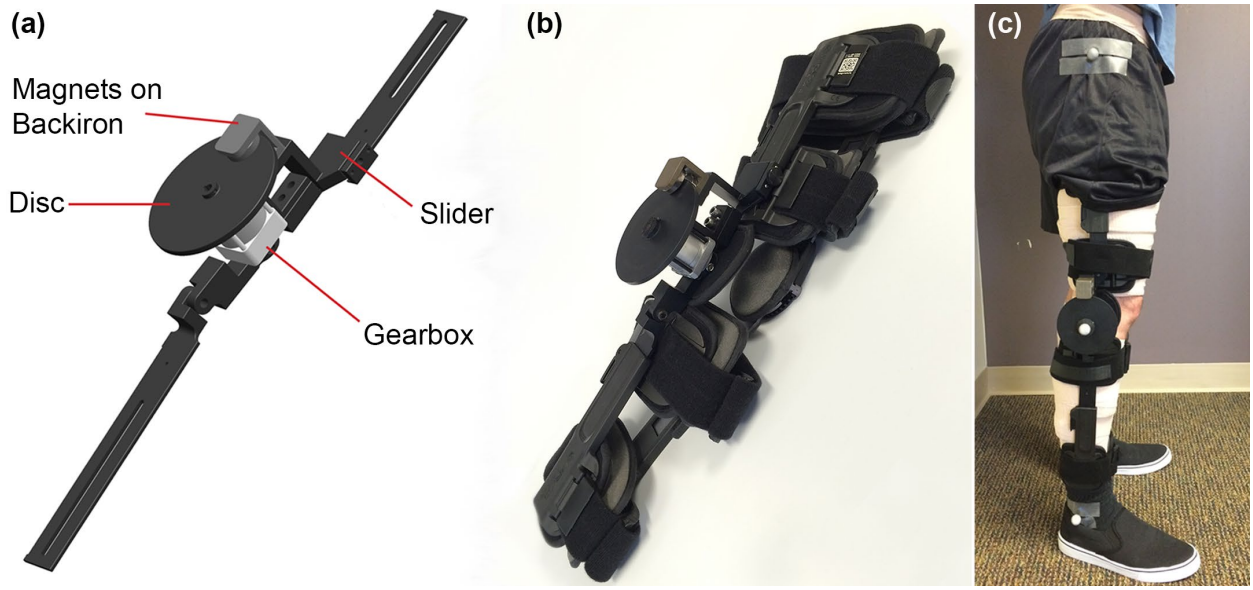

Figure 2.2 (a) Three-dimensional CAD rendering of the eddy current braking device. A slider allows us to change the area of magnetic field exposed to the disc, thus providing a variable torque. **(b)** A close-up view of the actual device showing the details of its attachment to a commercially available adjustable knee brace. **(c)** A subject wearing the device as it was in the experimental setup.

2.2.2 Human Subject Experiment

During phase two, the biomechanical effects of the wearable resistive device were tested on human subjects during a brief walking exercise under various loading conditions. Subjects (n = 7) with no signs of neurological or orthopedic impairment participated in the study. All experiments were carried out in accordance with the University of Michigan Human Subjects Institutional Review Board. Prior to the experiment, three 19 mm diameter retroreflective markers were placed over the subject’s right greater trochanter, lateral femoral epicondyle, and lateral malleolus. Additionally, eight surface electromyographic (EMG) electrodes (Trigno, Delsys, Natick, MA) were placed over the muscle bellies of vastus medialis (VM), rectus femoris (RF), medial hamstring (MH), lateral hamstring (LH), tibialis anterior (TA), medial gastrocnemius (MG), soleus (SO), and gluteus medius (GM) according to the established

guidelines (www.seniam.org) (Krishnan et al., 2013; Ranganathan & Krishnan, 2012). The EMG electrodes were tightly secured to the skin using self-adhesive tapes and cotton elastic bandages. The quality of the EMG signals was visually inspected to ensure that the electrodes were appropriately placed. The participant then performed maximum voluntary contractions (MVCs) of their hip abductors, knee extensors, knee flexors, ankle dorsiflexors, and ankle plantar flexors against a manually imposed resistance (Krishnan et al., 2013). The EMG activities obtained during the maximum contractions were used to normalize the EMG data obtained during walking.

The EMG and kinematic data were collected using custom software written in LabVIEW 2011 (National Instruments Corp., Austin, TX, USA). EMG data were recorded at 1000 Hz, and the kinematic data were recorded at 30 Hz using a real-time tracking system described elsewhere (Krishnan et al., 2015). Briefly, retroreflective markers placed on the hip, knee, and ankle joints were tracked using an image processing algorithm written in LabVIEW Vision Assistant. A three-point model was then created from the hip, knee, and ankle markers to obtain sagittal plane hip and knee kinematics using the following equations (Equation 2.2):

$$\theta_{Hip} = \arctan2\big([x_{knee} - x_{hip}]|[y_{hip} - y_{knee}]\big)$$

$$\theta_{Knee} = (90 - Hip\ Angle) - \big(\arctan2([y_{ankle} - y_{knee}]|[x_{ankle} - x_{knee}])\big)$$

Equation 2.2

Where θ_{Hip} (relative to the vertical trunk) and θ_{Knee} represent the anatomical joint angles, x_{hip}, x_{knee} and x_{ankle} represent the x-coordinates, and y_{hip}, y_{knee} and y_{ankle} represent the y-coordinates of the markers over the respective anatomical landmarks.

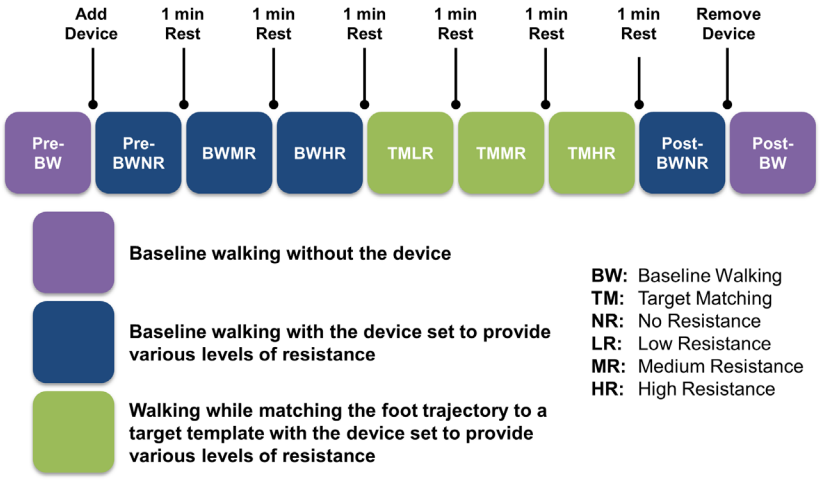

Figure 2.3 Schematic of the experimental protocol.

2.2.3 Experimental Protocol

A schematic of the experimental protocol is given in Figure 2.3. Testing began by having the subject walk on a treadmill (Woodway USA, Waukesha, WI) at 2 mph. A two-minute warm-up period was provided, after which the subject performed a baseline walking trial (pre-BW) for one minute. The subject then wore the resistive brace (with a marker on its joint axis) on their right leg and performed nine walking trials, with each trial lasting one minute. A one-minute rest period was provided between each trial. With the device, the subject first performed one baseline walking with no resistance (pre-BWNR) to characterize the transparency of the device. The subject then performed two more baseline walking trials where the device was set to provide either medium (BWMR) or high resistance (BWHR). Following which, the subject performed three target matching (TM) trials where they viewed the ensemble average of their pre-BWNR foot trajectory on the monitor and attempted to match their foot trajectory with the target. The foot trajectory refers to the x-y position of the lateral malleolus with respect to the subject's greater trochanter in the sagittal plane (Figure 2.4), and was computed using a forward-kinematic model that used hip and knee joint angles and the segment lengths of the thigh and shank (Banala et al., 2009; Krishnan et al., 2013). The target matching trials were performed for two reasons:

(1) matching the template ensured that their hip and knee kinematics were similar to their unresisted baseline walking kinematics and (2) it allowed us to evaluate the feasibility of combining functional resistance training with a motor learning task. During the three target matching trials, the resistance was set to low, medium, or high (corresponding to a quarter, half, and full magnetic exposure to the disc) to study the biomechanical effects of the device over a range of resistance settings. These trials were accordingly named as target matching with low resistance (TMLR), target matching with medium resistance (TMMR), and target matching with high resistance (TMHR). Following the target matching trials, the subject repeated the baseline walking with no resistance (post-BWNR) and baseline walking with no device (post-BW) trials. These trials were performed to see if there were any sustained changes in kinematics (i.e., aftereffects).

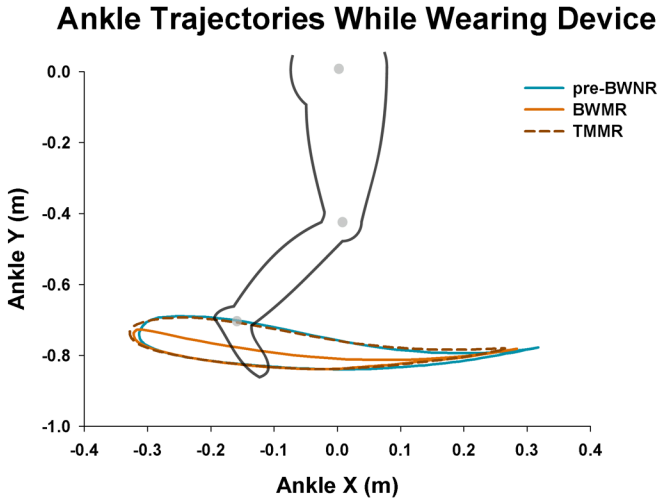

Figure 2.4 Sample ankle trajectories from a participant while walking on the treadmill under different loading conditions. The trajectories are x-y position of the lateral malleolus with respect to the greater trochanter of the hip in the sagittal plane. Ankle trajectories were computed using a forward-kinematic model that used hip and knee joint angles and the segment lengths of the thigh and shank. The leg's position on the plot corresponds to the mid-swing phase of gait. The pre-BWNR refers to baseline walking with no resistance condition prior to the target matching conditions. The BWMR refers to baseline walking with medium resistance condition. Here, the height of the ankle trajectory (i.e., Ankle Y) was observed to reduce due to torque exerted by the device. The TMMR refers to target matching with medium resistance condition. During target matching, the participant viewed their pre-BWNR trajectory on the monitor and attempted to match their foot trajectory with the target. The TMMR trajectory was very similar to that of pre-BWNR, indicating the participant was able to match the target without any difficulty. Note that for clarity purposes, only three conditions are shown in the figure.

2.2.4 Data Analysis

2.2.4.1 Electromyography

The device's effect on muscle activation was evaluated through the changes in EMG amplitude between walking conditions. The recorded raw EMG data were band-pass filtered (20–500 Hz), rectified, and smoothed using a zero phase-lag low-pass Butterworth digital filter (8^{th} order, 6 Hz Cut-off) (Krishnan et al., 2013). The resulting EMG profiles for baseline and target matching conditions were normalized using MVC contractions and ensemble averaged across strides to compute mean EMG profiles during each condition (EMG data of soleus muscle from one subject were excluded from the analysis due to electrode malfunction). Gait events were identified using accelerometer data collected from the Trigno™ EMG sensors. Ensemble averages of the gait cycle were then divided into two bins corresponding to the stance and swing phases of gait, and the average EMG activity was computed during each phase.

2.2.4.2 Kinematics

The kinematic data were ensemble averaged across strides and subjects to compute average profiles for each walking condition. The hip and knee excursions during baseline and target matching trials were calculated for each stride and averaged to determine the effect of resistive walking on sagittal plane kinematics, and to test the feasibility of target tracking during resisted walking. The hip and knee excursions during the first ten strides of the initial and final baseline walking conditions (i.e., pre-BW, pre-BWNR, post-BW, and post-BWNR) was averaged to recognize any short-lived aftereffects following the brief training with the resistive brace. Additionally, the instantaneous angular velocity of the knee joint during the target matching trials was calculated to estimate the resistance felt by the knee throughout the gait cycle.

2.2.4.3 Statistical Analysis

All statistical analyses were performed using SPSS for windows version 22.0 (SPSS Inc., Chicago, IL, USA). Descriptive statistics were computed for each variable and for assessing the results of benchtop testing. Prior to statistical analysis, the EMG data were log transformed ($\log_e$EMG) to minimize skewness and heteroscedasticity (Duschau-Wicke et al., 2010; Krishnan et al., 2013). To examine the effect of the device on subjects' muscle activation and joint kinematics during baseline walking, a linear mixed model analysis of variance (ANOVA) with trial (pre-BWNR, BWLR, BWMR, and BWHR) as a fixed factor and subject as a random factor was performed for each muscle during each time bin (Collins et al., 2015; Duschau-Wicke et al., 2010; West et al., 2014). A significant main effect was followed by post-hoc analyses using paired t-tests with Šídák-Holm correction for multiple comparisons to compare resisted baseline walking trials (i.e., BWMR and BWHR) with the unresisted baseline walking trial (i.e., pre-BWNR). To examine the effect of the device on subjects' muscle activation and joint kinematics during target matching trials, another linear mixed model ANOVA with trial (pre-BWNR, TMLR, TMMR, TMHR) as a fixed factor and subject as a random factor was performed for each muscle during each time bin. A significant main effect was followed by post-hoc analyses using paired t-tests with Šídák-Holm correction for multiple comparisons to compare resisted target matching trials (i.e., TMLR, TMMR, and TMHR) with the unresisted baseline walking trial (i.e., pre-BWNR). In order to evaluate the transparency of the device, paired t-tests were used to compare differences in muscle activation and joint kinematics between baseline walking with no device and baseline walking with no resistance trials (i.e., pre-BW and pre-BWNR). Paired t-tests were also used to compare differences in hip and knee joint excursions during the first ten strides between the pre-baseline and post-baseline walking trials (i.e., pre-BW vs. post-BW and

pre-BWNR vs. post-BWNR) to identify significant aftereffects. A significance level of $\alpha = 0.05$ was used for all statistical analyses.

2.3 Results

2.3.1 Benchtop Testing

The results of bench top testing verified that eddy current braking torque scaled linearly with velocity at the speeds used in this study (Figure 2.5). The resistive torque was also proportional to the area of magnetic field exposed to the disc and the thickness of the disc; however, torque appeared to plateau after 3 mm of disc thickness (Figure 2.5). Additionally, the maximum resistive torque attained using this small, portable form of eddy current braking was substantially large (26.85 N·m at 45 degrees per second using a 5mm thick disc; Figure 2.5). This observation suggested that the benchtop device was capable of generating a peak torque of about 180 N·m during normal gait because the peak angular velocity of the knee during normal gait can exceed 300 degrees per second (Goldberg et al., 2003). This meant that the size and strength of the magnets used in the device, and therefore the weight, could be greatly reduced while still providing sufficient torque for functional resistance training. For this reason, the number of magnetic pairs used for braking was reduced from two to one, while the strength of the magnets was reduced by about half (DX04B-N52, KJ Magnetics, Pipersville, Pa) before fitting the device to the leg brace. The new brake was thus capable of providing about 56 N·m of torque during normal gait.

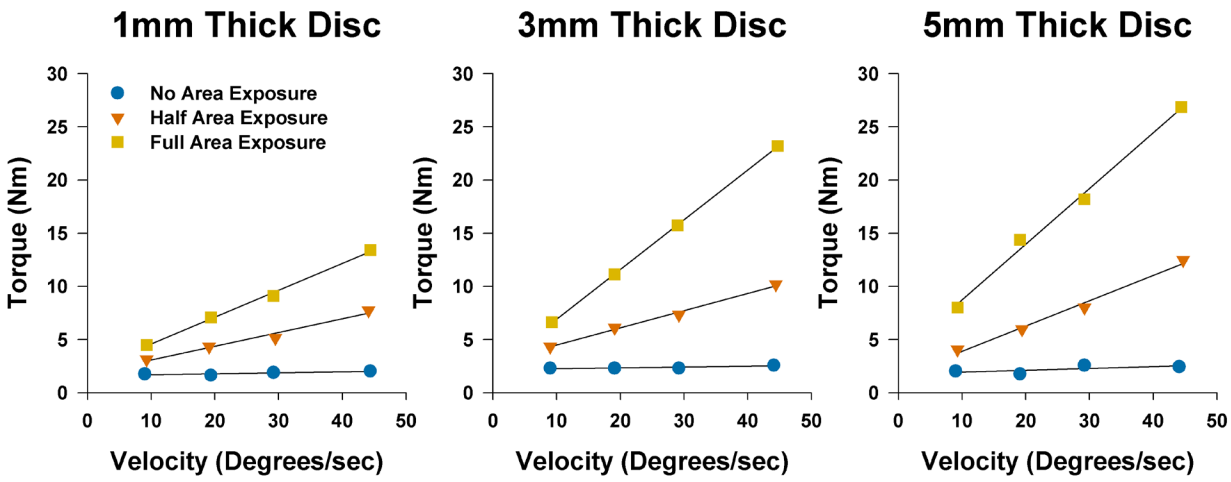

Figure 2.5 Plots showing the results of benchtop testing performed on a Biodex isokinetic dynamometer with the eddy current braking device. The torques generated at various velocities were evaluated for three different discs (1 mm, 3 mm, and 5 mm) at three different exposure levels (no exposure, half exposure, and full exposure). As expected, the resistive torque scaled linearly with the velocity of the disc. The resistive torque was also proportional to the area of magnetic field exposed to the disc. The thickness of the disc also scaled the torque; however, torque appeared to plateau after 3 mm of disc thickness.

2.3.2 Human Subjects Experiment

2.3.2.1 Electromyographic Changes during Baseline Walking

The muscle activation profiles observed during baseline walking trials are summarized in Figure 2.6. There was a significant main effect of trial on EMG activity of vastus medialis [$F(2,12) = 7.823$; $p = 0.007$], medial gastrocnemius [$F(2,12) = 17.696$; $p < 0.001$], and soleus [$F(2,10) = 5.021$; $p = 0.031$] during the *stance phase* of gait. Post-hoc analysis indicated that the EMG activity of vastus medialis was significantly higher during resisted walking than during unresisted walking [BWMR: $p = 0.020$; BWHR: $p = 0.006$]. On the contrary, the medial gastrocnemius and soleus had significantly lower activation during resisted walking [MG BWMR: $p = 0.046$; MG BWHR: $p < 0.001$; SO BWHR: $p = 0.021$]. There was a significant main effect of trial on EMG activity of tibialis anterior [$F(2,12) = 4.026$; $p = 0.046$] and soleus [$F(2,10) = 4.187$; $p = 0.048$] during the *swing phase* of gait. Post-hoc analysis showed a significant increase in soleus activation [BWHR: $p = 0.032$] and a trend towards significantly

higher tibialis anterior activation [BWMR: p = 0.056; BWHR: p = 0.063] during resisted walking.

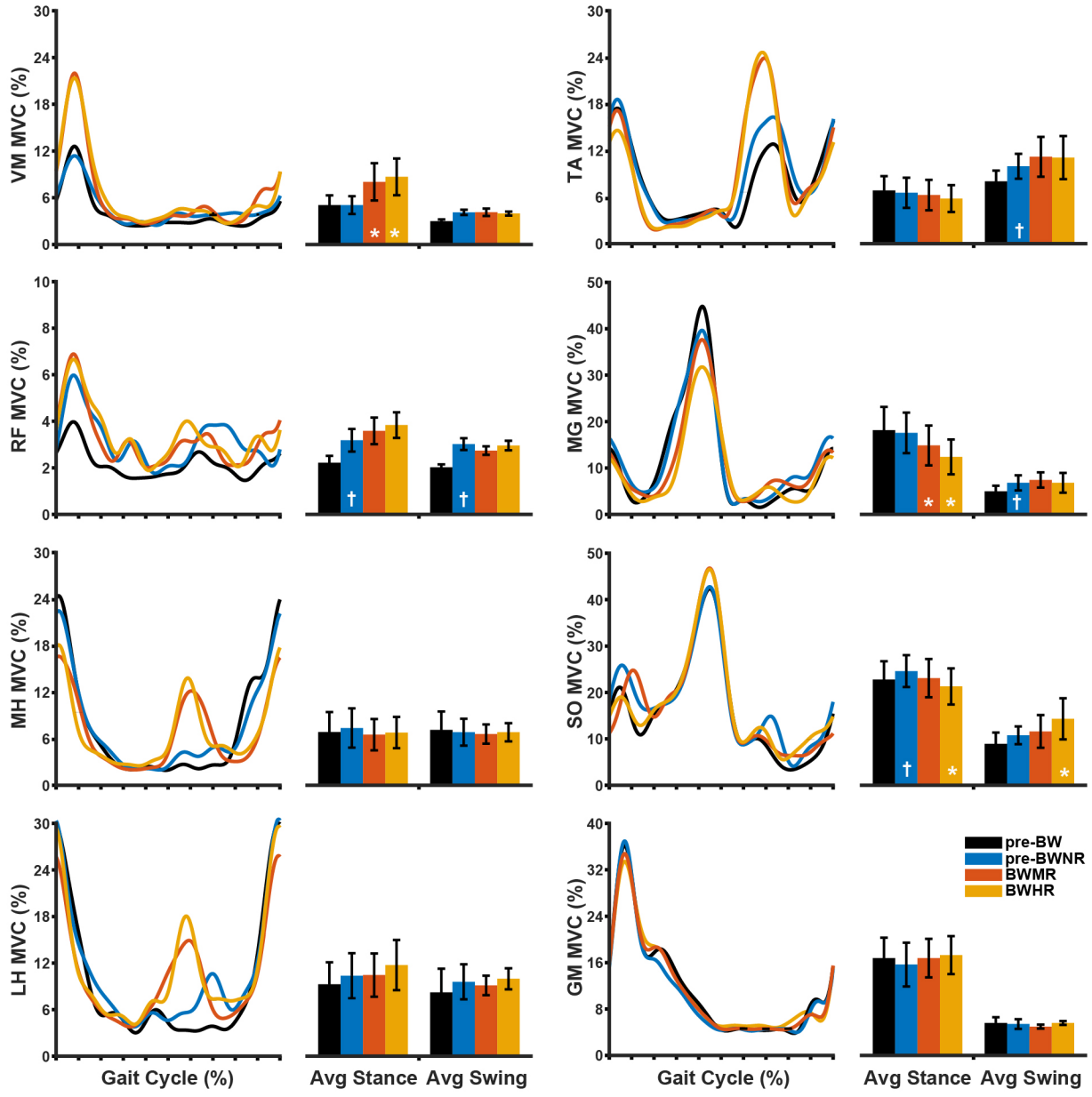

Figure 2.6 Average electromyographic activity of each muscle during the baseline walking conditions. Traces show the mean ensemble averaged activation profiles (across all participants) during each walking condition, while bars show the average activation during the stance and swing phase of each condition. Note that muscle activation increased for many of the muscles tested. Error bars show the standard error of the mean. Daggers indicate significant differences between pre-baseline walking (pre-BW) and pre-baseline walking with no resistance (pre-BWNR) trials, and asterisks indicate significance in comparison with the pre-baseline walking with no resistance (pre-BWNR) trial. BW: baseline walking; BWNR: baseline walking with no resistance; BWMR: baseline walking with medium resistance; BWHR: baseline walking with high resistance; VM: vastus medialis; RF: rectus femoris; MH: medial hamstring; LH: lateral hamstring; TA: tibialis anterior; MG: medial gastrocnemius; SO: soleus; GM: gluteus medius.

2.3.2.2 Kinematic Changes during Baseline Walking

There was a significant main effect of trial on knee joint excursion during baseline walking [$F(2,12) = 96.327$; $p < 0.001$] with the device; however, no changes were observed for the hip joint [$F(2,12) = 0.593$; $p = 0.568$] (Figure 2.7). Post-hoc analysis showed a significant reduction in knee joint excursion during resisted walking than during unresisted walking [BWMR: $-28.6 \pm 8.0°$, $p < 0.001$; BWHR: $-37.1 \pm 8.3°$, $p < 0.001$].

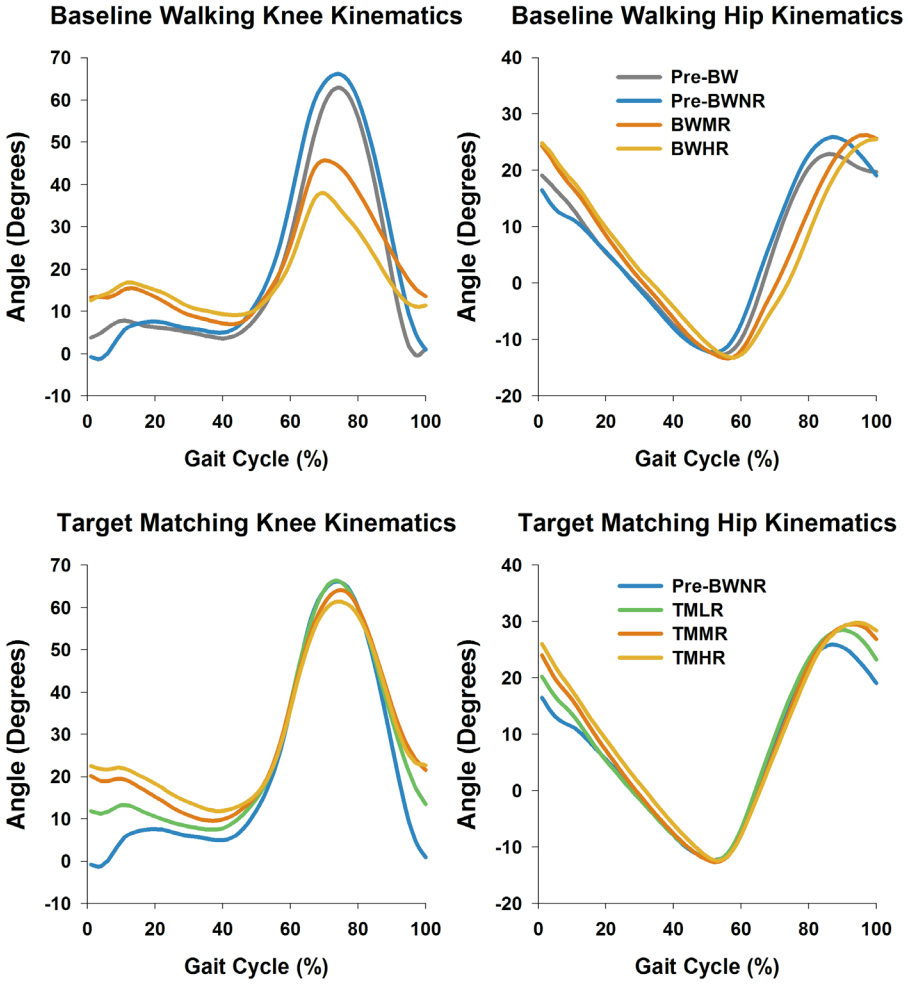

Figure 2.7 Average kinematic data of the hip and knee joints during baseline walking conditions (top) and target matching conditions (bottom). Traces show the mean ensemble averaged joint angles (across all participants) during each walking condition. Note that knee flexion was greatly decreased during resisted baseline walking, but approached the level of baseline walking without resistance when subjects were given a target matching task. BW: baseline walking; BWNR: baseline walking with no resistance; BWMR: baseline walking with medium resistance; BWHR: baseline walking with high resistance; TMLR: target matching with low resistance; TMMR: target matching with medium resistance; TMHR: target matching with high resistance.

2.3.2.3 Electromyographic Changes during Target Matching

The muscle activation profiles observed during target matching trials are summarized in Figure 2.8. There was a significant main effect of trial on EMG activity of vastus medialis [$F(3,18) = 14.086$; $p < 0.001$], rectus femoris [$F(3,18) = 6.672$; $p = 0.003$], medial hamstring [$F(3,18) = 4.034$; $p = 0.023$], lateral hamstring [$F(3,18) = 7.268$; $p = 0.002$] and gluteus maximus [$F(3,18) = 6.619$; $p = 0.003$] during the *stance phase* of gait. Post-hoc analysis indicated that the EMG activity was significantly greater during resisted target matching trials for the vastus medialis [TMMR: $p < 0.001$; TMHR: $p < 0.001$], rectus femoris [TMMR: $p = 0.016$; TMHR: $p = 0.006$], lateral hamstring [TMHR: $p = 0.011$], and gluteus medius [TMMR: $p = 0.028$; TMHR: $p = 0.005$] muscles. There was a significant main effect of trial on EMG activity of all the muscles during the *swing phase* of gait [$F(3,18) = 4.871$ to 27.519; $p = 0.015$ to $p < 0.001$]. Post-hoc analysis indicated the EMG activity was significantly greater during resisted target matching trials when compared with the unresisted baseline walking for all the muscles tested [$p = 0.036$ to $p < 0.001$; Figure 2.8].

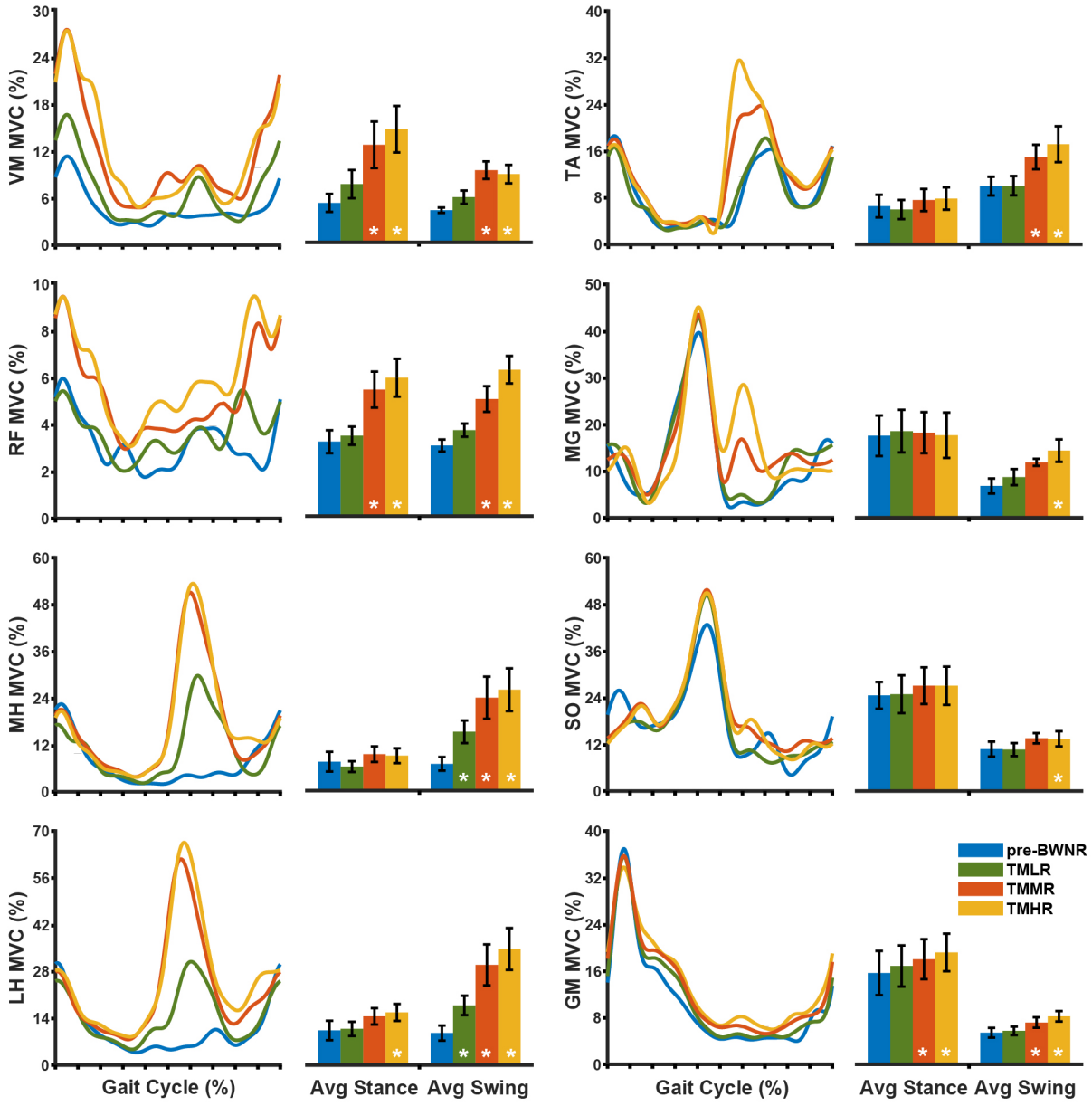

Figure 2.8 Average electromyographic activity of each muscle during the target matching conditions. Traces show the mean ensemble averaged activation profiles (across all participants) during each walking condition, while bars show the average activation during the stance and swing phase of each condition. Note that muscle activation increased several folds for many of the muscles during both stance and swing phase of the gait. Error bars show the standard error of the mean and asterisks indicate significance in comparison with the pre-baseline walking with no resistance (pre-BWNR) trial. BWNR: baseline walking no resistance; TMLR: target matching with low resistance; TMMR: target matching with medium resistance; TMHR: target matching with high resistance; VM: vastus medialis; RF: rectus femoris; MH: medial hamstring; LH: lateral hamstring; TA: tibialis anterior; MG: medial gastrocnemius; SO: soleus; GM: gluteus medius.

2.3.2.4 Kinematic Changes during Target Matching

There was a significant main effect of trial on hip [$F(3,18) = 6.907$; $p = 0.003$] and knee joint excursions [$F(3,18) = 23.420$; $p < 0.001$] during resisted target matching (Figure 2.7). Post-

hoc analysis showed that the hip joint excursions were greater during the target matching trials (TMMR: 4.5 ± 3.7°, p = 0.003; TMHR: 4.5 ± 3.1°, p = 0.002), but the knee joint excursions were smaller (TMLR: −7.8 ± 5.1°, p = 0.004; TMMR: −12.0 ± 7.2°, p < 0.001; TMHR: −16.4 ± 4.9°, p < 0.001) during the target matching trials when compared with baseline walking with no resistance.

2.3.2.5 Transparency of the Device during Baseline Walking

The EMG profiles observed during baseline walking with no resistance were relatively similar to those observed during baseline walking without the device (Figure 2.6). However, paired t-tests indicated small, but significantly greater activation of the rectus femoris (0.96 ± 1.03%; p = 0.035) and soleus (1.87 ± 1.76%; p = 0.030) muscles during the *stance phase*, and of the rectus femoris (1.0 ± 1.24%; p = 0.038), tibialis anterior (1.95 ± 1.94%; p = 0.017), and gastrocnemius (1.83 ± 3.64%; p = 0.029) muscles during the *swing phase* of the gait. There were no differences in hip (36.2 ± 2.8° and 39.1 ± 4.9°; p = 0.15) or knee (65.0 ± 2.5° and 69.6 ± 8.7°; p = 0.08) joint excursions during baseline walking and baseline walking with no resistance trials.

2.3.2.6 Kinematic Aftereffects of Resisted Target Matching

A brief period of training with the device resulted in significant increases in knee joint excursions during baseline walking with no device (4.2 ± 2.6°; p = 0.005) and baseline walking with no resistance trials (5.4 ± 4.7°; p = 0.023) (Figure 2.9a). Training also resulted in a significant increase in hip joint excursion during the baseline walking with no resistance trial (2.6 ± 1.6°; p = 0.005); however, no differences were observed in the baseline walking trial (−0.1 ± 1.4°; p = 0.825) (Figure 2.9b).

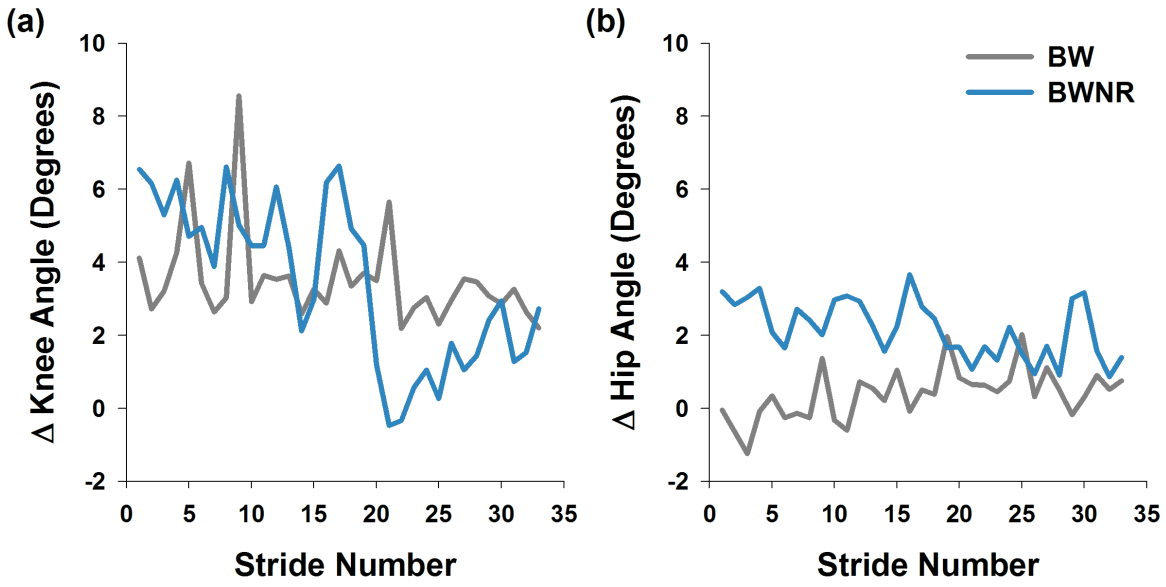

Figure 2.9 Plots showing changes in **(a)** knee joint and **(b)** hip joint excursions following a brief period (4 minutes) of training with the resistive brace. Note that hip and knee excursions increased after training; however, these aftereffects appear to be short-lived and reduced over time. BW: baseline walking; BWNR: baseline walking with no resistance.

2.4 Discussion

The aim of this study was to develop a wearable device that is capable of providing resistance across the knee joint for functional resistance training of gait. We found that eddy current braking is a feasible option for this application, as our benchtop testing indicated that it can generate the torque required for functional resistance training at a relatively small size and weight. Additionally, with the incorporation of a linear slider, we were able to obtain an adjustable resistance that can be regulated based on a subject's impairment level and functional capacity. The results from the human subjects experiment also indicated that the device was largely transparent, as there were minimal alterations in hip/knee kinematics (3° to 5°) and lower extremity muscle activation (< 2% MVC). However, once the resistance was added, knee excursions reduced substantially. This was expected because the nervous system is known to optimize metabolic and movement related costs during walking or reaching movements (Bertram, 2005; Ranganathan et al., 2013). Interestingly, despite the reduction in knee joint

excursions during resisted baseline walking, muscle activation still increased in some of the muscles. More importantly, when subjects performed target tracking to minimize kinematic slacking (i.e., a phenomenon where the motor system reduces muscle activation levels and movement excursions to minimize metabolic and movement related costs (Marchal-Crespo & Reinkensmeyer, 2009; Reinkensmeyer et al., 2009)) during resisted walking, the EMG activation increased several-fold in many of the muscles used in gait. Further, the aftereffects observed in hip and knee kinematics after a brief period of resisted target matching suggest that the device may have meaningful clinical potential, albeit further research is required to verify this premise.

The eddy current braking device is unique because it provides bidirectional resistance across the knee joint–as opposed to the endpoint–of the subject's leg. Accordingly, muscle activation during target matching scaled largest around the knee joint. Interestingly, we also found that providing a resistance across the knee elicited increased activity of muscles spanning the hip and the ankle joints. These findings are consistent with previous studies (Krishnan et al., 2013) and suggest that performing a motor learning task with the proposed device requires coordinated inputs from multiple muscles in the lower limb. The increased activation of the non-targeted muscles is potentially due to the synergistic and-or biarticular nature of some of the leg muscles (e.g. medial gastrocnemius), and recruitment of these muscles may have assisted in the process of overcoming the applied resistance (Clark et al., 2010; Krishnan et al., 2013).

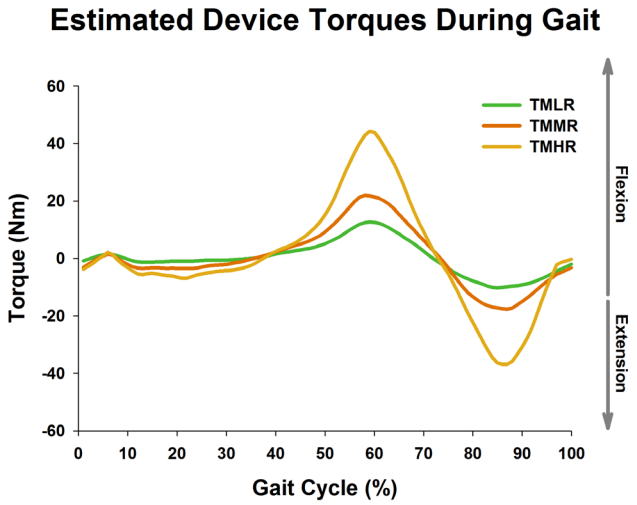

Figure 2.10 Data showing resistive torques applied by the device throughout the gait cycle during target matching. Resistive torques were estimated using the velocity profiles calculated from the kinematic data. TMLR: target matching with low resistance; TMMR: target matching with medium resistance; TMHR: target matching with high resistance.

The eddy current brake in this study produced large resistive forces when compared to other wearable devices (Sulzer et al., 2009). The estimated resistive torques during the target matching trials ranged between 10 to 45 N·m (Figure 2.10), which are quite large considering the weight of the device. Also, changes in EMG activation were larger in comparison to those observed during walking with a 4 or 8 kg weight attached to the foot (Browning et al., 2007). These results suggest that eddy current braking is a suitable alternative to loading the lower limb muscles during walking. However, it is important to note that subjects reduced their joint excursions during resisted walking. As a result, the changes in muscle activation were subtle during simple resisted walking (i.e., baseline resisted walking): with some muscles showing lower activation. Incorporating a target tracking task effectively minimized the kinematic slacking observed during resisted baseline walking. Further, muscle activation increased several-fold during target tracking trials. These findings emphasize the importance of kinematic feedback during functional resistance training, and failure to address kinematic slacking could reduce the effectiveness of functional resistance training and promote compensatory movements. The kinematic feedback could also assist in minimizing off-plane motions (e.g., increased hip

abduction/adduction) because the device in itself does not constrain those movements. In our experience, the device-induced off-plane motions were minimal (< 1°) in healthy subjects; however, certain patient populations (e.g., stroke) may behave differently due to abnormal synergistic coupling of motions across joints (Krishnan & Dhaher, 2012).

While testing the clinical benefits of this device was not the focus of this study, the proposed device may have value in physical rehabilitation. Past research indicates that an ideal rehabilitation device should (1) encourage activities specific to daily living, (2) be able to be taken home, (3) have adjustable resistance to meet client needs, (4) have the potential to provide biofeedback to the clients, and (5) cost under $6000 (Lu et al., 2011). The device in this study meets all these clinical guidelines. Additionally, functional resistance training with this device is advantageous because it is not confined to treadmill training. Instead, training can take place over-ground, where the behavior is more specific to tasks encountered during daily living. Appropriate feedback can be administered during over-ground walking in the form of instructor/auditory feedback (Duncan et al., 2007; Zanotto et al., 2013), obstacle training (Duncan et al., 2007), or even kinematic tracking using inertial measurement units (Rebula et al., 2013). Given that the device is lightweight and portable, it could also be taken home to greatly amplify the dosage of therapy outside the clinical setting or in remote areas where rehabilitative care is not readily available. The device is also inherently safe because eddy current brakes are passive actuators that dissipate energy, as opposed to active motors that add energy to the system–with an active device, if there is a malfunction or error in the controls, unexpected motions could bring serious injuries to the user. Further, the clinical relevance of the device may extend outside of therapy for neurological injury. For example, because thigh muscle strength is critical for adequate lower limb function and quality of life (Christiansen et al., 2013; Decker et

al., 2004; Palmieri-Smith & Lepley, 2015; Shelburne et al., 2005), we believe that the device could be beneficial for many subjects recovering from serious knee injuries, such as anterior cruciate ligament injury or repair, where thigh muscle strength deficits are profound (Lepley, 2015).

There were many design challenges faced while creating the device. Eddy current braking is capable of providing large levels of resistance, but these are generally coupled with high inertias (Gosline & Hayward, 2008). This limits the transparency of the device, as the resistive torque is dependent on the thickness, radius, and angular velocity of the disc, all of which increase rotational inertia. For this reason, we used a cable capstan coupling in our initial prototypes, as it allowed for a compact design with zero backlash during torque transmission, which provided a smoother feel to the user. However, the cable capstan was unable to withstand repeated wear. A planetary gearbox not only solved this issue, but also made the device modular (i.e., the gear ratios can be changed if necessary). However, we found that the set screws were prone to back off the gear shaft during repetitive loading. Adding an additional key on the gearing shaft and a through pin to the rotating shaft resolved this issue and kept the interfaces rigid without slipping. Further, by making the protruding arms of the device identical to those of the brace, the device fit seamlessly into the commercial leg brace. This proved to be a better option than superposing the device onto the brace, as it left the adjustability intact and reduced weight.

Further improvements are possible for better utilization of the device. The resistance setting of the current device is manually controlled using a linear slider. In the future, simple extensions to the design could be used to realize a computer-controlled resistance, with resistance programmed to be a function of time, gait kinematics, or muscle activations. For

example, a small motor in conjunction with microprocessor control could be added to modulate the area of the magnet exposed on the aluminum disc. Besides keeping the device passive (as the motors would not directly act on the subject's leg), it would also enable the therapist to modulate the resistance levels dynamically based on a subject's rehabilitation needs. Moreover, bidirectional resistance may not be appropriate for all patient groups, such as those that have muscle imbalances across a joint. The addition of computer control or even a simple ratcheting mechanism, where the disc could be engaged and disengaged based on the direction of the movement, would enable the device to provide unidirectional resistance. This would allow the device to resist the weak agonist while not loading the stronger antagonist.

A key limitation is that some of the kinematic changes observed may have been due to marker movements and kinematic model (vertical pelvis/trunk) used in this study. However, prior research indicates that sagittal plane motions are less affected due to marker movements and sagittal plane pelvic motions are minimal (<2°) during normal gait (Benoit et al., 2006; Castelli et al., 2015). Thus, we believe that the changes observed in this study are much larger than the anticipated errors due to marker movements and kinematic model. Future research should consider incorporating a better kinematic model and 3D camera system to elucidate fully the biomechanical effects of the device on the wearer, particularly when testing patient population.

In summary, we fabricated a lightweight yet high torque eddy current brake and packaged it into a commercially available knee brace to create a wearable device that is capable of providing resistance across the knee joint for functional resistance training. We also showed that the device increased muscle activation in many of the key muscles used in gait. Further, we demonstrated that a brief period of training with the resistive device induced positive kinematic

aftereffects in both the hip and knee joints. These results demonstrate that the resistive device described in this study is a feasible and promising approach to actively engage and strengthen the key muscles used in gait. However, further testing in an injured population is warranted to determine the therapeutic benefits (e.g., strength, coordination, and neural plasticity) that could emerge from this unique application of functional resistance training.

2.5 Acknowledgement

This work has been published in the Annals of Biomedical Engineering (Washabaugh et al., 2016). I would like to thank my co-authors on this article: Dr. R. Brent Gillespie, Dr. Ted Claflin, and Dr. Chandramlouli Krishnan for their contributions to the design of the device and experiments and editing of the manuscript. Research reported in this publication was supported by (1) National Institute of Biomedical Imaging and Bioengineering (NIBIB) of the National Institutes of Health (Grant# R01EB019834), (2) Fostering Innovation Grants, and (3) University of Michigan Office of Research Grant. The content is solely the responsibility of the authors and does not necessarily represent the official views of the National Institutes of Health. A Special thanks to Stephanie Prout, Elizabeth Mays, and Sarah Abdulhamid—the senior design group formerly known as team Promovi—for their work in creating preliminary versions of the device. Since the publication of this paper, this device has been patented (Title: Resistive device employing eddy current braking, Patent No: US20200061404A1).

Chapter 3

A Wearable Resistive Robot Facilitates Locomotor Adaptations in Individuals with Stroke

Abstract

Background: Resisted treadmill walking is a form of task-specific training that has been used to improve gait function in individuals with neurological injury, such as stroke, spinal cord injury, or cerebral palsy. Traditionally, these devices use active elements (e.g., motors or actuators) to provide resistance during walking, making them bulky, expensive, and less suitable for overground or in-home rehabilitation. We recently developed a low-cost, wearable brace that generates resistive torques across the knee joint using a simple magnetic brake. However, the possible effects of training with this device on gait function in a clinical population are currently unknown. *Objective:* The purpose of this study was to test the acute effects of resisted walking with this device on kinematics, muscle activation patterns, and gait velocity in chronic stroke survivors. *Methods:* Six stroke survivors wore the resistive brace and walked on a treadmill for 20 minutes (4 × 5 minutes) at their self-selected walking speed while simultaneously performing a foot trajectory-tracking task to minimize stiff-knee gait. Electromyography, sagittal plane gait kinematics, and overground gait velocity were collected to evaluate the acute effects of the device on gait function. *Results:* Resisted treadmill training resulted in a significant increase in quadriceps and hamstring EMG activity during walking. Significant aftereffects (i.e., improved joint excursions) were also observed on the hip and knee kinematics, which persisted for several steps after training. More importantly, training resulted in significant improvements in

overground gait velocity. These results were consistent in all the subjects tested. *Conclusion:* This study provides preliminary evidence indicating that resisted treadmill walking using our knee brace can result in meaningful biomechanical aftereffects that translate to overground walking.

3.1 Introduction

Individuals with stroke often experience significant walking dysfunction that limits their ability to safely and effectively ambulate in the community (Michael et al., 2005). Indeed, current evidence indicates that reduced gait speed is a significant predictor of falls and mobility outcomes after stroke (Michael et al., 2005; Ng et al., 2017). Thus, regaining locomotor function is a major goal of post-stroke rehabilitation (Teasell et al., 2003), and therapists often place a considerable amount of time and effort in restoring gait function after stroke.

Treadmill training and progressive resistance training are the two most commonly used techniques to improve locomotor function after stroke (Leon et al., 2017; Manella & Field-Fote, 2013; Pak & Patten, 2008; Polese et al., 2013; Seo et al., 2017; Visintin et al., 1998). These interventions have demonstrated improvements in gait performance, although outcomes are known to vary between studies, particularly for resistance training (Lamberti et al., 2017; Lund et al., 2017; Mehta et al., 2012; Nadeau et al., 2013; Park et al., 2015; Vahlberg et al., 2017). It is to be noted that resistance training is typically performed in a "nonfunctional" manner (e.g., exercises performed in seated or standing positions); whereas, it is known that training should be functional (i.e., specific to the task being targeted) to address sensorimotor deficits during functional tasks, such as walking because of practice specificity (Barnett et al., 1973; Dobkin, 2004; El Amki et al., 2017; Henry, 1968; Kleim & Jones, 2008; Manini et al., 2007; Proteau et al., 1992; Schmidt & Lee, 1988; Takahashi et al., 2008; Williams et al., 2014). Further, such

training of isolated muscle groups (without any functional context) does not facilitate the synchronized activation of multiple muscles (i.e., coordination), which is critical for gait recovery after stroke. Thus, interventions that collectively address strength and coordination deficits during walking could be beneficial for improving gait function after stroke.

Task-specific loading of the limbs—termed as functional resistance training or functional strength training—combines elements of resistance training and task-specific training for gait rehabilitation. Here, resistance is applied to the subject's limb during walking such that multiple muscles are engaged in a coordinated fashion (Gama et al., 2018; Washabaugh et al., 2016). A number of studies have evaluated the benefits of functional resistance training in healthy as well as neurologically impaired individuals. These studies collectively demonstrate that functional resistance training can (1) improve metabolic rate, (2) increase lower-extremity muscle activation, joint power, and kinematics, and (3) improve skilled overground walking performance (e.g., gait speed, endurance, balance, symmetry, etc.) (Browning et al., 2007; Duclos et al., 2014; Houldin et al., 2011; Klarner et al., 2013; Lam et al., 2015; Lam et al., 2011; Wu, Kim, et al., 2014; Wu, Landry, et al., 2014; Wu et al., 2012; Wu, Landry, et al., 2011; Yen et al., 2012). However, functional resistance training is often performed using devices with active elements, such as motors or actuators, to control the resistive forces/torques, which makes them bulky, expensive, and less suitable for overground or in-home rehabilitation. Further, these training methods typically do not incorporate any kinematic feedback during resisted walking, which is critical to incentivize participants to increase effort and maintain optimal spatiotemporal coordination.

To address these issues, we recently developed a low-cost, wearable knee brace that is capable of producing scalable resistive torques using a simple magnetic brake (Washabaugh et

al., 2016), and tested the biomechanical effects of this device on healthy, unimpaired individuals during treadmill walking. The training also incorporated a foot trajectory-tracking paradigm to ensure that subjects maintained appropriate hip/knee kinematics during resisted walking. The results of this study demonstrated that resisted walking significantly increased muscle activation of the lower-extremity muscles and induced kinematic aftereffects once the resistance was removed. However, the possible effects of training with this device on gait function in a clinical population—which is critical to understand the clinical potential of this device—are currently unknown. Therefore, this study tested the acute effects of resisted treadmill walking on quadriceps and hamstring muscle activation patterns, sagittal hip/knee kinematics, and overground gait velocity in chronic stroke survivors. We hypothesized that resisted treadmill walking will significantly increase muscle activation, hip and knee excursion, and gait velocity: these hypotheses were based on our prior experience with healthy adults (Washabaugh et al., 2016) and on existing literature in neurologically impaired individuals (Lam et al., 2011; Wu et al., 2012; Yen et al., 2012).

3.2 Materials and Methods

3.2.1 Participants

Six (3 males and 3 females) chronic stroke survivors (Age: 58.0 ± 8.5 years, Height: 1.70 ± 0.14 m, Weight: 76.0 ± 23.6 Kg, Time since stroke onset: 3.0 ± 2.7 years, Lower-extremity Fugl-Meyer score: 27.8 ± 6.2 [maximum possible = 34]) participated in this research study. Stroke subjects were included in this study if they 1) were between 18 and 75 years of age, 2) had a unilateral stroke at least 6 months prior to participation, 3) had a cortical or sub-cortical lesion that was documented by radiological (CT or MRI) or clinical findings, 4) were community ambulators and indicated that they can walk at least 20 minutes on a treadmill, and 5) had some

ability to bend their hip and knee. Exclusion criteria included: 1) a history of a recent lower-extremity injury, fracture, or surgery, 2) uncontrolled diabetes or hypertension, 3) Mini-Mental State Exam score < 22, and 4) a history of unstable or untreated cardiovascular diseases. All subjects provided written informed consent to participate in the study using a form that was approved by the University of Michigan Institutional Review Board.

3.2.2 Wearable Brace

Functional resistance training was performed using a resistive brace that was engineered with an eddy current brake. An in depth description of this device can be found in the previous chapter (Chapter 2). Briefly, eddy current brakes are non-contact brakes that utilize the motion of a conductive material through a magnetic field (an act that creates eddy currents within the conductive material) to generate dissipative resistance to that motion. The magnitude of the resistive torques generated by an eddy current disk brake (as used in this device) is governed by: $\tau = \sigma \times A \times d \times B^2 \times R^2 \times \omega$ (Gosline & Hayward, 2008). In this equation, the resistive torque τ depends on the conductivity of the disc material σ, area of the disc exposed to the magnetic field A, the thickness of the disc d, the magnitude of the magnetic field strength B, the effective radius of the disc R, and the angular velocity of the disc rotation ω (Figure 3.1a). Hence, magnitude of the resistance can be augmented by altering the area of the magnetic field exposed to the disk (i.e. greater magnetic exposure will result in greater resistive torques).

The eddy current brake of our device consists of two permanent magnets (DX04B-N52, KJ Magnetics, Pipersville, Pa) mounted on a ferromagnetic backiron, a planetary gearbox (P60, Banebots, Loveland, CO), and an aluminum disc (0.5 cm thickness, 10.16 cm diameter). The magnets and backiron are fixed to a linear slider, which allows us to control the magnitude of the resistance (Figure 3.1b). To properly convey the resistive torques to the user, the brake interfaces

with a commercially available knee brace (Figure 3.1c) (T Scope Premier Post-Op Knee Brace, Breg, Grand Prairie, TX). When this brace is worn, flexion or extension of the knee spins the aluminum disc and generates resistive torque to oppose this motion (via eddy currents) based on how the magnets are exposed to the disk.

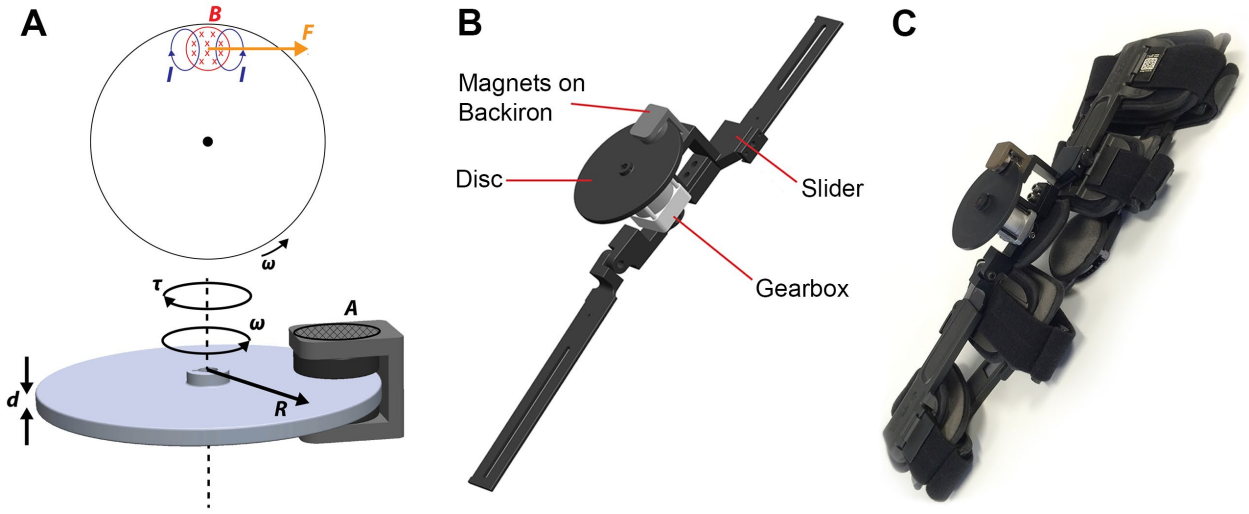

Figure 3.1 (a) Schematic showing the basis of resistive torque generation in an eddy current brake. As the disc rotates through a magnetic field (B) with angular velocity (ω), eddy currents (I) form within the disc. This results in a resistive force that always opposes the angular velocity. The resulting resistance τ is also dependent on the conductivity of the disc material σ, area of the disc exposed to the magnetic field A, the thickness of the disc d, the magnitude of the magnetic field strength B, the effective radius of the disc R, and the angular velocity of the disc rotation ω **(b)** Computer-aided design rendering of the eddy current brake. **(c)** A close-up view of the knee brace embedded with eddy current brake.

3.2.3 Experimental Protocol

The schematic of the experimental protocol is provided in Figure 3.2. Prior to the experiment, three 19 mm diameter retroreflective markers were placed over the subject's hip, knee, and ankle joints. Additionally, eight surface electromyographic (EMG) electrodes (Trigno, Delsys, Natick, MA) were placed over the muscle bellies of the vastus medialis (VM), rectus femoris (RF), medial hamstring (MH), and lateral hamstring (LH) according to the established guidelines (www.seniam.org) (Ranganathan & Krishnan, 2012; Ranganathan et al., 2016). The EMG electrodes were tightly secured to the skin using self-adhesive tapes and cotton elastic bandages. The quality of the EMG signals was visually inspected to ensure that the electrodes

were appropriately placed. After which, two inertial measurement units (IMUs) (Opal sensors, APDM, Inc., Portland, OR) were secured to the dorsum of both feet, which were used to minimize bias and objectively measure the overground gait speed of the subject prior to and after training. We chose to place the IMUs on the feet as opposed to ankle, as prior research has indicated that foot configuration is more accurate for measuring gait velocity (Washabaugh et al., 2017). The subject then performed two 3-second maximum voluntary contractions (MVCs) of their knee extensors and flexors in a seated position against a manually imposed resistance (Krishnan et al., 2013; Washabaugh et al., 2016). The peak EMG activities (i.e., the maximum of the two trials) obtained during the maximum contractions were used to normalize the EMG data obtained during walking.

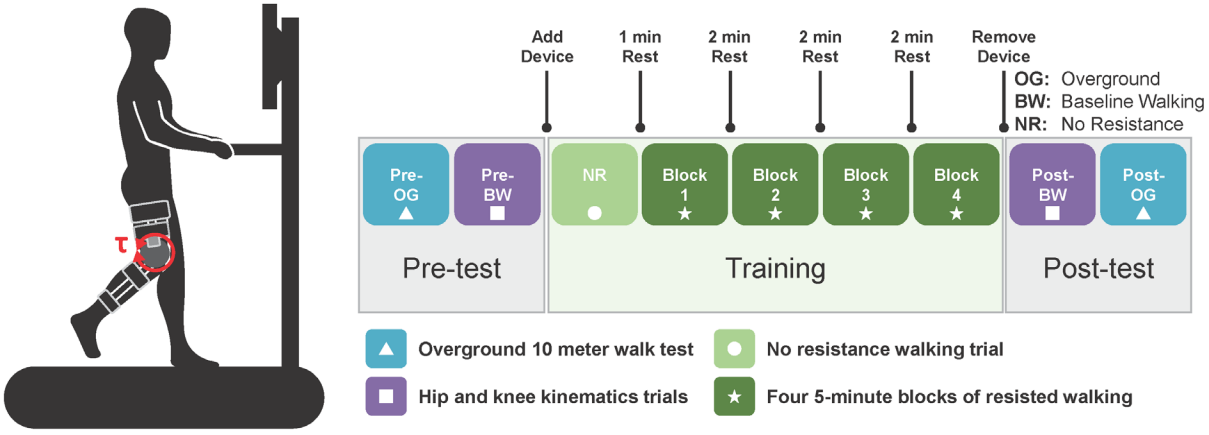

Figure 3.2 Schematic of the experimental protocol.

The experiment consisted of three phases: (1) pre-test phase, (2) training phase, and (3) post-test phase. During the *pre-test phase*, the subject's baseline overground walking speed and hip and knee gait kinematics were established. The 10-m walk test (10MWT) was used to evaluate the baseline walking speed. The 10MWT is a psychometrically robust measure of walking and mobility (Lin et al., 2010), and has excellent test-retest reliability (ICC > 0.9) (Lewek & Randall, 2011; Washabaugh et al., 2017). The subject performed three trials of the

10MWT at their self-selected pace and the average of the three trials was used in the analysis. The subject then walked on a motorized treadmill (Woodway USA, Waukesha, WI) with their hands placed over a custom-built treadmill rail system. After a 2-minute warm-up period, baseline kinematic data were recorded for one minute.

During the *training phase*, the subject first wore the resistive brace and walked over the treadmill at their comfortable walking speed without any resistance (no resistance – NR) for one minute. After which, the resistive properties of the device were adjusted based on the subject's self-reported ability and comfort level—i.e., resistance was set as the maximum comfortable resistance that the subject could walk with for the duration of the 5-minute block and was adjusted based on their feedback (forces on average were ~12% of their body-weight) (Wu et al., 2012; Yen et al., 2012). The subject then performed four 5-minute blocks of resisted walking while simultaneously attempting to match their foot trajectory to a template foot trajectory that was projected on a computer monitor placed in front of them for visual feedback. The template was created by scaling (10%-30% based on their ability) the ensemble average of their baseline hip/knee kinematics. This was performed to minimize stiff-knee gait and ensure that the subject was bending their hip and knee adequately during resisted walking (Krishnan et al., 2013; Washabaugh et al., 2016). Our previous research has shown that this type of training is effective in engaging the hamstring muscles (Washabaugh et al., 2016) and promotes locomotor recovery after stroke (Krishnan et al., 2012). The foot trajectory refers to the *x*–*y* position (X_a and $\boldsymbol{Y_a}$) of lateral malleolus with respect to the subject's greater trochanter in the sagittal plane, and was computed using a forward-kinematic model (Equation 3.1) that used hip (Θ_h) and knee (Θ_k) joint angles and the segment lengths of the thigh (l_1) and shank (l_2) (Krishnan et al., 2015; Saner et al., 2017).

$$\begin{bmatrix} X_a \\ Y_a \end{bmatrix} = \begin{bmatrix} sin\Theta_h & -\sin(\Theta_k - \Theta_h) \\ -cos\Theta_h & -\cos(\Theta_k - \Theta_h) \end{bmatrix} \begin{bmatrix} l_1 \\ l_2 \end{bmatrix}$$

Equation 3.1

During the *post-test phase*, the brace was removed and the subject's overground walking speed and hip and knee gait kinematics were recorded again in an identical fashion to those during the *pre-test phase*.

3.2.4 Data Analysis

The device's effect on muscle activation patterns was evaluated using the EMG data collected during treadmill walking with and without resistance. The raw EMG data were band-pass filtered (20–500 Hz), rectified, and smoothed using a zero phase-lag low-pass Butterworth digital filter (8th order, 6 Hz Cut-off) (Krishnan et al., 2013). The resulting EMG profiles were normalized to MVC data and ensemble averaged across strides using gait events generated from the accelerometer of the Trigno EMG sensors. The ensemble averaged EMG data were then divided into two bins corresponding to the stance and swing phases of gait, and the peak EMG activity was computed during each phase. The device's effect on Locomotor adaptations and aftereffects to resistance during walking was evaluated by comparing the changes in hip/knee kinematics (first 30 strides) and overground walking speed before and after the training.

3.2.5 Statistical Analysis

All statistical analyses were performed using SPSS for windows version 22.0 (SPSS Inc., Chicago, IL, USA). Wilcoxon signed-rank test was used to examine the effect of the device on subjects' muscle activation during the stance and swing phases of the gait—EMG data were compared between the no resistance trial (training NR) and final training trial (training block 4). Wilcoxon signed-rank test was also used to compare differences in hip and knee excursions and overground walking speed between pre-test and post-test walking trials. Spearman's rank

correlation test was used to determine if changes in hamstring muscle activation during training ($EMG_{block\ 4} - EMG_{NR}$) were related to the kinematic aftereffects induced by the training ($Kinematics_{post\text{-}BW} - Kinematics_{pre\text{-}BW}$). A significance level of $\alpha = 0.05$ was used for all statistical analyses and all tests were two-sided.

3.3 Results

The muscle activation profiles during resisted treadmill walking are provided in Figure 3.3. Resisted treadmill walking significantly increased EMG activity of the vastus medialis ($p = 0.028$), medial hamstring ($p = 0.028$) and lateral hamstring ($p = 0.028$) muscles during the swing phase of the gait. Wilcoxon signed-rank test also indicated that 20 minutes of resisted walking significantly increased the hip ($2.6° \pm 0.6°$, $p = 0.028$; Figure 3.4) and knee ($6.4° \pm 1.4°$, $p = 0.028$; Figure 3.4) joint excursions and overground gait velocity (0.05 ± 0.01 m/s, $p = 0.028$) of stroke survivors. Spearman's rank correlation test indicated a significant positive correlation between increase in hamstring muscle activation and kinematic aftereffects ($\rho = 0.89$, $p = 0.017$) at the knee, but not at the hip ($\rho = 0.53$, $p = 0.277$).

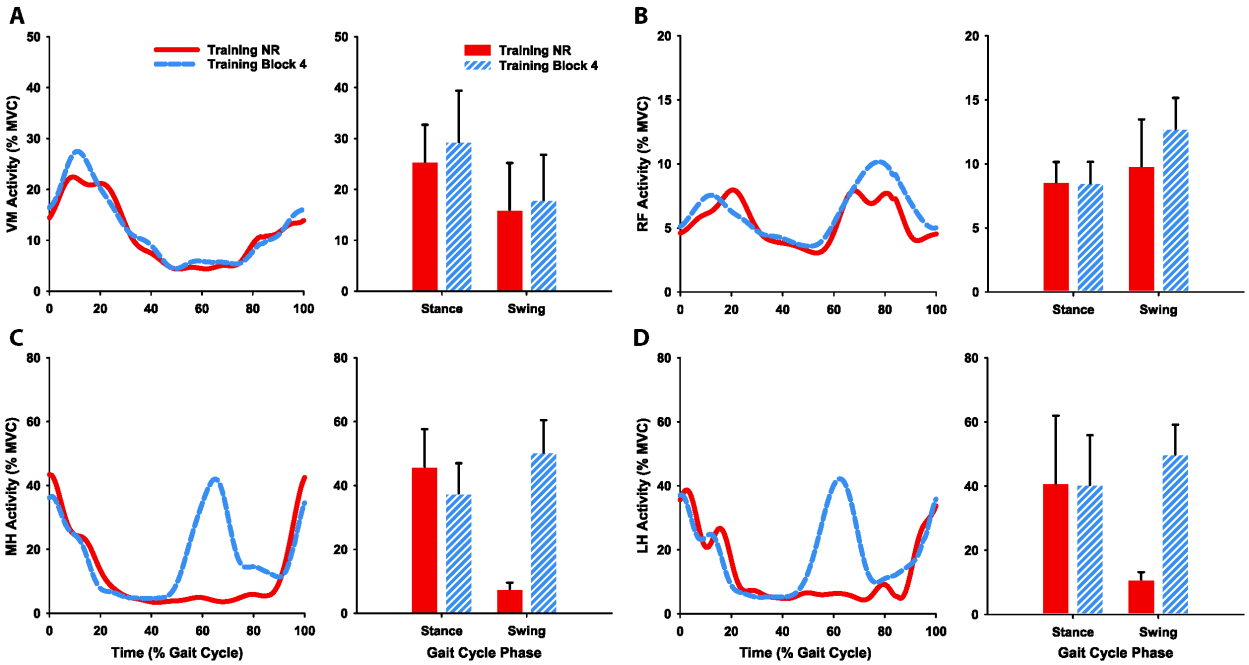

Figure 3.3 Traces showing the mean ensemble averaged EMG activation profiles (across all subjects) of each muscle during no resistance walking and the final (4th) block of resisted walking. Bars next to the traces show the peak activation of the respective muscle during the stance and swing phases of the gait. Error bars indicate the standard error of the mean.

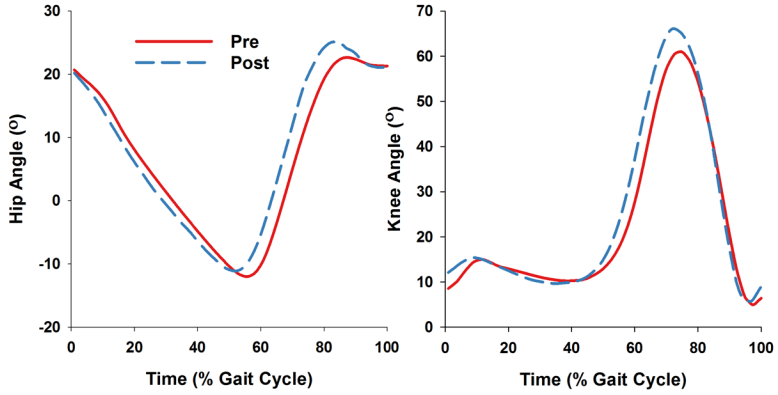

Figure 3.4 Traces showing the mean ensemble averaged (first 30 strides) sagittal plane hip and knee joint angles (across all subjects) before and after 20-minutes of resisted walking.

3.4 Discussion

This study pilot-tested the acute effects of resisted treadmill walking with a novel wearable knee brace on kinematics, muscle activation patterns, and gait velocity of stroke survivors. The results of this study indicate that robotic-resisted treadmill walking significantly increased the EMG activity of several of the key gait muscles during walking. Most notably, the

hamstring muscles, which were the primary muscles targeted during training, showed almost 5- to 7-fold increase in muscle activity. The increase in hamstring activity was also paralleled by significant improvements in hip and knee gait kinematics and overground gait velocity–a consistent finding that was observed in all the subjects (n = 6) tested in this study. These results provide preliminary evidence supporting that resisted walking with our knee brace induces meaningful biomechanical aftereffects that translates to overground walking, making it a feasible approach to improving locomotor functions after stroke.

A growing body of evidence indicates that resisted gait training improves the locomotor ability of individuals with various neurological conditions (e.g., stroke, cerebral palsy, and spinal cord injury) (Lam et al., 2015; Wu, Landry, et al., 2014; Wu et al., 2012; Wu, Landry, et al., 2011). The basic premise underlying this approach is that the functional benefits of strength training (e.g., gait function) are augmented when combined with task-specific training, and the combination may facilitate motor learning and neural plasticity (Kleim & Jones, 2008; Lam et al., 2006; Lam et al., 2015; Wu et al., 2012). When provided through a robotic interface, this training has the benefit of flexibility through the robotic controls (i.e., resistive forcefields can be easily scaled and redirected to be patient-specific based on deficits). However, robot based systems often utilize active actuators/motors to provide resistance—making them bulky, limited to use on a treadmill, and too expensive to be used in most rehabilitation settings (small clinic and home based). For these reasons, therapists often sacrifice controllability in order to cut costs and apply resistance using ankle weights or resistance bands (Lam et al., 2009), but these alternatives only allow rigid training schema (e.g., ankle weights have difficulty targeting the hamstring muscles and large resistive forces are only possible with excessively large weights). Our eddy current braking device was created as an intermediate step between active robots and

their passive alternatives—offering basic control in a package that is lightweight, useable overground, and inexpensive (< $2000). The forcefield provided by our device is very similar to how a Lokomat robot has been used to perform resistive gait training (Lam et al., 2015), but at a fraction of cost of the Lokomat ($3K vs $400K). Previous research indicates that the cumulative increase in gait speed after several weeks of resisted gait training is approximately 0.05-0.1 m/s (Hornby et al., 2008; Lam et al., 2015; Lam et al., 2011; Wu, Landry, et al., 2014), whereas the acute increase (i.e., within a single session) with our device was 0.05 m/s. Additionally, we saw a 5- to 7-fold increase in hamstring muscle activity with our device (that weighs only ~1.6kg) with only $1/4^{th}$ of maximum possible resistance, which is several times larger than walking with an 8kg weight or Lokomat-resisted walking (Browning et al., 2007; Houldin et al., 2011; Lam et al., 2008). Critically, this increase in hamstring muscle activity was strongly associated with the kinematic aftereffects (i.e., increase in knee joint excursion) observed at the knee joint, suggests that larger hamstring activity during resisted walking is crucial for inducing kinematic changes with training. Although our training primarily focused on the weaker hamstring muscles, we note that training can be easily customized to the quadriceps muscle group, either by incorporating a ratcheting joint into the brace or with servo control over the linear slider. Hence, low-cost passive robots such as our eddy current braking device could represent a substantial step forward in gait rehabilitation.

From a clinical standpoint, a key question that emerges is whether the improvements in hip/knee kinematics and overground gait speed observed in this study are clinically significant. First, we note that the reported improvements were seen within a single-session of training. Thus, we anticipate that repeated training would result in cumulative benefits that are larger than those observed in the current study. Further, the changes in hip and knee joint excursions and

overground gait velocity were indeed larger than the MDC values established (Perera et al., 2006; Saner et al., 2017) after accounting for the sample size of the group ($MDC_{group} = MDC_{individual}/\sqrt{n}$) (de Vet et al., 2001; Lu et al., 2008; Washabaugh et al., 2017). Most importantly, the changes observed in overground gait speed falls in the substantial meaningful change category for stroke survivors (Perera et al., 2006).

The low sample size is a key limitation of this study. However, as noted before, the positive outcomes observed in this study were very consistent across all subjects (6 out of 6) for EMG, kinematics, and gait speed, suggesting that a larger sample size would not have changed the study results. Another limitation is that we only chose moderate-to-high functioning individuals, which limits the generalizability to individuals with more severe impairments. We intentionally chose these subjects because prior research indicates that robotic-resisted training is particularly beneficial for individuals with relatively high function (Wu et al., 2012). Thus, it is likely that assistive therapy (rather than resistive therapy) may be more suitable for individuals with significant impairments. Finally, the therapeutic benefits of this device are not currently known, as this study was not designed to study the cumulative effects of training with the device. Future clinical trials will potentially inform us on the clinical potential of this device.

In summary, this study tested the immediate effects of resisted treadmill walking using a wearable knee brace on gait function in individuals with stroke. We found that training with the brace resulted in significant improvements in EMG, kinematics, and overground gait velocity. Importantly, this finding was very consistent across subjects, indicating that this type of training may have a significant clinical potential for gait training after stroke. To our knowledge, this is the first study to show that a wearable untethered exoskeleton device can induce meaningful locomotor adaptations in stroke subjects, which could also potentially translate to in home or

community based rehabilitation programs. However, further testing is required to verify the cumulative benefits of resistive gait training with this device.

3.5 Acknowledgment

This work has been published in Restorative Neurology and Neuroscience (Washabaugh & Krishnan, 2018). I would like to thank my co-author on this article, Dr. Chandramlouli Krishnan, for his contributions to the design of the experiments and editing of the manuscript. The research reported in this publication was supported in part by the National Institutes of Health (Grant# R01-EB019834) and by the National Science Foundation Grant No. DGE #1256260. Any opinions, findings, and conclusions or recommendations expressed in this material are those of the author(s) and do not necessarily reflect the views of the funding sources.

Chapter 4

Providing Kinematic Feedback as a Means to Reduce Motor Slacking during Functional Resistance Training of Walking

Abstract

Background: Functional resistance training is frequently applied to rehabilitate individuals with neuromusculoskeletal injuries. It is performed by applying resistance in conjunction with a task-specific training, such as walking. However, the benefits of this training may be limited by motor slacking. As the body reduces its motor output in response to the added resistance, it limits intensity. While techniques like feedback could reduce one's tendency to minimize effort during training, they are seldom used during training.

Research Question: Does functional resistance training during walking lead to motor slacking, and can techniques such as visual feedback be used to reduce these effects?

Methods: Fourteen able-bodied individuals participated in this experiment. Participants were trained by walking on a treadmill while a bidirectional resistance was applied to the knee using a robotic knee exoskeleton. During training, participants were either instructed to walk in a manner that felt natural or were provided real-time visual feedback of their kinematics. Electromyography and knee kinematics were measured to determine if adding resistance to the limb induced slacking and if feedback could reduce slacking behavior. Kinematic aftereffects were measured after training bouts to gauge adaptation.

Results: Functional resistance training without feedback significantly reduced knee flexion when compared to baseline walking, indicating the participants were slacking. This reduction in knee flexion did not improve with continued training. Providing visual feedback of knee joint kinematics during training significantly increased knee muscle activation and kinematic aftereffects.

Significance: These indicate that individuals are susceptible to motor slacking during functional resistance training, which could affect outcomes of this training. However, motor slacking can be reduced if training is provided in conjunction with a feedback paradigm. This finding underscores the importance of using additional methods that externally motivate motor adaptation when the body is not intrinsically motivated to do so.

4.1 Introduction

Injuries to the neuromuscular and skeletal systems can result in gait impairments and disability (Chen et al., 2005; Kuo et al., 2007; Pietrosimone et al., 2018). Often, these impairments are related to deficits in strength and altered motor control (Harvey, 2016; Olney & Richards, 1996). Hence, rehabilitation of these individuals requires some combination of strength training to improve force-generating capacity in the lower-extremity muscles and task-oriented training to promote re-learning of functional tasks like walking. However, it has been shown that when these training types have been implemented independently from one another, increases in one may not transfer to the other (Bohannon, 2007; Krebs et al., 2007; Sullivan et al., 2007). This disconnect has led to the development of new training methods that work to combine strength training with task oriented training.

One such method is functional resistance training, where a resistive exercise is applied in conjunction with a task-specific training (Donaldson et al., 2009; Yang et al., 2006). When functional resistance training is applied during walking, additional devices (e.g., leg braces, weighted cuffs, bands, or rehabilitation robots) are placed on the leg as means to provide resistance to the muscles used in the task. While this training technique has shown promise in its ability to increase functional metrics, such as walking speed (Alabdulwahab et al., 2015; Lam et al., 2009; Lam et al., 2015; Wu et al., 2017; Wu et al., 2012), studies that have analyzed strength have shown minimal improvements (Wu et al., 2012). This lack of strength gains may indicate that training is often not intense enough to improve force-generating capacity in the lower-extremity muscles.

Intensity may be reduced during training due to a phenomenon known as motor slacking, where the motor system reduces muscle activation levels and movement excursions as a means to minimize metabolic and movement-related costs (Reinkensmeyer et al., 2009). Indeed, studies on other functional tasks, such as reaching, have found that the body attempts to minimize movement-related costs in the presence of resistances (Izawa et al., 2008; Liu & Reinkensmeyer, 2004; Washabaugh et al., 2018). It is possible that motor slacking is less prominent during gait training, as there is some evidence to suggest that joint excursions reduce when the resistance is first added but improve with prolonged exposure (Lam et al., 2006; Savin et al., 2010). However, these studies often show that the kinematics rarely return to baseline levels. Thus, there is a critical need to determine if motor slacking occurs during training. It must also be ascertained whether additional methods, such as providing kinematic feedback, can improve muscular effort and movement excursions during functional resistance training.

Therefore, the purpose of this study was to determine how adding resistance to the leg during walking contributes to motor slacking. It also evaluated how motor slacking can be offset by including visual feedback of kinematics during the training. Resistance was provided using a knee brace that was fitted with a controllable brake, such that it provided resistance to knee flexion and extension during the swing phase of walking. To measure motor slacking during training, we evaluated changes in muscle activation and peak knee flexion during walking. We also measured kinematic aftereffects in knee angle, to determine if resisted walking with and without feedback altered adaptation. We hypothesized that functional resistance training without feedback would significantly reduce peak knee flexion during training. Additionally, the provision of kinematic feedback would significantly increase muscle activation and kinematic aftereffects during gait.

4.2 Materials and Methods

Fourteen able-bodied individuals participated in the study. However, one participants' data was excluded because they misunderstood training instructions. Analysis was performed on the remaining 13 participants (7 females; age: 21.0 ± 2.5 years; height: 171.9 ± 9.1 cm; mass: 67.2 ± 12.0 kg; self-selected walking speed: 1.46 ± 0.21 m/s; knee extensor strength: 185.7 ± 58.5 Nm; knee flexor strength: 106.2 ± 33.2 Nm [mean ± standard deviation]). Prior to the study, each participant reviewed and signed an informed consent document approved by the University of Michigan Institutional Review Board (HUM00093673, approved on 5/24/2018).

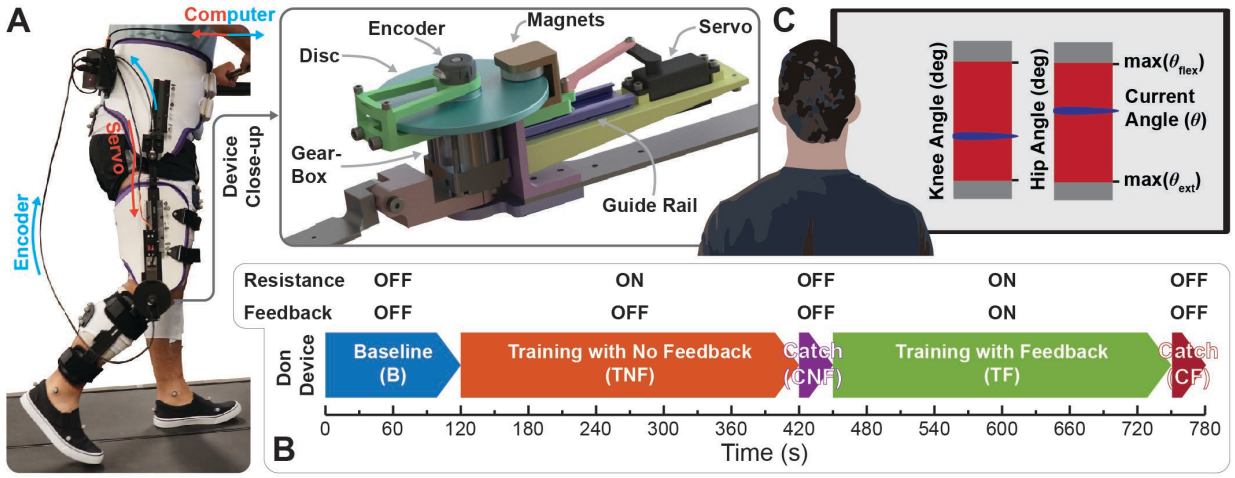

Figure 4.1 Schematic of the resistive device and experimental protocol. (A) A leg brace provides resistance to the knee via a controllable magnetic brake. Knee and hip angles are measured with encoders on the device and resistance is controlled by moving the magnets radially relative to the disc with a servomotor. (B) During the experiment, participants wore the device and trained while walking on a treadmill with resistance. Trainings varied based on the participants received kinematic feedback. Following each training session, resistance and feedback were removed during catch trials as we measured kinematic aftereffects. (C) Diagram of the real-time visual feedback paradigm. Participants walked and were encouraged to match their joint excursions to those measured from the baseline trial.

4.2.1 Experiment

In a separate session before training, we measured knee strength and self-selected gait speed. Knee strength was measured at 45 degrees of flexion in an isokinetic dynamometer (System Pro 4, Biodex, Shirley, NY). Participants were seated and secured into the device, warmed up with three submaximal contractions, then instructed to kick out or pull back maximally three times for each direction. Rest (120 s) was given between contractions. Self-selected walking speed was measured as the average of three 10-meter walk tests.

During the training session, intensity was measured using electromyography (EMG). We placed EMG sensors (Trigno Avanti, Delsys, Natick, MA, US) over the vastus medialis (VM), vastus lateralis (VL), rectus femoris (RF), medial hamstring (MH), and lateral hamstring (LH) muscles according to SENIAM guidelines. We assisted the participant in donning a controllable knee exoskeleton on their right leg (Figure 4.1 A) (Washabaugh et al., 2016; Washabaugh & Krishnan, 2018). We then measured the participant's baseline walking (B) over an instrumented

treadmill (Bertec, Columbus, OH, US) for 120 s at 60% of their self-selected walking speed without resistance (Figure 4.1 B). During baseline, encoders on the device measured knee angular velocity to calculate the device controls required to provide a bidirectional resistance (i.e., resisting both flexion and extension) with a magnitude of 15–20% of the participant's strength (Equation 4.1).

For training trials, participants walked for 300 s with resistance. The first trial was performed without visual feedback (TNF) and participants were instructed to walk in a manner that felt natural. After this trial, the resistance was removed and participants underwent a 30 s catch trial (CNF). During catch trials, participants were instructed to walk naturally as we measured the aftereffects of the training. During the second training trial, participants walked as they received visual feedback (TF) of their hip and knee joint angles as measured with the encoders on the device. Lastly, feedback and resistance were removed and participants performed another catch trial (CF).

Feedback consisted of bar plots for the hip and knee joints that displayed the average maximum and minimum joint angles from the baseline trial along with a cursor of the real-time joint angle (Figure 4.1 C). Participants were encouraged to reach peak knee flexion/hip extension during early swing and peak knee extension/hip flexion when they approached heel-strike. Feedback was created using a custom LabVIEW vi (v2013, National Instruments Corp., Austin, TX, US) and displayed on a monitor in front of the treadmill.

4.2.2 Device

Resistance was provided to the knee joint during training using a wearable exoskeleton device previously developed in our lab (Washabaugh et al., 2016). During operation, movement of the joint spins an aluminum disk and permanent magnets are exposed to the disk to provide

resistance (greater magnet exposure increases resistance) (Figure 4.1 A). In previous versions of the device, the resistance had to be manually controlled; however, the device was modified to be servo-controlled (1207 TG, Power HD, Pololu Corporation, Las Vegas, US). This allowed us to provide different resistances to the knee flexors and extensors according to:

$$T = -\beta\dot{\theta},$$

$$where\ \beta = \frac{0.17}{1 + e^{-\frac{(x-0.56)}{0.16}}}$$

$$\text{such that } |T| = \begin{cases} \%\ MVIC_{flex}, & \text{if } \dot{\theta} = \max(\dot{\theta}_{flex}) \\ \%\ MVIC_{ext}, & \text{if } \dot{\theta} = \max(\dot{\theta}_{ext}) \end{cases}.$$

Equation 4.1

In this equation, *T* was the torque generated by the device, β was the damping coefficient (units: Nm s deg-1), and $\dot{\theta}$ was the angular velocity of the joint. β was characterized using a dynamometer that measured torque over a range of movement velocities and magnet exposures (*x*); these data were then fit to a sigmoid curve. During training, magnet exposure was determined separately for flexion and extension. When $\dot{\theta}$ was equal to the extrema of the average knee velocity profile measured during baseline trials [i.e., $\max(\dot{\theta}_{flex})$ or $\max(\dot{\theta}_{ext})$], the magnitude of T was equal to a percentage of the participants strength.

The device was fitted to hip-knee orthosis consisting of a custom pelvis and thigh segments (Newport Bilateral MC & Newport Universal Thigh; Orthomerica Products, Inc.; Orlando, FL, US) and a modified orthopedic knee brace (T-Scope Premier Post-Op Knee Brace; Breg, Inc.; Carlsbad, CA, US). A freely moving joint was fit between the pelvis and thigh segments. Optical encoders were placed on each joint of the device (E4T-360, US Digital, Vancouver, WA, US) and used to measure joint angles and velocities during use. Data were

logged and devices were controlled using a custom LabVIEW program that communicated with a microprocessor (Arduino UNO, Arduino, Somerville, MA, US).

4.2.3 Data Processing

Raw EMG and force plate data were collected in QTM at 2000 Hz. Using a custom LabVIEW program, EMG data were band-pass filtered (20-500 Hz) and rectified. Both EMG and force data were then smoothed using a zero phase-lag low-pass Butterworth digital filter (EMG: 8th order, 6 Hz; force: 6th order, 100 Hz). EMG data were then segmented at heel strike (20 N threshold from the vertical force data) and ensemble averaged across strides to compute mean EMG profiles during each trial. We normalized these profiles to the peak amplitude during the baseline trial (i.e., in units of %B), then calculated the maximum muscle activation for each trial. These values were then log transformed to minimize skewness and heteroscedasticity (Krishnan et al., 2013).

During each trial, we measured knee angle using an encoder on the device at a rate of 62.5 Hz using a custom LabVIEW program. For processing, these data were filtered using a zero phase-lag low-pass Butterworth digital filter (6th order, 100 Hz). We then calculated the maximum knee flexion angle for each stride and averaged these values across strides.

4.2.4 Statistical Analysis

Statistics were performed using JASP computer software (Version 0.14.1). During training, muscle activation was analyzed using a two-way repeated-measures ANOVA (muscle [5 levels: VM, VL, RF, MH, LH] × trial [3 levels: B, TNF, and TF]) while knee kinematics were measured with a one-way repeated measures ANOVA (3 levels: B, TNF, and TF). We also performed a planned comparison to see if knee flexion changed within the TNF trial, where we compared the knee joint angle of the first five strides with the last five strides with a paired t-test.

Kinematic aftereffects were analyzed using one-way repeated measures ANOVA (3 levels: B, CNF, and CF). Following significant ANOVA main effects, we performed post hoc pairwise comparisons using paired t-tests with Holm correction ($\alpha = 0.05$). Note, to help with interpretation, we also report the non-transformed average difference for muscle activation data.

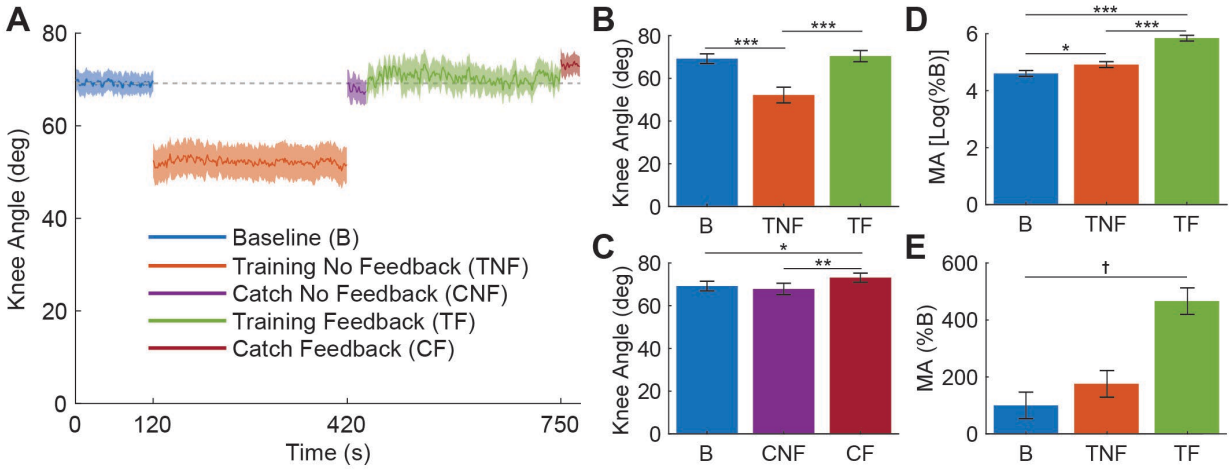

Figure 4.2 (A) Average stride-by-stride maximum knee flexion angle throughout the experiment. For viewing purposes, stride-by-stride data were interpolated so they could be plotted against time. The shaded region above and below the line corresponds to the standard error of the mean. (B) Knee angle during training: the knee angle reduced significantly when training without feedback, which would indicate participants were susceptible to motor slacking. (C) Knee angle during catch trials: there were significant aftereffects following training with feedback. (D) Log transformed muscle activation (MA) during training: muscle activation increased significantly during both training methods. However, amplitude was much larger when training with feedback. Bars represent the marginal means of the analysis. (E) Non-transformed muscle activation, presented to improve interpretation of how muscle activation changed during training. Error bars indicate the standard error of the mean. Symbols: * $p < 0.05$; ** $p < 0.01$; *** $p < 0.001$; † statistics were not run on these data, for visualization purposes only.

4.3 Results

Motor slacking was monitored throughout the study using knee joint angles and muscle activation. The average knee flexion angle throughout the experiment is displayed in Figure 4.2 A. Analysis of the knee joint data during training indicated that there was a significant difference between trials [$F(2,24) = 49.402$, $p < 0.001$]. Post hoc comparisons indicated that the knee angle significantly reduced when training without feedback when compared with baseline [$\Delta = -17.0$ (95% CI = −21.4 – −12.5) degrees, $p < 0.001$, $d = -2.299$]. However, with feedback, peak joint angles matched closely with their baseline levels [$\Delta = 1.2$ (95% CI = −3.2 – 5.7) degrees, $p = 0.548$, $d = 0.169$] (Figure 4.2 B). When analyzing planned comparisons of joint angle within the

no feedback trial, we did not find that joint angle was changed between the beginning and end of the trial [$\Delta = 0.07$ (95% CI = −2.12 – 2.25) degrees, $p = 0.949$, $d = 0.018$].

Kinematic aftereffects (Figure 4.2 C) produced a significant main effect between trials [$F(2,24) = 6.227$, $p = 0.007$]. Post hoc comparisons indicated that there was a significant aftereffect of increased peak knee flexion following training with visual feedback [$\Delta = 3.9$ (95% CI = 0.6 – 7.3) degrees, $p = 0.037$, $d = 0.702$], but not after training without feedback [$\Delta = -1.3$ (95% CI = −4.7 – 2.1) degrees, $p = 0.396$, $d = -0.240$]. The aftereffects from training with feedback were also larger than those from training without feedback [$\Delta = 5.3$ (95% CI = 1.9 – 8.7) degrees, $p = 0.007$, $d = 0.942$].

When analyzing muscle activation (Figure 4.2 D) there was a significant main effect for trial [$F(2,24) = 43.713$, $p < 0.001$]. Post hoc analysis indicated that muscle activation was significantly increased when training with visual feedback when compared with baseline [$\Delta =$ 1.238 (95% CI = 0.937 – 1.539) log(%B), $p < 0.001$, $d = 2.492$; non-transformed: $\Delta = 336.0$ %B]. While muscle activation also significantly increased without feedback, this effect was much smaller [Δ=0.311 (95% CI = 0.01 – 0.612) log(%B), $p = 0.034$, $d = 0.625$; non-transformed: $\Delta = 75.6$ %B]. When comparing both training trials, the muscles were more activated when training with feedback than without [$\Delta = 0.928$ (95% CI = 0.627 – 1.229) log(%B), $p < 0.001$, $d = 1.867$; non-transformed: $\Delta = 290.4$ %B].

4.4 Discussion

This study investigated how functional resistance training during walking can be augmented using visual feedback. Specifically, we tested how knee joint kinematics and muscle activation were altered when a resistance was applied to the knee during walking, and how visual feedback could then be used to reduce the motor slacking associated with this training. We found

that: (1) the knee joint excursion was significantly reduced during functional resistance training, where resistive torques were applied to the knee extensors and flexors during gait; (2) the reduction in knee joint excursion did not improve with continued functional resistance training; and (3) minimizing motor slacking by providing visual feedback of knee joint kinematics significantly increased knee muscle activation and kinematic aftereffects. These results emphasize the importance of providing feedback during functional resistance training while walking. The increase in muscle loading and active engagement that feedback provides could greatly augment the outcomes of this training.

A key finding of this study was that the intensity of functional resistance training was augmented when the training was provided in conjunction with a feedback paradigm. Specifically, while training with feedback there was an approximately three-fold increase in muscle activation when compared to training without feedback. Muscle activity during walking is correlated with metabolic cost (Hortobagyi et al., 2011). Hence, it appears that when feedback was not provided, the body worked to reduce the metabolic cost of walking with the added resistance to the knee. This effect was more evident when looking at the knee kinematics while walking, which were greatly reduced (~17 degrees) when walking without feedback. Importantly, this reduction in knee excursion persisted throughout the training period and did not reach the levels of baseline walking without resistance. Such motor slacking is problematic for a training like functional resistance training, where one of the main goals is to increase strength through greater loading of the muscles (Donaldson et al., 2009; Yang et al., 2006). While it is unclear if longer durations of training would help in minimizing the slacking that was observed in the no feedback condition, our results suggest that this issue can be effectively addressed by providing kinematic feedback.

The long-term effects of functional resistance training during walking in clinical populations have been somewhat conflicting. While some studies have shown there are benefits to applying resistance during walking as opposed to providing assistance (Wu et al., 2017; Wu et al., 2016), others have shown this training has a small or no-effect (Lam et al., 2009; Wu, Landry, et al., 2014). However, a majority of these trainings have been performed without feedback; hence, it is possible that patients were kinematically slacking and not exerting enough effort during training. Indeed, the results of our study showed that the thigh muscles were minimally engaged when feedback was not provided, but were substantially engaged when walking with visual feedback. Moreover, we found that participants adapted more during training with feedback, as aftereffects were only observed when training was performed with visual feedback. It is often believed that if a perturbation does not result in aftereffects, then the training is less valuable because the nervous system is not being engaged. This belief likely stems from how aftereffects have been seen to transfer to overground walking (Reisman et al., 2009; Savin et al., 2014; Wu et al., 2016). However, if reducing movement-related costs is the body's predominant goal (Finley et al., 2013; Izawa et al., 2008; Ranganathan et al., 2013), then it is logical that the body would attempt to mitigate resistive perturbations and not correct the errors they introduce (Liu & Reinkensmeyer). As with any exercise, users will likely have to be externally motivated to train, and feedback may reprioritize the body's control scheme to provide motivation that drives adaptation. While there are numerous ways that feedback can be applied during training (e.g., via coaching, visual feedback, object avoidance, or games), this study underscores the importance of using additional methods that externally motivate training to bolster both intensity and adaptation.

4.4.1 Limitations

A primary limitation is related to the small sample size of this study. Although our sample size is consistent with many short-term motor adaptation studies (Blanchette & Bouyer, 2009; Noble & Prentice, 2006; Savin et al., 2010), our overall sample size was limited due to COVID restrictions. Thus, it is unclear if we had adequate power to realize findings with small effect sizes. Further, we did not randomize the order that the conditions were presented in this study. We intentionally chose not to randomize because we felt that introducing participants to the visual feedback condition first would disproportionately confound their performance without feedback (i.e., reduce their ability to walk normally). Given that aftereffects were not present after training without feedback, we do not feel that the feedback condition was significantly confounded by the carryover effects from the no feedback condition. We also note that repeated exposure to resistance can reduce the magnitude of aftereffects (Blanchette et al., 2012); thus our testing order likely produced a more conservative estimate of the effects of visual feedback. However, additional insights may have been gained if feedback was a between-subjects factor. Next, most studies often allow aftereffects to wash out (i.e., prolonged walking until walking returns to normal) between trials. We did not provide wash out between the no feedback and feedback conditions. However, this again should not have affected our results because the no feedback condition did not produce significant aftereffects. Lastly, participants were only trained for five minutes in each condition. While this is a common duration for measuring acute aftereffects, and steady state adaptation often occurs after the first several steps (Emken & Reinkensmeyer, 2005; Lam et al., 2006), it is still a much shorter duration than would be provided during an intervention. Hence, it is possible that participants could become more engaged if training was provided for a longer duration.

4.5 Conclusion

In conclusion, the results of this study indicate that individuals are susceptible to motor slacking during functional resistance training, which could affect outcomes of this training. However, motor slacking can be reduced if training is provided in conjunction with a feedback paradigm. We found that training while receiving visual feedback of gait kinematics increased intensity and produced larger aftereffects. Although training without feedback was slightly more intensive than normal walking, the aftereffects due to this training were not pronounced. This finding underscores the importance of using additional methods that externally motivate the user during functional resistance training, especially if the body is not intrinsically motivated to do so.

4.6 Acknowledgment

This work was supported in part by the National Institutes of Health (Grant R21 HD092614), the National Science Foundation (Grant DGE 1256260), and the UM-BICI Collaboratory Initiative. Any opinions, findings, and conclusions or recommendations expressed in this material are those of the authors and do not necessarily reflect the views of the funding sources. I would like to thank my adviser Dr. Chandramouli Krishnan for his contribution in study design and writing. I would like to thank Luis Cubillos for his assistance in data processing and creating figures, Mary Koje for her help in data processing, as well as Belinda Cargile and Alexandra Nelson for the work they did collecting data and initial drafting. Several others also assisted in collecting these data, including Tom Augenstein, Scott Brown, Kaitlyn Ford, Jiajie Qiu, Samantha Steinberg, Miranda Santos, and Michael Volyanyuk.

Chapter 5

Design and Preliminary Assessment of a Passive Elastic Leg Exoskeleton for Resistive Gait Rehabilitation

Abstract

Objective: This study aimed to develop a unique exoskeleton to provide different types of elastic resistances (i.e., resisting flexion, extension, or bidirectionally) to the leg muscles during walking. *Methods:* We created a completely passive leg exoskeleton, consisting of counteracting springs, pulleys, and clutches, to provide different types of elastic resistance to the knee. We first used a benchtop setting to calibrate the springs and validate the resistive capabilities of the device. We then tested the device's ability to alter gait mechanics, muscle activation, and kinematic aftereffects when walking on a treadmill under the three resistance types. *Results:* Benchtop testing indicated that the device provided a nearly linear torque profile and could be accurately configured to alter the angle where the spring system was undeformed (i.e., the resting position). Treadmill testing indicated the device could specifically target knee flexors, extensors, or both, and increase eccentric loading at the joint. Additionally, these resistance types elicited different kinematic aftereffects that could be used to target user-specific spatiotemporal gait deficits. *Conclusion:* These results indicate that the elastic device can provide various types of targeted resistance training during walking. *Significance:* The proposed elastic device can provide a diverse set of resistance types that could potentially address user-specific muscle weaknesses and gait deficits through functional resistance training.

5.1 Introduction

Gait impairments are a prominent source of disability after neurological or orthopedic injuries (Chen et al., 2005; Kuo et al., 2007; Pietrosimone et al., 2018; Waite et al., 2000). For example, following a stroke—which is the leading cause of long-term disability in the United States (Mozaffarian et al., 2015)—only 50% of survivors are able to ambulate in the community following conventional therapy (Perry et al., 1995). Such impairment can greatly affect independence and quality of life (Brandes et al., 2008); hence, retraining gait following an injury is of the utmost importance. Applying functional resistance training during walking is an emerging method for treating individuals with gait impairments. This training is administered by having a patient perform a task-specific training (in this case, walking) while a load is applied to resist the movement (Cooke et al., 2010; Donaldson et al., 2009; Washabaugh et al., 2016). This works simultaneously to improve muscle strength and coordination, which are often underlying sources of gait impairment (Blackburn et al., 2016; Hsu et al., 2003; Kautz & Brown, 1998).

Most studies have applied functional resistance training using simple rehabilitation equipment, such as ankle weights (Browning et al., 2007; Duclos et al., 2014; Lam et al., 2009; Simao et al., 2019). While these devices are low-cost and widely available in clinics, they are limited in their ability to target patient-specific muscle weakness during walking. This is because the load is tethered to the user's ankle (i.e., the distal end of the shank); hence, resistance is automatically coupled between the user's hip and knee joints (Washabaugh, Augenstein, & Krishnan, 2020). This problem can be remedied by devices that directly resist the motion of the joint (i.e., a joint-space approach). Joint-space based devices include wearable leg braces and exoskeletons and allow resistance to be targeted to a single joint if desired. This is potentially beneficial for rehabilitation, as therapists often measure strength at the joint level using clinical

tests (e.g., manual muscle testing) or dynamometry (Bohannon, 2001). Hence, joint-space based devices can directly target these patient specific weaknesses while providing resistance during functional tasks. For this reason, there have been several joint-space devices developed in recent years for providing functional resistance training during walking (Blanchette et al., 2014; Conner et al., 2020; Lam et al., 2006; Martini et al., 2019; Noel et al., 2008; Washabaugh et al., 2016; Washabaugh & Krishnan, 2018).

While all of these devices apply resistance in the joint space, they differ in the type of resistance that they are designed to provide. For example, a majority of these devices provide viscous loads to the participant during walking (Lam et al., 2006; Washabaugh et al., 2016; Washabaugh & Krishnan, 2018)), meaning their resistance is proportional and opposite the velocity of the joint (i.e. a negative power constraint). While there are several benefits to viscous resistances (Stoeckmann et al., 2009)—such as the ease of use, smoothness, and controllability of the device—this negative power constraint also means that this strategy can only target muscles during concentric contractions (i.e. the muscle shortens while in tension). This is a potential limitation, as many key elements of walking rely on eccentric loading (i.e. muscle lengthening while in tension). For example, the hamstrings work eccentrically to slow knee extension in preparation for heel-strike; however, viscous devices cannot provide this type of resistance. To study these potential resistive paradigms, we will need to develop strategies that can remove the negative power constraint by allowing energy to be exerted on the user.

The type of actuator used to generate resistance determines whether a device can exert energy on the user. Most rehabilitation robots use active actuators (e.g., motors), which add external energy to the user in order to provide resistance. However, active actuators are typically expensive, bulky, and potentially unsafe if not programmed correctly. These issues can be

addressed by using passive actuators (e.g., masses, springs, and dampers), which are relatively cost-effective, light-weight, and inherently safe, as they do not add external energy to the user but convert/store the user's own energy. Hence, we anticipate that passive devices are more feasible for small clinics or in-home use. Also, if the device is low-cost enough to be purchased by the patient there could be additional therapeutic benefits (Kleim & Jones, 2008), as this could increase the dosage of training and allow for more variable training that is specific to everyday life.

Therefore, this study aimed to develop a unique, low-cost, and passive exoskeleton device that can provide different types of targeted elastic resistance during walking. An elastic resistance was desired because elastic elements (such as springs) store elastic potential energy when they are deformed (i.e. stretched or compressed), then return that energy back to the user as they recoil. Hence, with an elastic exoskeleton it is possible to engage the muscle during concentric contraction as the elastic element is deformed, and during eccentric contraction while the element recoils. While several passive elastic exoskeletons have been developed in the past (e.g., leg braces that incorporate leaf springs (Cherry et al., 2016), torsion springs (Cherry et al., 2006; Mankala et al., 2009; Sulzer et al., 2009), extension springs (Collins et al., 2015), and compression springs (Shamaei et al., 2014, 2015)), these devices typically have been used to provide assistance to movement, whereas the purpose for our device was to apply resistance. Our device further differs from these past devices because it can alter the joint angle where the elastic element of the device is undeformed (i.e., the resting position); thus, allowing the device to resist any joint motion (i.e., joint flexion, extension, or both), and accommodate any restrictions in a patient's range of motion. In this paper, we provide an overview of the governing principles and

design of this device. We also verify its use in a benchtop testing scenario and when worn on the knee during treadmill walking.

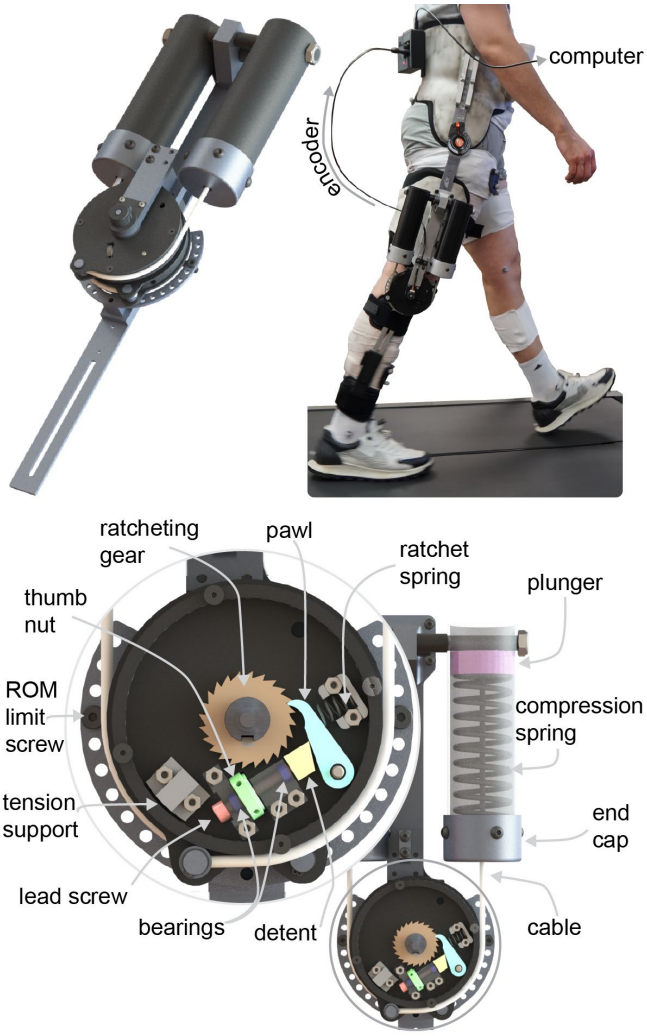

Figure 5.1 An elastic leg brace for functional resistance training during walking. **(Top Left)** A rendering of the device. **(Top Right)** The device fit to the knee of a hip and knee orthosis. **(Bottom)** Schematic depicting the components of a spring-pulley-clutch subassembly. When providing resistance, a ratcheting gear fixed to the joint engages a pawl; hence, rotation of the joint (clockwise in this depiction) rotates the pulley, which compresses the spring to provide a linear torque profile to the leg. Alternatively, a lead screw can actuate a detent, which disengages the pawl and removes the resistance.

5.2 Methods

5.2.1 Developing an Elastic Mechanism

To obtain the level of functionality and adjustability that we desired from this device, we created a novel mechanism that used counteracting subassemblies containing springs, pulleys,

and clutches (Figure 5.1). A single subassembly could provide resistance to a single direction of motion (i.e., flexion or extension); hence, two subassemblies oriented in opposing directions permitted resistance to flexion and/or extension (i.e., unidirectional or bidirectional) with the single device.

Each subassembly consisted of a compression spring housed within a cylinder along with a plunger that compressed the spring when pulled on by a custom nylon-coated cable assembly (2126SN6, Carl Stahl Sava Industries, Inc., Riverdale, NJ, US) (Figure 5.1 Bottom). The top end of the cable contained a threaded plug fitting that fastened to a countersunk nut atop the plunger. The bottom end of the cable contained a ball and shank fitting, which was routed through an opening in the cylinder's end cap then fixed to a point along the edge of the pulley (Diameter: 10.54 cm) using a quick-release mechanism. The pulley was centered on the joint of the device and provided a constant lever arm for the spring force, which permitted a linear relationship between the output torque and angle of the device.

Within the pulley was a clutch mechanism that allowed us to select the angular position where the spring was uncompressed (i.e., the resting position). The clutch consisted of a ratcheting gear fixed to the device's joint, a pawl, a ratchet spring, and a detent that traveled along a lead screw (Figure 5.1 Bottom). When the detent was retracted, the ratchet spring held the pawl engaged with the ratcheting gear. In this configuration, the device provided resistance because the pulley would rotate along with the user's joint to pull the cable and compress the spring. However, the resistance could also be removed by disengaging the clutch. This was accomplished by turning the lead screw (using a hex key or thumb nut) so that the detent traveled to disengage the pawl.

With two of these subassemblies, the net resistive torque output by the device was the difference between their respective torques:

$$\mathrm{T} = \tau_1 - \tau_2,$$

Equation 5.1

where T was the net torque generated by the device (i.e., the device moment) and τ_i was the torque for each subassembly where the subscript (i.e., 1 or 2) indicates which spring-pulley-clutch subassembly the variable was associated with. The net torque from the device could also be expressed based on the spring and pulley parameters:

$$\mathrm{T} = k_1(\theta - \theta_{r1}) - k_2(\theta_{r2} - \theta); \text{ where } \theta_{r1} \leq \theta \leq \theta_{r2}.$$

Equation 5.2

In these equations θ was the current angle of the device, k_i was the calibrated torsional stiffness of the spring in each subassembly, and θ_{ri} was the angle where the clutch associated with that spring was engaged (i.e., where the spring becomes uncompressed). During operation, θ was measured using an encoder mounted atop the joint of the device (E4T-360, US Digital, Vancouver, WA, US) that communicated with a computer via an microprocessor (Arduino UNO, Arduino, Somerville, MA, US). The ratcheting gears allowed the clutch to be engaged in 15 deg increments. We constrained θ in these equations because, if θ exceeded those limits, the cable would lose tension and could come off the pulley. If there was no spring located in the cylinder or if one of the clutches was disengaged, the subassembly did not contribute to the output torque and the device provided unidirectional resistance. When both subassemblies were engaged, the device provided bidirectional resistance.

The device was designed to permit quick alterations in resistive capability by exchanging springs of different stiffnesses. Springs could be exchanged by doing the following: with the clutch disengaged, the distal end of the cable could be disconnected from the pulley using the

quick-release mechanism. The end cap on the cylinder could then be removed by undoing the bayonet mount fastener (Figure 5.1 Bottom). With the end cap off, the spring would be easily accessible and could be replaced with a spring of a different stiffness. For this study, we purchased several stock compression springs (Acxess Spring, Colton, CA, US), meant to permit a range of resistances between approximately 5 and 50 Nm of peak torque for a joint excursion of about 70 deg. We selected compression springs because they have high stiffness and deflection capabilities, can be easily enclosed for safety, are less fragile than other types of springs (e.g., extension springs), and can be purchased as stock components for springs with the same form factor. The angular stiffness of these springs (k) was measured during benchtop testing.

The output torque of the device could also be expressed as a simple spring system:

$$\mathrm{T} = k_{eff}(\theta - \theta_R), \text{where}$$

Equation 5.3

$$k_{eff} = k_1 + k_2.$$

Equation 5.4

In this system, k_{eff} was the effective spring constant for the device and θ_R was the angular position where the spring system was at rest (i.e., the resting position). In our device, θ_R could be manually controlled based on the spring stiffnesses (k_i) and the positions where the clutches were engaged (θ_{ri}). Hence, when operating in bidirectional mode, we could control the position where the transition between flexion and extension resistance occurred. This position was calculated by finding where the net torque of the device was zero (i.e., the position that effectively negated pre-tensions in both subassemblies):

$$0 = k_1(\theta_R - \theta_{r1}) - k_2(\theta_{r2} - \theta_R); \text{thus,}$$

Equation 5.5

$$\theta_R = \frac{k_1\theta_{r1} + k_2\theta_{r2}}{k_1 + k_2} \xrightarrow{k_1=k_2} \frac{\theta_{r1} + \theta_{r2}}{2}.$$

Equation 5.6

If the θ_{ri} required to pre-tension a spring was located within the user's range of motion, θ_{ri} could be set by instructing the user to move their joint to the desired position before engaging the ratchet on each subassembly. However, for some values of θ_{ri} (e.g., if θ_R= 10, θ_{r1}= −50 and θ_{r2}= 70) the clutches may need to be set outside the user's anatomical range of motion. In our device, this was achieved safely by locking the joint, then placing a rod through a hole in the side of the pulley and into the tension support (Figure 5.1 Bottom), which gave us leverage to rotate the pulley to the desired position before engaging the clutch.

The device was designed in SolidWorks 3D Design Software (v2019, SolidWorks Corp., Waltham, MA, US) so as to withstand 100 Nm of torque (i.e., a 2x safety factor) about the joint (verified through finite element analysis [FEA]). The device was custom fabricated primarily using aluminum (6061 and 7075) and polyoxymethylene (POM). POM was used in many sliding/bearing applications (e.g., plunger/cylinder) due to its low coefficient of friction with other surfaces. Information on parts, materials, costs, and machining techniques can be found at: http://neurro-lab.engin.umich.edu/downloads (Bill of Materials).

To complete the exoskeleton, the elastic device was fitted to the knee joint of a custom hip-knee orthosis (Figure 5.1 Top Right), consisting of pelvis and thigh segments (Newport Bilateral MC & Newport Universal Thigh; Orthomerica Products, Inc.; Orlando, FL, US) and a modified orthopedic knee brace (T-Scope Premier Post-Op Knee Brace; Breg, Inc.; Carlsbad, CA, US). A freely moving joint was fit between the pelvis and thigh segments to eliminate sliding of the knee device, but the elastic device could potentially be fit between the pelvis and thigh to permit resistance at the hip joint. We selected the knee joint as a target for resistance

because of the following reasons: (1) the segments spanning the knee joint have relatively less soft tissue when compared with the hip joint, which makes it easier to convey resistance to the leg, (2) the inertia of the device at the knee would be lower than at the ankle, which reduces the confounding effects of inertia on gait mechanics and muscle activation, and (3) we wanted to address thigh muscle strength during walking as it has been linked to functional outcomes in various populations (Krishnan & Theuerkauf, 2015; Pak & Patten, 2008). Overall, the elastic device that was designed in this study (i.e., the resistive component) had a mass of 1.9 kg, while the mass of the entire exoskeleton (including braces) was approximately 4.4 kg. The mass of the individual springs used in the ranged from 75g (k=0.125) to 350g (k=0.605) for the benchtop experiment and from 75g (k=0.125) to 250g (k=0.501) during the human subject experiment.

5.2.2 Benchtop Validation of the Device

A benchtop setup was used to measure the stiffness of (i.e., calibrate) the springs and to validate our ability to alter the resting position of the device. In this setup, the upper and lower arms of the device (i.e., the portion of the device that interfaces with the leg brace) were rigidly attached to an isokinetic dynamometer (System Pro 4, Biodex, Shirley, NY) using a custom built jig (Figure 5.2 Left). Care was then taken to ensure that the axis of the dynamometer aligned with the joint of the elastic device. The dynamometer was programmed to cycle between 0 deg (defined as vertical) and 70 deg at an angular velocity of 1 deg s^{-1} while the torque and position were logged using the dynamometer's built-in functionality. We used 0 and 70 deg to approximate the knee range of motion during walking.

To calibrate the springs used in the device, individual springs were placed into the cylinder of the lower subassembly (Figure 5.2 Left; Cylinder 1) and the clutch was engaged at 0 deg (i.e., θ_{r1}= 0). Meanwhile, the upper cylinder was left empty. The program on the

dynamometer was executed twice to both measure the spring stiffness and to measure repeatability.

To validate our ability to alter the resting position of the device, springs were loaded into the top and bottom cylinders of the device (i.e., $k_1 = k_2 = 0.215$ N m deg^{-1}). To set the resting position of the device at different angles, the clutches of the counteracting subassemblies were engaged at various positions (θ_{r1} and θ_{r2}) in accordance with Equation 5.2 and Equation 5.6. The resting positions were set as follows: $\theta_{r1} = -50$ and $\theta_{r2} = 70$ for $\theta_R = 10$; $\theta_{r1} = -30$ and $\theta_{r2} = 70$ for $\theta_R = 20$; $\theta_{r1} = -10$ and $\theta_{r2} = 70$ for $\theta_R = 30$; $\theta_{r1} = 0$ and $\theta_{r2} = 70$ for $\theta_R = 35$; $\theta_{r1} = 0$ and $\theta_{r2} = 80$ for $\theta_R = 40$; $\theta_{r1} = 0$ and $\theta_{r2} = 100$ for $\theta_R = 50$; and $\theta_{r1} = 0$ and $\theta_{r2} = 120$ for $\theta_R = 60$ deg. Once the spring mechanism was set, the arm was relocated to the zero position and the dynamometer program was run.

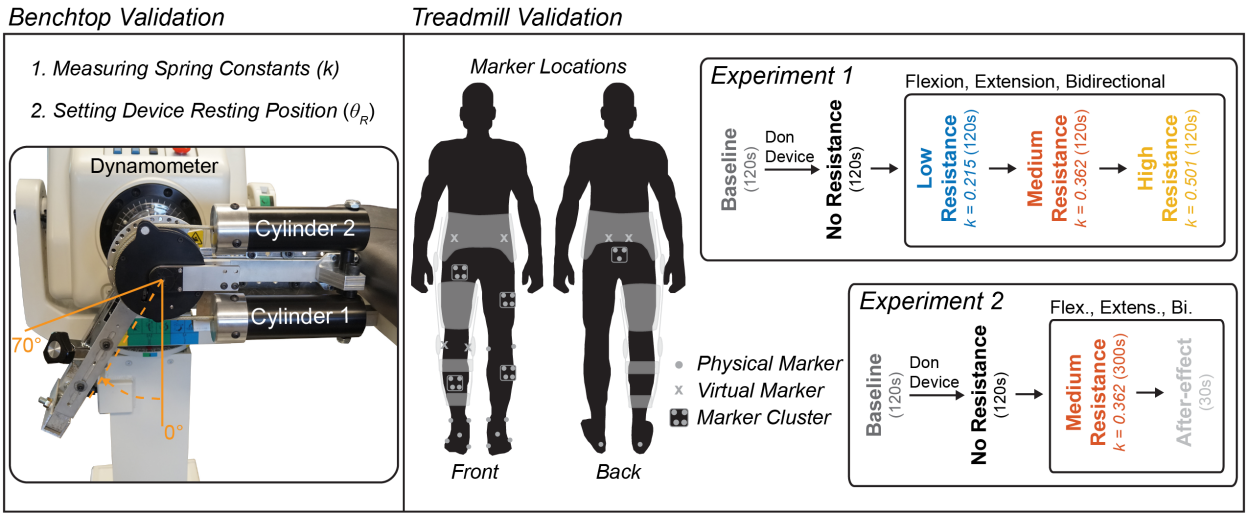

Figure 5.2 Schematic depicting benchtop and treadmill validation experiments. **(Left)** For benchtop testing the device was connected to a dynamometer to measure the stiffness of (i.e., calibrate) the springs and validate our ability to alter the resting position of the spring system. **(Right)** The device was worn over the knee to test its ability to convey forces to the leg during treadmill walking. Separate experiments were run to see (1) how the device performed under three different conditions (i.e., resisting knee flexion, extension, or bidirectionally) at multiple resistance levels and (2) how these conditions augment adaptation with the device, as we measured kinematics, kinetics, and muscle activation.

5.2.3 Evaluation of the Device during Treadmill Walking

To evaluate the ability of the device to provide resistance during walking, the elastic leg brace was worn by a healthy participant (male, aged: 24 years, height: 185 cm, mass: 93 kg, dominant leg: right) during two validation experiments. The first experiment evaluated the device during walking under various loading conditions—including having the device provide resistance to knee flexion, extension, or bidirectionally—at several resistance intensities, as we measured electromyography (EMG), kinematics, and kinetics. The second experiment was devised to see how the device could influence motor adaptation by measuring the kinematic aftereffects that occurred after sustained walking under these loading conditions. In preparation for these experiments, the participant reviewed and signed an informed consent document approved by the University of Michigan Institutional Review Board (HUM00093673, approved on 5/24/2018).

5.2.3.1 Experiment 1: Device Performance during Walking

The protocol for experiment 1 (Figure 5.2 Right) was as follows: EMG sensors (Trigno Avanti, Delsys, Natick, MA, US) were placed over several lower extremity muscles used during walking (incl. the quadriceps [vastus medialis, VM; rectus femoris, RF], hamstrings [medial hamstring, MH; lateral hamstring, LH], tibialis anterior, medial gastrocnemius, soleus, and gluteus medius). Reflective markers were then placed for motion capture (Qualisys Track Manager [QTM], Qualisys, Göteborg, SE). Refer to Appendix B.1 for additional details about the experimental setup, such as marker placements. We then measured the participant's static posture (see Appendix B.2.1 for details) without the device. Next, the participant performed a Baseline trial, where he walked on an instrumented split-belt treadmill (Bertec, Columbus, OH, US) at 1 m s^{-1} for a duration of 120s (note, this was the speed throughout all experiments). We

then assisted the participant in donning the device. Once the device was fitted properly, we performed a second static trial in case any marker clusters had shifted. The participant then walked on the treadmill while wearing the device with no resistance (i.e., with the clutches disengaged and without springs in the cylinders). From this trial, we measured the maximum knee flexion and extension angles (i.e., the range of motion limits: ROM_{min} = 0 degrees and ROM_{max} = 66 degrees) using the encoder on the device. These angles were used to provide real-time feedback that encouraged the participant to walk with their normal range of motion during resisted trials (see Appendix B.3 for details).

The participant then walked with the device providing resistance to their knee joint during three loading conditions (Resisting Flexion, Extension, and Bidirectional) at three intensities that used different spring stiffnesses (Low [k_i= 0.215 N m deg^{-1}, Medium [k_i= 0.362 N m deg^{-1}], and High [k_i= 0.501 N m deg^{-1}]). For each condition, the participant walked for 120 s with resistance, then was given 60 s of rest before progressing to the next intensity. To resist flexion, the spring was inserted into the first cylinder (k_1) and the clutch for that cylinder was engaged while the participant's leg was fully extended (θ_{r1}= ROM_{min}). To resist extension, the spring was inserted into the second cylinder (k_2) and the clutch was engaged while the participant's leg was flexed to the peak flexion angle (θ_{r2}= ROM_{max}). To resist bidirectionally, the springs were placed into both cylinders (k_1 and k_2) and the clutch on the first cylinder was engaged at ROM_{min} while the clutch for the second cylinder was engaged at ROM_{max}; hence, the resting position of the device was now located in the center of the range of motion (θ_R=(ROM_{max}−ROM_{min})/2=33 deg) and the spring stiffness (k_{eff}) was doubled so that the peak device moments matched those of the flexion and extension conditions.

5.2.3.2 Experiment 2: Aftereffects Following Adaptation

Experiment 2 occurred on a separate day; however, the protocol (Figure 5.2 Right) and experimental setup were very similar to the first experiment. Following the no resistance trial, we configured the device to resist knee flexion using a medium stiffness spring (k= 0.362 N m deg^{-1}). The participant then walked on the treadmill for 300 s with resistance and visual feedback. Once 300 s had elapsed, we stopped the treadmill then removed the resistance and feedback. The participant was then instructed to walk in a manner that feels natural, and they walked for an additional 30 s while we measured the aftereffect. The participant then received a break (120 s), after which he walked again for 300 s without resistance to wash-out any lingering effects from the previous condition. Following the washout, we repeated this procedure for the Extension and Bidirectional configurations.

5.2.4 Data Processing

5.2.4.1 Benchtop Validation of the Device

Throughout the benchtop validation experiments, torque and position data were recorded from the dynamometer at a frequency of 100 Hz. These data were then imported into MATLAB for processing (vR2019a, MathWorks, Natick, MA, US). For each spring, we performed a linear regression to find the slope relationship (i.e., spring stiffness k) between the output torque and the angle of the device. These measured values were then compared with those provided by the spring manufacturer. Additionally, we calculated Pearson's correlation coefficient, and slope of the regression line, and coefficient of variation between the two sets of calibration data in order to measure repeatability (see Appendix B.4 for details). For validating our ability to alter the resting position of the device, the torque data were plotted against the angle of the device. We

then measured the angle at which the torque crossed zero and compared that with the predicted value determined using Equation 5.2.

5.2.4.2 Evaluation of the Device During Treadmill Walking

Electromyography

The amplitude of surface EMG was used to determine how the device's various loading configurations could alter muscle activation during walking. Raw EMG data were collected in Qualisys Track Manager (QTM) and sampled at 2000 Hz. Using a custom LabVIEW program, these raw data were band-pass filtered (20-500 Hz), rectified, and smoothed using a zero phase-lag low-pass Butterworth digital filter (8th order, 6 Hz). The resulting EMG profiles were then normalized using maximum voluntary contractions; hence units were expressed as a percentage of this activation (% MVC). We ensemble averaged the EMG data across strides to compute mean EMG profiles during each trial. Strides were determined to begin at heel-strike. Processed EMG data for all muscles can be downloaded at: http://neurro-lab.engin.umich.edu/downloads (Experiment 1 EMG Data).

Device Moments and Powers

The torque and power that the device generated was calculated using the calibrated spring constants and the encoder data from the device. During each trial involving the leg brace, we collected the device angle from the encoder at a rate of 62.5 Hz using a custom LabVIEW program. For processing, we upsampled the encoder data to 2000 Hz, so that it matched the force plate data. We then performed a numerical derivative on the angle data to calculate the angular velocity. We used Equation 5.3 to estimate the output torque, then multiplied this torque by the

angular velocity to estimate power. These data were segmented into strides and ensemble averaged to yield a profile representing the average torque and power for each trial.

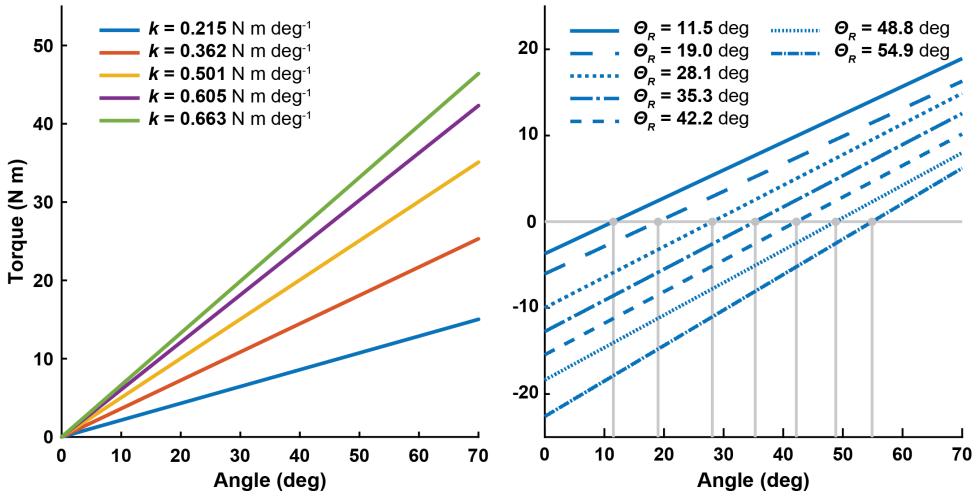

Figure 5.3 Results from benchtop testing. (Left) The stiffness of the calibrated springs (***k***) is indicated by the slope of a linear fit. (Right) The subassemblies were configured to alter the resting position ($\boldsymbol{\theta_R}$) of the device. The angle where the torque crossed zero using the lightest spring (***k***=0.215 N m deg^{-1}) is indicated with a vertical line extending down to the x-axis. In both plots, the y-axis indicates torque and the x-axis indicates the angle as measured with the dynamometer.

Kinematics and Kinetics

Motion capture and force plate data were collected using QTM and sampled at 200 Hz and 2000 Hz, respectively. Gaps in the motion capture data were filled and markers were labeled in QTM. These data were then exported to Visual3D (C-Motion Inc., Germantown, MD, US) for further processing (see Appendix B.2.3 for full details). Briefly, skeletal models were constructed from the static trials (see Appendix B.2.2 for details) and applied to the dynamic walking trials. The marker position data and force plate data were low-pass filtered using a zero phase-lag Butterworth digital filter (6 Hz) to remove motion artifacts and high frequency noise due to the treadmill motors, respectively. From these filtered data, we then computed the sagittal plane kinematics and kinetics (internal moments and powers) of the hip, knee, and ankle joints of the right leg (the leg that was wearing the brace). These data were segmented at heel-strike and ensemble averaged across strides. We then subtracted the average device moment and power

from the knee data to account for the device's contribution. Processed kinematics and kinetics data (for all joints) can be downloaded at: http://neurro-lab.engin.umich.edu/downloads (Experiment 1 Biomechanics Data). Note that only kinematics from the aftereffect trials were compared for experiment 2.

5.3 Results

5.3.1 Benchtop Validation of the Device

Calibration curves for the individual springs can be found in Figure 5.3 (Left). These data are compared with theoretical stiffnesses (based on the factory spring calibrations) in Table B.1. Overall, the results indicated that the stiffness parameters (k_i) of the device could be accurately altered in evenly spaced increments (approximately 0.112 N m deg^{-1} change in stiffness between springs). On average, the absolute percentage error in spring stiffness measured from the device, when compared with our theoretical calculations, was 9.8%. Interestingly, our measured stiffnesses were higher than theoretical for the smaller springs, and lower than theoretical for the larger (stiffer) springs. These errors likely occurred due to hysteresis caused by friction in the system, or deformation of the system, respectively (Figure B.3). Additionally, these characterization curves were repeatable over two cycles of loading (see Appendix B.4).

Additionally, we validated the ability to change the resting position of the device (θ_R). A linear fit of these data can be found in Figure 5.3 (Right). We then compared our measured resting position with the theoretical resting position calculated based on Equation 5.6 (Table B.1). On average, the absolute difference between our measured values and the theoretical values was 1.9 deg. This is much smaller than the minimum increment of the ratchet gear, 15 deg.

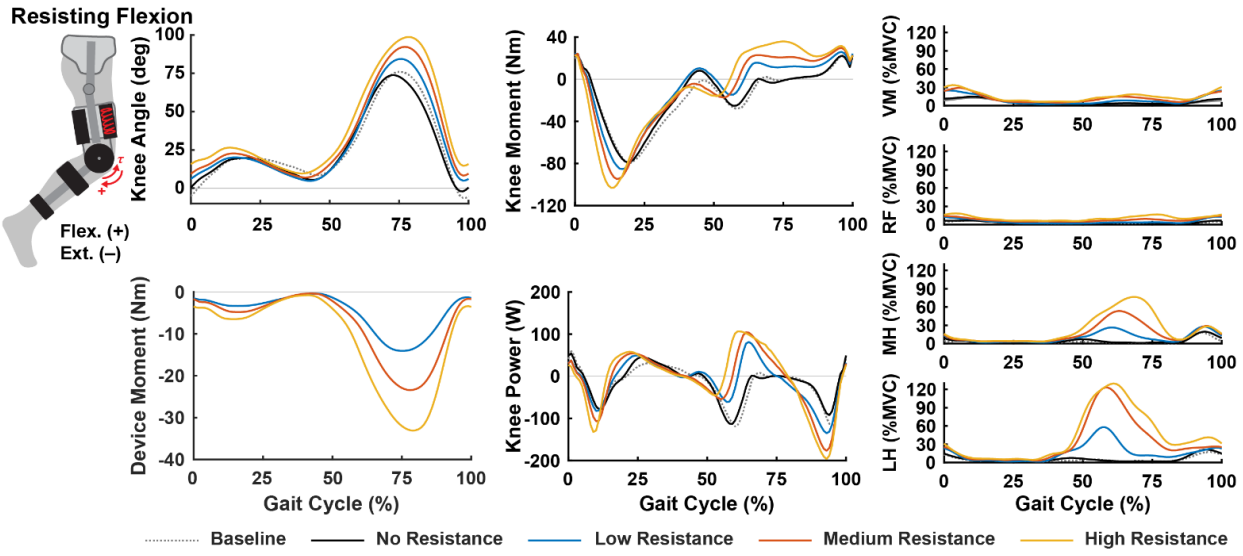

Figure 5.4 Gait biomechanics and electromyography while walking with the device set to resist knee flexion. The device was configured to provide three levels (Low, Medium, and High) of resistance to the leg during flexion (i.e., the device was providing an extension torque). The diagram at the top left shows the sign convention for angles and moments. Positive knee powers indicate the joint was generating power (i.e., contracting concentrically) while negative powers indicate the joint was absorbing power (i.e., contracting eccentrically). Plots on the far right show the muscle activation of the quadriceps (vastus medialis [VM], rectus femoris [RF]) and hamstring muscles (medial hamstring [MH], and lateral hamstring [LH]). In all plots, the x-axis indicates the percentage of the gait cycle over a stride. Units: deg = degrees, Nm = newton meters, W = watts, %MVC = percentage of maximum voluntary contraction.

5.3.2 Experiment 1: Device Performance during Walking

5.3.2.1 Resisting Flexion

Walking with the device set to provide *no resistance* did not have a large effect on any of the metrics measured in this experiment when compared with baseline walking (Figure 5.4). When resisting flexion, the device output max resistances of 14.1, 23.4, and 33.1 Nm for the low, medium, and high resistances, respectively. The peak resistance occurred during early swing, where knee flexion is typically the largest. Consequently, we found the knee flexion moment was increased during the swing phase. Surprisingly, the knee extension moment increased during the stance phase—a movement that should have been assisted during this condition. We believe this occurred because the knee was flexed at heel-strike; hence, knee extension had to counteract the bodyweight. Interestingly, we saw that the joint power was more negative (i.e., absorption

increased) during early stance and late swing. Meanwhile, joint power was more positive (i.e., generation increased) during the early swing phase. Muscle activation of the hamstrings was increased during late stance and throughout the swing phase of gait. Quadriceps muscle activation was slightly increased during early stance.

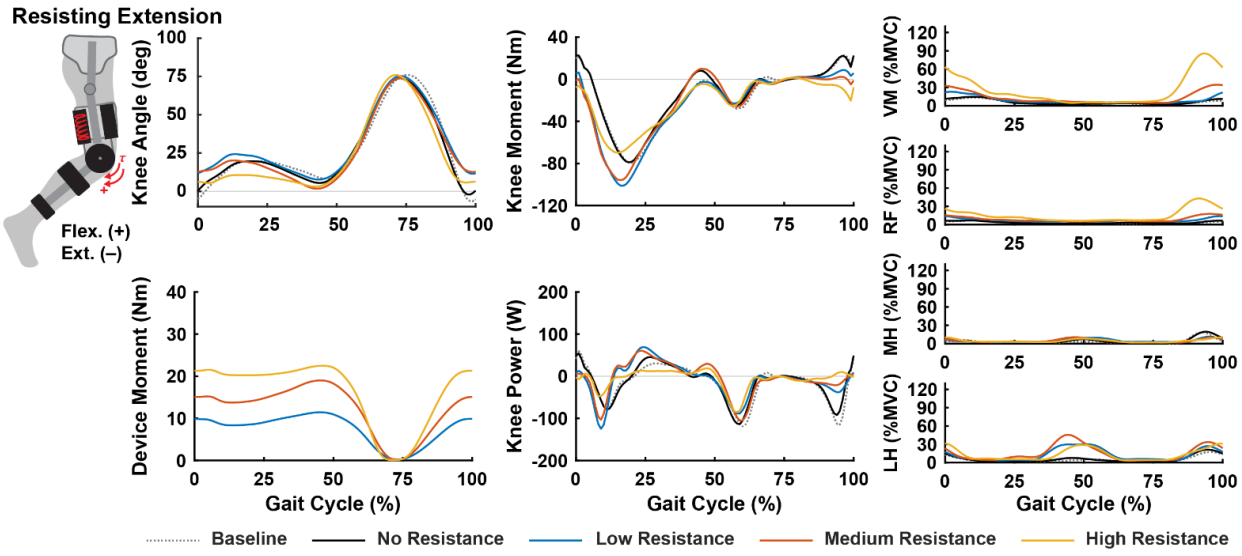

Figure 5.5 Gait biomechanics and electromyography while walking with the device set to resist knee extension. The device was configured to provide three levels (Low, Medium, and High) of resistance to the leg during extension (i.e., the device was providing a flexion torque). The diagram at the top left shows the sign convention for angles and moments. Positive knee powers indicate the joint was generating power (i.e., contracting concentrically) while negative powers indicate the joint was absorbing power (i.e., contracting eccentrically). Plots on the far right show the muscle activation of the quadriceps (vastus medialis [VM], rectus femoris [RF]) and hamstring muscles (medial hamstring [MH], and lateral hamstring [LH]). In all plots, the x-axis indicates the percentage of the gait cycle over a stride. Units: deg = degrees, Nm = newton meters, W = watts, %MVC = percentage of maximum voluntary contraction.

5.3.2.2 Resisting Extension

During this condition, the device output maximum resistances of 11.4, 19.0, and 22.5 Nm for the low, medium, and high resistances, respectively (Figure 5.5). This peak occurred during the stance and late swing phases, where the knee is extended. Generally, the device increased the knee extension moment during the stance and the late swing phase. Joint power was more negative during the early stance phase (i.e., absorption increased). During late swing, a period of the gait cycle where the hamstrings usually act eccentrically, we saw less power absorption.

Muscle activations of the quadriceps muscles were greatly increased during early–mid stance and late swing. The hamstrings showed some increased muscle activation during late stance.

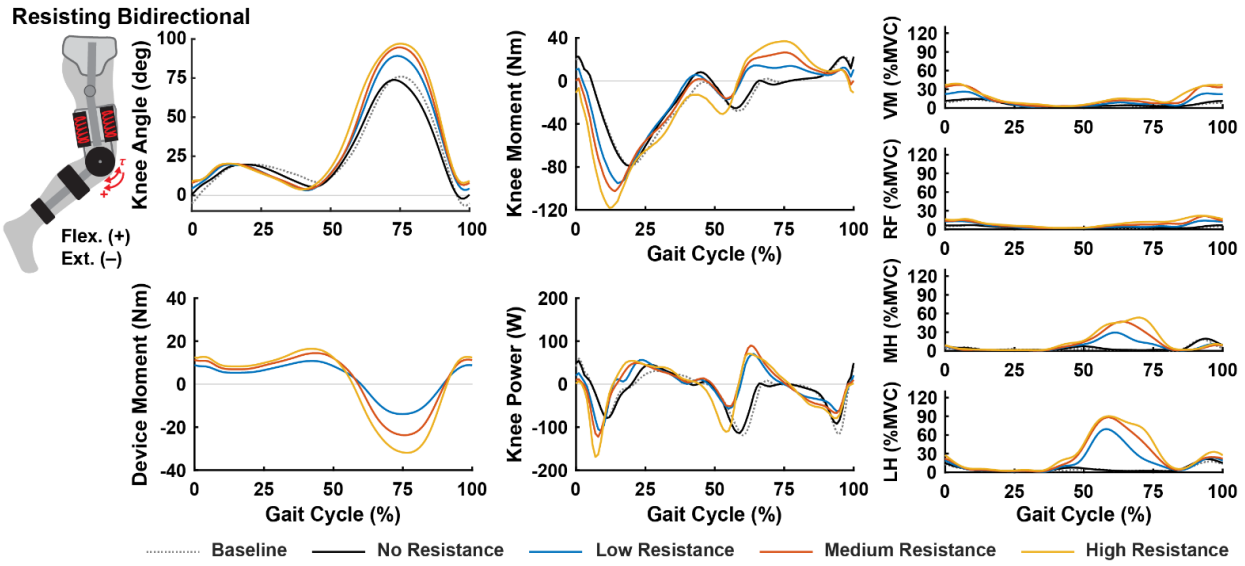

Figure 5.6 Gait biomechanics and electromyography while walking with the device set to resist the knee bidirectionally (i.e., resisting both flexion and extension). The device was configured to provide three levels (Low, Medium, and High) of bidirectional resistance. The diagram at the top left shows the sign convention for angles and moments. Positive knee powers indicate the joint was generating power (i.e., contracting concentrically) while negative powers indicate the joint was absorbing power (i.e., contracting eccentrically). Plots on the far right show the muscle activation of the quadriceps (vastus medialis [VM], rectus femoris [RF]) and hamstring muscles (medial hamstring [MH], and lateral hamstring [LH]). In all plots, the x-axis indicates the percentage of the gait cycle over a stride. Units: deg = degrees, Nm = newton meters, W = watts, %MVC = percentage of maximum voluntary contraction.

5.3.2.3 Resisting Bidirectionally

During the bidirectional resistance condition, the device succeeded in providing both flexion and extension resistances (Figure 5.6). During this condition, the device output maximum extension torques (i.e., resisting flexion) of 13.9, 23.7, and 31.9 Nm, and maximum flexion torques (i.e., resisting extension) of 10.8, 14.4, and 16.4 Nm for the low, medium, and high resistances, respectively. On average, the bidirectional resistance was 10% below what was seen during the unidirectional resistance conditions, and these discrepancies were more pronounced when resisting extension. All springs elicited increases in knee extension moment during the early stance phase and knee flexion moment during early–mid swing. The extra knee extension moment during the stance phase led to more negative power (i.e., absorption increased) after

heel-strike, followed by an increase in positive power (i.e., increased generation) in early-mid stance. These were paralleled by increases in quadriceps muscle activation at these phases. At the beginning of the swing phase joint power was more positive (i.e., generation increased), which was paralleled by large increases in hamstring muscle activation.

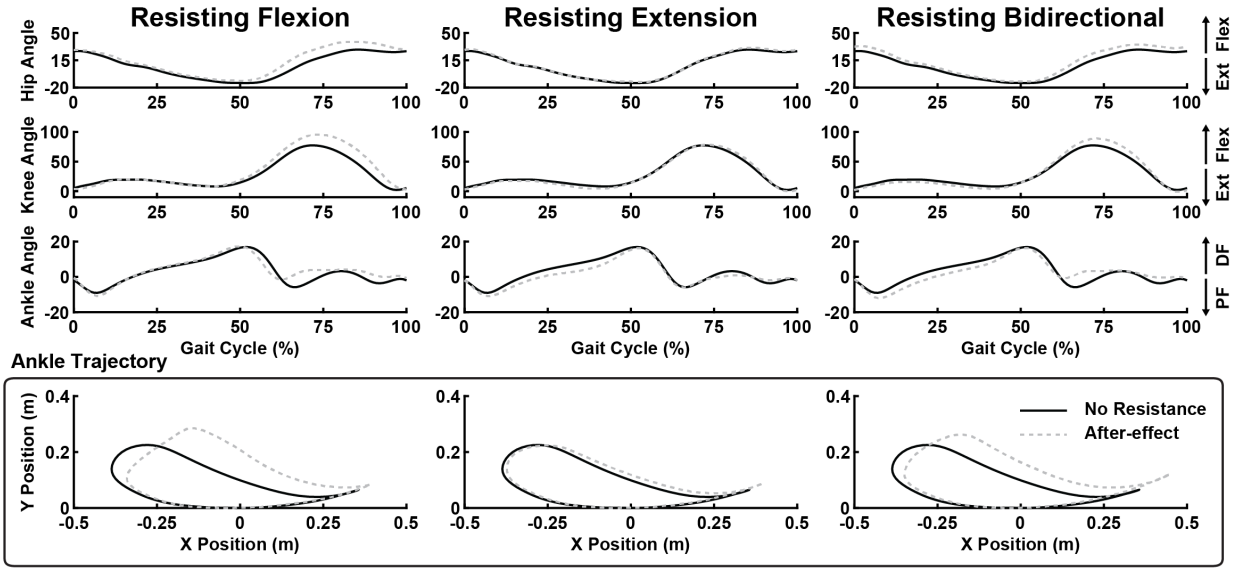

Figure 5.7 Kinematic aftereffects following the removal of resistance. Comparing the kinematics before and after a training allowed us to measure the aftereffects for each resistance configuration. The top three rows depict the sagittal hip, knee, and ankle joint angles. The y-axis indicates the angle in degrees, while the x-axis indicates the percentage of the gait cycle over a stride. The bottom row depicts the sagittal ankle trajectories (i.e., the path that the ankle traveled) relative to the hip and offset from ground. In these plots, the y-axis indicates movement in the vertical direction (in meters), while the x-axis indicates movement in the anterior-posterior direction. Hence, an increase in y means the foot was being lifted higher, while an increase in x-excursion could indicate a larger step length.

5.3.3 Experiment 2: Aftereffects Following Adaptation

Removing the resistance and visual feedback resulted in kinematic aftereffects that varied based on the type of resistance provided (Figure 5.7). After walking with resistance to knee flexion, hip and knee flexion angles increased and the ankle was more dorsiflexed throughout the swing phase when compared with the walking with no resistance. When viewed as an ankle trajectory, the participant was lifting their foot higher during the swing phase. Walking with resistance to knee extension resulted in increased knee extension and ankle plantarflexion during the stance phase of the aftereffect trial. The ankle trajectory aftereffect had a larger x-excursion,

indicating a longer step length. Walking with bidirectional resistance appeared to combine the effects seen in the flexion and extension conditions. Hip flexion, knee flexion, and ankle dorsiflexion increased during the swing phase, while knee extension and ankle plantarflexion increased during the stance phase. This resulted in an ankle trajectory where the foot was lifted higher and step length was larger. Notably, knee kinematics returned to the levels seen during the no resistance trial following the washout trials (Figure B.4).

5.4 Discussion

The goal of this research was to develop a unique exoskeleton device that could provide various types of elastic resistance during walking. Subsequently, we created a novel elastic mechanism then fit the resulting device to a hip and knee orthosis, so as to provide resistance to the knee. During benchtop validation, we found the elastic mechanism could provide a nearly linear torque profile, and the device could be configured to alter the resting position of the spring system with high accuracy; thus, permitting resistance to flexion, extension, or both (i.e., bidirectionally). When validating during treadmill walking, we found that these resistance configurations could be used to target preferentially knee flexion, extension, or both. Moreover, the device could be used to increase power absorption at the joint, which could be used to eccentrically load the leg muscles. Lastly, once the resistance was removed, the different resistance configurations elicited different kinematic aftereffects. Thus, elastic devices such as this could serve as a diverse tool for functional resistance training paradigms aimed at targeting specific weaknesses or kinematic outcomes.

Through the treadmill walking validation experiment, we found that the resistance configurations could be used to target resistance to their respective joint motions. Specifically, while resisting knee flexion, the device increased knee flexion moment and hamstring activation

during the swing phase; while resisting knee extension, the device increased knee extension moments and quadriceps activation during the early stance and late swing phases; and under a bidirectional resistance, the device increased both flexion and extension moments and activated each muscle group at their respective times. These were exciting findings, as most elastic devices are not capable of providing this level of targeted resistance; instead, they are limited to resisting a single joint motion (Cherry et al., 2006; Cherry et al., 2016; Mankala et al., 2009; Shamaei et al., 2014; Sulzer et al., 2009). Additionally, we found this device could return energy to the user, which could be used to elicit eccentric contractions. This was clearly demonstrated during the late swing phase when the device was resisting knee flexion, as we found increased power absorption at the knee paired with increased hamstring activation. Hence, the hamstrings could have been acting eccentrically at that time.

The second walking validation experiment measured the aftereffects produced after training with the device. Aftereffects are believed to contain information about how the nervous system is adapting (Gordon et al., 2013; Morton & Bastian, 2006; Shadmehr & Mussa-Ivaldi, 1994) and may serve as a marker for potential therapeutic gains, as aftereffects have been seen to transfer to overground walking (Regnaux et al., 2008; Reisman et al., 2009). In our experiment, we measured the kinematic aftereffects (i.e., changes in hip and knee angles, and ankle trajectory) elicited by the three different resistance configurations as the user received visual feedback. We found that resisting flexion increased hip and knee flexion, which resulted in a higher step height; resisting extension increased knee extension, which resulted in an increased step length; and resisting bidirectionally combined these effects to produce a higher step with longer length. Hence, the different device configurations could be used to elicit different control strategies for walking, and perhaps, the device configuration could be selected to treat patient-

specific gait deficits. However, we would like to note that the aftereffects we observed are likely a result of the combined resistance and visual feedback. Further, research on a larger group of patients would be needed to elucidate the added effects of visual feedback and to demonstrate the cumulative effects of repeated training with the device.

While the device mostly performed as intended, we also saw that performance reduced when storing large amounts of energy. During use, the device stored up to 28.35 J of energy (equivalent to lifting a 100 kg mass 3 cm). Under such high-energy conditions, we saw (1) errors between the theoretical and measured stiffnesses of springs during benchtop testing, and (2) diminished device moments with stiff springs during treadmill walking. Concerning (1), some errors arose in the form of hysteresis during loading/unloading due to friction between the plunger and cylinder (Figure B.3). While only a small amount of friction was present at low loads, the problem was worse at high loads. This did not affect the functionality of the device, but friction could influence how the device feels to the user. Another source of error that could have contributed to (1) is the deformation of structural components within the device under large loads, which led to nonlinearity in the stiffness profile (and an underestimation of stiffness, Figure B.3). Regarding (2), deformation of the leg brace components (i.e., the custom orthoses) hindered the devices ability to convey forces to the leg during walking. This was especially prominent when the device was resisting extension (Figure 5.5). While walking, the large amount of energy stored by the device caused soft tissues and padding on the brace to compress, which caused the brace joint to shift relative to the participant's leg. When this happened, the device was unable to output a torque that scaled relative to the spring stiffness. Hence, when resisting extension, although the spring stiffness scaled by 38% between the medium and high

stiffness conditions, the peak device moment only scaled by 18%. However, many of these problems can be addressed with future iterations of the device.

While the current prototype provides a good starting point for this device, there are many alterations that could be incorporated into future iterations to improve general usability and expand the capabilities of the device. To improve usability, future iterations could minimize friction in the device, either by using a more rigid material for the cylinder or changing the type of spring so a cylinder is not needed (e.g., extension springs). However, we note that there are many benefits of compression springs (e.g., large force/deflection capability, small footprint, safety) that could outweigh the drawbacks of other types of springs (e.g., fragile, difficult to interface with, etc.). Additionally, the leg braces we used were never intended to convey external forces to the leg. Rather, they are typically used to limit range of motion after surgical procedures. Hence, forces could be better conveyed to the leg if the brace were designed to fit more snugly and contact bony places on the leg. Finally, there are a few alterations that could expand the capabilities of the device. First, the resistance of the device could be put under computer control. Typically, it is difficult to control elastic systems, as control is achieved by exchanging the spring or adding pre-tension, which requires a lot of power. This is a drawback to elastic devices and a reason why viscous devices are intriguing, as they offer more potential to be continuously controlled (Washabaugh et al., 2016; Washabaugh et al., 2019). However, with this elastic brace, computer control could be achieved by controlling the clutches similar to an elastic device that has been used to reduce knee loading (Shamaei et al., 2015). This modification would allow the device to remain passive (as power would not be introduced to the user) and would greatly increase the likelihood of the device being worn during everyday life. Lastly, the current device can be adapted to provide resistance to other joints and during other functional tasks.

Although providing resistance to walking was the goal of this paper, the potential for such a device is far-reaching.

5.5 Conclusion

In this study, we developed a unique exoskeleton device to provide elastic resistances to the knee during walking. The elastic mechanism we designed allowed us to alter the stiffness of the device and control the resting position of the spring system. Thus, the device could be configured to provide resistance to joint flexion, extension, or bidirectionally. During walking, these configurations were shown to target specific joint motions and muscle groups. Additionally, the device was able to increase power absorption at the joint, which is atypical for many resistive leg braces. Lastly, the different resistance configurations elicited different kinematic aftereffects. Hence, such elastic devices could serve as a diverse tool for functional resistance training paradigms.

5.6 Acknowledgment

This work has been published in Transactions on Biomedical Engineering (Washabaugh, Augenstein, Ebenhoeh, et al., 2020). I would like to thank my co-authors on this article: Thomas E. Augenstein, Alissa M. Ebenhoeh, Jiajie Qiu, Kaitlyn A. Ford, and Dr. Chandramlouli Krishnan, for their contributions to the design of the device, data collection, data processing, and drafting/editing of the manuscript. This work was supported in part by the National Institutes of Health (Grant R21 HD092614), the National Science Foundation (Grant DGE 1256260), and the UM-BICI Collaboratory Initiative. Any opinions, findings, and conclusions or recommendations expressed in this material are those of the authors and do not necessarily reflect the views of the funding sources. I would also like to thank Justin Lee for helping with designs, Jeffrey Wensman

and the Orthotics and Prosthetics Center for procuring custom leg bracing, and Jim Tice and the LSA Scientific Instrument Shop for their guidance and the use of their equipment.

Chapter 6

Comparing how the Resistance Type and Targeted Joint Acutely Affects Functional Resistance Training during Walking

Abstract

Applying resistance to the leg during walking is an emerging approach that is being used to rehabilitate individuals with neuromuscular or orthopedic injuries. When this training is applied using a wearable exoskeleton or leg brace, resistance can be targeted to a weakened leg joint. However, the kinetics of training with these devices can vary greatly based on the type of resistance that is used. Hence, this study was designed to examine how functional resistance training of walking differs while using viscous and elastic resistances, or when targeting the hip or knee joints. Fourteen able-bodied individuals came into the lab on separate visits at least 96 hours apart, where they were trained with either a device that provided viscous resistance to the knee, elastic resistance to the knee, or viscous resistance to the hip and knee in a bidirectional (i.e., targeting joint flexion and extension) manner. We measured gait biomechanics and muscle activation during training, as well as kinematic aftereffects and changes in peripheral fatigue and neural excitability after training. We found that the resistance type and targeted joints differentially altered gait kinetics during training. However, these differences did not translate to device-specific differences in aftereffects, peripheral fatigue, or neural excitability. Instead, each group showed similar changes in these variables. The results of this study demonstrated how different resistance types can be used to alter gait biomechanics during functional resistance

training. Although we did not find resistance-specific changes in neural adaptation following an acute training session, it is still possible that prolonged training could produce differential effects.

6.1 Introduction

Resistance training is a widely used approach for promoting strength and recovery during physical therapy (Cramp et al., 2006; Flansbjer et al., 2008; Lima et al., 2013; Liu & Latham, 2009; Pak & Patten, 2008). However, there are many different types of resistive loads that can be used for strength training. For example, clinics may use free weights, elastic resistance bands, pneumatic/hydraulic exercise machines, or even pools to apply resistance during training (Stoeckmann et al., 2009). When training with these different methods, the kinetics of the training are going to vary greatly depending on the type of resistive element that is used (Stoeckmann et al., 2009). For example, free-weight-based resistances depend on the acceleration of the movement, elastic resistances scale based on the position, and viscous resistances depend on velocity. Undoubtedly, these types of elements yield resistances that differ in how they engage the muscles during use and how they feel to the user. Because of these differences, it is often debated which type of resistance is most beneficial for certain exercises or types of training (Aboodarda et al., 2016; Anderson et al., 2008; Brandt et al., 2013; Lima et al., 2018; Stoeckmann et al., 2009).

Functional resistance training is a technique that is frequently used in clinics to combat the strength deficits and functional limitations that follow ageing or neural and orthopedic injuries. It is administered by having patients perform a functional task (e.g., converting between a sit and a stand) while additional loading is used to make the task more difficult (Blundell et al., 2003; Donaldson et al., 2009; Kerr et al., 2017; Lohne-Seiler et al., 2013; Yang et al., 2006). By

design, the task-specific nature of this training should reinforce neural circuits while the resistance strengthens the key muscles used in the task (Carroll et al., 2001; Donaldson et al., 2009; Krebs et al., 2007; Sullivan et al., 2007). Recently this technique has been widely applied to retrain walking. Again, there are many different types of resistive loads, including basic resistive methods that are common in clinics (i.e., weighted cuffs and elastic bands) (Blanchette & Bouyer, 2009; Browning et al., 2007; Duclos et al., 2014; Gottschall & Kram, 2003; Noble & Prentice, 2006) and wearable leg braces/exoskeletons (Blanchette et al., 2014; Conner et al., 2020; Lam et al., 2006; Martini et al., 2019; Noel et al., 2008; Washabaugh et al., 2016; Washabaugh & Krishnan, 2018). Wearable exoskeletons have large promise for this type of training because they can target the resistance to a weakened leg joint and give therapists greater control over the treatment. However, there are two important questions to be considered when using these devices: 1) what type of resistance should be applied and 2) to which joints should resistance be applied.

While there are numerous types of resistances that can be applied for functional resistance training during walking, wearable exoskeleton devices have commonly provided resistances that behave as viscous (Lam et al., 2006; Washabaugh et al., 2016; Washabaugh & Krishnan, 2018) or elastic (Blanchette et al., 2014; Washabaugh, Augenstein, Ebenhoeh, et al., 2020). The widespread use of viscous resistances is not surprising, as viscous resistances have the benefits of smoothness and safety. However, because viscous resistances are velocity-dependent, they are only able to resist muscles during concentric contractions (i.e. the muscle shortens while in tension). Meanwhile, elastic resistances are position-dependent, which makes them capable of resisting both concentric and eccentric contractions (i.e. the muscle shortens while in tension) during functional resistance training (Washabaugh, Augenstein, Ebenhoeh, et

al., 2020). Such differences could alter several aspects of training. For example, when comparing concentric and eccentric training, concentric contractions have been found to acutely increase muscular fatigue (Pasquet et al., 2000), while the cumulative effects of eccentric training have been found to better promote strength (Kaminski et al., 1998; Roig et al., 2009). However, no studies have directly compared the effects of functional resistance training during walking with different types of resistances.

There is a similar paucity of research examining the joint that is targeted for functional resistance training during walking. While there have been studies that have targeted the hip (Houldin et al., 2012; Houldin et al., 2011), knee (Diaz et al., 1997; Washabaugh, Augenstein, Ebenhoeh, et al., 2020; Washabaugh et al., 2016; Washabaugh & Krishnan, 2018), both the hip and the knee (Klarner et al., 2013; Lam et al., 2006; Zabukovec et al., 2013), and the ankle (Barthélemy et al., 2012; Blanchette et al., 2011; Conner et al., 2020), no studies have directly compared any of these training methods. Ultimately, the joint that is targeted could be of more importance than the type of resistance that is provided, as each joint has a specific role in the control of walking (Whittle, 2007). Moreover, neuromuscular injuries often affect one or many of these joints at a time. For example, individuals recovering from an anterior cruciate ligament injury will have greater weakness in the muscles surrounding the knee (Arangio et al., 1997; Palmieri-Smith & Lepley, 2015), while a neurological injury (such as stroke) may have weakness down the entire leg (Awad et al., 2020; Lomaglio & Eng, 2008; Mulroy et al., 2003). However, it can be difficult to convey large resistances to the leg using wearable exoskeleton devices. Hence, research in this area would help determine how specific injuries could be treated and identify future areas for resistive exoskeleton development.

In this study, we ran two experiments to compare different methods for functional resistance training during walking. In the first experiment, we compared how elastic and viscous resistive elements differ in their ability to provide bidirectional (i.e., resisting both flexion and extension) resistance to the knee during walking. In the second experiment, we compared training with different joint configurations of the viscous device—we provided bidirectional resistance to either the knee or both the hip and knee together. During both experiments, resistive strategies were compared acutely (i.e., after a single training session) based on how they altered gait biomechanics and muscle activation during training, as well as kinematic aftereffects, peripheral fatigue, and neural excitability after training. In both experiments, we hypothesized that the resistance type or device configuration would alter kinetics and muscle activation during training. Also, that kinematic aftereffects, peripheral fatigue, and neural excitability would be altered based on these training effects. Specifically, in experiment 1, we hypothesized the elastic resistance would resist the quadriceps during the stance phase when compared with training with the viscous resistance. Hence, the elastic device would produce greater peripheral fatigue and changes in neural excitability of this muscle group. In experiment 2, we hypothesized that the hip-knee configuration would increase the hip extension moment and hamstring activation during the stance phase and would also increase hip flexion moment and quadriceps activation during the swing phase when compared with the knee configuration. Hence, the hip-knee configuration would produce larger changes in aftereffects, peripheral fatigue, and neural excitability for these joint movements/muscle groups.

6.2 Materials and Methods

Fourteen healthy individuals participated in the study (Table 6.1). All participants were determined to be right leg dominant based on which leg they preferred to use to kick a ball

(Krishnan & Williams, 2014). Prior to the study, all participants reviewed and signed an informed consent document approved by the University of Michigan Institutional Review Board (HUM00093673, approved on 5/24/2018). After signing the informed consent, participants were required to complete four testing sessions.

Table 6.1 Demographic information, strength, and overground gait velocity

Participant	Sex	Age	Height	Mass	Hip Ext	Hip Flex	Knee Ext	Knee Flex	Gait Speed
		(yr)	(cm)	(kg)			(Nm)		(m/s)
1	F	21	163	54	87.7	97.9	187.8	71.0	1.71
2	F	20	168	64	80.6	86.8	148.6	88.1	1.36
3*	F	21	168	59	71.0	114.4	151.6	101.0	1.22
4	M	22	173	74	97.8	103.8	201.1	125.8	1.32
5	M	18	173	68	80.6	107.4	156.7	122.1	1.18
6	F	22	175	68	74.0	92.6	137.4	70.3	1.33
7	F	26	163	50	70.6	79.3	170.5	89.5	1.89
8	F	20	160	68	92.8	123.1	170.1	99.3	1.26
9	F	18	172	59	56.6	64.3	131.8	83.5	1.38
10	F	20	158	53	64.6	72.6	100.5	54.8	1.36
11*	M	25	185	80	157.5	166.5	282.9	161.3	1.66
12	M	24	185	93	126.5	151.4	299.2	142.3	1.39
13	M	19	180	66	108.4	144.6	185.0	126.9	1.43
14	M	22	180	77	133.4	119.4	242.6	145.1	1.65
Average		21	172	67	93.0	108.9	183.3	105.8	1.44
Average*		21	171	66	89.5	103.6	177.6	101.6	1.44

* Participants were excluded from biomechanics data analysis because of either an equipment malfunction or the participant misunderstood instructions.

6.2.1 Preliminary Session

Prior to training, we measured the participant's strength and self-selected walking speed. Strength of the right (training) leg was measured by having participants perform maximum voluntary isometric contractions (MVICs) of the knee and hip extensors and flexors while in a Biodex dynamometer (System Pro 4, Biodex, Shirley, NY). When measuring knee strength, participants were seated and fastened in the dynamometer with their hip at 85 degrees and their right knee fixed at 45 degrees of flexion. When measuring hip strength, participants stood upright as the arm of the dynamometer was aligned with their hip joint center and affixed to their thigh. During contractions, participants stabilized themselves by holding firmly to a rigid portion of the dynamometer. Participants warmed up by performing submaximal contractions of 25%,

50%, and 75% of their perceived maximum. Participants then performed three MVICs for each movement which were averaged to represent strength (Table 6.1). Between MVICs participants were given 120 s of rest.

Self-selected walking speed was measured using the 10-meter walk test, where participants walked on a 12-meter straight walkway, while a stopwatch was used to time the intermediate 10-meter walk. The average of three 10-meter walk tests was used to calculate self-selected walking speed (Table 6.1). Participants were given at least four days of rest between laboratory visits.

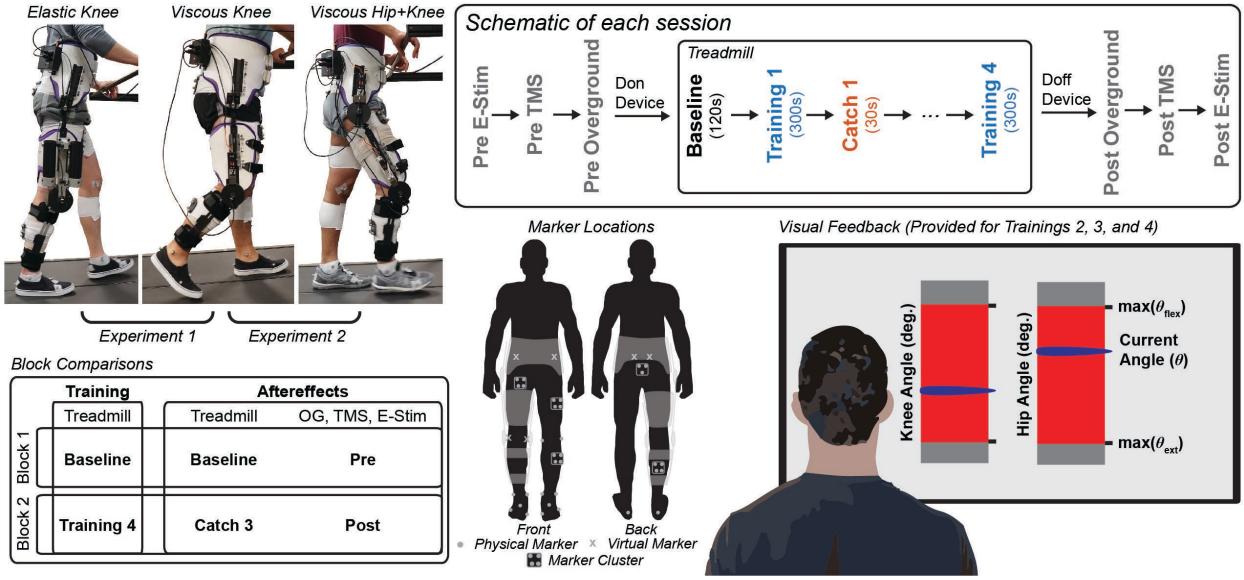

Figure 6.1 Summary of the training protocol. Participants came to the lab for three training sessions that differed based on the resistive method that was used for functional resistance training during walking (Top Left), including a viscous resistance at the knee, elastic resistance at the knee, or viscous resistance to the hip and knee. All devices operated in a bidirectional manner (i.e., targeting joint flexion and extension). (Top Right) During the training protocol, we used electrical stimulation of the thigh muscles to measure peripheral fatigue (E-Stim) and transcranial magnetic stimulation (TMS) to measure neural excitability. We measured normal gait kinematics while the participant walked overground and during a baseline trial on the treadmill. The participant underwent four training trials, where they walked with resistance, that were interspersed with catch trials, where they walked with the resistance removed. (Bottom Right) During training trials 2–4 participants received visual feedback based on the joint angles as measured with encoders of the device. They were encouraged to use feedback of their current angle to match their average maximum and minimum joint angles as measured during the baseline trial. (Bottom Middle) A schematic indicating where markers were placed for motion capture, including physical markers and marker clusters, as well as virtual markers that were placed with a stylus if the device obstructed a bony landmark. (Bottom Left) A schematic indicating which blocks were used to identify how resistance type or device configuration would alter kinetics and muscle activation during training, as well as kinematic aftereffects, peripheral fatigue, and neural excitability following training.

6.2.2 Training Sessions

Participants returned to the lab for three additional sessions where, during each session, we trained them using a different method for providing resistance during walking, including walking with a bidirectional viscous resistance at the knee, bidirectional elastic resistance at the knee, and a bidirectional viscous resistance at the hip and knee (Figure 6.1). The order in which participants were exposed to these trainings was pseudo-randomized to minimize the effect that training order could have when comparing the resistances. The protocol for these training sessions can be found in Figure 6.1.

6.2.2.1 Electrical Stimulation

At the beginning of each training session, we evaluated the mechanical properties (i.e., twitch tension) of the quadriceps and hamstring muscles using previously established procedures (Krishnan & Williams, 2011). The skin of the anterior and posterior right thigh was cleansed with alcohol swabs, then a pair of self-adhesive carbon electrodes were placed over the proximal and distal quadriceps (electrode dimensions: 2.75 × 5.0 in) and hamstring muscles (electrode dimensions: 2.0 × 3.5 in). Participants were seated in the dynamometer as they were during strength testing (Figure 6.2), and electrical pulses were delivered using a high-voltage, constant-current electrical stimulator (DS7AH; Digitimer, Hertfordshire, U.K.). During the first session, the current intensity for each participant was determined by stimulating each muscle group at rest with singlet pulses (200-μs pulse duration, 400 V) in sequential steps until the evoked torque failed to increase, but decreased (Krishnan & Williams, 2011). For the quadriceps and hamstrings, sequential stimulations began at 100 mA and 80 mA and were stepped in 100 mA and 20 mA increments, respectively. Once the torque decreased, the current was then reduced by half the step magnitude and a final stimulation was provided. The current that elicited the largest

twitch amplitude was selected for the remainder of the study. Each muscle group was then stimulated with three sets of triplet pulse trains of 20 Hz and we measured the resulting twitch torque from the dynamometer.

6.2.2.2 Electromyography

We then placed electromyography (EMG) surface electrodes (Trigno Avanti, Delsys, Natick, MA, US) over the muscle bellies of several lower-extremity muscles: 1) quadriceps muscles (vastus medialis [VM], vastus lateralis [VL], and rectus femoris [RF]), 2) hamstring muscles (medial hamstring [MH], and lateral hamstring [LH]), 3) an ankle dorsiflexor muscle (tibialis anterior [TA]), 4) ankle plantar flexor muscles (medial gastrocnemius [MG], and soleus [SO]), and 5) a hip abductor muscle (gluteus medius [GM]). These sensors were placed on the right leg according to the established guidelines at www.seniam.org. Sensor positions were slightly altered from established guidelines if the leg brace hindered placement. EMG electrodes were tightly secured to the skin using self-adhesive tapes and cotton elastic bandages.

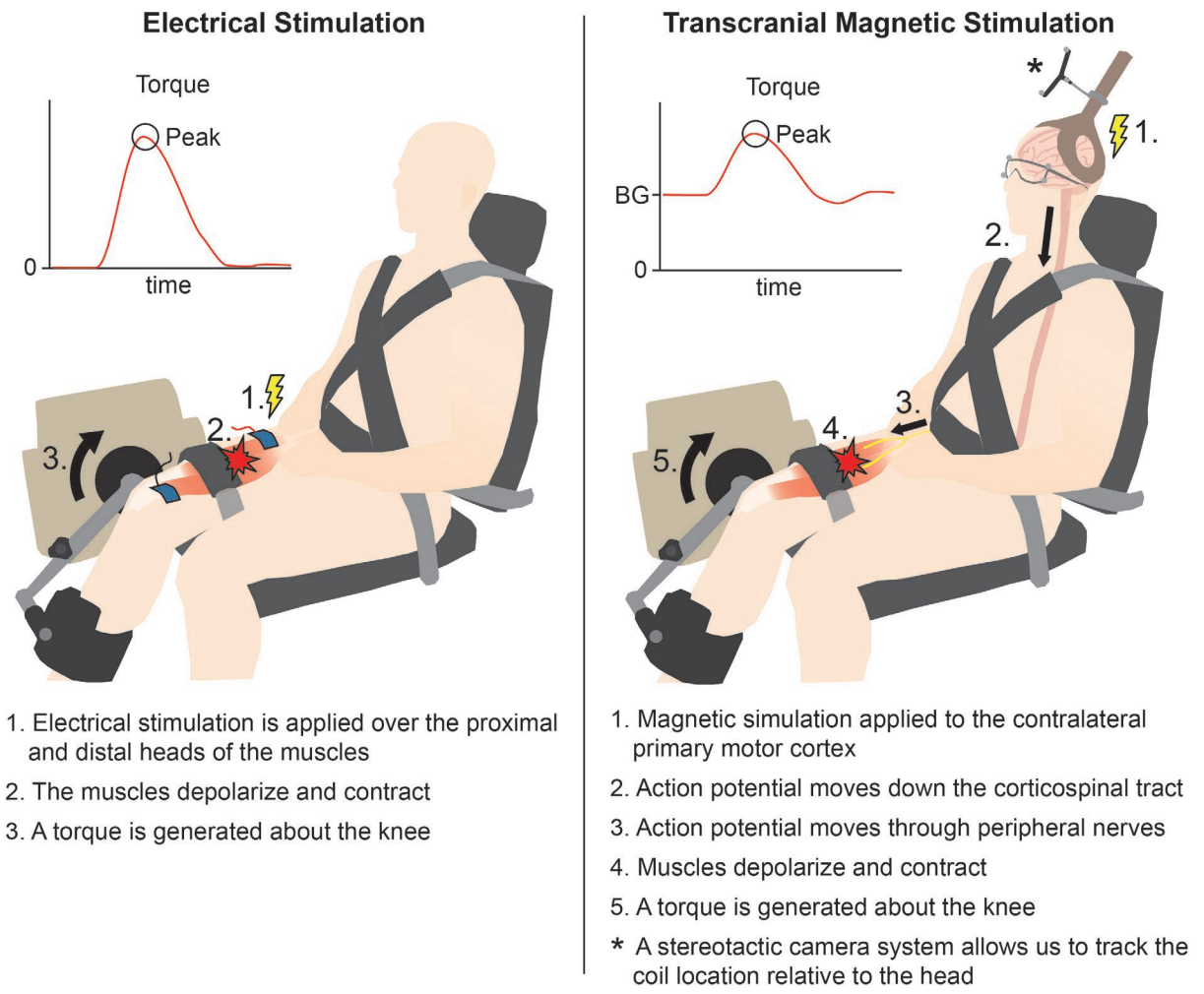

Figure 6.2 Schematic depicting how electrical stimulation and transcranial magnetic stimulation were used to measure peripheral fatigue and neural excitability, respectively.

6.2.2.3 Transcranial Magnetic Stimulation

Transcranial magnetic stimulation was then performed to get a baseline with which to compare neural excitability of the corticospinal tract (Figure 6.2). Again, participants were seated in the dynamometer and TMS was applied during both knee flexion and extension while participants performed a task to match 10% of their MVIC (i.e., a background contraction). Motor-evoked responses were elicited using a Magstim 200^2 stimulator (Magstim Co Ltd, Whitland, UK) via a 110-mm diameter double-cone coil. The coil was oriented to induce a posterior-to-anterior current flow in the cortex. The hotspot location was determined by first

measuring 1.0 cm posterior and 2.0 cm lateral from the vertex, such that the hotspot was contralateral to the leg being tested. From this location, the coil was systematically moved to determine the location that elicited the largest and most consistent motor-evoked responses for both muscle groups (i.e., flexion and extension). This hotspot location was then registered using a stereotactic navigation system that located the coil relative to the participant's scalp (Rodseth et al., 2017). Active motor threshold (AMT) was determined individually for each muscle group as the minimum intensity that elicited a motor-evoked response discernable from background noise with a 60% success rate (i.e., 3 out of 5 stimuli). We then performed 25 stimulations at an intensity of 140% AMT and measured the evoked torque for each muscle group.

6.2.2.4 Motion Capture

Prior to each session, we calibrated the capture volume of our motion capture system (Qualisys Track Manager [QTM], Qualisys, Göteborg, SE), which consisted of 12 infrared tracking cameras (Miqus M3) and two video cameras (Miqus Video), and performed an analog zeroing of our instrumented split-belt treadmill (Bertec, Columbus, OH, US). Following TMS, reflective markers were placed on the legs for motion capture (Figure 6.1); we used the CAST (calibrated anatomical systems technique) lower extremity marker set (Cappozzo et al., 1995). For both legs, individual markers were placed over the anterior and posterior iliac spine, medial and lateral femoral epicondyles, medial and lateral malleoli of the ankle, and at the 1st, 2nd, and 5th metatarsals and calcaneus of the foot. Additionally, marker clusters were placed on the thighs and shanks. In our implementation, because the leg brace obstructed our ability to place physical markers over the iliac spine and right femoral epicondyles, several markers were placed virtually with a stylus; hence, an additional cluster was required on the back of the pelvis to aid in tracking of the virtual iliac spine markers (Washabaugh, Augenstein, Ebenhoeh, et al., 2020). All

individual markers were secured to the leg using self-adhesive tapes, whereas clusters were secured via hook-and-loop fastener elastic wraps (MediWrap, fabrifoam, Exton, PA, US).

Once markers were placed, we collected a static trial where the participant stood upright and motionless on the treadmill as the cameras recorded the positions of the physical markers. With each static trial, we also performed a pointer trial, where the participant remained upright as we used a stylus (a calibrated rigid body) to indicate the positions for virtual markers. During this pointer trial, an event was created in the motion capture software (i.e., the time point was saved) when the stylus was in the correct position for each virtual marker.

6.2.2.5 Overground Walking

Participants walked overground as we measured gait kinematics to see if any aftereffects transferred to overground walking. Overground walking took place on a 6 m long walkway that was integrated with the instrumented treadmill. Participants traversed the walkway two times as we measured kinematics.

6.2.2.6 Training

We then assisted the participant in donning the resistive device for that session. Once the device was fitted properly, we performed a second static trial, then a baseline trial where the participant walked on the treadmill for a duration of 120 s while wearing the device with no resistance (i.e., with the magnet exposure removed from the disk or with the springs disengaged). The treadmill speed was set to 60% of the participant's self-selected walking speed (Table 6.1) for all treadmill trials. For safety purposes, participants were permitted to rest their hands on the treadmill's front railing but were instructed to apply minimal pressure.

Finally, participants trained with the device. In total, there were four 300 s training trials interspersed with 30 s catch trials. During each training trial, the resistance of the device was set

for each joint action (i.e., flexion or extension) to be 15-20% of their MVIC. These resistance settings for the device were determined based on the average kinematics during the baseline trial (See Equation 6.1 and Equation 6.2). During the first training trial, participants were instructed to walk in a manner that felt natural and did not receive any additional feedback. During the remaining three training trials, participants walked as they received visual feedback of their hip and knee joint angles as measured with the encoders on the device. Feedback consisted of bar plots for each joint that displayed the average maximum and minimum joint angles from the baseline trial along with a cursor of the real-time joint angle (Figure 6.1). The participants were encouraged to reach peak flexion during early swing and peak extension when they approached heel-strike. Feedback was created using a custom LabVIEW vi (v2013, National Instruments Corp., Austin, TX, US) and displayed on a 177.8 cm (70 in) monitor located approximately 2.5 m in front of the treadmill.

After each the first three training trials, the feedback and resistance were quickly removed, and the participants walked on the treadmill for a 30 s catch trial. Before the catch trial, participants were again instructed to walk in a way that felt natural. These catch trials allowed us to monitor adaptation during the training session.

After the last training trial, the experimenters helped the participants doff the device and repeated overground walking. We then performed a third static trial, removed all reflective markers, then repeated our procedures for transcranial magnetic stimulation and electrical stimulation.

6.2.3 Devices for Providing Resistances

Resistances were provided using wearable exoskeleton devices previously developed in our lab (Washabaugh, Augenstein, Ebenhoeh, et al., 2020; Washabaugh et al., 2016). The elastic

device operated using a pair of counteracting springs and pulleys. Calibrated compression springs were housed within the cylinders on the device and connected to the pulleys using cables. Within each pulley was a clutch mechanism that allowed us to create offsetting pre-tensions within each spring. For this study, the mechanism was configured to provide a bidirectional resistance (i.e., having both flexion and extension components) that varied linearly with joint angle according to:

$$\mathrm{T}_k = \tau_{flex} - \tau_{ext} = k_{flex}(\max(\theta_{ext}) - \theta_k) - k_{ext}\big(\theta_k - \max(\theta_{flex})\big),$$

$$\text{such that } |\mathrm{T}_k| = \begin{cases} \%\, MVIC_{flex}, & \text{if } \theta_k = \max(\theta_{flex}) \\ \%\, MVIC_{ext}, & \text{if } \theta_k = \max(\theta_{ext}) \end{cases}$$

Equation 6.1

where T_k was the net device torque about the knee and τ_{flex} and τ_{ext} were the individual torque components that resisted flexion and extension, respectively. Within each of these components, k_{flex} was the stiffness of the spring that was resisting knee flexion, k_{ext} was the stiffness of the spring resisting extension (units: Nm deg^{-1}), θ_k was the real-time knee angle, and $\max(\theta_{ext})$ and $\max(\theta_{flex})$ were the maximum extension and flexion angles measured from the average knee angle profile during the baseline trial, and represent the angle where each clutch was engaged. Spring stiffnesses k_{ext} and k_{flex} were selected in this study so that when θ_k was equal to either $\max(\theta_{ext})$ or $\max(\theta_{flex})$, the magnitude of T_k was equal to a percentage of the participants extension or flexion maximum voluntary isometric contraction (MVIC) as measured before training, respectively.

The viscous device used a miniature magnetic disk brake in order to provide a velocity-dependent resistance to the joint. Magnetic brakes provide resistance when a conductive material is moved through a magnetic field. In this instance, the conductor was an aluminum disk and the magnetic field was provided using permanent rare-earth magnets. The resistive capabilities of

this mechanism were altered by changing the area of the magnetic field that is exposed to the disk (i.e., more magnet exposure increased the damping coefficient). While the magnet exposure of our previous device had to be manually adjusted, the device in this experiment was modified so that we could specifically target the training needs of knee extensors or flexors. This was done by making the device semi-passive; hence, the manual mechanism was replaced with a servo-controlled mechanism (1207 TG, Power HD, Pololu Corporation, Las Vegas, US). Thus, magnet settings could be adjusted based on the joint that the device was resisting and whether the joint was being flexed or extended. The torque of the device was set according to:

$$\mathrm{T}_{h/k} = -\beta_{h/k}\dot{\theta}_{h/k},$$

$$where\ \beta_h = \frac{0.42}{1 + e^{-\frac{(x_h - 0.59)}{0.15}}}$$

$$and\ \beta_k = \frac{0.17}{1 + e^{-\frac{(x_k - 0.56)}{0.16}}}$$

$$\text{such that } \left|\mathrm{T}_{h/k}\right| = \begin{cases} \%\ MVIC_{flex}, & \text{if } \dot{\theta}_{h/k} = \max(\dot{\theta}_{flex}) \\ \%\ MVIC_{ext}, & \text{if } \dot{\theta}_{h/k} = \max(\dot{\theta}_{ext}) \end{cases}.$$

Equation 6.2

In this equation, β was the damping coefficient (units: Nm s deg^{-1}), $\dot{\theta}$ was the angular velocity of the joint, and the subscripts *h* or *k* indicated whether the device was applied to the hip or knee joints. β was characterized for each device using a dynamometer that measured torque over a range of movement velocities and magnet exposures (x); these data were then fit to a sigmoid curve using the MATLAB Curve Fitting Toolbox. Note that β was larger for the hip joint when compared with the knee joint [$\max(\beta_h) = .39$ and $\max(\beta_k) = .16$ Nm s deg^{-1}] because that device had an additional pair of magnets to account for the joint's slower movement velocities. During training, for each joint, magnet exposure was determined separately for flexion and

extension such that, when $\dot{\theta}$ was equal to the extrema of the average knee velocity profile measured during baseline trials [i.e., max($\dot{\theta}_{flex}$) or max($\dot{\theta}_{ext}$)], the magnitude of T was equal to a percentage of the participants (MVIC) as measured before training.

These devices were fitted to hip-knee orthosis consisting of a custom pelvis and thigh segments (Newport Bilateral MC & Newport Universal Thigh; Orthomerica Products, Inc.; Orlando, FL, US) and a modified orthopedic knee brace (T-Scope Premier Post-Op Knee Brace; Breg, Inc.; Carlsbad, CA, US). When resistance was only being applied to the knee, a freely moving joint was fit between the pelvis and thigh segments. Optical encoders were placed on each joint of the device (E4T-360, US Digital, Vancouver, WA, US) which were used to measure joint angles and velocities during use. Data were logged and devices were controlled using a custom LabVIEW program that communicated with a microprocessor (Arduino UNO, Arduino, Somerville, MA, US).

6.2.4 Data Processing

6.2.4.1 Electrical Stimulation

Torque data and a sync signal corresponding to stimulation onset were sampled at a frequency of 2000 Hz. Using a custom LabVIEW processing software, the torque data were recursively filtered using a low-pass Butterworth filter (10 Hz, 4th order) (Garcia, Rodriguez, et al., 2020). The sync signal was used to automatically calculate the max amplitude of the evoked torque after stimulation (within 500 ms). The torque value at stimulation onset was then subtracted from the max amplitude. Note, the time window used to calculate the maximum torque amplitude was manually adjusted to account for volitional and reflex responses, which were monitored by comparing latencies within the trial and between time points (i.e., Pre to Post). These procedures were carried out for each stimulation, then the average amplitude was

calculated for each block. Between blocks, a decrease in the electrically stimulated torque indicated peripheral muscular fatigue and an increase indicated potentiation.

6.2.4.2 Transcranial Magnetic Stimulation

MEP data were collected from the torque sensor on the dynamometer at a frequency of 2000 Hz, along with a sync signal that corresponded to stimulation onset. Processing was performed with a custom LabVIEW program. Raw data were segmented from 200 ms prior to the stimulation over a window of 500 ms for each of the 25 stimulations. These segmented data were then ensemble averaged to yield an average torque curve at each time point. From this curve, we measured the mean of the background contraction (i.e., the 80 ms prior to the stim) and the peak torque. For our measure of corticospinal excitability, the peak torque data were normalized to the background contraction (MEP_T). In another analysis, to determine if alterations in corticospinal excitability were due to neural changes or just changes in the muscle properties (i.e., peripheral fatigue), the peak torque elicited during TMS was normalized to the peak torque elicited during electrical stimulation ($MEP_{T/E}$).

6.2.4.3 Electromyography

EMG signals were processed so that we could evaluate muscle activation throughout the study. Raw EMG data were collected in Qualisys Track Manager (QTM) and sampled at 2000 Hz. Using a custom LabVIEW program, these raw data were band-pass filtered (20-500 Hz), rectified, and smoothed using a zero phase-lag low-pass Butterworth digital filter (8th order, 6 Hz). These data were segmented at heel strike (i.e., when the vertical axis of the force plate data exceeded 20N) then ensemble averaged across strides to compute mean EMG profiles for each trial. These profiles were then normalized to the peak amplitude of the EMG during the baseline trial.

6.2.4.4 Device Kinetics

During each trial involving the leg brace, we collected the device angle from the encoder at a rate of 62.5 Hz using a custom LabVIEW program. For processing, we upsampled the encoder data to 2000 Hz, so that it matched the force plate data. We then performed a numerical derivative on the angle data to calculate the angular velocity. With the device angle and velocity, we used Equation 6.1 and Equation 6.2 to estimate the output torque, then multiplied this torque by the angular velocity to estimate power. These data were segmented into strides and ensemble averaged to yield a profile representing the average torque and power for each trial.

6.2.4.5 Gait Kinematics and Kinetics

Motion capture and force plate data were collected using QTM and sampled at 200 Hz and 2000 Hz, respectively. Gaps in the motion capture data were filled and markers were labeled in QTM. These data were then exported to Visual3D (C-Motion Inc., Germantown, MD, US) for further processing (see Appendix B.2.3 for full details). Briefly, skeletal models were constructed from the static trials (see Appendix B.2.2 for details) and applied to the walking trials. The marker position data and force plate data were low-pass filtered using a zero phase-lag Butterworth digital filter (6 Hz) to remove motion artifacts and high frequency noise due to the treadmill motors. From these filtered data, we then computed the sagittal plane kinematics and kinetics (internal moments and powers) of the hip, knee, and ankle joints. These data were segmented at heel-strike and ensemble averaged across strides. We then subtracted the average device moment and power from the hip and knee data to account for the device's contribution.

6.2.5 Statistical Analysis

For both experiments, all gait variables (i.e., kinematics, kinetics, and muscle activation) were analyzed using one-dimensional statistical parametric mapping (SPM1D, version 0.4,

https://spm1d.org/) in MATLAB (vR2019a, MathWorks, Natick, MA, US) over the full gait cycle. Specifically, for each comparison, we performed two-way ANOVAs (resistance type [2 levels] × block [2 levels]) with repeated measures on both factors (see Figure 6.1 for specific blocks that were used in this model). SPM avoids many of the issues of conventional statistical procedures when performing time-series analysis (i.e., high error rates and loss of data) by using random field theory to generate a distribution and critical thresholds for hypothesis testing based on the smoothness of the data (Pataky et al., 2013). We note that during treadmill walking, two participants had to be removed from the analysis. In one instance there was an equipment malfunction and in the other the participant misunderstood instructions. For our analysis, all gait variables were piecewise linear length normalized (Helwig et al., 2011; Sadeghi et al., 2000) to align with distinctive features of the baseline kinematic profiles of the hip, knee, and ankle (Figure C.1). Muscle activation data were then log transformed to minimize skewness and heteroscedasticity (Krishnan et al., 2013). SPM{F} statistic curves were calculated at each time point of the gait cycle for both main effects and an interaction. We then identified significant clusters (i.e., groups of points along the time axis) that exceeded the critical threshold ($\alpha = 0.05$). After a significant main effect, we reported the marginal means for each level over each cluster. If there was a significant interaction, we ignored all main effects that overlapped with the interaction and performed planned post hoc SPM1D paired t-tests (i.e., for each resistance type, comparing both blocks; for each block, comparing both resistance types) with Bonferroni correction ($p < 0.0125$). We then identified all significant clusters that overlapped with the interaction and reported the cell means over the cluster. To improve interpretation, we report muscle activation as non-log normalized values.

Our analyses of peripheral fatigue and corticospinal excitability were performed in SPSS for windows version 27.0 (SPSS Inc., Chicago, IL, USA). For each of these variables, we used a two-way ANOVA (resistance type [2 levels] × block [2 levels; Pre and Post]) model with repeated measures on both factors. Following significant main effects, we reported mean difference and standard error of the marginal means. If there was a significant interaction, we ignored the main effects and performed planned post hoc paired t-tests (see above) with Šidák correction and reported cell means. A significance level of $\alpha = 0.05$ was used for these analyses.

6.3 Results

We ran two experiments to test how elastic and viscous resistances compare in their ability to resist the knee during walking, and how training with a viscous resistance at the knee joint differs from training with the resistances at the hip and knee joints. While we only present certain variables of interest in the results sections, additional results can be found in Appendix C.

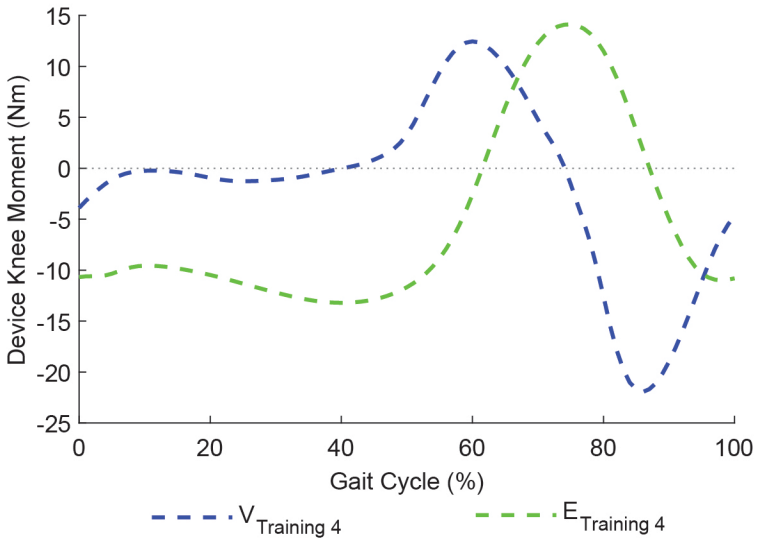

Figure 6.3 Experiment 1: profiles of the resistive moments that were provided to the knee by the viscous (V) and elastic (E) devices during experiment 1. Note that a positive moment meant the device was resisting knee flexion while a negative moment was resisting extension.

6.3.1 Experiment 1: Elastic vs. Viscous Resistance

6.3.1.1 Training

Resistance Characteristics

While both resistance types successfully provided a bidirectional torque (i.e., resisting both extension and flexion) about the knee during training, the characteristics of the torque provided by each resistance type varied greatly (Figure 6.3). The Elastic device resisted knee extension throughout the stance phase and knee flexion during mid-swing, then returned to resisting extension during the terminal swing phase. Meanwhile, the Viscous device did not impart much resistance during the stance phase but resisted knee flexion during pre-swing and knee extension during mid swing. Overall, the peak flexion and extension resistances were 12.4±5.1 (mean ± standard deviation) and 20.9±9.3 Nm for the Viscous device and 14.0±5.6 and 13.1±5.3 for the Elastic device, respectively. We note that the devices were set so that the participant should have received a resistance that approximated 15–20% of their maximum voluntary isometric contraction during training. Hence, while the kinetics of the devices differed, the actual magnitude of the resistance during training underestimated the prescribed torque by approximately 36% for all conditions (i.e., for both resistance types and joint actions). After participants completed both the Viscous and Elastic training sessions, they were asked which of the resistance types they found to be more enjoyable to train with, and which one they found to be a better exercise. We found that most participants found the Viscous resistance to be more enjoyable (10/14 participants) while a similar proportion found the Elastic resistance provided a better exercise (9/14 participants).

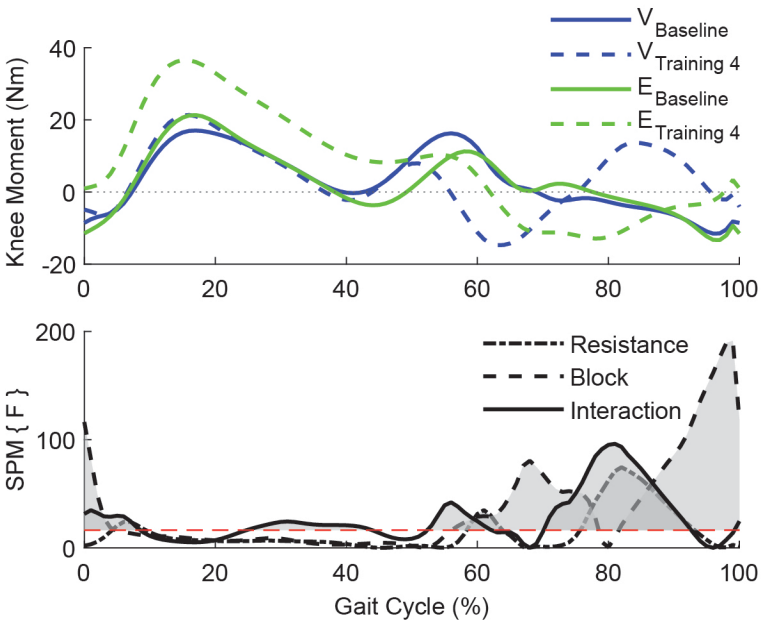

Effect	DoF	Range	Mean$_1$	Mean$_2$	*p*
Interaction	(1, 11)	0.0 – 8.6			**0.001**
		24.8 – 43.9			**< 0.001**
		52.3 – 62.1			**< 0.001**
		70.1 – 92.6			**< 0.001**
		99.2 – 100.0			**0.049**
Post hoc	$t_{V1\ E1}$	70.8 – 75.7	-2.1	1.9	**0.001**
		80.3 – 84.3	-3.6	-2.2	**0.005**
		96.8 – 97.2	-11.5	-13.3	0.049
	$t_{V2\ E2}$	1.2 – 9.7	-0.9	11.5	**0.003**
		56.0 – 65.5	-10.5	2.1	**0.002**
		73.1 – 93.0	8.3	-8.9	**< 0.001**
	$t_{V1\ V2}$	52.3 – 71.3	7.9	-7.5	**< 0.001**
		76.7 – 100.0	-6.2	7.1	**< 0.001**
	$t_{E1\ E2}$	0.0 – 10.9	-1.8	12.3	**< 0.001**
		63.2 – 84.7	0.6	-10.6	**< 0.001**
		92.6 – 100.0	-11.5	-1.2	**0.006**

Figure 6.4 Experiment 1: knee moment during training. (Top) Traces depict the internal knee moment profile over the gait cycle while walking with the viscous resistance (V) and the elastic resistance (E). Positive moments indicate joint extension while negative moments indicate flexion (Middle) SPM{F} statistics plotted over the gait cycle. Traces that exceed the threshold (red dashed line) are considered significant and are shaded gray. (Bottom) Table indicating the averages and significance of clusters that exceeded the threshold. For post hoc testing, mean 1 is the average of the first cell in the t-test, and mean 2 is the average for of the second cell. P-values are in bold if they are considered significant.

Internal Joint Moment

The two resistance types differed in their ability to augment knee joint moments during training, as shown by significant interactions throughout both the stance and swing phases (Figure 6.4). Post hoc testing indicated that, during the stance phase, the Elastic resistance significantly increased the knee extension moment. Notably, the Viscous device failed to alter

joint moments during the stance phase. At toe-off (i.e., pre- and initial-swing), the Viscous resistance elicited a significant increase in knee flexion moment, which was also larger than the Elastic resistance at this phase of the gait cycle. However, during mid-swing, these roles reversed: the Elastic device now resisted flexion while the Viscous device began targeting knee extension. During terminal swing, both resistance types elicited a significant increase in knee extension moment; however, they were not significantly different from one another. Note there were small differences between the devices during baseline walking when there was no resistance, but these differences were relatively small in magnitude (< 4 Nm; Figure 6.4).

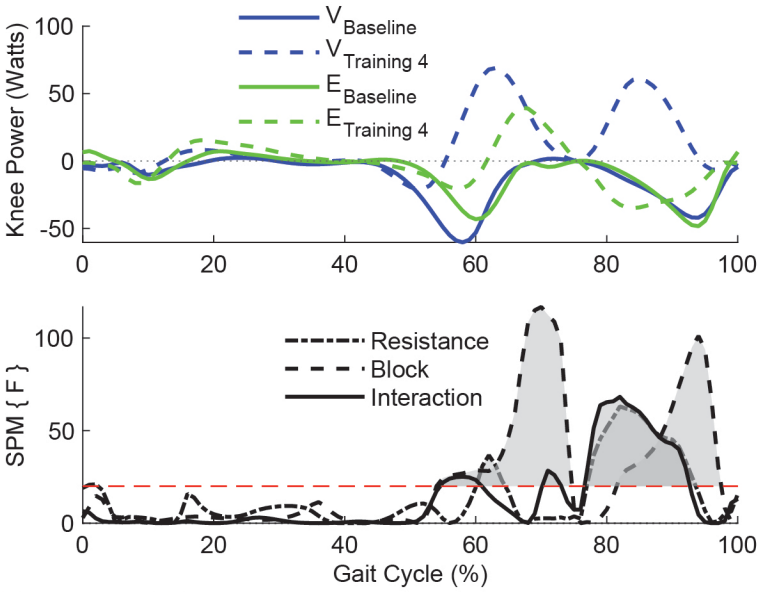

Effect	DoF	Range	Mean$_1$	Mean$_2$	*p*
Resistance	(1, 11)	0.6 – 2.3	-4.8	2.5	**0.025**
Interaction	(1, 11)	54.6 – 60.9			**< 0.001**
		70.1 – 73.1			**0.008**
		76.6 – 92.7			**< 0.001**
Post hoc	$t_{V1\ E1}$	52.9 – 59.2	-52.1	-26.1	**< 0.001**
		71.4 – 74.6	1.2	-2.8	**0.002**
	$t_{V2\ E2}$	59.4 – 65.2	63.4	6.8	**< 0.001**
		76.7 – 93.2	37.2	-26.9	**< 0.001**
	$t_{V1\ V2}$	52.8 – 71.5	-28.2	34.4	**< 0.001**
		77.3 – 96.9	-23.4	30.6	**< 0.001**
	$t_{E1\ E2}$	65.4 – 74.3	-3.6	27.6	**< 0.001**
		76.8 – 84.2	-5.1	-23.8	**< 0.001**
		91.8 – 97.2	-40.9	-15.2	**< 0.001**

Figure 6.5 Experiment 1: knee power during training. (Top) Traces depict the power profile over the gait cycle while walking with the viscous resistance (V) and the elastic resistance (E). Positive power indicates power generation while negative indicates absorption. (Middle) SPM{F} statistics plotted over the gait cycle. Traces that exceed the threshold (red dashed line) are

considered significant and are shaded gray. (Bottom) Table indicating the averages and significance of clusters that exceeded the threshold. For resistance main effects, mean 1 is the average for the viscous device over the cluster, and mean 2 is the average for the elastic device over the cluster. For post hoc testing, mean 1 is the average of the first cell in the t-test, and mean 2 is the average for of the second cell. P-values are in bold if they are considered significant.

Joint Power

There were several significant differences in how these resistance types were able to augment knee power during walking, as shown by significant interactions throughout the swing phase (Figure 6.5). Post hoc testing indicated that the Viscous resistance began to elicit a significant increase in power generation at the knee as early as the pre-swing phase. Notably, when worn without resistance, this device also required more power absorption when compared with the Elastic device at this phase of the gait cycle. While the Elastic resistance significantly increased power generation during initial swing, this increase was not as large as the result that was seen with the Viscous resistance. During mid-swing, the Viscous resistance again began to significantly elicit increased power generation at the knee. Conversely, the Elastic resistance was promoting power absorption at that time. While both resistance types reduced the need for power absorption during terminal swing, they were not significantly different from one another over that phase.

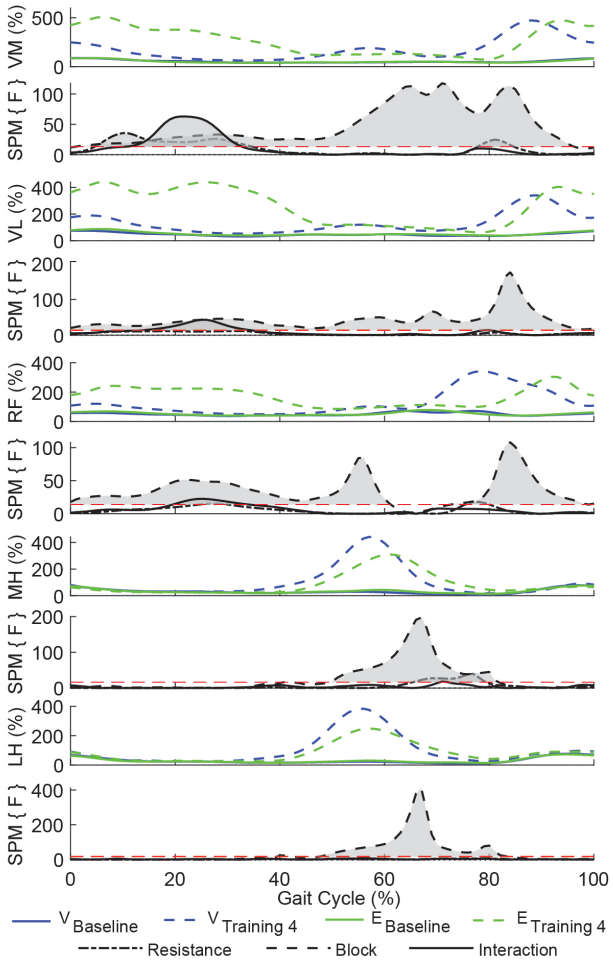

Effect	DoF	Range	Mean$_1$	Mean$_2$	p
VM					
Resistance	(1, 11)	77.8 – 84.7	168.0	71.5	**0.030**
Block	(1, 11)	0.9 – 96.2	51.7	213.4	**< 0.001**
Interaction	(1, 11)	10.4 – 32.8			**< 0.001**
Post hoc	$t_{V2\ E2}$	6.2 – 33.6	104.6	377.8	**< 0.001**
	$t_{V1\ V2}$	6.4 – 8.2	80.6	190.3	0.040
	$t_{E1\ E2}$	4.0 – 79.0	49.8	236.8	**< 0.001**
VL					
Block	(1, 11)	0.0 – 100.0	49.5	193.8	**< 0.001**
Interaction	(1, 11)	13.7 – 34.4			**< 0.001**
		79.3 – 80.0			**0.049**
Post hoc	$t_{V2\ E2}$	17.9 – 33.8	65.4	412.7	**< 0.001**
		78.8 – 81.8	165.0	71.9	0.042
	$t_{V1\ V2}$	1.8 – 17.2	62.9	146.5	**< 0.001**
		31.2 – 38.6	32.7	55.4	**0.002**
		66.4 – 94.5	41.0	189.0	**< 0.001**
	$t_{E1\ E2}$	0.0 – 78.1	52.0	256.6	**< 0.001**
		80.0 – 100.0	53.6	275.9	**< 0.001**
RF					
Resistance	(1, 11)	75.4 – 80.0	201.9	77.3	**0.031**
Block	(1, 11)	0.0 – 61.2	48.2	125.3	**< 0.001**
		72.7 – 98.9	51.1	218.4	**< 0.001**
		99.1 – 100.0	57.6	142.8	**0.049**
Interaction	(1, 11)	19.6 – 33.9			**0.002**
Post hoc	$t_{V2\ E2}$	18.4 – 38.0	57.3	211.7	**< 0.001**
	$t_{V1\ V2}$	16.3 – 23.6	45.4	72.4	**0.003**
	$t_{E1\ E2}$	0.8 – 44.6	50.4	203.7	**< 0.001**
MH					
Block	(1, 11)	40.8 – 42.1	21.2	55.0	**0.046**
Interaction	(1, 11)	70.6 – 72.1			**0.045**
Post hoc	$t_{V2\ E2}$	67.8 – 80.4	41.0	97.0	**< 0.001**
	$t_{V1\ V2}$	50.7 – 73.0	21.9	254.6	**< 0.001**
	$t_{E1\ E2}$	49.3 – 81.9	28.4	175.3	**< 0.001**
LH					
Block	(1, 11)	39.5 – 42.5	15.9	52.2	**0.029**
		47.6 – 83.9	19.5	154.4	**< 0.001**

Figure 6.6 Experiment 1: muscle activation of the thigh muscles during training. (Left) Traces depict the muscle activation over the gait cycle while walking with the viscous resistance (V) and the elastic resistance (E) as well as SPM{F} statistics plotted over the gait cycle. SPM{F} traces that exceed the threshold (red dashed line) are considered significant and are shaded gray. (Right) Table indicating the averages and significance of clusters that exceeded the threshold. For resistance main effects, mean 1 is the average for the viscous device over the cluster, and mean 2 is the average for the elastic device over the cluster. For block main effects, mean 1 is the average over the cluster for the baseline block, and mean 2 is the average over the cluster for the training 4 block. For post hoc testing, mean 1 is the average of the first cell in the t-test, and mean 2 is the average for of the second cell. P-values are in bold if they are considered significant. Muscle abbreviations: VM (vastus medialis), VL (vastus lateralis), RF (rectus femoris), MH (medial hamstring), LH (lateral hamstring).

Muscle Activation

Thigh muscle activation (i.e., of the quadriceps [vastus medialis VM, vastus lateralis VL, and rectus femoris RF] and hamstrings [medial MH and lateral hamstrings LH]) showed differences in how it was altered in response to walking with the different types of resistance (Figure 6.6). The largest difference was in the quadriceps muscles during mid-stance, where significant interactions and post hoc testing indicated that, while both devices significantly

increased activation of these muscles, the effect was larger when walking with the Elastic resistance. Both resistance types significantly increased muscle activation of the quadriceps during the swing phase, as was shown by significant block main effects for each muscle. An interaction during mid-swing in the vastus lateralis muscle likely arose due to timing of when the muscle was active during swing. The Viscous resistance increased quadriceps activation earlier (initial – mid-swing) than the Elastic resistance (mid – terminal swing). Hamstring muscle activation was relatively unaffected for the first half the stance phase when walking with both resistance types. However, significant main effects for Block indicated that muscle activation began to increase for both resistance types during terminal stance. This increased activation was maintained well into the swing phase (mid-swing). While swing phase muscle activation was similar in the lateral hamstring for both resistance types, a significant interaction and post hoc testing in the medial hamstring indicated that the Elastic resistance maintained this heightened activation for longer.

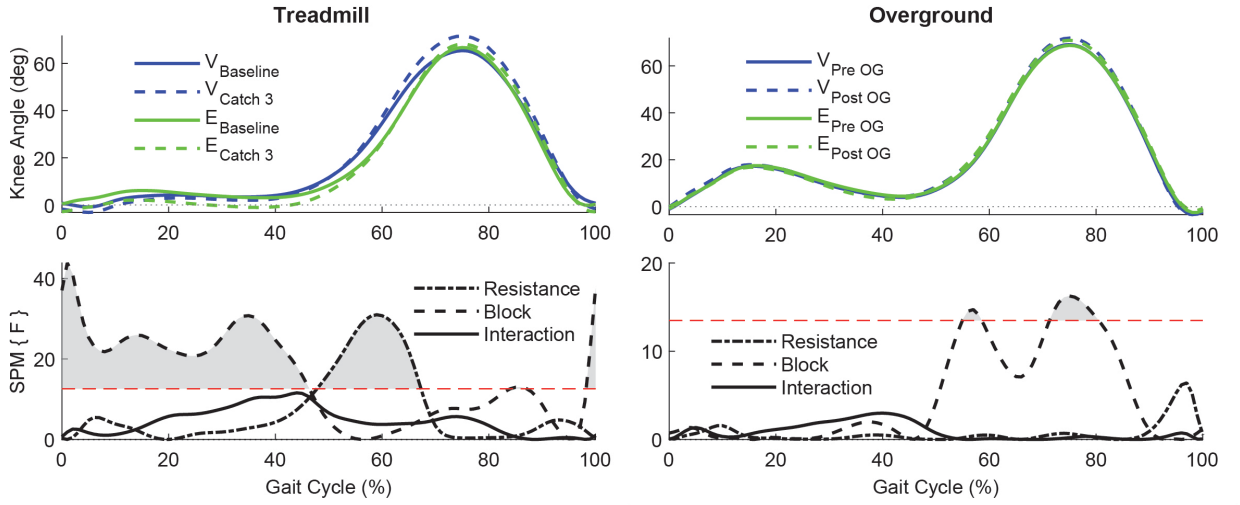

Effect	DoF	Range	Mean$_1$	Mean$_2$	*p*
Resistance	(1, 11)	47.8 – 67.3	30.5	23.4	**0.002**
		0.0 – 46.4	3.6	0.9	**< 0.001**
Block	(1, 11)	84.0 – 87.1	44.4	48.6	**0.046**
		98.2 – 100.0	0.7	-1.8	**0.049**

Effect	DoF	Range	Mean$_1$	Mean$_2$	*p*
Knee					
Block	(1, 11)	54.9 – 58.6	18.7	20.6	**0.042**
		71.3 – 80.5	67.2	69.6	**0.017**

Figure 6.7 Experiment 1: knee kinematic aftereffects. Plots indicate kinematics when walking on the treadmill (Left) and overground (Right). For each joint, (Top) traces depict the kinematic profile over the gait cycle while walking with the viscous resistance (V) and the elastic resistance (E). Below the kinematic traces, SPM{F} statistics are plotted over the gait cycle. Traces

that exceed the threshold (red dashed line) are considered significant and are shaded gray. (Bottom) Tables indicating the averages and significance of clusters that exceeded the threshold. For resistance main effects, mean 1 is the marginal mean for the viscous resistance and mean 2 is the marginal mean for the elastic resistance. For block main effects over the treadmill, mean 1 is the marginal mean during Baseline over the cluster, and mean 2 is the marginal mean during Catch 3 over the cluster. For block main effects overground, mean 1 is the average over the cluster for the Pre Overground block and mean 2 is the average over the cluster for the Post Overground block. P-values are in bold if they are considered significant.

6.3.1.2 Aftereffects

Treadmill Walking Kinematics

While walking on the treadmill, both resistance types elicited significant aftereffects for knee angle (as shown by a main effect for Block; Figure 6.7). However, we failed to find a significant interaction to indicate that participants adapted differently while walking with Viscous or Elastic resistances. From the significant block effect, we found that walking with resistance increased the knee extension angle during the stance phase and increased the knee flexion angle during the mid-swing phase. There was also a significant main effect for resistance during pre-swing. This occurred because participants started flexing their knee earlier while walking with the Viscous leg brace during both the baseline and catch trials, which could have been due to the slight increase in rotational inertia due to the spinning disk on this device.

Overground Kinematics

Some kinematic aftereffects for the knee angle were maintained once the resistance was removed and the participants walked overground (Figure 6.7). Specifically, there was a significant block effect that occurred during mid-swing, indicating that the knee was also more flexed at this phase of the gait cycle when walking overground. Notably, the increased knee extension during the stance phase that was seen while walking on the treadmill did not translate to overground walking. We also found a significant block effect during pre-swing, which indicated the knee was more flexed at this phase.

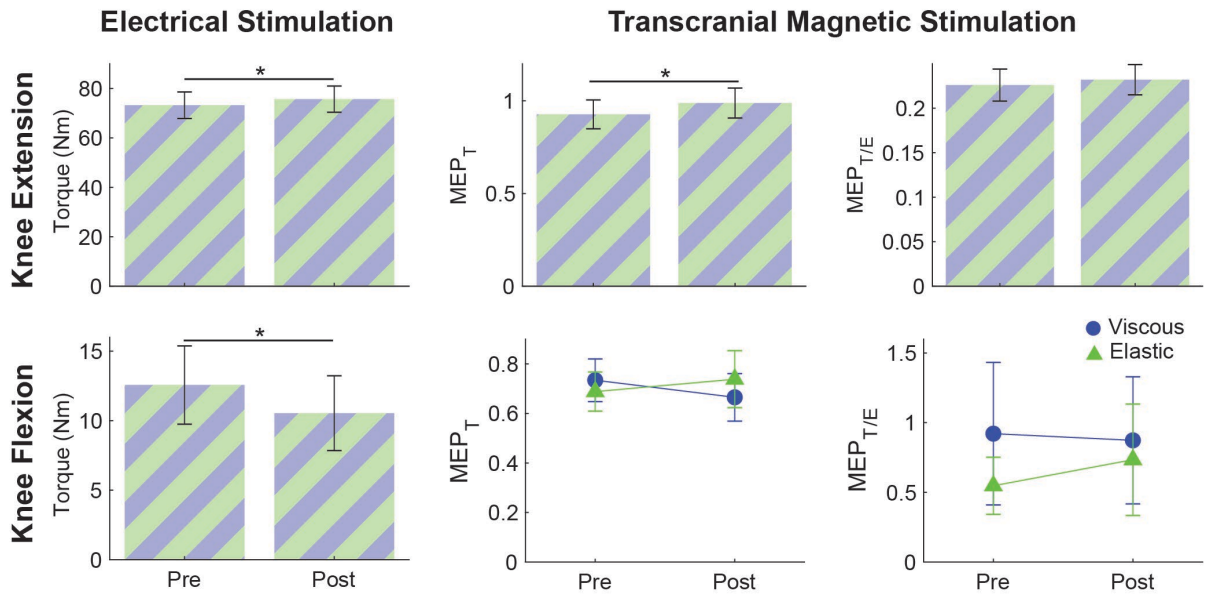

Figure 6.8 Experiment 1: results from electrical stimulation and transcranial magnetic stimulation procedures. Bar plots represent main effects for Block and line plots represent interactions (Block*Resistance). Electrical stimulation of the muscles indicated that knee extension was potentiated while knee flexion was fatigued. While there was a significant increase in extensor MEP_T, this effect disappeared once transcranial magnetic stimulation evoked torque was normalized to electrical stimulation ($MEP_{T/E}$). Note MEP_T and $MEP_{T/E}$ are both normalized and do not have units. (*: $p < 0.05$).

6.3.1.3 Electrical Stimulation

We failed to find any significant interactions when analyzing the electrical stimulation data, which indicated that both resistance types had a similar effect on peripheral fatigue. However, we did find several significant main effects for block (i.e., Pre–Post) during both flexion and extension (Figure 6.8). During flexion, the evoked torque significantly decreased [$F(1,13) = 10.34$, $p = 0.007$, $\Delta = -2.03 \pm 0.63$ Nm (mean ± standard error)], indicating the hamstring muscles were fatigued. During extension, the evoked torque significantly increased [$F(1,13) = 12.85$, $p = 0.007$, $\Delta = 2.47 \pm 0.63$ Nm], indicating the quadriceps were potentiated.

6.3.1.4 Neural Excitability

Neural excitability appeared altered following training while walking under these different resistance types (Figure 6.8). During knee extension, there was a significant main effect for block [$F(1,13) = 5.63$, $p = 0.034$] when analyzing MEP_T to indicate that excitability was

increased following training (Δ = 6.1 ± 2.6%) with both resistance types. During knee flexion, there was a significant interaction [F(1,13) = 7.11, p = 0.019] but post hoc testing did not reveal any differences between the blocks or resistance types (p > 0.161). However, once we normalized the MEPs to peripheral factors (i.e., the torque evoked during electrical stimulation [$MEP_{T/E}$]) all significant effects disappeared (p > 0.40; Figure 6.8). Hence, all changes in excitability may have been attributable to changes at the muscle level and not the neural level.

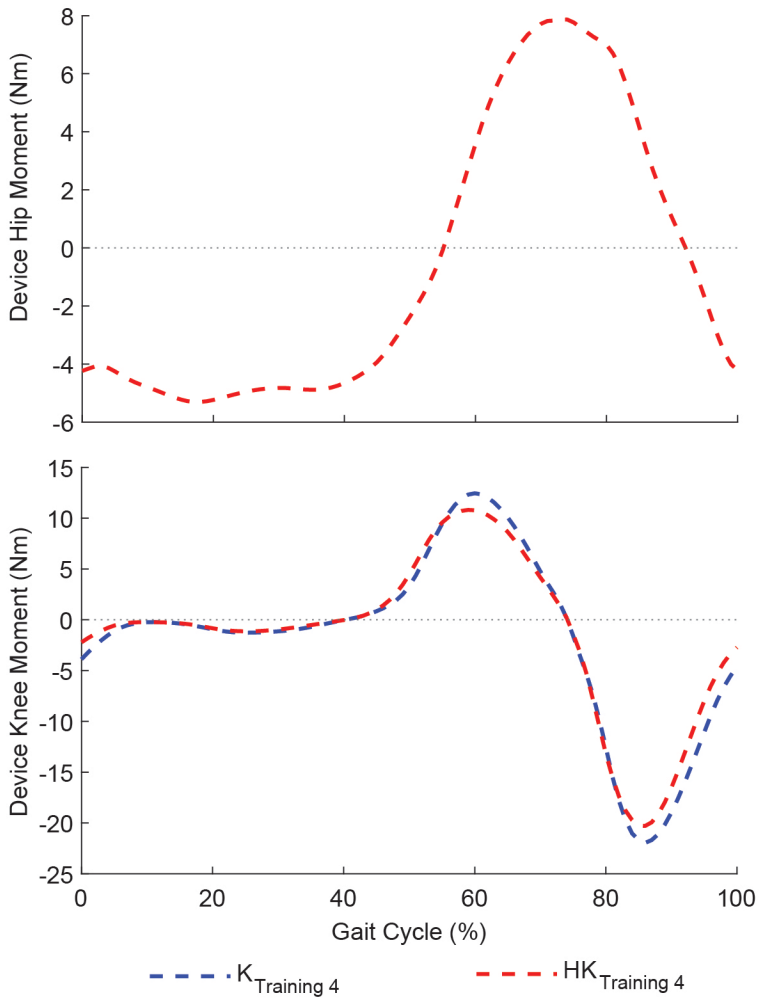

Figure 6.9 Experiment 2: profiles of the resistive moments that were provided to the hip and knee by the Knee (K) and Hip-Knee (HK) device configurations during experiment 2. Note that a positive moment meant the device was resisting flexion while a negative moment was resisting extension of the joint.

6.3.2 Experiment 2: Viscous Resistance at the Knee vs. at the Hip and Knee

6.3.2.1 Training

Resistance Characteristics

With the Hip-Knee configuration, the device provided a resistance to hip flexion throughout the stance phase, extension from the loading response to terminal swing, then extension again at the end of the swing phase (Figure 6.9). The resistance provided at the knee joint during both configurations was relatively similar: while each configuration did not impart much resistance during the stance phase, they resisted knee flexion during pre-swing and knee extension during mid swing. Again, we saw that both configurations did not provide the correct prescribed torque during training. However, it was most pronounced with the Hip-Knee configuration at the hip joint. For the hip, the max flexion and extension torques were 8.8±3.9 and 6.3±2.1 Nm, respectively. Hence, the prescribed torque was underestimated by approximately 56%.

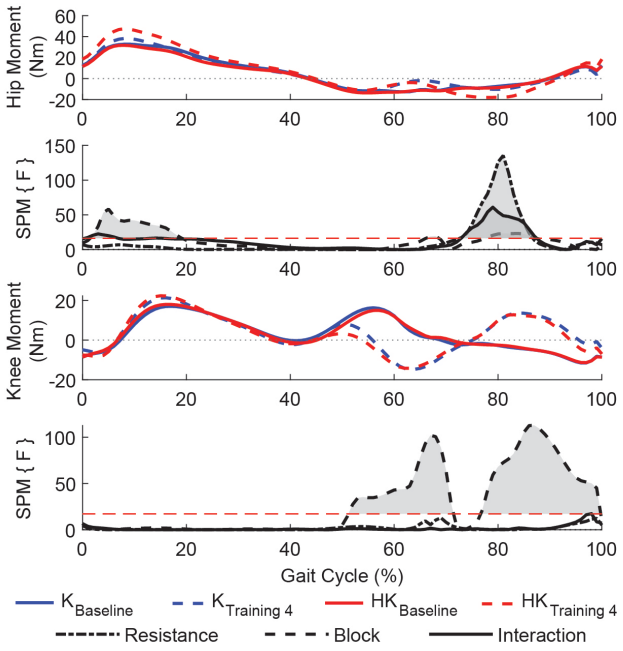

Effect	DoF	Range	Mean$_1$	Mean$_2$	p
Hip					
Block	(1, 11)	66.2 – 68.6	-11.3	-5.2	**0.037**
Interaction	(1, 11)	0.5 – 6.8			**0.006**
		13.4 – 15.2			**0.043**
		72.9 – 87.4			**< 0.001**
Post hoc	$t_{K2\ HK2}$	72.5 – 87.2	-8.5	-16.0	**< 0.001**
	$t_{K1\ K2}$	5.7 – 9.2	32.4	37.5	0.015
		66.1 – 69.2	-11.0	-3.0	0.020
	$t_{HK1\ HK2}$	0.0 – 20.6	25.9	37.7	**< 0.001**
		75.2 – 89.3	-6.5	-14.6	**< 0.001**
		99.9 – 100.0	11.4	18.1	0.050
Knee					
Block	(1, 11)	51.2 – 71.4	8.0	-7.2	**< 0.001**
		76.7 – 99.8	-6.2	6.3	**< 0.001**
Interaction	(1, 11)	97.9 – 98.0			**0.050**
Post hoc	$t_{K1\ K2}$	76.7 – 100.0	-6.2	7.1	**< 0.001**
	$t_{HK1\ HK2}$	77.1 – 98.3	-6.0	6.3	**< 0.001**

Figure 6.10 Experiment 2: hip and knee internal moments during training. (Left) Traces depict the joint moment profile over the gait cycle while walking with the viscous device in the Knee configuration (K) and the Hip-Knee configuration (HK). Positive moments indicate joint extension while negative moments indicate flexion. Under each moment plot, SPM{F} statistics are plotted over the gait cycle. SPM traces that exceed the threshold (red dashed line) are considered significant and are shaded gray. (Right) Table indicating the averages and significance of clusters that exceeded the threshold. For block main effects, mean 1 is the average over the cluster for the Baseline block, and mean 2 is the average over the cluster for the Training 4 block. For post hoc testing, mean 1 is the average of the first cell in the t-test, and mean 2 is the average for of the second cell. P-values are in bold if they are considered significant.

Internal Joint Moments

The Hip-Knee configuration altered the internal hip joint moment during training beyond what was seen while walking with the Knee configuration, as shown by significant interactions during the loading response and mid-swing (Figure 6.10). However, post hoc testing indicated that the Hip-Knee configuration only significantly increased the hip flexion moment beyond the Knee configuration during mid-swing. Both configurations increased hip extension during the loading response. While hip extension during the loading response was increased more with the Hip-Knee configuration, this difference was not significant. At the knee, both configurations behaved similarly. This was shown by significant block effects during toe off and terminal swing that indicated internal knee flexion moments and extension moments increased during these periods, respectively.

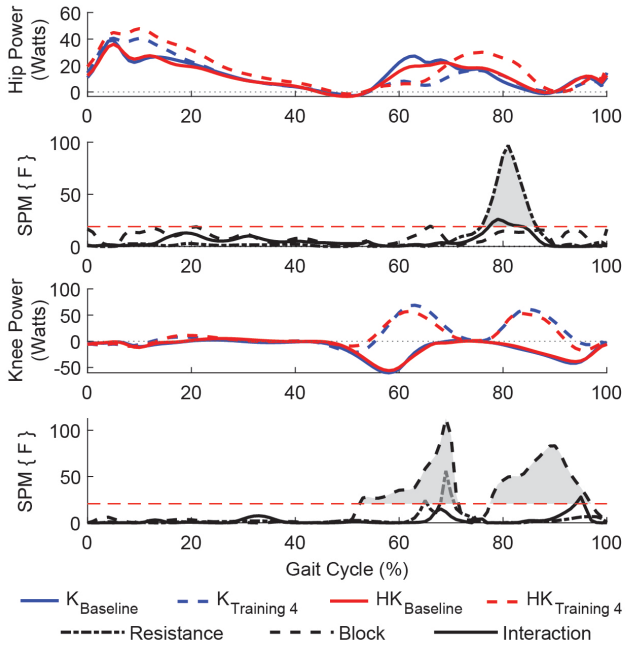

Effect	DoF	Range	Mean$_1$	Mean$_2$	p
Hip					
Block	(1, 11)	65.9 – 66.2	21.3	8.1	**0.049**
Interaction	(1, 11)	77.3 – 83.7			**< 0.001**
Post hoc	$t_{K1\ HK1}$	78.4 – 83.7	6.3	10.6	**< 0.001**
	$t_{K2\ HK2}$	76.3 – 85.9	9.7	22.7	**< 0.001**
Knee					
Resistance	(1, 11)	64.7 – 65.4	26.4	16.1	**0.044**
		67.9 – 70.7	12.4	6.5	**0.006**
Block	(1, 11)	52.4 – 71.4	-28.3	31.6	**< 0.001**
		77.5 – 96.9	-22.5	26.9	**< 0.001**
Interaction	(1, 11)	94.0 – 95.6			**0.026**
Post hoc	$t_{K2\ HK2}$	94.9 – 96.6	-5.4	-16.7	0.024
	$t_{K1\ K2}$	77.3 – 96.9	-23.4	30.6	**< 0.001**
	$t_{HK1\ HK2}$	79.6 – 95.0	-22.5	29.2	**< 0.001**

Figure 6.11 Experiment 2: hip and knee power during training. (Left) Traces depict the joint power profile over the gait cycle while walking with the viscous device in the Knee configuration (K) and the Hip-Knee configuration (HK). Positive power indicates power generation while negative indicates absorption. Under each power plot, SPM{F} statistics are plotted over the gait cycle. SPM traces that exceed the threshold (red dashed line) are considered significant and are shaded gray. (Right) Table indicating the averages and significance of clusters that exceeded the threshold. For block main effects, mean 1 is the average over the cluster for the Baseline block, and mean 2 is the average over the cluster for the Training 4 block. For post hoc testing, mean 1 is the average of the first cell in the t-test, and mean 2 is the average for of the second cell. P-values are in bold if they are considered significant.

Joint Power

Both configurations augmented joint power by increasing power generation during walking (Figure 6.11). At the hip, a significant interaction indicated that the Hip-Knee configuration required more power generation than the Knee-configuration during the mid-swing phase of gait. However, both configurations actually decreased power generation during initial swing, as shown by a significant block effect. Given this effect applies to both configurations this could have been an artifact of the target-matching task that the participants performed. At the knee, both configurations increased power generation surrounding toe-off and during mid – terminal swing, as shown by significant block effects during these phases. While it appears slightly more power was generated with the Knee configuration—as shown by significant resistance effects and an interaction—the overall curves appear similar throughout the gait cycle.

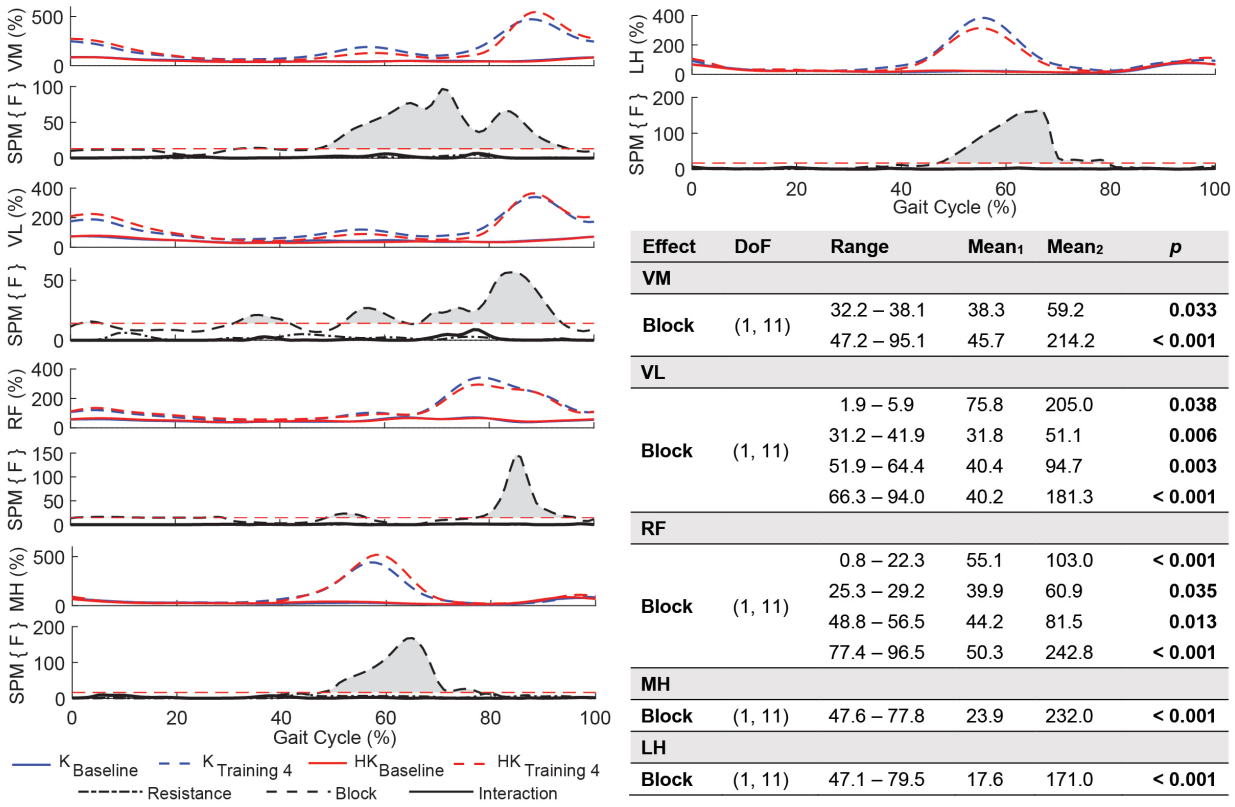

Effect	DoF	Range	Mean$_1$	Mean$_2$	p
VM					
Block	(1, 11)	32.2 – 38.1	38.3	59.2	**0.033**
		47.2 – 95.1	45.7	214.2	**< 0.001**
VL					
Block	(1, 11)	1.9 – 5.9	75.8	205.0	**0.038**
		31.2 – 41.9	31.8	51.1	**0.006**
		51.9 – 64.4	40.4	94.7	**0.003**
		66.3 – 94.0	40.2	181.3	**< 0.001**
RF					
Block	(1, 11)	0.8 – 22.3	55.1	103.0	**< 0.001**
		25.3 – 29.2	39.9	60.9	**0.035**
		48.8 – 56.5	44.2	81.5	**0.013**
		77.4 – 96.5	50.3	242.8	**< 0.001**
MH					
Block	(1, 11)	47.6 – 77.8	23.9	232.0	**< 0.001**
LH					
Block	(1, 11)	47.1 – 79.5	17.6	171.0	**< 0.001**

Figure 6.12 Experiment 2: muscle activation of the thigh muscles during training. (Left) Traces depict the muscle activation over the gait cycle while walking with the viscous device in the Knee configuration (K) and the Hip-Knee configuration (HK) as well as SPM{F} statistics plotted over the gait cycle. SPM{F} traces that exceed the threshold (red dashed line) are considered significant and are shaded gray. (Right) Table indicating the averages and significance of clusters that exceeded the threshold. For block main effects, mean 1 is the average over the cluster for the baseline block, and mean 2 is the average over the cluster for the training 4 block. P-values are in bold if they are considered significant. Muscle abbreviations: VM (vastus medialis), VL (vastus lateralis), RF (rectus femoris), MH (medial hamstring), LH (lateral hamstring).

Muscle Activation

Muscle activation did not significantly differ between the two configurations (Figure 6.12). Given that resistance was added to the hip in the Hip-Knee configuration, we would have expected several of the bi-articular muscles (i.e., the rectus femoris, and hamstrings muscles) that span the hip and knee joints would have been more activated with this configuration; however, there were no significant interactions. We did find several block main effects, indicating that the quadriceps were more active during both stance and swing phases. The hamstrings were more activated during the swing phase with both configurations.

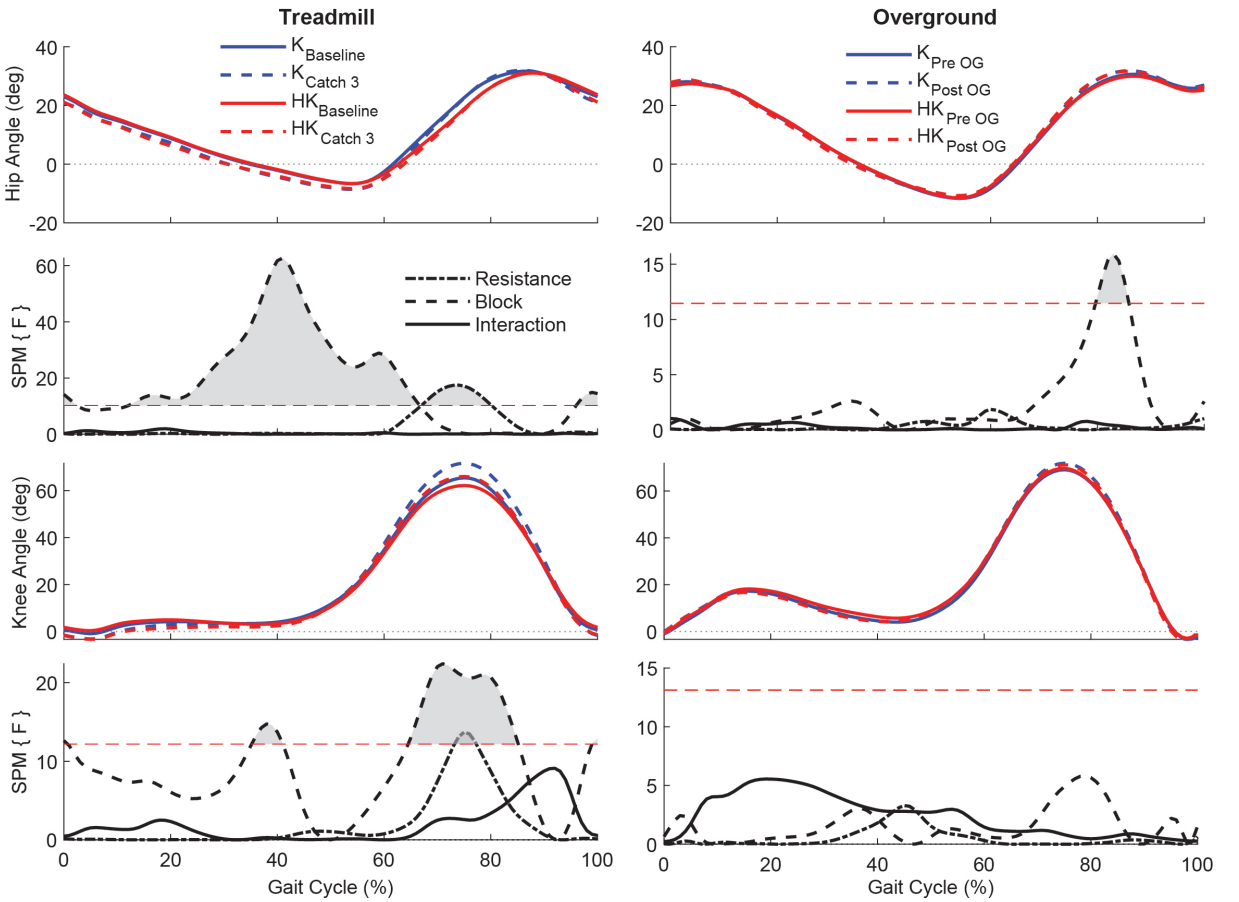

Effect	DoF	Range	Mean$_1$	Mean$_2$	*p*
Hip					
Resistance	(1, 11)	67.0 – 80.1	19.8	16.3	**0.036**
Block	(1, 11)	0.0 – 2.5	22.2	20.0	**0.049**
		12.1 – 66.7	1.3	-0.8	**< 0.001**
		96.0 – 100.0	24.9	22.8	**0.049**
Knee					
Resistance	(1, 11)	73.2 – 77.3	68.2	63.8	**0.045**
Block	(1, 11)	0.0 – 0.7	1.2	-1.7	**0.050**
		35.2 – 41.1	3.5	2.3	**0.040**
		64.5 – 85.2	58.1	62.6	**0.003**
		99.0 – 100.0	1.6	-1.1	**0.050**

Effect	DoF	Range	Mean$_1$	Mean$_2$	*p*
Hip					
Block	(1, 11)	79.6 – 85.9	28.9	30.7	**0.042**

Figure 6.13 Experiment 2: hip and knee kinematic aftereffects. Plots indicate kinematics when walking on the treadmill (Left) and overground (Right). For each joint, (Top) traces depict the kinematic profile over the gait cycle while walking with the viscous device in the Knee configuration (K) and the Hip-Knee configuration (HK). Below the kinematic traces, SPM{F} statistics are plotted over the gait cycle. Traces that exceed the threshold (red dashed line) are considered significant and are shaded gray. (Bottom) Tables indicating the averages and significance of clusters that exceeded the threshold. For resistance main effects, mean 1 is the marginal mean for the Knee configuration and mean 2 is the marginal mean for the Hip-Knee configuration. For block main effects over the treadmill, mean 1 is the marginal mean during Baseline over the cluster, and mean 2 is the marginal mean during Catch 3 over the cluster. For block main effects during overground walking, mean 1 is the average over the cluster for the Pre Overground block and mean 2 is the average over the cluster for the Post Overground block. P-values are in bold if they are considered significant.

6.3.2.2 Aftereffects

Treadmill Walking Kinematics

While walking on the treadmill, both configurations elicited significant aftereffects for hip and knee angle (Figure 6.13). For the hip, significant block effects indicated that the hip was more extended at heel strike and throughout mid stance – initial swing. A significant resistance effect during mid-swing indicated that the addition of the resistance element at the hip (regardless of if it was set to provide resistance or not) made the joint less flexed during this phase. At the knee, significant block effects indicated that both configurations increased the knee extension angle at heel strike and during mid-stance, and knee flexion angle during mid-swing. Additionally, there was a significant main effect for resistance during mid-swing, which likely occurred because peak knee flexion was reduced with the Hip-Knee configuration during training and baseline walking.

Overground Kinematics

Interestingly, none of the effects that were observed during treadmill walking transferred to overground walking. Instead, at the hip, there was a block effect that indicated the hip was more extended during mid-swing with both configurations (Figure 6.13). While this was not seen during treadmill walking, this effect was also present during overground walking in experiment 1 (Figure C.7). No significant effects were found for the knee when walking overground.

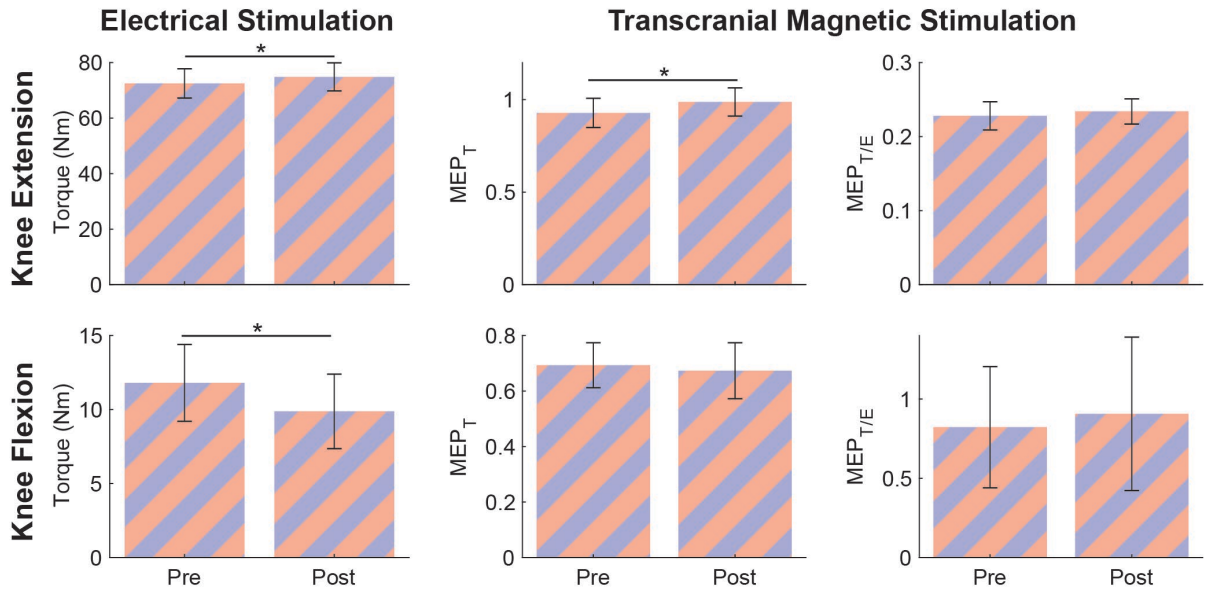

Figure 6.14 Experiment 2: results from electrical stimulation and transcranial magnetic stimulation procedures. Bar plots represent main effects for Block. Electrical stimulation of the muscles indicated that knee extension was potentiated while knee flexion was fatigued. While there was a significant increase in extensor MEP_T, this effect disappeared once transcranial magnetic stimulation evoked torque was normalized to electrical stimulation ($MEP_{T/E}$). Note MEP_T and $MEP_{T/E}$ are both normalized and do not have units. (*: $p < 0.05$).

6.3.2.3 Electrical Stimulation

We failed to find any interactions when analyzing the electrical stimulation data. Hence, adding resistance to the hip did not significantly alter peripheral fatigue beyond what was found with the knee configuration. However, we still found several significant main effects for block during flexion and extension (Figure 6.14). During flexion, the evoked torque significantly decreased during [$F(1,13) = 7.87$, $p = 0.015$, $\Delta = -1.93 \pm 0.69$ Nm], indicating the hamstring muscles were fatigued. During extension, the evoked torque significantly increased [$F(1,13) = 7.18$, $p = 0.019$, $\Delta = 2.33 \pm 0.87$ Nm], indicating the quadriceps were potentiated.

6.3.2.4 Neural Excitability

Our findings for neural excitability for experiment 2 closely matched what we found during experiment 1 (Figure 6.14). Again, during knee extension, there was a significant main effect for block [$F(1,13) = 5.39$, $p = 0.037$] to indicate that both resistance methods increased

excitability ($\Delta = 5.9 \pm 2.6\%$). There were no significant effects during flexion ($p > 0.060$). Once MEPs were normalized to peripheral factors ($MEP_{T/E}$) the significant effect for extension disappeared ($p > 0.47$). Hence, observed changes in excitability may have been attributable to changes at the muscle level and not the neural level of the corticospinal tract.

6.4 Discussion

In this study, we compared several different methods for providing functional resistance training during walking that varied based on the type of resistance that was used and to which joints the resistance was provided. Specifically, we compared how training differs between elastic and viscous resistive elements when providing bidirectional resistance to the knee, and how training with a device configured to resist the knee compares with resistance to the hip and knee. During training, as hypothesized, we found the viscous and elastic resistance types altered the magnitude, direction, and phase of gait where biomechanical changes occurred. However, contrary to our hypothesis, this training did not translate to resistance-specific differences in kinematic aftereffects, peripheral fatigue, or neural excitability. Similarly, training with a configuration that targeted the hip and knee joints altered the kinetics of training at the hip joint beyond what was seen when just targeting the knee joint. However, this did not translate to differences in kinematic aftereffects, peripheral fatigue, or neural excitability between the two configurations. Although we did not find different resistance types altered neural adaptation following an acute training session, it is still possible that prolonged training could produce differential effects. These findings provide new insight into how functional resistance training can be applied during walking.

We found that the resistance type altered gait biomechanics during training. Mainly, we saw knee extensor moment and quadriceps activation were increased during the stance phase

when training with the elastic device, but not when training with the viscous device. Additionally, the viscous device increased power generation at the knee to a larger extent than the elastic device. However, there were phases (i.e., mid-swing) where the elastic device increased power absorption at the knee. These findings represent many of the key differences between these two resistance types. That is, because resistance scales with the joint velocity with the viscous device, it appears that a viscous resistance can better promote power generation. Also, because the elastic device is capable of storing energy, it was able to hold the muscles in tension during the stance and mid-swing phases and increase power absorption. Due to the fact that the quadriceps muscles were activated throughout the stance phase with the elastic device, we assumed that the elastic resistance would fatigue the quadriceps more than the viscous device. However, we did not see that the muscles were more fatigued after the elastic training.

The intensity at which functional resistance training should be administered is a debated issue in this field (Akagi et al., 2020; Raymond et al., 2013; Schoenfeld et al., 2015). For conventional strength training, it is generally believed that high intensity (~70% of max strength) repetitions until fatigue are best for promoting strength (Izquierdo et al., 2006; Nobrega & Libardi, 2016). However, it would not be possible to provide this level of intensity during a functional task like walking (without substantially reducing the number of steps taken during training). Instead, we must rely on low intensity training, which has also been shown to augment strength when performed to fatigue (Schoenfeld et al., 2015). In this study, we applied a low intensity of resistance (15-20% of MVIC), which is comparable to what has been used in other studies (Houldin et al., 2011; Tang et al., 2019; Yen et al., 2014). One aspect that is unique to our study is that we used electrical stimulation to benchmark how training with these devices altered peripheral fatigue. We found that the hamstrings were fatigued after training, but the quadriceps

were actually potentiated. Hence, the intensity that we used may have been sufficient to train the hamstrings, but more resistance may have to be added to engage the quadriceps to the same extent.

Our findings highlight several of the difficulties of designing wearable exoskeleton devices so that they can convey large resistances to the leg. During both of our experiments, we repeatedly saw that the actual resistance output by the device was lower than what we had prescribed. This issue was abundantly clear when we attempted to add resistance to the hip joint in experiment 2, as the torque at the hip underestimated the prescribed torque by approximately 56%. Such diminished conveyance of resistance is common with wearable devices (Yandell et al., 2017), but this could have affected our results. Typically, the conveyance of resistance is hindered in wearable devices due to anatomical factors and the need to make the device comfortable. Resistive torques can easily be conveyed through rigid bodies, but anatomically, our rigid components (i.e., bones) are usually obstructed by several layers of pliable tissues (i.e., skin, fat, and muscle). Additionally, to increase comfort of the device, leg braces typically have a layer of foam padding that goes between the device and leg. Hence, under resistance, these soft and pliable components deform and the full resistance does not get conveyed to the leg. This is less of an issue when interfacing with the knee joint as the shin is relatively bony, but the hip appears to be a more difficult target, likely because the device must transfer resistance through the more pliable thigh and pelvis. We anticipated this issue and attempted to mitigate it by using a pelvis brace that extended up the torso. However, our results in experiment 2 were still affected—even though we saw significant differences in hip kinetics during training, this did not translate to increased muscle activation of the bi-articular rectus femoris or hamstrings when compared with the knee configuration. In the future, we would redesign the pelvis brace so that it

came in better contact with bony landmarks (e.g., the sacrum and anterior superior iliac spine) so that resistance is more directly transfers to the pelvis.

During both experiments, we still found that training resulted in significant kinematic aftereffects once the resistance was removed. Aftereffects are typically measured to determine if motor adaptation—a form of motor learning where the nervous system gradually develops new movement commands in response to perturbations of movement—is taking place (Emken & Reinkensmeyer, 2005; Lam et al., 2006; Shadmehr & Mussa-Ivaldi, 1994). Many times, aftereffects have been seen to transfer to overground walking (Reisman et al., 2009; Savin et al., 2014; Wu et al., 2016), or even persist for months following an intervention (Reisman et al., 2013; Rode et al., 2015). In our studies, we perturbed walking by adding resistance to the leg joints. We found that walking with bidirectional resistance to the knee joint resulted in aftereffects of increased extension during the stance phase and flexion during the swing phase regardless of the type of resistance used. Moreover, the aftereffect of increased knee flexion during swing transferred to overground walking. Notably, adding resistance to the hip did not alter the aftereffects measured for the hip joint. This was unexpected based on the findings of other studies (Lam et al., 2006), but this discrepancy is likely stems from the hip braces inability to convey proper resistances during training.

While aftereffects are believed to contain information about how the neural system is altered due to training, in this study, we also directly measured neural excitability using transcranial magnetic stimulation. We hypothesized that our findings from transcranial magnetic stimulation would match those of our aftereffects (i.e., an increase in knee extension and flexion in experiment 1). While this was not the case during knee flexion, we did find that neural excitability (MEP_T) increased during knee extension. However, once we normalized the motor

evoked responses to the torque elicited during electrical stimulation ($MEP_{T/E}$; i.e., removed the effects of muscle potentiation), there appeared to be no changes in neural excitability. This finding suggests that the neural excitability changes observed during knee extension were primarily mediated by peripheral changes in the quadriceps muscles. It is to be noted that we report only the acute effects of functional resistance training, and preliminary evidence from past research suggests that long-term training can result in sustained changes in neural excitability of the quadriceps muscles (Brown et al., 2021).

6.4.1 Limitations

A primary limitation of this study is related to the small sample size. Although our sample size is consistent with other studies that have done similar research (Blanchette & Bouyer, 2009; Noble & Prentice, 2006; Savin et al., 2010; Stoeckmann et al., 2009), our overall sample size was limited due to COVID restrictions. Thus, it is unclear if we had adequate power to realize findings with small effect sizes. Further, there are several considerations that must be made when comparing resistance types. Mainly we had to control for the joint motions that were being resisted and the magnitude of the resistance. We selected a bidirectional resistance because a majority of research on wearable exoskeleton devices has used viscous bidirectional resistances (Houldin et al., 2012; Houldin et al., 2011; Klarner et al., 2013; Lam et al., 2006; Washabaugh et al., 2016; Washabaugh & Krishnan, 2018; Zabukovec et al., 2013). However, we could have designed the study to target flexion or extension. It is possible that these resistance types would behave differently in these scenarios. Finally, we only tested the effects of these devices during a single training session. To truly understand how the resistance type can affect functional resistance training during walking will require comparing these devices during an intervention.

6.5 Conclusion

This study compared how providing resistance to the leg during gait training is affected by the type of resistance used as well as the specific joints that are targeted. We compared training with viscous and elastic bidirectional resistance to the knee, and how having resistance at the knee compares with resisting the hip and knee together. The methods that we used differentially altered the joint kinetics and muscle activation during training. However, this did not translate to differences in adaptation, peripheral fatigue, or neural excitability once the resistance was removed. Rather, the body adapted similarly to the resistance in each experiment. This may indicate that the resistance type does not have a large effect on functional resistance training during walking. However, we note that this was only an acute study, and differences could arise due to the cumulative effects of training. Also, there are several factors, such as how the resistance is controlled, the intensity and dosage of the training, and the device's ability to properly convey resistance to the leg that could alter our findings.

6.6 Acknowledgment

This work was supported in part by the National Institutes of Health (Grant R21 HD092614), the National Science Foundation (Grant DGE 1256260), and the UM-BICI Collaboratory Initiative. Any opinions, findings, and conclusions or recommendations expressed in this material are those of the authors and do not necessarily reflect the views of the funding sources. I would like to thank my adviser Dr. Chandramouli Krishnan for his assistance in developing some of the methods used in this study. Additionally, I would like to thank the numerous colleagues, research assistants, and students that helped me in collecting and analyzing the tremendous amounts of data included in this study, including Scott Brown, Tom Augenstein,

Mary Koje, Belinda Cargile, Kaitlyn Ford, Jiajie Qiu, Samantha Steinberg, Miranda Santos, and Michael Volyanyuk.

Chapter 7

Functional Resistance Training During Walking: Using Musculoskeletal Modeling to Determine if the Method of Application Differentially Affects Gait Biomechanics and Muscle Activation Patterns

Abstract

Background: Task-specific loading of the limbs—termed as functional resistance training—is commonly used in gait rehabilitation; however, the biomechanical and neuromuscular effects of various forms of functional resistance training have not been studied systematically. This information is crucial for correctly selecting the appropriate method of applying functional resistance training when treating individuals with gait disorders. *Research question:* To comprehensively evaluate the biomechanical (i.e., joint moment and power) and muscle activation changes with different forms of functional resistance training that are commonly used in clinics and research using biomechanical simulation-based analyses. *Methods:* We developed simulations of functional resistance training during walking using OpenSim (Gait2354, 23 degrees of freedom and 54 muscles) and custom MATLAB scripts. We investigated five methods of applying functional resistance training that have been commonly used in clinics or in research: (1) a weight attached at the ankle, (2) an elastic band attached at the ankle, (3) a viscous device attached to the hip and knee, (4) a weight attached at the pelvis, and (5) a constant backwards pulling force at the pelvis. Lower-extremity joint moments and powers were computed using inverse dynamics and muscle activations were estimated using

computed muscle control while walking with each device under multiple resistance levels: normal walking with no resistance, and walking with 30, 60, and 90 Newtons of resistance. *Results:* The results indicate that the way in which resistance is applied during gait training differentially affects the internal joint moments, powers, and muscle activations as well as the joints and phase of the gait cycle where the resistance was experienced. *Significance:* The results highlight the importance of understanding the joints and muscles that are targeted by various methods of providing functional resistance training and carefully choosing the best method of training that meets the specific therapeutic needs of the patient.

7.1 Introduction

Injuries to the neuro-musculoskeletal system (e.g., stroke, spinal cord injury, lower-extremity injuries, osteoarthritis, etc.) can result in profound gait deficits that can lead to reduced function and long-term health-related quality of life (Moseley et al., 1993; Naili et al., 2017; Pietrosimone et al., 2018). Leg muscle weakness has been consistently linked to abnormal gait patterns and poor biomechanical symmetry in these individuals (Blackburn et al., 2016; Lewek et al., 2002; Lindmark & Hamrin, 1995; Nakamura et al., 1985). Accordingly, rehabilitation efforts are often concentrated on restoring muscle strength and control. However, clinical interventions addressing muscle weakness are often performed in a non-functional manner (i.e., exercises performed in a seated or standing position), which may not be optimal for transfer of benefits of training to functional activities, such as walking, because of the phenomenon of "practice specificity" (Morrissey et al., 1995; Proteau et al., 1992; Williams et al., 2014). Task-specific loading of the limbs—commonly known as functional resistance training or functional strength training—has been purported as a potential approach to address this issue. Functional resistance training can be applied by having subjects perform weight-bearing exercises (e.g., sit-to-stand,

step-ups, etc.) (Blundell et al., 2003; Kerr et al., 2017; Lohne-Seiler et al., 2013), as well as by applying additional external loads to the limbs during walking (Chang et al., 2018; Duclos et al., 2014; Lam et al., 2015; Wu et al., 2017). The key advantages of the latter approach are that it is more specific to walking and allows the resistance to be scaled according to the needs of the patient. In the past decade, a number of studies have evaluated the short-term and long-term effects of applying external resistive loads during walking on physiological, biomechanical, and clinical outcomes (Browning et al., 2007; Chang et al., 2018; Duclos et al., 2014; Klarner et al., 2013; Lam et al., 2015; Washabaugh et al., 2016; Wu et al., 2017). Collectively, these studies have shown that functional resistance training during walking: (1) increases metabolic cost, (2) positively affects biomechanical outcomes, such as muscle activation, joint kinetics, and kinematics, and (3) improves gait function.

It is to be noted, though, that functional resistance training during walking can be performed in multiple ways. For example, studies have used simple devices, such as ankle weights and weighted-vests, to more sophisticated active and passive robotic devices (Browning et al., 2007; Chang et al., 2018; Lam et al., 2015; Puthoff et al., 2006; Wu et al., 2017). More importantly, these devices can provide resistance directly to the joints or as end-point forces (e.g., weights tethered to the ankle) and during different phases of gait. Thus, the resulting human-device interactions and muscle activation patterns may differ considerably between these various modes of functional resistance training. Given that functional resistance training is becoming increasingly popular for gait rehabilitation, it is imperative to understand the differential effects of these devices on lower-extremity biomechanics and muscle activation patterns during gait. However, studying the biomechanical effects of these devices in human subjects is challenging because of experimental constraints such as matching resistive loads

between devices and subjects, controlling for the confounding effects of fatigue during testing, and studying muscle activation from a large number of lower-extremity muscles.

Computer simulations that utilize musculoskeletal models can be a valuable tool for evaluating the biomechanical effects of different resistive exercises (Schellenberg et al., 2015). Previous researchers have used musculoskeletal modeling to compute muscle/joint forces and also to gain insight into how various musculoskeletal properties (e.g., muscle strength, limb lengths, muscle moment arms, etc.) affect biomechanical and functional outcomes (e.g. the kinematics, kinetics, muscle activation, joint loads, jump height, etc.) (Dorn et al., 2015; Escamilla et al., 2009; Fregly et al., 2015; Lewis et al., 2009; Pandy et al., 1990; Pluss et al., 2018; Schellenberg et al., 2015). Such studies have helped in determining movement control during exercise and locomotion (Dorn et al., 2015; Pandy et al., 1990), appropriate kinematics for training (Escamilla et al., 2009; Fregly et al., 2015; Lewis et al., 2009; Pluss et al., 2018), and how different exercise schemes affect muscle activation (Dorn et al., 2015; Pluss et al., 2018). Although previous studies have used musculoskeletal modeling to answer biomechanical questions related to exercise and human locomotion, there are no studies that have comprehensively evaluated how different modes of applying functional resistance training affect gait biomechanics and muscle activation patterns, which may have meaningful implications for how therapy is prescribed in the clinic. Hence, in this study, we used a biomechanical simulation to evaluate the effects of different modes of functional resistance training on gait biomechanics and lower-extremity muscle activation patterns during gait.

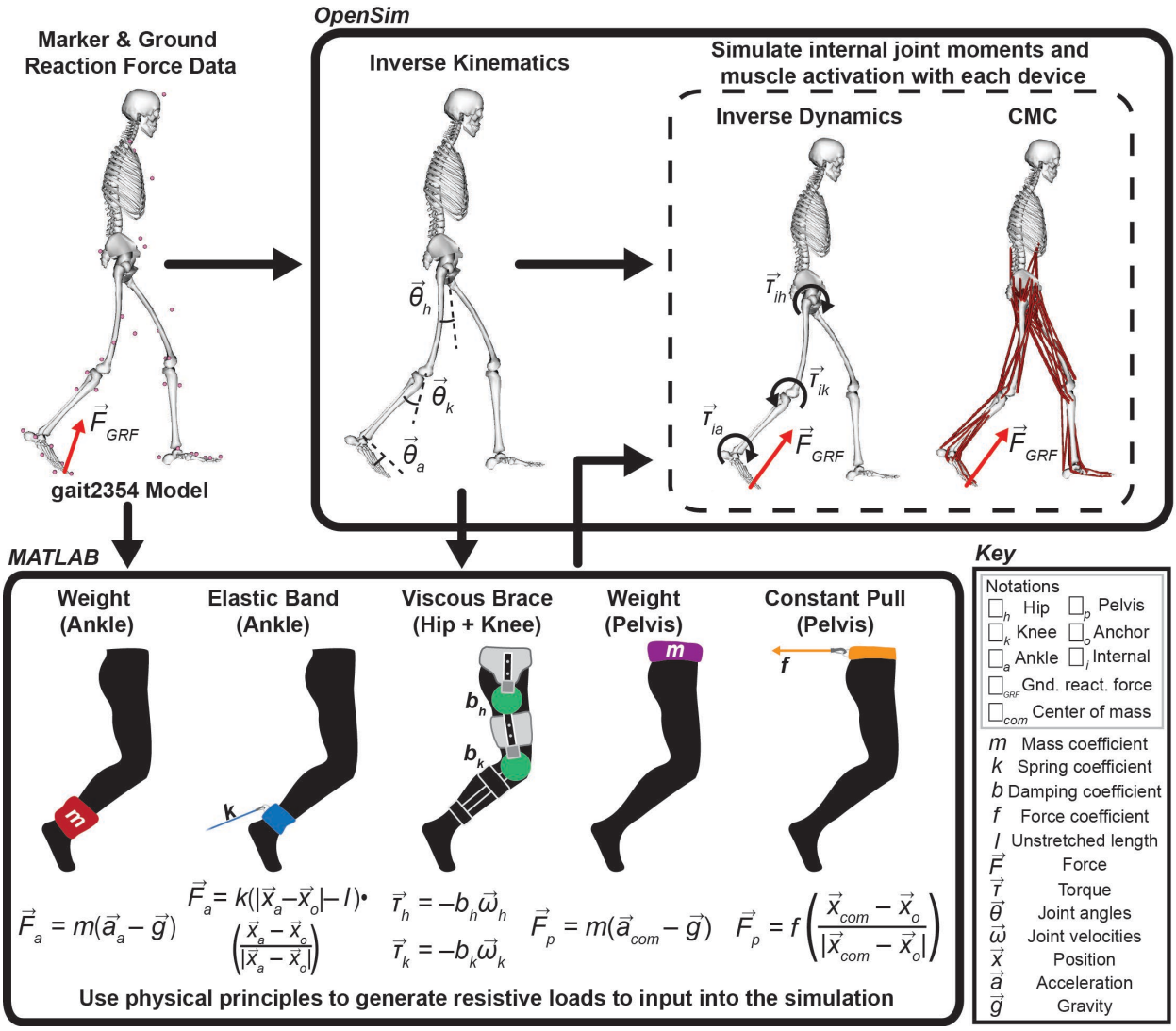

Figure 7.1 A schematic of the simulation-based analysis used to estimate the biomechanical effects of walking under various modes of applying resistance. The simulation used the Gait2354 dynamic musculoskeletal model with OpenSim to first generate kinematics from marker trajectories. The kinematics and a file containing the external forces acting on the model were then input into MATLAB to generate time-varying force information for each resistive mode. An updated external force file and the kinematics were then used to run inverse dynamics to generate internal joint moments and power and used in the computed muscle control algorithm (CMC) to generate muscle activations.

7.2 Methods

For this study, we investigated five functional resistance training paradigms (i.e., methods) that have been commonly used in clinics or research: (1) a weight attached at the ankle (Browning et al., 2007; Lam et al., 2009), (2) an elastic band attached at the ankle (Wu et al., 2017), (3) a viscous device attached to the hip and knee (i.e., a device that applies velocity-dependent resistance to the hip and knee joints) (Chang et al., 2018; Lam et al., 2008), (4) a

weight attached at the pelvis (e.g. weighted vest) (Kubinski & Higginson, 2012; Puthoff et al., 2006), and (5) a constant backwards pulling force at the pelvis (e.g. pulling a weighted sled) (Lawrence et al., 2013; Mun et al., 2017). To determine the effects of these various modes of functional resistance training, we devised a simulation-based analysis (Figure 7.1) to extract joint moments, powers, and muscle activations while walking with each device under multiple resistance levels: normal walking with no resistance, and walking with 30, 60, and 90 N of resistance. A simulation was ideal for this analysis because it allowed us to maintain exact kinematics across all modes and levels of resistance, monitor activation of muscles that are difficult to measure with surface electromyography, and perform a wide battery of tests without fatiguing a participant.

7.2.1 Biomechanical Simulation in OpenSim

The simulation was run in OpenSim (Version 3.3) using the Gait2354 dynamic musculoskeletal model (23 degrees of freedom and 54 muscles) and modeling tools (Delp et al., 1990). We set up the analysis using two marker trajectory files and an external force file provided by OpenSim for this model: the first marker trajectory file tracked a participant (weighing 72.6 kg) standing in a static pose, the second tracked the participant walking over a treadmill for several seconds, and the external force file contained all forces acting on the model during walking (i.e., ground reaction forces). We used the Scale Tool with the static marker file to scale the model to the participant's anthropometry. We then used the Inverse Kinematics Tool with the walking marker file to determine the participant's kinematics during walking. The external force file was then modified based on the mode and level of the resistance (more details on this procedure are provided below). The kinematics and external force files were then fed into the Inverse Dynamics Tool to find joint moments and calculate power, as well as the Computed

Muscle Control (CMC) Tool (Thelen et al., 2003) to simulate lower-extremity muscle activation. The maximum isometric force of each muscle in the model was adjusted uniformly in order to prevent muscle activation from saturating during CMC while maintaining each muscle's relative contribution to walking.

7.2.2 Modeling Various Modes of Functional Resistance Training

Custom MATLAB (version R2017b) programs were written in order to emulate the various modes of applying resistance and modify the external force file. For each mode of resistance, the programs modified the original external force file to (1) include the resistance that was added to the model and (2) adjust the ground reaction forces to balance new external forces. These programs used the kinematics and the governing physical principles of the resistance modes to generate time-varying force information during walking (Figure 7.1). The coefficients for each resistance mode (i.e., mass, stiffness, damping, and force constant) were set to provide either 30, 60, or 90 N of resistance to the model, determined as the average force added to the model over the gait cycle. Thus, the amount of resistance applied during walking was similar across all resistance modes. The methods used to calculate these resistances are detailed in Appendix D. To balance the external forces that were added to the model, a force equal and opposite to the external force was added to the ground reaction forces of the leg during stance. However, simply adding this balancing force to the ground reaction force resulted in large discrete events at heel strike and toe-off. To smoothen these discrete events, the balancing force was multiplied by a scalar that increased linearly from 0 (at heel strike) to 1 (at flat foot) and decreased linearly back to 0 at toe-off (i.e., trapezoidal windowing function). This force balancing was only necessary for the external forces added by the ankle weight, elastic band,

pelvis weight, and constant pelvis force. The resistive forces added by the viscous device were internal to the model, and therefore, did not alter ground reaction forces.

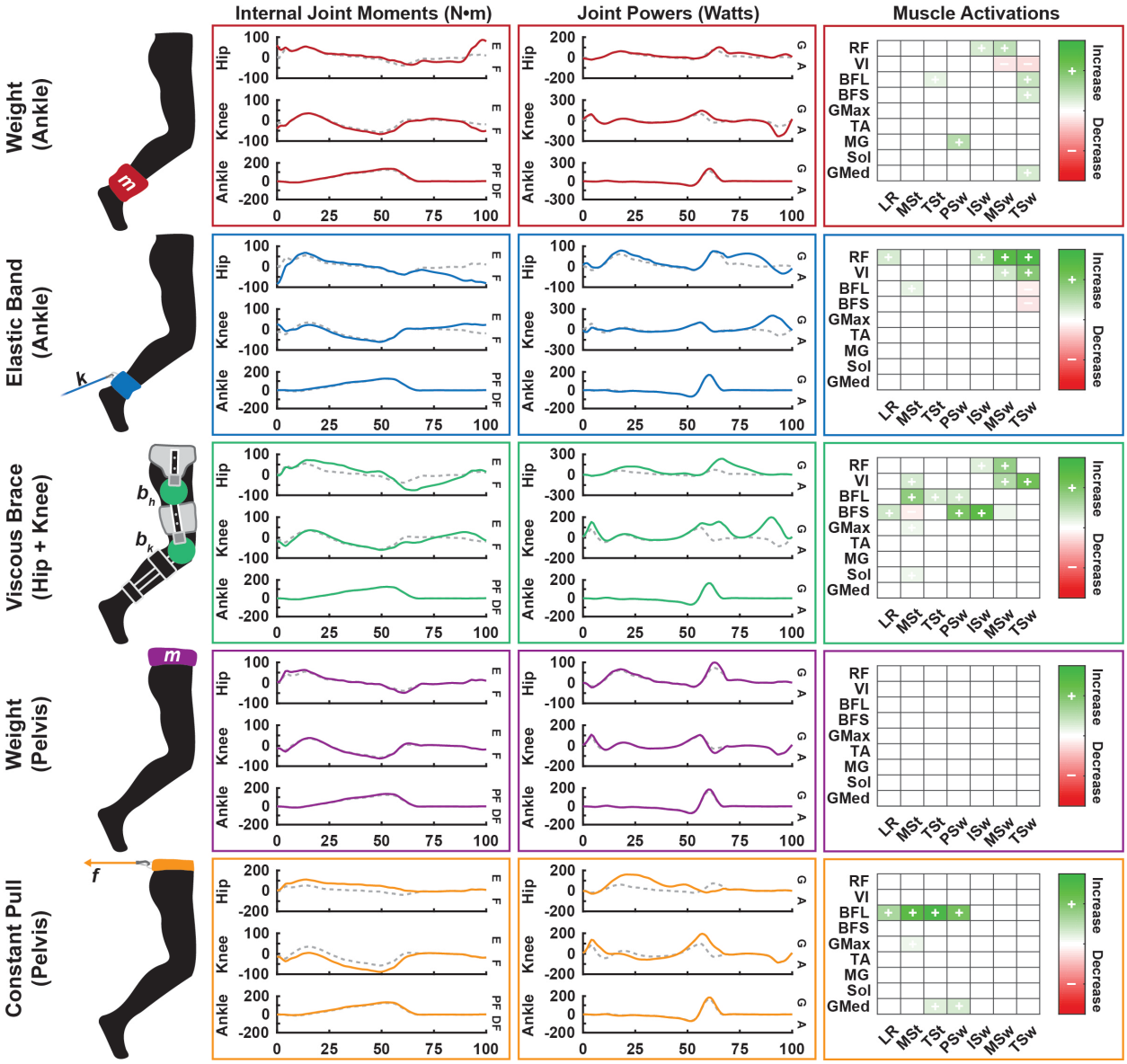

Figure 7.2 Simulated joint moments, powers, and muscle activations resulting from common resistance types applied while walking. Plots depict the result of a 60N resistive force applied using a weight placed at the ankle, an elastic band located at the ankle, a viscous resistance at the hip and knee, a weight placed at the pelvis, and a constant force pulling backwards at the pelvis. Joint moments and powers are plotted against the percentage of the gait cycle, where solid lines represent walking with the load and dashed lines represent normal walking. Labels to the right of the moment plots indicate the direction for extension, flexion, plantarflexion, and dorsiflexion. Labels on the power plots indicate a power generation or absorption. Muscle activations are depicted as a heat map of the muscles and the phase of the gait cycle, and indicate a change in muscle activation between resisted and normal walking. Muscle abbreviations: RF (rectus femoris), VI (vastus intermedius), BFL (biceps femoris long head), BFS (biceps femoris short head), GMax (gluteus maximus), TA (tibialis anterior), MG (medial gastrocnemius), Sol (soleus), GMed (gluteus medius). Gait phase abbreviations: LR (loading response), MSt (mid-stance), TSt (terminal stance), PSw (pre-swing), ISw (initial-swing), MSw (mid-swing), TSw (terminal swing).

7.2.3 Variables Extracted from the Simulation

For our analysis, we evaluated the internal joint moments and joint power of the right hip, knee, and ankle in the sagittal plane. In addition to the temporal representation of these variables, we measured the maximum and minimum moments and powers during the stance and swing phases of gait. We also evaluated the muscle activation of the rectus femoris (RF), vastus intermedius (VI), biceps femoris long head (BFL), biceps femoris short head (BFS), gluteus maximus (GMax), tibialis anterior (TA), medial gastrocnemius (MG), soleus (Sol), and gluteus medius (GMed) muscles. The model included three GMed and three GMax muscles, and we used the average activation of these muscles in our analyses. For visualization purposes, muscle activation data were depicted as heat maps that highlight the muscles and gait cycle segments where a muscle's activation either increased or decreased when compared with normal walking. In order to highlight only meaningful changes from normal walking, heat maps included muscle activation data only when the product of the percentage change in muscle activation from normal walking and the difference between resisted and normal walking muscle activations exceeded a certain threshold (1.25) (e.g., a 25% increase from baseline with at least a change of 0.05 in activation). The gait cycle was divided into loading response (LR), mid-stance (MSt), terminal stance (TSt), pre-swing (PSw), initial-swing (ISw), mid-swing (MSw), and terminal swing (TSw) to better elucidate when each resistance mode is effective during gait.

7.3 Results

Traces of the internal joint moments and joint powers, and heatmaps of muscle activations during the 60 N of resistance condition are depicted in Figure 7.2. Additionally, the maximum and minimum internal joint moments and powers and the average percent change in muscle activation during the stance and swing phases for all modes and levels of resistance are

provided in Table 7.1 and Table 7.2. The results for the 60N resistance condition are summarized below. Note that all percentages represent the percentage change of the variable with respect to normal walking with no resistance.

Table 7.1 Maximum and minimum sagittal joint moments and powers for each mode of applying functional resistance training.

Joint Moments (N·m)

		Hip				Knee				Ankle			
		Stance		Swing		Stance		Swing		Stance		Swing	
Mode	**R**	**Max**	**Min**	**Max**	**Min**	**Max**	**Min**	**Max**	**Min**	**Max**	**Min**	**Max**	**Min**
NW	–	55.1	−38.6	15.1	−8.5	35.2	−57.6	3.2	−19.1	125.4	−11.9	0.8	−2.5
Ankle Weight	30	54.8	−34.3	50.8	−15.1	35.4	−62.2	6.1	−35.7	130.7	−12.8	0.8	−2.3
	60	60.2	−35.0	87.1	−21.8	35.5	−66.7	9.1	−52.4	136.3	−13.9	0.8	−2.2
	90	88.8	−41.2	123.4	−31.9	35.7	−71.2	12.2	−69.0	141.8	−15.0	0.8	−2.2
Elastic Band	30	61.2	−38.9	−11.1	−33.8	29.3	−59.5	11.7	0.7	126.5	−7.5	0.8	−2.4
	60	67.7	−84.7	−15.0	−80.9	26.1	−60.8	27.9	3.8	127.2	−3.2	0.8	−2.4
	90	74.3	−130.6	−18.9	−128.4	46.8	−62.2	46.5	4.6	128.0	−1.1	0.8	−2.3
Viscous Brace	30	63.5	−53.4	19.1	−38.6	35.6	−58.7	12.1	−16.4	125.4	−11.9	0.8	−2.5
	60	72.0	−75.7	23.4	−68.7	36.5	−60.0	27.5	−22.6	125.4	−11.9	0.8	−2.5
	90	84.4	−104.3	27.8	−98.8	37.4	−61.5	43.6	−34.7	125.4	−11.9	0.8	−2.5
Pelvis Weight	30	59.0	−43.8	15.1	−8.9	36.5	−60.1	3.2	−19.1	130.8	−12.1	0.8	−2.4
	60	63.4	−49.1	15.1	−9.2	37.8	−62.6	3.2	−19.1	136.3	−12.3	0.8	−2.3
	90	67.8	−54.3	15.1	−9.6	39.3	−65.1	3.2	−19.1	141.8	−12.5	0.8	−2.3
Pelvis Constant	30	83.3	−17.4	15.1	−7.6	20.0	−73.1	3.2	−19.1	128.9	−9.3	0.8	−2.3
	60	111.6	−6.8	15.1	−6.8	4.7	−88.6	3.2	−19.1	132.5	−7.1	0.8	−2.2
	90	139.8	−3.2	15.1	−6.3	−2.6	−104.1	3.2	−19.1	136.1	−4.8	0.8	−2.3

Joint Powers (Watts)

		Hip				Knee				Ankle			
		Stance		Swing		Stance		Swing		Stance		Swing	
Mode	**R**	**Max**	**Min**	**Max**	**Min**	**Max**	**Min**	**Max**	**Min**	**Max**	**Min**	**Max**	**Min**
NW	–	73.4	−18.1	26.6	−0.1	100.2	−44.0	5.9	−86.7	163.3	−69.0	2.6	−2.6
Ankle Weight	30	82.6	−18.6	47.4	0.1	119.9	−46.1	11.1	−159.0	182.4	−71.9	2.6	−2.5
	60	102.3	−19.7	68.2	0.3	143.0	−48.1	16.2	−231.9	203.1	−74.8	2.6	−2.3
	90	122.9	−20.8	89.0	0.5	168.8	−50.2	21.4	−305.5	223.8	−77.7	2.6	−2.1
Elastic Band	30	74.7	−16.8	44.0	−13.2	103.7	−31.8	81.3	−15.3	165.0	−69.6	2.6	−2.6
	60	78.9	−16.1	64.7	−34.0	104.9	−35.6	204.7	−19.3	165.1	−70.0	2.6	−2.5
	90	87.7	−15.4	92.7	−54.9	106.1	−70.8	336.9	−23.7	165.2	−70.4	2.6	−2.5
Viscous Brace	30	143.4	−16.0	121.3	0.0	120.6	−36.4	84.6	−26.3	163.3	−69.0	2.6	−2.6
	60	234.2	−14.6	215.9	0.1	156.6	−29.9	199.2	−9.1	163.3	−69.0	2.6	−2.6
	90	329.1	−13.1	310.6	0.2	245.0	−26.7	317.5	−4.7	163.3	−69.0	2.6	−2.6
Pelvis Weight	30	85.3	−20.0	27.8	−0.1	102.3	−51.8	5.9	−86.7	172.7	−72.0	2.6	−2.5
	60	98.5	−22.4	29.1	−0.1	107.8	−72.1	5.9	−86.7	182.1	−75.0	2.6	−2.5
	90	111.8	−24.8	30.3	−0.1	117.7	−92.4	5.9	−86.7	191.5	−78.0	2.6	−2.4
Pelvis Constant	30	107.3	−22.3	24.0	−0.1	143.3	−41.4	5.9	−86.7	172.7	−71.0	2.6	−2.4
	60	160.6	−27.0	21.4	−0.1	193.7	−57.1	5.9	−86.7	182.8	−72.9	2.6	−2.2
	90	220.0	−44.1	18.7	−0.1	246.8	−76.2	5.9	−86.7	193.3	−74.9	2.6	−2.0

Abbreviations: R (resistance level [N]), NW (normal walking with no resistance); Mass of the subject in the model: 72.6 [kg]. For hip and knee joint moments, (+) indicates extension and (−) indicates flexion. For the ankle moments, (+) indicates plantarflexion and (−) indicates dorsiflexion. For all powers, (+) indicates a concentric contraction (power generation) and (−) indicates an eccentric contraction (power absorption).

The ankle weight mainly increased hip extension and knee flexion moments (477% and 174%, respectively) and increased power absorption (167%) at the knee joint at the end of the

swing phase. The muscle activation of the hamstrings (biceps femoris long and short heads) was increased during the terminal swing (35% and 17%, respectively). This increased hamstring muscle activation corresponded to eccentric contraction of the hamstring muscles because the knee joint was absorbing power over this phase. Interestingly, the ankle weight also reduced the activation of a quadriceps muscle (vastus intermedius) during swing (−48%).

The elastic band increased hip flexion and knee extension moments during the swing phase of gait (852% and 772%, respectively) when compared with normal walking with no resistance. The hip generated more power during the early swing phase (143%) then began absorbing more power towards the end of the swing phase (>1000%). The knee primarily showed an increase in power generation during the swing phase (>1000%). The muscle activation of the quadriceps muscles (rectus femoris and vastus intermedius) was increased during the swing phase (198% and 148%, respectively), while that of the hamstring muscles (biceps femoris long and short heads) was decreased during the swing phase (−22% and −9%, respectively).

The viscous device increased hip extension moments during the stance phase (31%) and hip flexion moments during the swing phase (708%) when compared with normal walking with no resistance. In the knee, it increased flexion moments during early swing (18%) and increased extension moments during late swing (759%). The viscous device increased power generation at the hip during the stance and swing phases (219% and 712%, respectively), and also increased power generation at the knee during the swing phase (>1000%). The muscle activation of the hamstring muscles (biceps femoris long and short heads) was increased during the stance (59% and 32%, respectively) and initial swing phases (20% and 90%, respectively), and that of the quadriceps muscles (rectus femoris and vastus intermedius) was increased during the swing

phase (66% and 194%, respectively). These increased quadriceps and hamstring muscle activation corresponded to concentric contractions of these muscles because the hip and knee joints were generating power at these instances.

Table 7.2 Average percentage change in muscle activation from normal walking for each mode of applying functional resistance training.

Muscle Activation (% Change)											
Mode	**R**	**Phase**	**RF**	**VI**	**BFL**	**BFS**	**GMax**	**TA**	**MG**	**Sol**	**GMed**
Ankle Weight	30	Stance	−2	−3	4	0	−6	6	8	−1	−2
		Swing	30	−40	20	1	6	1	4	0	11
	60	Stance	−11	−5	10	2	−6	12	14	2	−2
		Swing	46	−48	35	17	9	2	8	−1	31
	90	Stance	−11	−4	18	7	−3	20	21	8	0
		Swing	69	−53	58	32	2	4	17	1	50
Elastic Band	30	Stance	2	−7	3	0	0	−11	1	2	−1
		Swing	108	75	−17	−2	−11	0	1	0	−12
	60	Stance	47	−10	17	6	9	−18	5	−4	1
		Swing	198	148	−22	−9	−10	0	1	0	−10
	90	Stance	70	−12	22	6	17	−24	8	−6	3
		Swing	281	208	−28	−11	−12	0	1	0	−19
Viscous Brace	30	Stance	−26	15	30	20	11	−5	0	3	3
		Swing	42	114	22	45	6	0	1	−2	−4
	60	Stance	−31	36	59	32	27	−5	0	3	8
		Swing	66	194	20	90	14	1	1	4	−1
	90	Stance	−34	61	92	51	40	−4	1	5	15
		Swing	104	257	27	122	29	3	11	0	5
Pelvis Weight	30	Stance	2	1	−1	−1	1	1	3	4	2
		Swing	9	−2	5	1	0	0	1	1	−2
	60	Stance	5	3	−1	1	1	6	7	13	4
		Swing	9	3	8	4	−1	1	2	2	−1
	90	Stance	7	5	1	1	5	8	11	18	8
		Swing	13	0	12	0	−3	2	3	3	2
Pelvis Constant	30	Stance	−31	−7	67	3	18	−5	6	−5	9
		Swing	4	0	−2	5	−1	0	3	−3	−5
	60	Stance	−32	−4	156	7	38	−14	6	13	28
		Swing	5	0	0	−4	0	2	10	1	5
	90	Stance	−32	−5	249	8	61	−28	5	21	47
		Swing	3	−2	−3	5	3	2	6	2	−3

Abbreviations: R (resistance level [N]), RF (rectus femoris), VI (vastus intermedius), BFL (biceps femoris long head), BFS (biceps femoris short head), GMax (gluteus maximus), TA (tibialis anterior), MG (medial gastrocnemius), Sol (soleus), GMed (gluteus medius). The average percentage change in muscle activation was calculated as: ((resisted − normal)/normal)*100.

The weight belt at the pelvis had a minimal effect on gait mechanics at the resistance levels studied in this experiment. The moments, powers, and muscle activation measured while applying resistance closely resembled those of normal walking with no resistance. The most notable change was an increase in knee absorption power during the stance phase (64%).

However, quadriceps muscle activation changes during the stance phase were minimal as a result of the added resistance (≤5%).

The backwards force pulling on the pelvis resulted in increased hip extension and knee flexion moments during the stance phase (103% and 54%, respectively) when compared with normal walking with no resistance. Power generation increased at the hip for most of the stance phase (119%) but decreased during the pre-swing phase (−122%). The knee generated more power during the loading response (56%), absorbed more power during mid-stance (112%), then generated more power again during pre-swing (93%). This mode of resistance mostly increased muscle activation of hip extensor muscles (biceps femoris long head and gluteus medius) during the stance phase (156% and 28%, respectively).

7.4 Discussion

Functional resistance training is increasing in popularity for gait rehabilitation, and several devices have been used in clinics and research to provide resistance to the leg while walking. However, the resulting human-device interactions and muscle activation patterns may differ considerably based on the mode in which the resistance is applied. An understanding of the biomechanical and neuromuscular effects of different modes of functional resistance training is crucial for tailoring training to patient-specific needs. This is the first study to comprehensively characterize the effects of various modes of functional resistance training on lower-extremity biomechanics and muscle activation during gait using a complex biomechanical simulation-based analysis. We specifically evaluated the effects of an ankle weight, an elastic band attached to the ankle, a viscous device attached to the hip and knee, a weight belt on the pelvis, and a constant backwards pulling force on the pelvis, which are the most commonly used methods in clinics and research. We found that the mode of applying resistance had differential effects on

the internal joint moments, powers, and muscle activations—greatly influencing the joints and phase of the gait cycle where the resistance was experienced, as well as the muscles that must counteract the applied resistance.

Our results indicate that, when applying functional resistance training during gait, the mode of resistance can be chosen to account for specific strength deficits or walking impairments. Ankle weights primarily increased internal hip extension and knee flexion moments at the end of the swing phase and provided resistance to the hamstring muscles. An elastic band placed at the ankle increased internal hip flexion and knee extension at the end of the swing phase and provided resistance primarily to the quadriceps muscles. The viscous device at the hip and knee was able to provide resistance to the hamstring muscles over the stance phase and initial swing, and the quadriceps muscles during mid- and late-swing. A weight placed at the pelvis was not very effective at providing resistance during walking. The constant backwards pulling force on the pelvis was the most effective mode for resisting hip extension and knee flexion during stance. Overall, these findings were consistent with previous studies on human subjects (Browning et al., 2007; Chang et al., 2018; Duclos et al., 2014; Klarner et al., 2013; Lam et al., 2006; Lam et al., 2008; Lawrence et al., 2013; Mun et al., 2017; Savin et al., 2010; Washabaugh et al., 2016), albeit, with some exceptions. A key discrepancy was that a constant backwards pulling force on the pelvis has been shown to increase both quadriceps and hamstring activation during stance (Lawrence et al., 2013; Mun et al., 2017), whereas only the hamstring muscles were active in our study. We believe this occurred because participants typically are allowed to adjust their kinematics when walking against a resistance, whereas we constrained the kinematics to normal walking. Thus, the increased hip, knee, and trunk flexion that are

commonly observed when walking with a constant backward pulling force could have resulted in more contribution from the quadriceps muscles (Mun et al., 2017).

An important finding of this study was that a weight placed at the pelvis minimally altered joint moments and muscle activation during resisted walking. Other studies that have investigated this mode of resistance at similar resistance levels have also found that it is ineffective for altering the internal joint moments during walking (Browning et al., 2007; Kubinski & Higginson, 2012). It is possible that the mass used for these studies was too small to elicit meaningful effects, as studies that have applied much larger resistances (up to 40% of bodyweight) found increases in quadriceps muscle activation (Simpson et al., 2011). We did not apply resistances this large because we controlled for the amount of external force applied to the model to allow for proper comparison between resistive modes, and we feel masses that large would not be practical for training patients with gait impairments. Similar to a weight placed at the pelvis, a weight placed at the ankle only had a small effect on internal joint moments/powers even with a large mass. Additionally, the increases in internal moments and powers due to a weight placed at the ankle were mainly observed during the terminal swing, which greatly limits how this approach can be applied for functional resistance training during walking.

In our simulation, we constrained the kinematics of the model to match a normal gait pattern without any resistance. Notably, this assumption does not account for kinematic adaptations that would typically occur when resistance is added during walking, which may lead to differences between the simulation results and what would be found through experiments on human subjects. However, there is a strong rationale for constraining the kinematics to normal walking. There is evidence that resisted walking leads to motor slacking (Washabaugh et al., 2016), where the motor system reduces muscle activation levels and movement excursions to

minimize metabolic and movement-related costs (Reinkensmeyer et al., 2009). To reduce slacking during functional resistance training of gait, many studies instruct subjects to walk as normally as possible (Barthélemy et al., 2012; Lam et al., 2006; Lam et al., 2008) or provide kinematic feedback (Klarner et al., 2013; Washabaugh et al., 2016) when the resistance is applied. This helps ensure that the muscles are appropriately loaded so the benefits of functional resistance training can be fully realized. Moreover, studies have shown that, although participants reduce their hip and knee flexion angles during the early part of functional resistance training, they typically adapt to the applied resistance and resume walking with more normal flexion angles with continued training (Lam et al., 2006). From these aspects, the model adequately accounted for the effort that the participant will have to exert while walking with resistance and resembled the way in which functional resistance training is performed in the clinic or research.

7.5 Limitations

There are some potential limitations to this study. We used a generic musculoskeletal model based on healthy participants in our simulations, which limits the generalizability of the findings to clinical populations (e.g., stroke) that often present with altered biomechanics and muscle weakness. However, it is to be noted that clinical populations with gait deficiencies share many kinematic gait features with normal walking (e.g., the leg must swing forward and backward throughout the gait cycle to complete a stride); hence, we believe that many of the general findings presented in this study will carry over to clinical populations. Another limitation is that we do not know how much change in muscle activation or moment data is needed to induce meaningful physiological adaptations (e.g., increase in gait speed). However, the observed biomechanical changes are in general similar to or greater than those reported in the

literature (Browning et al., 2007; Houldin et al., 2011; Mun et al., 2017; Savin et al., 2010; Yen et al., 2013)—a change that has been shown to positively affect gait outcomes in patient populations after a course of an intervention (Lam et al., 2009; Lam et al., 2015; Wu et al., 2017). There are also several assumptions made during musculoskeletal modeling. For example, biomechanical simulations typically rely on a minimum effort principle (e.g., the sum of the squared muscle activations, as done in this study) to simulate muscle activation. While this approximation of a human's motor control objective may be reasonable for a healthy population, it may not hold when predicting the muscle activation of a pathological gait, which can be influenced by other factors such as pain or fatigue. In these cases, patients may alter their motor control to more heavily favor stability or preserve joint integrity by increasing antagonist muscle activity, which a minimum effort principle fails to predict (Bergmann et al., 2004; Schellenberg et al., 2015). As a result, caution should be exercised when generalizing the study results to a patient population.

7.6 Conclusion

In summary, using a simulation-based analysis we show that the mode of applying resistance greatly affects joint moments, powers, and muscle activation, as well as the phase of the gait cycle where the resistance was experienced. Specifically, we show that providing resistance via an elastic band at the ankle can be used to isolate and target the quadriceps muscles during the swing phase, whereas a viscous hip and knee device could be used to target both hip/knee flexors and extensors. A constant backward pulling force at the pelvis could be used to primarily target the hip extensors during the stance phase. A weight placed at the pelvis or at the ankle minimally altered joint moments and muscle activation during resisted walking. Thus, the detailed biomechanical and muscle activation changes described in this study can be

used to guide rehabilitation so that resistances for functional resistance training during gait can be prescribed to better account for patient-specific strength deficits or walking impairments.

7.7 Acknowledgment

This work has been published in Gait and Posture (Washabaugh, Augenstein, & Krishnan, 2020). I would like to thank my co-authors on this article: Thomas E. Augenstein and Dr. Chandramlouli Krishnan for their contributions to the data processing, analysis, and drafting/editing of the manuscript. This work was partly supported by the National Institute of Child Health and Human Development of the National Institutes of Health (Grant # R21 HD092614), (2) National Science Foundation Graduate Research Fellowship Program (DGE #1256260), (3) The U-M-BICI (Beijing Institute of Collaborative Innovation) Collaboratory, and (4) Disability and Rehabilitation Engineering Program of the National Science Foundation (Grant # 1804053).

Chapter 8

Conclusion

8.1 Summary

This dissertation presents considerable work studying strategies for providing resistance to the leg for functional resistance training during walking. Overall, this research worked toward two common themes. In the first theme, we worked to compare how resistive gait strategies that have been commonly used in the literature could be used to target patient-specific weakness. In the second theme, we worked to develop new low-cost devices that could provide utility in the clinic and in home.

In line with the first theme, our literature review in Chapter 1 identified several methods that have been used to provide resistance to the legs during walking and summarized how these methods have been able to augment the acute effects of training. Similarly, in Chapter 7, we used musculoskeletal modeling in OpenSim to directly compare several strategies that have been used to provide functional resistance training to gait in the clinic or laboratory setting. Our review may better represent how patients will naturally adapt to resistance. However, musculoskeletal modeling offered a unique environment to make these comparisons because it allowed us to closely match the magnitude of the resistance and controlled for the kinematics of the model (i.e., the model could not kinematically slack). In both instances, we found that devices differed in their ability to alter gait parameters during walking. Hence, we believe the information presented in these chapters could be of use to clinicians when selecting a resistive strategy

informed by their patient's impairments and functional goals, while remaining feasible for use in their clinic or in the patient's home. It could also be of use to engineers who are looking to design new rehabilitation strategies for providing resistance during walking.

As for our second theme, we found that passive devices have been more commonly used for this type of training. This may be because passive devices (e.g., weighted cuffs and resistance bands) provide an extremely low-cost and easy-to-use option for providing resistance to the legs during walking. However, putting factors like cost and ease of use aside, it appears that wearable robotic exoskeleton devices have the most upside for this type of training. With a robotic exoskeleton, a single device can be used to resist a wide array of gait abnormalities and training can be easily controlled or monitored by the operator. Still, the large cost of these devices can disincentivize their widespread use in most clinical or home settings. To remedy this, we proposed the use of passive and semi-passive exoskeleton devices for this training, as they balance the affordability of passive devices with the controllability and patient monitoring capabilities of robotic devices. In Chapters 2 – 5 we developed and tested two passive wearable exoskeleton devices for providing resistance to the leg.

Chapter 2 documented the design of our passive damper based device, which provided a viscous (i.e., velocity-dependent) resistance to the knee using a magnetic, eddy current brake. This device was unique because the resistive properties of the device (i.e., the damping coefficient) could be easily adjusted by altering the exposure of the magnets over the disk. Preliminary testing with this device on able-bodied participants (Chapter 2) and stroke survivors (Chapter 3) indicated that the device provided resistance levels suitable for functional resistance training in a package that was both lightweight and wearable. Walking with this device at the knee resulted in significant increases in activation of many of the muscles tested. A brief period

of training also resulted in significant aftereffects once the resistance was removed. In stroke survivors, this training resulted in significant improvements in overground gait velocity. These results supported the feasibility of this device for providing functional resistance training during walking. Notably, in Chapter 4 this device was then upgraded so that the brake could be controlled by a computer (i.e., made semi-passive).

However, Chapter 4 had an additional purpose related to the application of training, which may also have design ramifications. In our previous experiments, we noted that participants often reduced their joint excursions when walking with resistance, which we believed to be a form of motor slacking. Hence, we ran an experiment to determine if participants were slacking during training, and if visual feedback could be used to augment the training and reduce any slacking behavior. We found that training without feedback significantly reduced knee flexion, indicating the participants were kinematically slacking. Also, providing visual feedback of knee joint kinematics during training significantly increased knee muscle activation and kinematic aftereffects (i.e., reduced slacking). These findings underscored the importance of using additional methods to externally motivate functional resistance training during walking. While there are many ways that feedback can be applied for this training (e.g., via coaching, visual feedback, object avoidance, or games), robotic devices are more likely to have the instrumentation required to provide more salient treatment.

In Chapter 5, we designed a passive elastic exoskeleton and tested how it could be used to resist the knee of an able-bodied participant. We were interested in elastic resistances because elastic elements are capable of storing energy (when a spring is compressed) then returning that energy to the user (when the spring recoils). Exerting energy on the user is a minimum requirement for providing resistance for eccentric muscle contractions. Notably, viscous

resistances cannot exert energy on the user. While there have been several elastic exoskeletons that have been used to assist/resist gait, the device we designed was unique in that it was highly configurable, meaning it could be used to provide resistance to joint flexion, extension, or to both (i.e., bidirectionally). Hence, the device could be used to target patient-specific weaknesses based on the configuration. During testing, we found the different device configurations could be used to target resistance more towards the knee extensor or flexor muscles. Also, knee joint power absorption was increased at several points on the gait cycle, meaning the device was exerting energy on the user.

Chapter 6 consisted of two experiments. The first compared functional resistance training while using the viscous and elastic knee braces to provide a bidirectional resistance at the knee. The second compared training with a resistance targeted to the knee with resistance targeted to both the hip and knee. In both experiments, we found that gait biomechanics were altered during training. Hence, the resistance type and targeted joint altered joint moments, powers, and muscle activation patterns. However, these training methods did not differ from one another in their ability to produce kinematic aftereffects, alter neural excitability, or fatigue the leg muscles during training. While this may indicate that the body is not very sensitive to the type of resistance that is used for training, there are several other ways that these devices could be controlled or configured that may change this interpretation. Additionally, differences may appear if we tested the cumulative effects of training with these two devices (i.e., in a clinical intervention). These experiments also provided new insight into how training can be dosed (i.e., how much resistance should be provided) during an intervention, as 15-20% of the participant's isometric strength fatigued the hamstring muscles but not the quadriceps. However, the ability to

properly dose a training may be limited based on the leg braces ability to transfer resistances to the leg.

In summary, we have examined how existing strategies for providing resistance during walking can be used to provide patient-specific treatments. Additionally, we have identified a gap within these strategies, and propose the use of passive and semi-passive exoskeleton devices for use in this training. We then designed two of these devices and tested their effects on able-bodied individuals and a small sample of stroke survivors. While our results so far have been promising, there are several lines of research that must be explored to further the themes presented in this dissertation.

8.2 Future Directions

Areas of research that should be further explored include redesigning of leg brace devices and translation of this research into clinical populations. When redesigning these resistive devices, first, the resistive mechanisms can be made smaller and more compact. Currently, the devices use many off-the-shelf parts which makes them larger than necessary. Several parts could be customized to reduce the size of these devices. For example, the gear mechanism for the magnetic brake could be customized to be lower profile, which would make the device sit much closer to the leg. During this process, we could also re-configure the gear ratio, disk diameter, and number of magnets so that the rotational inertia of the device could be reduced. Likewise, the ratcheting system for the elastic brake largely dictates the size of the device. If the ratchet and pawl were smaller, we could likely use springs that have a smaller footprint but are stiffer. Hence, the size/weight of the whole device could potentially be reduced.

Second, the wearable braces need to be revised so that they are better able to convey forces from the device to the leg. This was a major limiting factor in some of our studies. For

example, in Chapter 6, we attempted to apply 15-20% of the participant's hip flexor and extensor torque but were only able to convey approximately half of the desired value. Although we used a custom configuration of leg braces in these studies, the brace was still comprised of off-the-shelf components. Further, these components were designed to limit range of motion and stabilize the joint. Hence, they were never intended to convey large resistances. In the future, we would redesign the pelvis and thigh braces so that they came in better contact with bony landmarks (e.g., the sacrum and anterior superior iliac spine). Further, it would improve the user experience if the device were easier for the patient to put on themselves.

Third, we tested the effects of these devices at the knee and the hip, but we have not attempted to target the ankle. This decision was intentional, as many stroke survivors are prescribed an ankle foot orthosis and we did not want to disrupt this treatment. However, the ankle plays a very important role in gait and would be a worthwhile training target. Indeed, stroke survivors often have an impaired ability to generate ankle plantarflexion moment (i.e., are unable to push off) at the end of the stance phase (Olney & Richards, 1996). While the ankle can present additional design challenges (e.g., the weight of the device will add more inertia to the leg, as the ankle is further from the center of mass), it is likely that the viscous and elastic mechanisms could be modified for this purpose.

Beyond device redesigns, there is a large need to translate this research into clinical populations. While the majority of research into functional resistance training is motivated to rehabilitate individuals with neurological injuries, only a small portion of research has been performed on these individuals. Even in this dissertation, we only tested the viscous device on a small group of stroke survivors. While we had intended to collect more data from stroke survivors, this was not possible because of research restrictions during the COVID pandemic. It

is important that more research be conducted on clinical populations because research on able-bodied individuals may not translate into individuals with neurological injuries. For example, in Chapter 6 we tested how training was able to induce fatigue. While our results indicated that the training was likely not intense enough for the quadriceps muscles of able-bodied individuals, this may not be the case for patients that have clinical signs of muscle weakness and gait impairments. Testing in clinical populations will also be necessary to educate our device redesigns, as human factors and requirements for usability will likely be altered in these populations.

Lastly, we have done substantial testing on the acute effects of functional resistance training with these devices; however, the findings from these studies must be substantiated through a clinical intervention. For example, in our studies, we tested how these devices could be used to alter internal joint moments, power, and muscle activation during walking. Ideally, an intervention with these devices would increase strength in these joints/muscles. However, that must still be verified. We also measured kinematic aftereffects. While it is often assumed that aftereffects measured during acute studies can be reinforced with continued training, this also must be verified. Clinical interventions on functional resistance training during gait should also work to determine if there are cumulative neural effects of this training, as such findings may elucidate clinical populations that could benefit from this training.

References

Aboodarda, S. J., Page, P. A., & Behm, D. G. (2016). Muscle activation comparisons between elastic and isoinertial resistance: A meta-analysis. *Clinical Biomechanics (Bristol, Avon)*, *39*, 52-61. https://doi.org/10.1016/j.clinbiomech.2016.09.008

Akagi, R., Sato, S., Hirata, N., Imaizumi, N., Tanimoto, H., Ando, R., Ema, R., & Hirata, K. (2020). Eight-Week Low-Intensity Squat Training at Slow Speed Simultaneously Improves Knee and Hip Flexion and Extension Strength. *Frontiers in Physiology*, *11*, 893. https://doi.org/10.3389/fphys.2020.00893

Alabdulwahab, S. S., Ahmad, F., & Singh, H. (2015). Effects of functional limb overloading on symmetrical weight bearing, walking speed, perceived mobility, and community participation among patients with chronic stroke. *Rehabilitation Research and Practice*, *2015*, 241519. https://doi.org/10.1155/2015/241519

Anderson, C. E., Sforzo, G. A., & Sigg, J. A. (2008). The effects of combining elastic and free weight resistance on strength and power in athletes. *Journal of Strength and Conditioning Research*, *22*(2), 567-574. https://doi.org/10.1519/JSC.0b013e3181634d1e

Arangio, G. A., Chen, C., Kalady, M., & Reed, J. F., 3rd. (1997). Thigh muscle size and strength after anterior cruciate ligament reconstruction and rehabilitation. *Journal of Orthopaedic and Sports Physical Therapy*, *26*(5), 238-243. https://doi.org/10.2519/jospt.1997.26.5.238

Awad, L. N., Lewek, M. D., Kesar, T. M., Franz, J. R., & Bowden, M. G. (2020). These legs were made for propulsion: Advancing the diagnosis and treatment of post-stroke propulsion deficits. *Journal of Neuroengineering and Rehabilitation*, *17*(1), 139. https://doi.org/10.1186/s12984-020-00747-6

Banala, S. K., Kim, S. H., Agrawal, S. K., & Scholz, J. P. (2009). Robot assisted gait training with active leg exoskeleton (ALEX). *IEEE Transactions on Neural Systems and Rehabilitation Engineering*, *17*(1), 2-8. https://doi.org/10.1109/TNSRE.2008.2008280

Barnett, M. L., Ross, D., Schmidt, R. A., & Todd, B. (1973). Motor skills learning and the specificity of training principle. *Research Quarterly*, *44*(4), 440-447. http://www.ncbi.nlm.nih.gov/pubmed/4532277

Barthélemy, D., Alain, S., Grey, M. J., Nielsen, J. B., & Bouyer, L. J. (2012). Rapid changes in corticospinal excitability during force field adaptation of human walking. *Experimental Brain Research*, *217*(1), 99-115. https://doi.org/10.1007/s00221-011-2977-4

Bastian, A. J. (2008). Understanding sensorimotor adaptation and learning for rehabilitation. *Current Opinion in Neurology*, *21*(6), 628-633. https://doi.org/10.1097/WCO.0b013e328315a293

Benoit, D. L., Ramsey, D. K., Lamontagne, M., Xu, L., Wretenberg, P., & Renstrom, P. (2006). Effect of skin movement artifact on knee kinematics during gait and cutting motions measured in vivo. *Gait and Posture*, *24*(2), 152-164. https://doi.org/10.1016/j.gaitpost.2005.04.012

Bergmann, G., Graichen, F., & Rohlmann, A. (2004). Hip joint contact forces during stumbling. *Langenbecks Archives of Surgery*, *389*(1), 53-59. https://doi.org/10.1007/s00423-003-0434-y

Bertram, J. E. (2005). Constrained optimization in human walking: Cost minimization and gait plasticity. *Journal of Experimental Biology*, *208*(Pt 6), 979-991. https://doi.org/10.1242/jeb.01498

Blackburn, J. T., Pietrosimone, B., Harkey, M. S., Luc, B. A., & Pamukoff, D. N. (2016). Quadriceps function and gait kinetics after anterior cruciate ligament reconstruction. *Medicine and Science in Sports and Exercise*, *48*(9), 1664-1670. https://doi.org/10.1249/MSS.0000000000000963

Blanchette, A. K., & Bouyer, L. J. (2009). Timing-specific transfer of adapted muscle activity after walking in an elastic force field. *Journal of Neurophysiology*, *102*(1), 568-577. https://doi.org/10.1152/jn.91096.2008

Blanchette, A. K., Lambert, S., Richards, C. L., & Bouyer, L. J. (2011). Walking while resisting a perturbation: Effects on ankle dorsiflexor activation during swing and potential for rehabilitation. *Gait and Posture*, *34*(3), 358-363. https://doi.org/10.1016/j.gaitpost.2011.06.001

Blanchette, A. K., Moffet, H., Roy, J.-S., & Bouyer, L. J. (2012). Effects of repeated walking in a perturbing environment: A 4-day locomotor learning study. *Journal of Neurophysiology*, *108*(1), 275-284. http://jn.physiology.org/cgi/doi/10.1152/jn.01098.2011

Blanchette, A. K., Noel, M., Richards, C. L., Nadeau, S., & Bouyer, L. J. (2014). Modifications in ankle dorsiflexor activation by applying a torque perturbation during walking in persons post-stroke: a case series. *Journal of Neuroengineering and Rehabilitation*, *11*, 98. https://doi.org/10.1186/1743-0003-11-98

Blundell, S. W., Shepherd, R. B., Dean, C. M., Adams, R. D., & Cahill, B. M. (2003). Functional strength training in cerebral palsy: A pilot study of a group circuit training class for children aged 4-8 years. *Clinical Rehabilitation*, *17*(1), 48-57. https://doi.org/10.1191/0269215503cr584oa

Bohannon, R. W. (2001). Measuring knee extensor muscle strength. *American Journal of Physical Medicine and Rehabilitation*, *80*(1), 13-18. https://doi.org/10.1097/00002060-200101000-00004

Bohannon, R. W. (2007). Muscle strength and muscle training after stroke. *Journal of Rehabilitation Medicine*, *39*(1), 14-20. https://doi.org/10.2340/16501977-0018

Bonnard, M., Camus, M., Coyle, T., & Pailhous, J. (2002). Task-induced modulation of motor evoked potentials in upper-leg muscles during human gait: A TMS study. *European Journal of Neuroscience*, *16*(11), 2225-2230. https://doi.org/10.1046/j.1460-9568.2002.02295.x

Brandes, M., Schomaker, R., Mollenhoff, G., & Rosenbaum, D. (2008). Quantity versus quality of gait and quality of life in patients with osteoarthritis. *Gait and Posture*, *28*(1), 74-79. https://doi.org/10.1016/j.gaitpost.2007.10.004

Brandt, M., Jakobsen, M. D., Thorborg, K., Sundstrup, E., Jay, K., & Andersen, L. L. (2013). Perceived loading and muscle activity during hip strengthening exercises: Comparison of elastic resistance and machine exercises. *International Journal of Sports Physical Therapy*, *8*(6), 811-819. https://www.ncbi.nlm.nih.gov/pubmed/24377067

Brown, S. R., Washabaugh, E. P., Dutt-Mazumder, A., Wojtys, E. M., Palmieri-Smith, R. M., & Krishnan, C. (2021). Functional resistance Training to improve knee ftrength and function after acute anterior cruciate ligament reconstruction: A case study. *Sports Health*, *13*(2), 136-144. https://doi.org/10.1177/1941738120955184

Browning, R. C., Modica, J. R., Kram, R., & Goswami, A. (2007). The effects of adding mass to the legs on the energetics and biomechanics of walking. *Medicine and Science in Sports and Exercise*, *39*(3), 515-525. https://doi.org/10.1249/mss.0b013e31802b3562

Cajigas, I., Koenig, A., Severini, G., Smith, M., & Bonato, P. (2017). Robot-induced perturbations of human walking reveal a selective generation of motor adaptation. *Science Robotics*, *2*(6). https://doi.org/10.1126/scirobotics.aam7749

Cappozzo, A., Catani, F., Croce, U. D., & Leardini, A. (1995). Position and orientation in space of bones during movement: Anatomical frame definition and determination. *Clinical Biomechanics (Bristol, Avon)*, *10*(4), 171-178. https://doi.org/10.1016/0268-0033(95)91394-t

Carroll, T. J., Riek, S., & Carson, R. G. (2001). Neural adaptations to resistance training: implications for movement control. *Sports Medicine*, *31*(12), 829-840. https://doi.org/10.2165/00007256-200131120-00001

Carroll, T. J., Riek, S., & Carson, R. G. (2002). The sites of neural adaptation induced by resistance training in humans. *Journal of Physiology*, *544*(Pt 2), 641-652. https://doi.org/10.1113/jphysiol.2002.024463

Carroll, T. J., Selvanayagam, V. S., Riek, S., & Semmler, J. G. (2011). Neural adaptations to strength training: Moving beyond transcranial magnetic stimulation and reflex studies. *Acta Physiologica (Oxford, England)*, *202*(2), 119-140. https://doi.org/10.1111/j.1748-1716.2011.02271.x

Castelli, A., Paolini, G., Cereatti, A., & Della Croce, U. (2015). A 2D markerless gait analysis methodology: Validation on healthy subjects. *Computational and Mathematical Methods in Medicine*, *2015*, 186780. https://doi.org/10.1155/2015/186780

Chang, C.-K., Washabaugh, E. P., Gwozdziowski, A., Remy, C. D., & Krishnan, C. (2018). A Semi-passive Planar Manipulandum for Upper-Extremity Rehabilitation. *Annals of Biomedical Engineering*, *46*(7), 1047-1065. https://doi.org/10.1007/s10439-018-2020-z

Chen, G., Patten, C., Kothari, D. H., & Zajac, F. E. (2005). Gait differences between individuals with post-stroke hemiparesis and non-disabled controls at matched speeds. *Gait and Posture*, *22*(1), 51-56. https://doi.org/10.1016/j.gaitpost.2004.06.009

Cherry, M. S., Choi, D. J., Deng, K. J., Kota, S., & Ferris, D. P. (2006, January). Design and fabrication of an elastic knee orthosis: Preliminary results. ASME 2006 International Design Engineering Technical Conferences and Computers and Information in Engineering Conference, Philadelphia, PA, USA.

Cherry, M. S., Kota, S., Young, A., & Ferris, D. P. (2016). Running with an elastic lower limb exoskeleton. *Journal of Applied Biomechanics*, *32*(3), 269-277. https://doi.org/10.1123/jab.2015-0155

Chisholm, A. E., Peters, S., Borich, M. R., Boyd, L. A., & Lam, T. (2015). Short-term Cortical Plasticity Associated With Feedback-Error Learning After Locomotor Training in a Patient With Incomplete Spinal Cord Injury. *Physical Therapy*, *95*(2), 257-266. https://academic.oup.com/ptj/article-lookup/doi/10.2522/ptj.20130522

Chow, D. H., Kwok, M. L., Au-Yang, A. C., Holmes, A. D., Cheng, J. C., Yao, F. Y., & Wong, M. S. (2005). The effect of backpack load on the gait of normal adolescent girls. *Ergonomics*, *48*(6), 642-656. https://doi.org/10.1080/00140130500070921

Christiansen, C. L., Bade, M. J., Weitzenkamp, D. A., & Stevens-Lapsley, J. E. (2013). Factors predicting weight-bearing asymmetry 1month after unilateral total knee arthroplasty: A cross-sectional study. *Gait and Posture*, *37*(3), 363-367. https://doi.org/10.1016/j.gaitpost.2012.08.006

Clark, D. J., Ting, L. H., Zajac, F. E., Neptune, R. R., & Kautz, S. A. (2010). Merging of healthy motor modules predicts reduced locomotor performance and muscle coordination complexity post-stroke. *Journal of Neurophysiology*, *103*(2), 844-857. https://doi.org/10.1152/jn.00825.2009

Collins, S. H., Wiggin, M. B., & Sawicki, G. S. (2015). Reducing the energy cost of human walking using an unpowered exoskeleton. *Nature*, *522*(7555), 212-215. https://doi.org/10.1038/nature14288

Conner, B. C., Luque, J., & Lerner, Z. F. (2020). Adaptive ankle resistance from a wearable robotic device to improve muscle recruitment in cerebral palsy. *Annals of Biomedical Engineering*, *48*(4), 1309-1321. https://doi.org/10.1007/s10439-020-02454-8

Cooke, E. V., Tallis, R. C., Clark, A., & Pomeroy, V. M. (2010). Efficacy of functional strength training on restoration of lower-limb motor function early after stroke: Phase I randomized controlled trial. *Neurorehabilitation and Neural Repair*, *24*(1), 88-96. https://doi.org/10.1177/1545968309343216

Corti, M., McGuirk, T. E., Wu, S. S., & Patten, C. (2012). Differential effects of power training versus functional task practice on compensation and restoration of arm function after stroke. *Neurorehabilitation and Neural Repair*, *26*(7), 842-854. https://doi.org/10.1177/1545968311433426

Cramp, M. C., Greenwood, R. J., Gill, M., Rothwell, J. C., & Scott, O. M. (2006). Low intensity strength training for ambulatory stroke patients. *Disability and Rehabilitation*, *28*(13-14), 883-889. https://doi.org/10.1080/09638280500535157

Damiano, D. L., & Abel, M. F. (1998). Functional outcomes of strength training in spastic cerebral palsy. *Archives of Physical Medicine and Rehabilitation*, *79*(2), 119-125. https://doi.org/10.1177/1545968311433426

de Vet, H. C., Bouter, L. M., Bezemer, P. D., & Beurskens, A. J. (2001). Reproducibility and responsiveness of evaluative outcome measures. Theoretical considerations illustrated by an empirical example. *International Journal of Technology Assessment in Health Care*, *17*(4), 479-487. https://www.ncbi.nlm.nih.gov/pubmed/11758292

Decker, M. J., Torry, M. R., Noonan, T. J., Sterett, W. I., & Steadman, J. R. (2004). Gait retraining after anterior cruciate ligament reconstruction. *Archives of Physical Medicine and Rehabilitation*, *85*(5), 848-856. https://doi.org/10.1016/j.apmr.2003.07.014

Delp, S. L., Loan, J. P., Hoy, M. G., Zajac, F. E., Topp, E. L., & Rosen, J. M. (1990). An interactive graphics-based model of the lower extremity to study orthopaedic surgical procedures. *IEEE Transactions on Biomedical Engineering*, *37*(8), 757-767. https://doi.org/10.1109/10.102791

Diaz, G. Y., Averett, D. H., & Soderberg, G. L. (1997). Electromyographic analysis of selected lower extremity musculature in normal subjects during ambulation with and without a Protonics knee brace. *Journal of Orthopaedic and Sports Physical Therapy*, *26*(6), 292-298. https://doi.org/10.2519/jospt.1997.26.6.292

Dobkin, B. H. (2004). Strategies for stroke rehabilitation. *Lancet Neurology*, *3*(9), 528-536. https://doi.org/10.1016/S1474-4422(04)00851-8

Dobkin, B. H. (2008). Training and exercise to drive poststroke recovery. *Nature Clinical Practice: Neurology*, *4*(2), 76-85. https://doi.org/10.1038/ncpneuro0709

Donaldson, C., Tallis, R., Miller, S., Sunderland, A., Lemon, R., & Pomeroy, V. M. (2009). Effects of conventional physical therapy and functional strength training on upper limb motor recovery after stroke: A randomized phase II study. *Neurorehabilitation and Neural Repair*, *23*(4), 389-397. https://doi.org/10.1177/1545968308326635

Dorn, T. W., Wang, J. M., Hicks, J. L., & Delp, S. L. (2015). Predictive simulation generates human adaptations during loaded and inclined walking. *PloS One*, *10*(4), e0121407. https://doi.org/10.1371/journal.pone.0121407

Duclos, C., Nadeau, S., Bourgeois, N., Bouyer, L., & Richards, C. L. (2014). Effects of walking with loads above the ankle on gait parameters of persons with hemiparesis after stroke. *Clinical Biomechanics (Bristol, Avon)*, *29*(3), 265-271. https://doi.org/10.1016/j.clinbiomech.2013.12.012

Duffell, L. D., Jordan, S. J., Cobb, J. P., & McGregor, A. H. (2017). Gait adaptations with aging in healthy participants and people with knee-joint osteoarthritis. *Gait and Posture*, *57*, 246-251. https://doi.org/10.1016/j.gaitpost.2017.06.015

Duncan, P. W., Sullivan, K. J., Behrman, A. L., Azen, S. P., Wu, S. S., Nadeau, S. E., Dobkin, B. H., Rose, D. K., Tilson, J. K., & Leaps Investigative Team. (2007). Protocol for the Locomotor Experience Applied Post-stroke (LEAPS) trial: A randomized controlled trial. *BMC Neurology*, *7*, 39. https://doi.org/10.1186/1471-2377-7-39

Duschau-Wicke, A., Caprez, A., & Riener, R. (2010). Patient-cooperative control increases active participation of individuals with SCI during robot-aided gait training. *Journal of Neuroengineering and Rehabilitation*, *7*, 43. https://doi.org/10.1186/1743-0003-7-43

El Amki, M., Baumgartner, P., Bracko, O., Luft, A. R., & Wegener, S. (2017). Task-specific motor rehabilitation therapy after stroke improves performance in a different motor task: Translational evidence. *Translational Stroke Research*, *8*(4), 347-350. https://doi.org/10.1007/s12975-016-0519-x

Emken, J. L., & Reinkensmeyer, D. J. (2005). Robot-enhanced motor learning: Accelerating internal model formation during locomotion by transient dynamic amplification. *IEEE Transactions on Neural Systems and Rehabilitation Engineering*, *13*(1), 33-39. https://doi.org/10.1109/TNSRE.2004.843173

Eng, J. J., & Tang, P. F. (2007). Gait training strategies to optimize walking ability in people with stroke: A synthesis of the evidence. *Expert Review of Neurotherapeutics*, *7*(10), 1417-1436. https://doi.org/10.1586/14737175.7.10.1417

Escamilla, R. F., Zheng, N., Macleod, T. D., Edwards, W. B., Imamura, R., Hreljac, A., Fleisig, G. S., Wilk, K. E., Moorman, C. T., 3rd, & Andrews, J. R. (2009). Patellofemoral joint force and stress during the wall squat and one-leg squat. *Medicine and Science in Sports and Exercise*, *41*(4), 879-888. https://doi.org/10.1249/MSS.0b013e31818e7ead

Finley, J. M., Bastian, A. J., & Gottschall, J. S. (2013). Learning to be economical: The energy cost of walking tracks motor adaptation. *Journal of Physiology*, *591*(4), 1081-1095. https://doi.org/10.1113/jphysiol.2012.245506

Flansbjer, U.-B., Miller, M., Downham, D., & Lexell, J. (2008). Progressive resistance training after stroke: Effects on muscle strength, muscle tone, gait performance and perceived participation. *Journal of Rehabilitation Medicine*, *40*(1), 42-48. https://doi.org/10.2340/16501977-0129

Fregly, B. J., Fregly, C. D., & Kim, B. T. (2015). Computational prediction of muscle moments during ARED squat exercise on the international space station. *Journal of Biomechanical Engineering*, *137*(12), 121005. https://doi.org/10.1115/1.4031795

Gama, G. L., Savin, D. N., Keenan, T., Waller, S. M., & Whitall, J. (2018). Comparing the effects of adapting to a weight on one leg during treadmill and overground walking: A pilot study. *Gait and Posture*, *59*, 35-39. https://doi.org/10.1016/j.gaitpost.2017.09.025

Garcia, S. A., Curran, M. T., & Palmieri-Smith, R. M. (2020). Longitudinal assessment of quadriceps muscle morphology before and after anterior cruciate ligament reconstruction and its associations with patient-reported outcomes. *Sports Health*, *12*(3), 271-278. https://doi.org/10.1177/1941738119898210

Garcia, S. A., Rodriguez, K. M., Krishnan, C., & Palmieri-Smith, R. M. (2020). Type of measurement used influences central and peripheral contributions to quadriceps weakness after anterior cruciate ligament (ACL) reconstruction. *Physical Therapy in Sport 46*, 14-22. https://doi.org/10.1016/j.ptsp.2020.08.001

Goldberg, S. R., Ounpuu, S., & Delp, S. L. (2003). The importance of swing-phase initial conditions in stiff-knee gait. *Journal of Biomechanics*, *36*(8), 1111-1116. http://www.ncbi.nlm.nih.gov/pubmed/12831736

Gordon, K. E., Kinnaird, C. R., & Ferris, D. P. (2013). Locomotor adaptation to a soleus EMG-controlled antagonistic exoskeleton. *Journal of Neurophysiology*, *109*(7), 1804-1814. https://doi.org/10.1152/jn.01128.2011

Gosline, A. H. C., & Hayward, V. (2008). Eddy current brakes for haptic interfaces: Design, identification, and control. *IEEE/ASME Transactions on Mechatronics*, *13*(6), 669-677. https://doi.org/10.1109/TMECH.2008.2004623

Gottschall, J. S., & Kram, R. (2003). Energy cost and muscular activity required for propulsion during walking. *Journal of Applied Physiology*, *94*(5), 1766-1772. https://doi.org/10.1152/japplphysiol.00670.2002

Haraguchi, M., & Furusho, J. (2013, June). Passive-type rehabilitation system for upper limbs which can display the exact resistance force in the orientation opposite to hand motion. IEEE International Conference on Rehabilitation Robotics (ICORR), Seattle, WA, USA.

Harvey, L. A. (2016). Physiotherapy rehabilitation for people with spinal cord injuries. *Journal of Physiotherapy*, *62*(1), 4-11. https://doi.org/10.1016/j.jphys.2015.11.004

Harvey, R. L. (2009). Improving poststroke recovery: Neuroplasticity and task-oriented training. *Current Treatment Options in Cardiovascular Medicine*, *11*(3), 251-259. https://doi.org/10.1007/s11936-009-0026-4

Helwig, N. E., Hong, S., Hsiao-Wecksler, E. T., & Polk, J. D. (2011). Methods to temporally align gait cycle data. *Journal of Biomechanics*, *44*(3), 561-566. https://doi.org/10.1016/j.jbiomech.2010.09.015

Henry, F. M. (1968). *Specificity vs. generality in learning motor skill* (R. C. Brown & G. S. Kenyon, Eds.). Prentice Hall.

Hesse, S. (2001). Locomotor therapy in neurorehabilitation. *NeuroRehabilitation*, *16*(3), 133-139. https://doi.org/10.3233/NRE-2001-16302

Higbie, E. J., Cureton, K. J., Warren, G. L. r., & Prior, B. M. (1996). Effects of concentric and eccentric training on muscle strength, cross-sectional area, and neural activation. *Journal of Applied Physiology*, *81*(5), 2173-2181. https://doi.org/10.1152/jappl.1996.81.5.2173

Hornby, T. G., Campbell, D. D., Kahn, J. H., Demott, T., Moore, J. L., & Roth, H. R. (2008). Enhanced gait-related improvements after therapist- versus robotic-assisted locomotor training in subjects with chronic stroke: A randomized controlled study. *Stroke*, *39*(6), 1786-1792. https://doi.org/10.1161/STROKEAHA.107.504779

Hortobagyi, T., Finch, A., Solnik, S., Rider, P., & DeVita, P. (2011). Association between muscle activation and metabolic cost of walking in young and old adults. *Journals of Gerontology. Series A: Biological Sciences and Medical Sciences*, *66*(5), 541-547. https://doi.org/10.1093/gerona/glr008

Houldin, A., Chua, R., Carpenter, M. G., & Lam, T. (2012). Limited interlimb transfer of locomotor adaptations to a velocity-dependent force field during unipedal walking. *Journal of Neurophysiology*, *108*(3), 943-952. https://doi.org/10.1152/jn.00670.2011

Houldin, A., Luttin, K., & Lam, T. (2011). Locomotor adaptations and aftereffects to resistance during walking in individuals with spinal cord injury. *Journal of Neurophysiology*, *106*(1), 247-258. https://doi.org/10.1152/jn.00753.2010

Hsu, A. L., Tang, P. F., & Jan, M. H. (2003). Analysis of impairments influencing gait velocity and asymmetry of hemiplegic patients after mild to moderate stroke. *Archives of Physical Medicine and Rehabilitation*, *84*(8), 1185-1193. https://doi.org/10.1016/s0003-9993(03)00030-3

Izawa, J., Rane, T., Donchin, O., & Shadmehr, R. (2008). Motor adaptation as a process of reoptimization. *Journal of Neuroscience*, *28*(11), 2883-2891. https://doi.org/10.1523/JNEUROSCI.5359-07.2008

Izquierdo, M., Ibanez, J., Gonzalez-Badillo, J. J., Hakkinen, K., Ratamess, N. A., Kraemer, W. J., French, D. N., Eslava, J., Altadill, A., Asiain, X., & Gorostiaga, E. M. (2006). Differential effects of strength training leading to failure versus not to failure on hormonal responses, strength, and muscle power gains. *Journal of Applied Physiology*, *100*(5), 1647-1656. https://doi.org/10.1152/japplphysiol.01400.2005

Kaminski, T. W., Wabbersen, C. V., & Murphy, R. M. (1998). Concentric versus enhanced eccentric hamstring strength training: Clinical implications. *J Athl Train*, *33*(3), 216-221. https://pubmed.ncbi.nlm.nih.gov/16558513/

Kautz, S. A., & Brown, D. A. (1998). Relationships between timing of muscle excitation and impaired motor performance during cyclical lower extremity movement in post-stroke hemiplegia. *Brain*, *121 (Pt 3)*, 515-526. https://doi.org/10.1093/brain/121.3.515

Kerr, A., Clark, A., Cooke, E. V., Rowe, P., & Pomeroy, V. M. (2017). Functional strength training and movement performance therapy produce analogous improvement in sit-to-stand early after stroke: Early-phase randomised controlled trial. *Physiotherapy*, *103*(3), 259-265. https://doi.org/10.1016/j.physio.2015.12.006

Kim, C. M., & Eng, J. J. (2003). The relationship of lower-extremity muscle torque to locomotor performance in people with stroke. *Physical Therapy*, *83*(1), 49-57. http://www.ncbi.nlm.nih.gov/pubmed/12495412

Klarner, T., Blouin, J. S., Carpenter, M. G., & Lam, T. (2013). Contributions to enhanced activity in rectus femoris in response to Lokomat-applied resistance. *Experimental Brain Research*, *225*(1), 1-10. https://doi.org/10.1007/s00221-012-3345-8

Kleim, J. A., & Jones, T. A. (2008). Principles of experience-dependent neural plasticity: Implications for rehabilitation after brain damage. *Journal of Speech, Language, and Hearing Research*, *51*(1), S225-239. https://doi.org/10.1044/1092-4388(2008/018)

Krebs, D. E., Scarborough, D. M., & McGibbon, C. A. (2007). Functional vs. strength training in disabled elderly outpatients. *American Journal of Physical Medicine and Rehabilitation*, *86*(2), 93-103. https://doi.org/10.1097/PHM.0b013e31802ede64

Krishnan, C., & Dhaher, Y. (2012). Corticospinal responses of quadriceps are abnormally coupled with hip adductors in chronic stroke survivors. *Experimental Neurology*, *233*(1), 400-407. https://doi.org/10.1016/j.expneurol.2011.11.007

Krishnan, C., Ranganathan, R., Dhaher, Y. Y., & Rymer, W. Z. (2013). A pilot study on the feasibility of robot-aided leg motor training to facilitate active participation. *PloS One*, *8*(10), e77370. https://doi.org/10.1371/journal.pone.0077370

Krishnan, C., Ranganathan, R., Kantak, S. S., Dhaher, Y. Y., & Rymer, W. Z. (2012). Active robotic training improves locomotor function in a stroke survivor. *Journal of Neuroengineering and Rehabilitation*, *9*, 57. https://doi.org/10.1186/1743-0003-9-57

Krishnan, C., & Theuerkauf, P. (2015). Effect of knee angle on quadriceps strength and activation after anterior cruciate ligament reconstruction. *Journal of Applied Physiology*, *119*(3), 223-231. https://doi.org/10.1152/japplphysiol.01044.2014

Krishnan, C., Washabaugh, E. P., & Seetharaman, Y. (2015). A low cost real-time motion tracking approach using webcam technology. *Journal of Biomechanics*, *48*(3), 544-548. https://doi.org/10.1016/j.jbiomech.2014.11.048

Krishnan, C., & Williams, G. N. (2011). Factors explaining chronic knee extensor strength deficits after ACL reconstruction. *Journal of Orthopaedic Research*, *29*(5), 633-640. https://doi.org/10.1002/jor.21316

Krishnan, C., & Williams, G. N. (2014). Effect of knee joint angle on side-to-side strength ratios. *Journal of Strength and Conditioning Research*, *28*(10), 2981-2987. https://doi.org/10.1519/JSC.0000000000000476

Krupenevich, R., Rider, P., Domire, Z., & DeVita, P. (2015). Males and females respond similarly to walking with a standardized, heavy load. *Military Medicine*, *180*(9), 994-1000. https://doi.org/10.7205/MILMED-D-14-00499

Kubinski, A. J., & Higginson, J. S. (2012). Strategies used during a challenging weighted walking task in healthy adults and individuals with knee osteoarthritis. *Gait and Posture*, *35*(1), 6-10. https://doi.org/10.1016/j.gaitpost.2011.07.012

Kuo, H. K., Leveille, S. G., Yu, Y. H., & Milberg, W. P. (2007). Cognitive function, habitual gait speed, and late-life disability in the National Health and Nutrition Examination Survey (NHANES) 1999-2002. *Gerontology*, *53*(2), 102-110. https://doi.org/10.1159/000096792

Lam, T., Anderschitz, M., & Dietz, V. (2006). Contribution of feedback and feedforward strategies to locomotor adaptations. *Journal of Neurophysiology*, *95*(2), 766-773. https://doi.org/10.1152/jn.00473.2005

Lam, T., Luttmann, K., Houldin, A., & Chan, C. (2009). Treadmill-based locomotor training with leg weights to enhance functional ambulation in people with chronic stroke: A pilot study. *Journal of Neurologic Physical Therapy*, *33*(3), 129-135. https://doi.org/10.1097/NPT.0b013e3181b57de5

Lam, T., Pauhl, K., Ferguson, A., Malik, R. N., Krassioukov, A., & Eng, J. J. (2015). Training with robot-applied resistance in people with motor-incomplete spinal cord injury: Pilot study. *Journal of Rehabilitation Research and Development*, *52*(1), 113-129. https://doi.org/10.1682/JRRD.2014.03.0090

Lam, T., Pauhl, K., Krassioukov, A., & Eng, J. J. (2011). Using robot-applied resistance to augment body-weight-supported treadmill training in an individual with incomplete spinal cord injury. *Physical Therapy*, *91*(1), 143-151. https://doi.org/10.2522/ptj.20100026

Lam, T., Wirz, M., Lunenburger, L., & Dietz, V. (2008). Swing phase resistance enhances flexor muscle activity during treadmill locomotion in incomplete spinal cord injury. *Neurorehabilitation and Neural Repair*, *22*(5), 438-446. https://doi.org/10.1177/1545968308315595

Lamberti, N., Straudi, S., Malagoni, A. M., Argiro, M., Felisatti, M., Nardini, E., Zambon, C., Basaglia, N., & Manfredini, F. (2017). Effects of low-intensity endurance and resistance training on mobility in chronic stroke survivors: A pilot randomized controlled study. *European Journal of Physical and Rehabilitation Medicine*, *53*(2), 228-239. https://doi.org/10.23736/S1973-9087.16.04322-7

Langhorne, P., Bernhardt, J., & Kwakkel, G. (2011). Stroke rehabilitation. *Lancet*, *377*(9778), 1693-1702. https://doi.org/10.1016/S0140-6736(11)60325-5

Lawrence, M., Hartigan, E., & Tu, C. (2013). Lower limb moments differ when towing a weighted sled with different attachment points. *Sports Biomechanics*, *12*(2), 186-194. https://doi.org/10.1080/14763141.2012.726639

Leon, D., Cortes, M., Elder, J., Kumru, H., Laxe, S., Edwards, D. J., Tormos, J. M., Bernabeu, M., & Pascual-Leone, A. (2017). tDCS does not enhance the effects of robot-assisted gait training in patients with subacute stroke. *Restorative Neurology and Neuroscience*, *35*(4), 377-384. https://doi.org/10.3233/RNN-170734

Lepley, L. K. (2015). Deficits in quadriceps strength and patient-oriented outcomes at return to activity after ACL reconstruction: A review of the current literature. *Sports Health*, *7*(3), 231-238. https://doi.org/10.1177/1941738115578112

Lepley, L. K., Lepley, A. S., Onate, J. A., & Grooms, D. R. (2017). Eccentric exercise to enhance neuromuscular control. *Sports Health*, *9*(4), 333-340. https://doi.org/10.1177/1941738117710913

Lepley, L. K., Wojtys, E. M., & Palmieri-Smith, R. M. (2015). Combination of eccentric exercise and neuromuscular electrical stimulation to improve quadriceps function post-ACL reconstruction. *Knee*, *22*(3), 270-277. https://doi.org/10.1016/j.knee.2014.11.013

Lewek, M., Rudolph, K., Axe, M., & Snyder-Mackler, L. (2002). The effect of insufficient quadriceps strength on gait after anterior cruciate ligament reconstruction. *Clinical Biomechanics (Bristol, Avon)*, *17*(1), 56-63. https://doi.org/10.1016/s0268-0033(01)00097-3

Lewek, M. D., & Randall, E. P. (2011). Reliability of spatiotemporal asymmetry during overground walking for individuals following chronic stroke. *Journal of Neurologic Physical Therapy*, *35*(3), 116-121. https://doi.org/10.1097/NPT.0b013e318227fe70

Lewis, C. L., Sahrmann, S. A., & Moran, D. W. (2009). Effect of position and alteration in synergist muscle force contribution on hip forces when performing hip strengthening exercises. *Clinical Biomechanics (Bristol, Avon)*, *24*(1), 35-42. https://doi.org/10.1016/j.clinbiomech.2008.09.006

Lima, F. F., Camillo, C. A., Gobbo, L. A., Trevisan, I. B., Nascimento, W. B. B. M., Silva, B. S. A., Lima, M. C. S., Ramos, D., & Ramos, E. M. C. (2018). Resistance training using low cost elastic tubing is equally effective to conventional weight machines in middle-aged to older healthy adults: A quasi-randomized controlled clinical trial. *Journal of Sports Science & Medicine*, *17*(1), 153-160. https://www.ncbi.nlm.nih.gov/pubmed/29535589

Lima, L. O., Scianni, A., & Rodrigues-de-Paula, F. (2013). Progressive resistance exercise improves strength and physical performance in people with mild to moderate Parkinson's disease: A systematic review. *Journal of Physiotherapy*, *59*(1), 7-13. https://doi.org/10.1016/S1836-9553(13)70141-3

Lin, J. H., Hsu, M. J., Hsu, H. W., Wu, H. C., & Hsieh, C. L. (2010). Psychometric comparisons of 3 functional ambulation measures for patients with stroke. *Stroke*, *41*(9), 2021-2025. https://doi.org/10.1161/STROKEAHA.110.589739

Lindmark, B., & Hamrin, E. (1995). Relation between gait speed, knee muscle torque and motor scores in post-stroke patients. *Scandinavian Journal of Caring Sciences*, *9*(4), 195-202. https://www.ncbi.nlm.nih.gov/pubmed/8578040

Liu, C.-J., & Latham, N. K. (2009). Progressive resistance strength training for improving physical function in older adults. *Cochrane Database of Systematic Reviews*, *2009*(3), CD002759. https://doi.org/10.1002/14651858.CD002759.pub2

Liu, J., & Reinkensmeyer, D. (2004, September). Motor adaptation as an optimal combination of computational strategies. Conference Proceedings of the Annual International Conference of the IEEE Engineering in Medicine and Biology Society, San Francisco, CA, USA.

Lohne-Seiler, H., Torstveit, M. K., & Anderssen, S. A. (2013). Traditional versus functional strength training: Effects on muscle strength and power in the elderly. *Journal of Aging and Physical Activity*, *21*(1), 51-70. https://doi.org/10.1123/japa.21.1.51

Lomaglio, M. J., & Eng, J. J. (2008). Nonuniform weakness in the paretic knee and compensatory strength gains in the nonparetic knee occurs after stroke. *Cerebrovascular Diseases*, *26*(6), 584-591. https://doi.org/10.1159/000165111

Lu, E. C., Wang, R. H., Hebert, D., Boger, J., Galea, M. P., & Mihailidis, A. (2011). The development of an upper limb stroke rehabilitation robot: Identification of clinical practices and design requirements through a survey of therapists. *Disabil Rehabil Assist Technol*, *6*(5), 420-431. https://doi.org/10.3109/17483107.2010.544370

Lu, W. S., Wang, C. H., Lin, J. H., Sheu, C. F., & Hsieh, C. L. (2008). The minimal detectable change of the simplified stroke rehabilitation assessment of movement measure. *Journal of Rehabilitation Medicine*, *40*(8), 615-619. https://doi.org/10.2340/16501977-0230

Lund, C., Dalgas, U., Gronborg, T. K., Andersen, H., Severinsen, K., Riemenschneider, M., & Overgaard, K. (2017). Balance and walking performance are improved after resistance and aerobic training in persons with chronic stroke. *Disability and Rehabilitation*, 1-8. https://doi.org/10.1080/09638288.2017.1336646

Maier, M., Ballester, B. R., & Verschure, P. F. M. J. (2019). Principles of neurorehabilitation after stroke based on motor learning and brain plasticity mechanisms. *Frontiers in Systems Neuroscience*, *13*, 74. https://doi.org/10.3389/fnsys.2019.00074

Manella, K. J., & Field-Fote, E. C. (2013). Modulatory effects of locomotor training on extensor spasticity in individuals with motor-incomplete spinal cord injury. *Restorative Neurology and Neuroscience*, *31*(5), 633-646. https://doi.org/10.3233/RNN-120255

Manini, T., Marko, M., VanArnam, T., Cook, S., Fernhall, B., Burke, J., & Ploutz-Snyder, L. (2007). Efficacy of resistance and task-specific exercise in older adults who modify tasks of everyday life. *Journals of Gerontology. Series A: Biological Sciences and Medical Sciences*, *62*(6), 616-623. https://doi.org/10.1093/gerona/62.6.616

Mankala, K. K., Banala, S. K., & Agrawal, S. K. (2009). Novel swing-assist un-motorized exoskeletons for gait training. *Journal of Neuroengineering and Rehabilitation*, *6*, 24. https://doi.org/10.1186/1743-0003-6-24

Marchal-Crespo, L., & Reinkensmeyer, D. J. (2009). Review of control strategies for robotic movement training after neurologic injury. *Journal of Neuroengineering and Rehabilitation*, *6*, 20. https://doi.org/10.1186/1743-0003-6-20

Mares, K., Cross, J., Clark, A., Barton, G. R., Poland, F., O'Driscoll, M. L., Watson, M. J., McGlashan, K., Myint, P. K., & Pomeroy, V. M. (2013). The FeSTivaLS trial protocol: A randomized evaluation of the efficacy of functional strength training on enhancing walking and upper limb function later post stroke. *International Journal of Stroke*, *8*(5), 374-382. https://doi.org/10.1111/j.1747-4949.2012.00778.x

Martin, T. A., Keating, J. G., Goodkin, H. P., Bastian, A. J., & Thach, W. T. (1996). Throwing while looking through prisms. I. Focal olivocerebellar lesions impair adaptation. *Brain*, *119 (Pt 4)*, 1183-1198. https://doi.org/10.1093/brain/119.4.1183

Martini, E., Crea, S., Parri, A., Bastiani, L., Faraguna, U., McKinney, Z., Molino-Lova, R., Pratali, L., & Vitiello, N. (2019). Gait training using a robotic hip exoskeleton improves metabolic gait efficiency in the elderly. *Scientific Reports*, *9*(1), 7157. https://doi.org/10.1038/s41598-019-43628-2

McGowan, C. P., Neptune, R. R., & Kram, R. (2008). Independent effects of weight and mass on plantar flexor activity during walking: Implications for their contributions to body support and forward propulsion. *Journal of Applied Physiology*, *105*(2), 486-494. https://doi.org/10.1152/japplphysiol.90448.2008

Mehta, S., Pereira, S., Viana, R., Mays, R., McIntyre, A., Janzen, S., & Teasell, R. W. (2012). Resistance training for gait speed and total distance walked during the chronic stage of stroke: A meta-analysis. *Topics in Stroke Rehabilitation*, *19*(6), 471-478. https://doi.org/10.1310/tsr1906-471

Michael, K. M., Allen, J. K., & Macko, R. F. (2005). Reduced ambulatory activity after stroke: The role of balance, gait, and cardiovascular fitness. *Archives of Physical Medicine and Rehabilitation*, *86*(8), 1552-1556. https://doi.org/10.1016/j.apmr.2004.12.026

Morrissey, M. C., Harman, E. A., & Johnson, M. J. (1995). Resistance training modes: Specificity and effectiveness. *Medicine and Science in Sports and Exercise*, *27*(5), 648-660. https://www.ncbi.nlm.nih.gov/pubmed/7674868

Morton, S. M., & Bastian, A. J. (2006). Cerebellar contributions to locomotor adaptations during splitbelt treadmill walking. *Journal of Neuroscience*, *26*(36), 9107-9116. https://doi.org/10.1523/JNEUROSCI.2622-06.2006

Moseley, A., Wales, A., Herbert, R., Schurr, K., & Moore, S. (1993). Observation and analysis of hemiplegic gait: Stance phase. *Australian Journal of Physiotherapy*, *39*(4), 259-267. https://doi.org/10.1016/S0004-9514(14)60486-4

Mozaffarian, D., Benjamin, E. J., Go, A. S., Arnett, D. K., Blaha, M. J., Cushman, M., de Ferranti, S., Despres, J. P., Fullerton, H. J., Howard, V. J., Huffman, M. D., Judd, S. E., Kissela, B. M., Lackland, D. T., Lichtman, J. H., Lisabeth, L. D., Liu, S., Mackey, R. H., Matchar, D. B., McGuire, D. K., Mohler, E. R., 3rd, Moy, C. S., Muntner, P., Mussolino, M. E., Nasir, K., Neumar, R. W., Nichol, G., Palaniappan, L., Pandey, D. K., Reeves, M. J., Rodriguez, C. J., Sorlie, P. D., Stein, J., Towfighi, A., Turan, T. N., Virani, S. S., Willey, J. Z., Woo, D., Yeh, R. W., Turner, M. B., American Heart Association Statistics Committee, & Stroke Statistics Subcommittee. (2015). Heart disease and stroke statistics--2015 update: A report from the American Heart Association. *Circulation*, *131*(4), e29-322. https://doi.org/10.1161/CIR.0000000000000152

Mulroy, S., Gronley, J., Weiss, W., Newsam, C., & Perry, J. (2003). Use of cluster analysis for gait pattern classification of patients in the early and late recovery phases following stroke. *Gait and Posture*, *18*(1), 114-125. https://doi.org/10.1016/s0966-6362(02)00165-0

Mun, K. R., Yeo, B. B. S., Guo, Z., Chung, S. C., & Yu, H. (2017). Resistance training using a novel robotic walker for over-ground gait rehabilitation: A preliminary study on healthy subjects. *Medical and Biological Engineering and Computing*, *55*(10), 1873-1881. https://doi.org/10.1007/s11517-017-1634-x

Nadeau, S. E., Wu, S. S., Dobkin, B. H., Azen, S. P., Rose, D. K., Tilson, J. K., Cen, S. Y., Duncan, P. W., & Team, L. I. (2013). Effects of task-specific and impairment-based training compared with usual care on functional walking ability after inpatient stroke rehabilitation: LEAPS Trial. *Neurorehabilitation and Neural Repair*, *27*(4), 370-380. https://doi.org/10.1177/1545968313481284

Naili, J. E., Wretenberg, P., Lindgren, V., Iversen, M. D., Hedstrom, M., & Brostrom, E. W. (2017). Improved knee biomechanics among patients reporting a good outcome in knee-related quality of life one year after total knee arthroplasty. *BMC Musculoskeletal Disorders*, *18*(1), 122. https://doi.org/10.1186/s12891-017-1479-3

Nakamura, R., Hosokawa, T., & Tsuji, I. (1985). Relationship of muscle strength for knee extension to walking capacity in patients with spastic hemiparesis. *Tohoku Journal of Experimental Medicine*, *145*(3), 335-340. https://doi.org/10.1620/tjem.145.335

Ng, M. M., Hill, K. D., Batchelor, F., & Burton, E. (2017). Factors predicting falls and mobility outcomes in patients with stroke returning home after rehabilitation who are at risk of falling. *Archives of Physical Medicine and Rehabilitation*. https://doi.org/10.1016/j.apmr.2017.05.018

Nielsen, J. B., Crone, C., & Hultborn, H. (2007). The spinal pathophysiology of spasticity--from a basic science point of view. *Acta Physiologica (Oxford, England)*, *189*(2), 171-180. https://doi.org/10.1111/j.1748-1716.2006.01652.x

Noble, J. W., & Prentice, S. D. (2006). Adaptation to unilateral change in lower limb mechanical properties during human walking. *Experimental Brain Research*, *169*(4), 482-495. https://doi.org/10.1007/s00221-005-0162-3

Nobrega, S. R., & Libardi, C. A. (2016). Is resistance training to muscular failure necessary? *Frontiers in Physiology*, *7*, 10. https://doi.org/10.3389/fphys.2016.00010

Noel, M., Cantin, B., Lambert, S., Gosselin, C. M., & Bouyer, L. J. (2008). An electrohydraulic actuated ankle foot orthosis to generate force fields and to test proprioceptive reflexes during human walking. *IEEE Transactions on Neural Systems and Rehabilitation Engineering*, *16*(4), 390-399. https://doi.org/10.1109/TNSRE.2008.926714

Olney, S. J., & Richards, C. L. (1996). Hemiparetic gait following stroke. Part I: Characteristics. *Gait and Posture*, *4*(2), 136-148. https://doi.org/10.1016/0966-6362(96)01063-6

Pak, S., & Patten, C. (2008). Strengthening to promote functional recovery poststroke: An evidence-based review. *Topics in Stroke Rehabilitation*, *15*(3), 177-199. https://doi.org/10.1310/tsr1503-177

Palmieri-Smith, R. M., & Lepley, L. K. (2015). Quadriceps strength asymmetry after anterior cruciate ligament reconstruction alters knee joint biomechanics and functional performance at time of return to activity. *American Journal of Sports Medicine*, *43*(7), 1662-1669. https://doi.org/10.1177/0363546515578252

Pandy, M. G., Zajac, F. E., Sim, E., & Levine, W. S. (1990). An optimal control model for maximum-height human jumping. *Journal of Biomechanics*, *23*(12), 1185-1198. https://doi.org/10.1016/0021-9290(90)90376-e

Park, B. S., Kim, M. Y., Lee, L. K., Yang, S. M., Lee, W. D., Noh, J. W., Shin, Y. S., Kim, J. H., Lee, J. U., Kwak, T. Y., Lee, T. H., Kim, J. Y., Park, J., & Kim, J. (2015). The effects of a progressive resistance training program on walking ability in patients after stroke: A pilot study. *Journal of Physical Therapy Science*, *27*(9), 2837-2840. https://doi.org/10.1589/jpts.27.2837

Pasquet, B., Carpentier, A., Duchateau, J., & Hainaut, K. (2000). Muscle fatigue during concentric and eccentric contractions. *Muscle and Nerve*, *23*(11), 1727-1735. https://doi.org/10.1002/1097-4598(200011)23:11<1727::aid-mus9>3.0.co;2-y

Pataky, T. C., Robinson, M. A., & Vanrenterghem, J. (2013). Vector field statistical analysis of kinematic and force trajectories. *Journal of Biomechanics*, *46*(14), 2394-2401. https://doi.org/10.1016/j.jbiomech.2013.07.031

Patten, C., Lexell, J., & Brown, H. E. (2004). Weakness and strength training in persons with poststroke hemiplegia: Rationale, method, and efficacy. *Journal of Rehabilitation Research and Development*, *41*(3A), 293-312. https://doi.org/10.1682/jrrd.2004.03.0293

Perera, S., Mody, S. H., Woodman, R. C., & Studenski, S. A. (2006). Meaningful change and responsiveness in common physical performance measures in older adults. *Journal of the American Geriatrics Society*, *54*(5), 743-749. https://doi.org/10.1111/j.1532-5415.2006.00701.x

Perry, J., Garrett, M., Gronley, J. K., & Mulroy, S. J. (1995). Classification of walking handicap in the stroke population. *Stroke*, *26*(6), 982-989. https://doi.org/10.1161/01.str.26.6.982

Pietrosimone, B., Blackburn, J. T., Padua, D. A., Pfeiffer, S. J., Davis, H. C., Luc-Harkey, B. A., Harkey, M. S., Pietrosimone, L. S., Frank, B. S., Creighton, R. A., Kamath, G. M., & Spang, J. T. (2018). Walking gait asymmetries 6 months following anterior cruciate ligament reconstruction predict 12-month patient-reported outcomes. *Journal of Orthopaedic Research*, *36*(11), 2932-2940. https://doi.org/10.1002/jor.24056

Platz, T. (2004). Impairment-oriented training (IOT)--scientific concept and evidence-based treatment strategies. *Restorative Neurology and Neuroscience*, *22*(3-5), 301-315. http://www.ncbi.nlm.nih.gov/pubmed/15502273

Plautz, E. J., Milliken, G. W., & Nudo, R. J. (2000). Effects of repetitive motor training on movement representations in adult squirrel monkeys: Role of use versus learning. *Neurobiology of Learning and Memory*, *74*(1), 27-55. https://doi.org/10.1006/nlme.1999.3934

Pluss, M., Schellenberg, F., Taylor, W. R., & Lorenzetti, S. (2018). Towards subject-specific strength training design through predictive use of musculoskeletal models. *Applied Bionics and Biomechanics*, *2018*, 9721079. https://doi.org/10.1155/2018/9721079

Polese, J. C., Ada, L., Dean, C. M., Nascimento, L. R., & Teixeira-Salmela, L. F. (2013). Treadmill training is effective for ambulatory adults with stroke: A systematic review. *Journal of Physiotherapy*, *59*(2), 73-80. https://doi.org/10.1016/S1836-9553(13)70159-0

Pollock, A., Baer, G., Campbell, P., Choo, P. L., Forster, A., Morris, J., Pomeroy, V. M., & Langhorne, P. (2014). Physical rehabilitation approaches for the recovery of function and mobility following stroke. *Cochrane Database of Systematic Reviews*, *2014*(4), CD001920. https://doi.org/10.1002/14651858.CD001920.pub3

Pouliot-Laforte, A., Parent, A., Hamdy, R., Marois, P., Lemay, M., & Ballaz, L. (2020). Relationship between lower limb strength and walking capacities in children with spastic bilateral cerebral palsy. *Disability and Rehabilitation*, 1-7. https://doi.org/10.1080/09638288.2020.1813819

Proteau, L., Marteniuk, R. G., & Levesque, L. (1992). A sensorimotor basis for motor learning: Evidence indicating specificity of practice. *Quarterly Journal of Experimental Psychology. A: Human Experimental Psychology*, *44*(3), 557-575. https://doi.org/10.1080/14640749208401298

Puthoff, M. L., Darter, B. J., Nielsen, D. H., & Yack, H. J. (2006). The effect of weighted vest walking on metabolic responses and ground reaction forces. *Medicine and Science in Sports and Exercise*, *38*(4), 746-752. https://doi.org/10.1249/01.mss.0000210198.79705.19

Ranganathan, R., Adewuyi, A., & Mussa-Ivaldi, F. A. (2013). Learning to be lazy: Exploiting redundancy in a novel task to minimize movement-related effort. *Journal of Neuroscience*, *33*(7), 2754-2760. https://doi.org/10.1523/JNEUROSCI.1553-12.2013

Ranganathan, R., & Krishnan, C. (2012). Extracting synergies in gait: Using EMG variability to evaluate control strategies. *Journal of Neurophysiology*, *108*(5), 1537-1544. https://doi.org/10.1152/jn.01112.2011

Ranganathan, R., Krishnan, C., Dhaher, Y. Y., & Rymer, W. Z. (2016). Learning new gait patterns: Exploratory muscle activity during motor learning is not predicted by motor modules. *Journal of Biomechanics*, *49*(5), 718-725. https://doi.org/10.1016/j.jbiomech.2016.02.006

Raymond, M. J., Bramley-Tzerefos, R. E., Jeffs, K. J., Winter, A., & Holland, A. E. (2013). Systematic review of high-intensity progressive resistance strength training of the lower limb compared with other intensities of strength training in older adults. *Archives of Physical Medicine and Rehabilitation*, *94*(8), 1458-1472. https://doi.org/10.1016/j.apmr.2013.02.022

Rebula, J. R., Ojeda, L. V., Adamczyk, P. G., & Kuo, A. D. (2013). Measurement of foot placement and its variability with inertial sensors. *Gait and Posture*, *38*(4), 974-980. https://doi.org/10.1016/j.gaitpost.2013.05.012

Regnaux, J. P., Pradon, D., Roche, N., Robertson, J., Bussel, B., & Dobkin, B. (2008). Effects of loading the unaffected limb for one session of locomotor training on laboratory measures of gait in stroke. *Clinical Biomechanics (Bristol, Avon)*, *23*(6), 762-768. https://doi.org/10.1016/j.clinbiomech.2008.01.011

Reid, M. J., & Prentice, S. D. (2001). Strategies associated with altered segment parameters during voluntary gait modifications. *Neuroscience Research Communications*, *29*(2), 79-87. https://doi.org/10.1002/nrc.1029

Reinkensmeyer, D. J., Akoner, O., Ferris, D. P., & Gordon, K. E. (2009, September). Slacking by the human motor system: Computational models and implications for robotic orthoses. Conference Proceedings of the Annual International Conference of the IEEE Engineering in Medicine and Biology Society, Minneapolis, MN, USA.

Reisman, D. S., McLean, H., Keller, J., Danks, K. A., & Bastian, A. J. (2013). Repeated split-belt treadmill training improves poststroke step length asymmetry. *Neurorehabilitation and Neural Repair*, *27*(5), 460-468. https://doi.org/10.1177/1545968312474118

Reisman, D. S., Wityk, R., Silver, K., & Bastian, A. J. (2009). Split-belt treadmill adaptation transfers to overground walking in persons poststroke. *Neurorehabilitation and Neural Repair*, *23*(7), 735-744. https://doi.org/10.1177/1545968309332880

Rocchi, J. E., Labanca, L., Luongo, V., & Rum, L. (2020). Innovative rehabilitative bracing with applied resistance improves walking pattern recovery in the early stages of rehabilitation after ACL reconstruction: A preliminary investigation. *BMC Musculoskeletal Disorders*, *21*(1), 1-9. https://doi.org/10.1186/s12891-020-03661-z

Rode, G., Lacour, S., Jacquin-Courtois, S., Pisella, L., Michel, C., Revol, P., Alahyane, N., Luauté, J., Gallagher, S., Halligan, P., Pélisson, D., & Rossetti, Y. (2015). Long-term sensorimotor and therapeutical effects of a mild regime of prism adaptation in spatial neglect. A double-blind RCT essay. *Annals of Physical and Rehabilitation Medicine*, *58*(2), 40-53. https://doi.org/10.1016/j.rehab.2014.10.004

Rodriguez, K. M., Palmieri-Smith, R. M., & Krishnan, C. (2020). How does anterior cruciate ligament reconstruction affect the functioning of the brain and spinal cord? A systematic review with meta-analysis. *J Sport Health Sci*. https://doi.org/10.1016/j.jshs.2020.07.005

Rodseth, J., Washabaugh, E. P., & Krishnan, C. (2017). A novel low-cost approach for navigated transcranial magnetic stimulation. *Restorative Neurology and Neuroscience*, *35*(6), 601-609. https://doi.org/10.3233/RNN-170751

Roemmich, R. T., & Bastian, A. J. (2018). Closing the loop: From motor neuroscience to neurorehabilitation. *Annual Review of Neuroscience*, *41*, 415-429. https://doi.org/10.1146/annurev-neuro-080317-062245

Roig, M., O'Brien, K., Kirk, G., Murray, R., McKinnon, P., Shadgan, B., & Reid, W. D. (2009). The effects of eccentric versus concentric resistance training on muscle strength and mass in healthy adults: A systematic review with meta-analysis. *British Journal of Sports Medicine*, *43*(8), 556-568. https://doi.org/10.1136/bjsm.2008.051417

Sadeghi, H., Allard, P., Shafie, K., Mathieu, P. A., Sadeghi, S., Prince, F., & Ramsay, J. (2000). Reduction of gait data variability using curve registration. *Gait and Posture*, *12*(3), 257-264. https://doi.org/10.1016/s0966-6362(00)00085-0

Saner, R. J., Washabaugh, E. P., & Krishnan, C. (2017). Reliable sagittal plane kinematic gait assessments are feasible using low-cost webcam technology. *Gait and Posture*, *56*, 19-23. https://doi.org/10.1016/j.gaitpost.2017.04.030

Savin, D. N., Morton, S. M., & Whitall, J. (2014). Generalization of improved step length symmetry from treadmill to overground walking in persons with stroke and hemiparesis. *Clinical Neurophysiology*, *125*(5), 1012-1020. https://doi.org/10.1016/j.clinph.2013.10.044

Savin, D. N., Tseng, S. C., & Morton, S. M. (2010). Bilateral adaptation during locomotion following a unilaterally applied resistance to swing in nondisabled adults. *Journal of Neurophysiology*, *104*(6), 3600-3611. https://doi.org/10.1152/jn.00633.2010

Savin, D. N., Tseng, S. C., Whitall, J., & Morton, S. M. (2013). Poststroke hemiparesis impairs the rate but not magnitude of adaptation of spatial and temporal locomotor features. *Neurorehabilitation and Neural Repair*, *27*(1), 24-34. https://doi.org/10.1177/1545968311434552

Scandalis, T. A., Bosak, A., Berliner, J. C., Helman, L. L., & Wells, M. R. (2001). Resistance training and gait function in patients with Parkinson's disease. *American Journal of Physical Medicine and Rehabilitation*, *80*(1), 38-43; quiz 44-36. https://doi.org/10.1097/00002060-200101000-00011

Schellenberg, F., Oberhofer, K., Taylor, W. R., & Lorenzetti, S. (2015). Review of modelling techniques for in vivo muscle force estimation in the lower extremities during strength training. *Computational and Mathematical Methods in Medicine*, *2015*, 483921. https://doi.org/10.1155/2015/483921

Schmidt, R. A., & Lee, T. D. (1988). *Motor Control & Learning: A Behavioral Emphasis*. Human Kinetics.

Schoenfeld, B. J., Peterson, M. D., Ogborn, D., Contreras, B., & Sonmez, G. T. (2015). Effects of low- vs. high-load resistance training on muscle strength and hypertrophy in well-trained men. *Journal of Strength and Conditioning Research*, *29*(10), 2954-2963. https://doi.org/10.1519/JSC.0000000000000958

Seo, H. G., Lee, W. H., Lee, S. H., Yi, Y., Kim, K. D., & Oh, B. M. (2017). Robotic-assisted gait training combined with transcranial direct current stimulation in chronic stroke patients: A pilot double-blind, randomized controlled trial. *Restorative Neurology and Neuroscience*. https://doi.org/10.3233/RNN-170745

Severini, G., Koenig, A., Adans-Dester, C., Cajigas, I., Cheung, V. C. K., & Bonato, P. (2020). Robot-Driven Locomotor Perturbations Reveal Synergy-Mediated, Context-Dependent Feedforward and Feedback Mechanisms of Adaptation. *Scientific Reports*, *10*(1), 5104. https://doi.org/10.1038/s41598-020-61231-8

Shadmehr, R., & Mussa-Ivaldi, F. a. (1994). Adaptive representation of dynamics during learning of a motor task. *Journal of Neuroscience*, *14*(5), 3208-3224. https://doi.org/10.1523/JNEUROSCI.14-05-03208.1994

Shamaei, K., Cenciarini, M., Adams, A. A., Gregorczyk, K. N., Schiffman, J. M., & Dollar, A. M. (2014). Design and evaluation of a quasi-passive knee exoskeleton for investigation of

motor adaptation in lower extremity joints. *IEEE Transactions on Biomedical Engineering*, *61*(6), 1809-1821. https://doi.org/10.1109/TBME.2014.2307698

Shamaei, K., Cenciarini, M., Adams, A. A., Gregorczyk, K. N., Schiffman, J. M., & Dollar, A. M. (2015). Biomechanical Effects of Stiffness in Parallel With the Knee Joint During Walking. *IEEE Transactions on Biomedical Engineering*, *62*(10), 2389-2401. https://doi.org/10.1109/TBME.2015.2428636

Shelburne, K. B., Torry, M. R., & Pandy, M. G. (2005). Effect of muscle compensation on knee instability during ACL-deficient gait. *Medicine and Science in Sports and Exercise*, *37*(4), 642-648. https://doi.org/10.1249/01.mss.0000158187.79100.48

Shin, Y. K., Lee, D. R., Kim, D. H., Lee, J. J., You, S. J. H., Yi, C. H., & Jeon, H. S. (2014). Effects of novel tubing gait on neuromuscular imbalance in cerebral palsy. *NeuroRehabilitation*, *35*(3), 587-596. https://doi.org/10.3233/NRE-141154

Silder, A., Delp, S. L., & Besier, T. (2013). Men and women adopt similar walking mechanics and muscle activation patterns during load carriage. *Journal of Biomechanics*, *46*(14), 2522-2528. https://doi.org/10.1016/j.jbiomech.2013.06.020

Simao, C. R., Regalado, I. C. R., Spaniol, A. P., Fonseca, D. O. S., Ribeiro, T. S., & Lindquist, A. R. (2019). Immediate effects of a single treadmill session with additional ankle loading on gait in children with hemiparetic cerebral palsy. *NeuroRehabilitation*, *44*(1), 9-17. https://doi.org/10.3233/NRE-182516

Simeu, E., & Georges, D. (1996). Modeling and control of an eddy current brake. *Control Engineering Practice*, *4*(1), 19-26. https://doi.org/10.1016/S1474-6670(17)45446-2

Simpson, K. M., Munro, B. J., & Steele, J. R. (2011). Backpack load affects lower limb muscle activity patterns of female hikers during prolonged load carriage. *Journal of Electromyography and Kinesiology*, *21*(5), 782-788. https://doi.org/10.1016/j.jelekin.2011.05.012

Stienen, A. H. A., Hekman, E. E. G., Van der Helm, F. C. T., Prange, G. B., Jannink, M. J. A., Aalsma, A. M. M., & Van der Kooij, H. (2007, June). Dampace: Dynamic force-coordination trainer for the upper extremities. 2007 IEEE 10th International Conference on Rehabilitation Robotics, Noordwijk, Netherlands.

Stoeckmann, T. M., Sullivan, K. J., & Scheidt, R. A. (2009). Elastic, viscous, and mass load effects on poststroke muscle recruitment and co-contraction during reaching: A pilot study. *Physical Therapy*, *89*(7), 665-678. https://doi.org/10.2522/ptj.20080128

Sullivan, K. J., Brown, D. A., Klassen, T., Mulroy, S., Ge, T., Azen, S. P., Winstein, C. J., & Physical Therapy Clinical Research Network. (2007). Effects of task-specific locomotor and strength training in adults who were ambulatory after stroke: Results of the STEPS randomized clinical trial. *Physical Therapy*, *87*(12), 1580-1602. https://doi.org/10.2522/ptj.20060310

Sulzer, J. S., Roiz, R. A., Peshkin, M. A., & Patton, J. L. (2009). A highly backdrivable, lightweight knee actuator for investigating gait in stroke. *IEEE Transactions on Robotics*, *25*(3), 539-548. https://doi.org/10.1109/TRO.2009.2019788

Takahashi, C. D., Der-Yeghiaian, L., Le, V., Motiwala, R. R., & Cramer, S. C. (2008). Robot-based hand motor therapy after stroke. *Brain*, *131*(Pt 2), 425-437. https://doi.org/10.1093/brain/awm311

Tang, R., Kim, J., Gaebler-Spira, D. J., & Wu, M. (2019). Gradual increase of perturbation load induces a longer retention of locomotor adaptation in children with cerebral palsy. *Hum Mov Sci*, *63*, 20-33. https://doi.org/10.1016/j.humov.2018.11.006

Teasell, R. W., Bhogal, S. K., Foley, N. C., & Speechley, M. R. (2003). Gait retraining post stroke. *Topics in Stroke Rehabilitation*, *10*(2), 34-65. https://doi.org/10.1310/UDXE-MJFF-53V2-EAP0

Teixeira-Salmela, L. F., Olney, S. J., Nadeau, S., & Brouwer, B. (1999). Muscle strengthening and physical conditioning to reduce impairment and disability in chronic stroke survivors. *Archives of Physical Medicine and Rehabilitation*, *80*(10), 1211-1218. https://doi.org/10.1016/s0003-9993(99)90018-7

Ten Brink, A. F., Visser-Meily, J. M. A., Schut, M. J., Kouwenhoven, M., Eijsackers, A. L. H., & Nijboer, T. C. W. (2017). Prism Adaptation in rehabilitation? No additional effects of prism adaptation on neglect recovery in the subacute phase poststroke: A randomized controlled trial. *Neurorehabilitation and Neural Repair*, *31*(12), 1017-1028. https://doi.org/10.1177/1545968317744277

Thelen, D. G., Anderson, F. C., & Delp, S. L. (2003). Generating dynamic simulations of movement using computed muscle control. *Journal of Biomechanics*, *36*(3), 321-328. https://doi.org/10.1016/s0021-9290(02)00432-3

Totah, D., Menon, M., Jones-Hershinow, C., Barton, K., & Gates, D. H. (2019). The impact of ankle-foot orthosis stiffness on gait: A systematic literature review. *Gait and Posture*, *69*, 101-111. https://doi.org/10.1016/j.gaitpost.2019.01.020

Vahlberg, B., Cederholm, T., Lindmark, B., Zetterberg, L., & Hellstrom, K. (2017). Short-term and long-term effects of a progressive resistance and balance exercise program in individuals with chronic stroke: A randomized controlled trial. *Disability and Rehabilitation*, *39*(16), 1615-1622. https://doi.org/10.1080/09638288.2016.1206631

van der Krogt, M. M., Bregman, D. J., Wisse, M., Doorenbosch, C. A., Harlaar, J., & Collins, S. H. (2010). How crouch gait can dynamically induce stiff-knee gait. *Annals of Biomedical Engineering*, *38*(4), 1593-1606. https://doi.org/10.1007/s10439-010-9952-2

Vashista, V., Agrawal, N., Shaharudin, S., Reisman, D. S., & Agrawal, S. K. (2013). Force adaptation in human walking with symmetrically applied downward forces on the pelvis. *IEEE Transactions on Neural Systems and Rehabilitation Engineering*, *21*(6), 969-978. https://doi.org/10.1109/TNSRE.2013.2243917

Vashista, V., Martelli, D., & Agrawal, S. K. (2016). Locomotor Adaptation to an Asymmetric Force on the Human Pelvis Directed Along the Right Leg. *IEEE Transactions on Neural Systems and Rehabilitation Engineering*, *24*(8), 872-881. https://doi.org/10.1109/TNSRE.2015.2474303

Visintin, M., Barbeau, H., Korner-Bitensky, N., & Mayo, N. E. (1998). A new approach to retrain gait in stroke patients through body weight support and treadmill stimulation. *Stroke*, *29*(6), 1122-1128. https://doi.org/10.1161/01.str.29.6.1122

Waite, L. M., Broe, G. A., Grayson, D. A., & Creasey, H. (2000). Motor function and disability in the dementias. *International Journal of Geriatric Psychiatry*, *15*(10), 897-903. https://doi.org/10.1002/1099-1166(200010)15:10<897::aid-gps215>3.0.co;2-c

Washabaugh, E. P., Augenstein, T. E., Ebenhoeh, A. M., Qiu, J., Ford, K. A., & Krishnan, C. (2020). Design and preliminary ssessment of a passive elastic leg exoskeleton for resistive gait rehabilitation. *IEEE Transactions on Biomedical Engineering*. https://doi.org/10.1109/TBME.2020.3038582

Washabaugh, E. P., Augenstein, T. E., & Krishnan, C. (2020). Functional resistance training during walking: Mode of application differentially affects gait biomechanics and muscle activation patterns. *Gait and Posture*, *75*, 129-136. https://doi.org/10.1016/j.gaitpost.2019.10.024

Washabaugh, E. P., Claflin, E. S., Gillespie, R. B., & Krishnan, C. (2016). A novel Application of eddy current braking for functional strength training during gait. *Annals of Biomedical Engineering*, *44*(9), 2760-2773. https://doi.org/10.1007/s10439-016-1553-2

Washabaugh, E. P., Guo, J., Chang, C. K., Remy, D., & Krishnan, C. (2019). A portable passive rehabilitation robot for upper-extremity functional resistance training. *IEEE Transactions on Biomedical Engineering*, *66*(2), 496-508. https://doi.org/10.1109/TBME.2018.2849580

Washabaugh, E. P., Kalyanaraman, T., Adamczyk, P. G., Claflin, E. S., & Krishnan, C. (2017). Validity and repeatability of inertial measurement units for measuring gait parameters. *Gait and Posture*, *55*, 87-93. https://doi.org/10.1016/j.gaitpost.2017.04.013

Washabaugh, E. P., & Krishnan, C. (2018). A wearable resistive robot facilitates locomotor adaptations during gait. *Restorative Neurology and Neuroscience*, *36*(2), 215-223. https://doi.org/10.3233/RNN-170782

Washabaugh, E. P., Treadway, E., Gillespie, R. B., Remy, C. D., & Krishnan, C. (2018). Self-powered robots to reduce motor slacking during upper-extremity rehabilitation: A proof of concept study. *Restorative Neurology and Neuroscience*, *36*(6), 693-708. https://doi.org/10.3233/RNN-180830

West, B. T., Welch, K. B., & Galecki, A. T. (2014). *Linear Mixed Models: A Practical Guide Using Statistical Software*. Chapman & Hall/CRC.

Whittle, M. W. (2007). *Gait Analysis: An Introduction* (4th ed.). Butterworth-Heinemann Elsevier.

Williams, G. N., Kahn, M., & Randall, A. (2014). Strength training for walking in neurologic rehabilitation is not task specific: A focused review. *American Journal of Physical Medicine and Rehabilitation*, *93*(6), 511-522. https://doi.org/10.1097/PHM.0000000000000058

Wouterse, J. H. (1991). Critical torque and speed of eddy current brake with widely separated soft iron poles. IEE Proceedings B (Electric Power Applications),

Wu, M., Hornby, T. G., Landry, J. M., Roth, H., & Schmit, B. D. (2011). A cable-driven locomotor training system for restoration of gait in human SCI. *Gait and Posture*, *33*(2), 256-260. https://doi.org/10.1016/j.gaitpost.2010.11.016

Wu, M., Kim, J., Arora, P., Gaebler-Spira, D. J., & Zhang, Y. (2014, August). Locomotor training through a 3D cable-driven robotic system for walking function in children with cerebral palsy: A pilot study. Conference Proceedings of the Annual International Conference of the IEEE Engineering in Medicine and Biology Society, Chicago, IL, USA.

Wu, M., Kim, J., Gaebler-Spira, D. J., Schmit, B. D., & Arora, P. (2017). Robotic resistance treadmill training improves locomotor function in children with cerebral palsy: A randomized controlled pilot study. *Archives of Physical Medicine and Rehabilitation*, *98*(11), 2126-2133. https://doi.org/10.1016/j.apmr.2017.04.022

Wu, M., Landry, J. M., Kim, J., Schmit, B. D., Yen, S.-C., & Macdonald, J. (2014). Robotic resistance/assistance training improves locomotor function in individuals poststroke: A randomized controlled study. *Archives of Physical Medicine and Rehabilitation*, *95*(5), 799-806. https://doi.org/10.1016/j.apmr.2013.12.021

Wu, M., Landry, J. M., Kim, J., Schmit, B. D., Yen, S. C., McDonald, J., & Zhang, Y. (2016). Repeat exposure to leg swing perturbations during treadmill training induces long-term retention of increased step length in human SCI: A pilot randomized controlled study. *American Journal of Physical Medicine and Rehabilitation*, *95*(12), 911-920. https://doi.org/10.1097/PHM.0000000000000517

Wu, M., Landry, J. M., Schmit, B. D., Hornby, T. G., & Yen, S.-C. (2012). Robotic resistance treadmill training improves locomotor function in human spinal cord injury: A pilot study. *Archives of Physical Medicine and Rehabilitation*, *93*(5), 782-789. https://doi.org/10.1016/j.apmr.2011.12.018

Wu, M., Landry, J. M., Yen, S.-C., Schmit, B. D., Hornby, T. G., & Rafferty, M. (2011, August). A novel cable-driven robotic training improves locomotor function in individuals post-stroke. Conference Proceedings of the Annual International Conference of the IEEE Engineering in Medicine and Biology Society, Boston, MA, USA.

Yandell, M. B., Quinlivan, B. T., Popov, D., Walsh, C., & Zelik, K. E. (2017). Physical interface dynamics alter how robotic exosuits augment human movement: Implications for optimizing wearable assistive devices. *Journal of Neuroengineering and Rehabilitation*, *14*(1), 40. https://doi.org/10.1186/s12984-017-0247-9

Yang, Y. R., Wang, R. Y., Lin, K. H., Chu, M. Y., & Chan, R. C. (2006). Task-oriented progressive resistance strength training improves muscle strength and functional performance in individuals with stroke. *Clinical Rehabilitation*, *20*(10), 860-870. https://doi.org/10.1177/0269215506070701

Yen, S.-C., Landry, J. M., & Wu, M. (2013). Size of kinematic error affects retention of locomotor adaptation in human spinal cord injury. *Journal of Rehabilitation Research and Development*, *50*(9), 1187-1200. https://doi.org/10.1682/JRRD.2012.09.0175

Yen, S.-C., Landry, J. M., & Wu, M. (2014). Augmented multisensory feedback enhances locomotor adaptation in humans with incomplete spinal cord injury. *Human Movement Science*, *35*, 80-93. https://doi.org/10.1016/j.humov.2014.03.006

Yen, S.-C., Schmit, B. D., Landry, J. M., Roth, H., & Wu, M. (2012). Locomotor adaptation to resistance during treadmill training transfers to overground walking in human SCI. *Experimental Brain Research*, *216*(3), 473-482. https://doi.org/10.1007/s00221-011-2950-2

Yen, S.-C., Schmit, B. D., & Wu, M. (2015). Using swing resistance and assistance to improve gait symmetry in individuals post-stroke. *Human Movement Science*, *42*, 212-224. https://doi.org/10.1016/j.humov.2015.05.010

Zabukovec, J. R., Boyd, L. A., Linsdell, M. A., & Lam, T. (2013). Changes in corticospinal excitability following adaptive modification to human walking. *Experimental Brain Research*, *226*(4), 557-564. https://doi.org/10.1007/s00221-013-3468-6

Zanotto, D., Rosati, G., Spagnol, S., Stegall, P., & Agrawal, S. K. (2013). Effects of complementary auditory feedback in robot-assisted lower extremity motor adaptation. *IEEE Transactions on Neural Systems and Rehabilitation Engineering*, *21*(5), 775-786. https://doi.org/10.1109/TNSRE.2013.2242902

Appendices

Appendix A

Chapter 1 Supplemental Materials

Table A.1 Summary of all the studies in Chapter 1 and the variables they measured

Reference	Population	Device	Mode	Type	Resisting	MA	Moments	Kinematics	Spatiotemporal	Neural
Browning et al. (2007)	AB	Passive	Point	Inertial	Foot/Shank/Thigh/Pelvis	Yes	Yes			
Noble & Prentice (2006)	AB	Passive	Point	Inertial	Shank		Yes	Yes	Yes	
Lam et al. (2008)	SCI	Passive/Active	Point/Joint	Inertial/Viscous	Shank/Hip+Knee	Yes		Yes		
Duclos et al. (2014)	Stroke	Passive	Point	Inertial	Shank		Yes			
Savin et al. (2010)	AB	Passive	Point	Inertial	Shank Back	Yes		Yes	Yes	
McGowan et al. (2008)	AB	Passive	Point	Inertial	Pelvis	Yes				
Krupenvich et al. (2015)	AB	Passive	Point	Inertial			Yes			
Kubinski & Higginson (2012)	AB/Knee OA	Passive	Point	Inertial	Torso		Yes			
Silder et al. (2013)	AB	Passive	Point	Inertial	Torso	Yes	Yes			
Simpson et al. (2011)	AB	Passive	Point	Inertial	Torso	Yes				
Chow et al. (2005)	AB	Passive	Point	Inertial	Torso		Yes			
Blanchette & Bouyer (2009)	AB	Passive	Point	Elastic	Foot Front	Yes			Yes	
Blanchette et al. (2012)	AB	Passive	Point	Elastic	Foot Front	Yes			Yes	
Shin et al. (2014)	AB/CP	Passive	Point	Elastic	Shank Front	Yes				
Gottschall & Kram (2003)	AB	Passive	Point	Elastic	Pelvis Back	Yes				
Tang et al. (2019)	CP	Active	Point	Viscoelastic	Shank Back	Yes			Yes	
Yen et al. (2013)	SCI	Active	Point	Viscoelastic	Shank Back	Yes			Yes	
Mun et al. (2017)	AB	Active	Point	Constant	Pelvis Back	Yes				
Vashista et al. (2016)	AB	Active	Point	Constant	Pelvis Down	Yes		Yes	Yes	

Reference	Population	Device	Mode	Type	Resisting	MA	Moments	Kinematics	Spatiotemporal	Neural
Barthélemy et al. (2012)	AB	Passive	Joint	Elastic	Ankle Dorsi	Yes		Yes		Yes
Houldin et al. (2011)	AB/SCI	Active	Joint	Viscous	Hip Bi	Yes		Yes	Yes	
Houldin et al. (2012)	AB	Active	Joint	Viscous	Hip Bi	Yes		Yes	Yes	
Klarner et al. (2013)	AB	Active	Joint	Viscous	Hip + Knee Bi	Yes				
Lam et al. (2006)	AB	Active	Joint	Viscous	Hip + Knee Bi	Yes		Yes		
Diaz et al. (1997)	AB	Active	Joint	Constant	Knee Flex/Knee Ext	Yes				
Blanchette et al. (2011)	AB	Active	Joint	Custom	Ankle Dorsi	Yes		Yes		
Conner et al. (2020)	CP	Active	Joint	Custom	Ankle Plantar	Yes				
Gama et al. (2018)	AB	Passive	Point	Inertial	Shank				Yes	
Savin et al. (2014)	AB/Stroke	Passive	Point	Inertial	Shank Back				Yes	
Savin et al. (2013)	Stroke	Passive	Point	Inertial	Shank Back				Yes	
Vashista et al. (2013)	AB	Passive	Point	Elastic	Pelvis Down			Yes		
Yen et al. (2014)	SCI	Active	Point	Viscoelastic	Shank Back				Yes	
Yen et al. (2015)	Stroke	Active	Point	Viscoelastic	Shank Back				Yes	
Yen et al. (2012)	SCI	Active	Point	Viscoelastic	Thigh Back				Yes	
Cajigas et al. (2017)	AB	Active	Joint	Custom	Shank Back				Yes	
Severini et al. (2020)	AB	Active	Joint	Custom	Shank Back				Yes	
Zabukovec et al. (2013)	AB	Active	Joint	Viscous	Hip + Knee Bi					Yes
Bonnard et al. (2002)	AB	Passive	Point	Elastic	Foot Up					Yes

Variable abbreviations: muscle activation (MA); population abbreviations: AB (able-bodied), SCI (spinal cord injury), CP (cerebral palsy), OA (osteoarthritis); resisting abbreviations: Flex (flexion), Ext (extension), Plant (plantarflexion), Dorsi (dorsiflexion), Bi (Bidirectional [e.g., Flex & Ext]); Front/Back/Down indicate the direction the device was pulling. Yes indicates that a variable was measured in the study. Note, many studies had additional variables that were not of interest to this study.

Appendix B

Chapter 5 Supplemental Materials

B.1 Experimental Setup

The setup was similar for both experiments. First, we calibrated the capture volume of the motion capture system (Qualisys Track Manager, Qualisys, Göteborg, SE), which consisted of 12 infrared tracking cameras (Miqus M3) and two video cameras (Miqus Video). We then zeroed the force plates of the instrumented split-belt treadmill (Bertec, Columbus, OH, US).

For experiment 1, we placed surface EMG electrodes (Trigno Avanti, Delsys, Natick, MA, US) over the muscle bellies of several quadriceps (vastus medialis [VM], and rectus femoris [RF]), and hamstring muscles (medial hamstring [MH], and lateral hamstring [LH]), and placed additional sensors on an ankle dorsiflexor muscle (tibialis anterior [TA]), ankle plantar flexor muscles (medial gastrocnemius [MG], and soleus [SO]), and a hip abductor muscle (gluteus medius [GM]). These sensors were placed on the right leg according to the established guidelines at www.seniam.org. Sensor positions were slightly altered from established guidelines if the leg brace hindered sensor placement. Once placed, the EMG electrodes were tightly secured to the skin using self-adhesive tapes and cotton elastic bandages. The quality of the EMG signals was visually inspected to ensure that the electrodes were appropriately placed. Finally, the participant performed two maximum voluntary contractions (MVCs) with each muscle group against a manually applied resistance, which were used later for normalization.

Next, for both experiments we placed markers on the legs for motion capture (Figure B.1). To track gait kinematics, we used the CAST (calibrated anatomical systems technique)

lower extremity marker set (Cappozzo et al., 1995). In this marker set, for the right and left leg, individual markers were placed over the anterior and posterior iliac spine, medial and lateral femoral epicondyles, medial and lateral malleoli of the ankle, and at the 1st, 2nd, and 5th metatarsals and calcaneus of the foot. Additionally, marker clusters were placed on the thigh and shank. In our implementation, because the leg brace obstructed our ability to place physical markers over the iliac spine and right femoral epicondyles, several markers were placed virtually with a stylus; hence, an additional cluster was required on the back of the pelvis to aid in tracking of the virtual iliac spine markers. All individual markers were secured to the leg using self-adhesive tapes, whereas clusters were secured via hook-and-loop fastener elastic wraps (MediWrap, fabrifoam, Exton, PA, US).

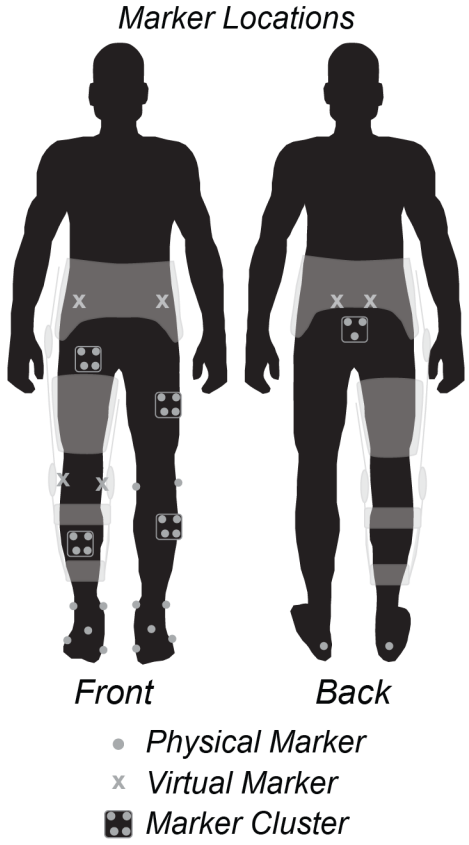

Figure B.1 Schematic depicting the locations where markers and marker clusters were located for motion capture.

B.2 Motion Capture

B.2.1 Static Trials

During static trials, we had the participant stand on the treadmill (either with or without wearing the device) motionless in an upright posture as the cameras recorded the positions of the physical markers. With each static trial, we also performed a pointer trial, where the participant remained upright as a study team member used a stylus (a calibrated rigid body) to indicate the positions for virtual markers. During this pointer trial, an event was created in the motion capture software (i.e., the time point was saved) when the stylus was in the correct position for each virtual marker. These events, along with the stylus position were later used to recreate virtual markers in Visual3D.

B.2.2 Building the Model

Using the CAST marker set, we created a model with pose estimation using six degrees of freedom segments to measure kinematics and kinetics during walking with the device. The pelvis segment was based on the CODA model (Charnwood Dynamics Ltd., UK), which uses the right and left iliac spine markers (these are virtual in our experiments) to estimate the location of the hip joint centers of the participant. The pelvis was tracked according to the cluster located on the posterior of the segment. The remainder of the segments were built using the standard Visual3D proximal and distal joint and radius definitions. Note if a radius is not specified, then it was automatically estimated based on medial and lateral markers of the joint. The thigh segments were defined proximally by the hip joint centers with radii of half the distance between the right and left hip joint centers. The distal definition of the thigh segments was the lateral and medial epicondyles of the femurs (these are virtual markers on the right leg in our experiments). The thighs were tracked according to the clusters placed anteriorly above the brace on the right thigh

segment and laterally on the left thigh segment. The shanks were defined proximally by the lateral and medial epicondyles of the femurs, and distally by the medial and lateral malleoli of the ankles. The shanks were tracked according to the clusters located anteriorly on the right segment and laterally on the left segment. The foot segments were defined proximally by the medial and lateral malleoli of the ankles, and distally by the 1st and 5th metatarsal markers on the feet. The foot segments were tracked using the 1st, 2nd, and 5th metatarsal markers, as well as the markers on the calcanei.

In addition to the previously mentioned segments, we also created multiple kinematic segments (sometimes referred to as virtual segments) so that our measures of joint angles were more anatomical and relative to the static posture. All of the kinematic segments were tracked using the same clusters/markers as defined for the segments above. To create a kinematic pelvis, we first had to create landmarks for the iliac crests. The iliac crest landmarks were said to be located at a set distance (half the distance between anterior iliac spine markers) directly above (using the lab coordinate system) the hip joint centers. The kinematic pelvis was then defined proximally using the iliac spine markers, and distally using the hip joint centers. This ensured the pelvis was perpendicular to the ground during the static posture, rather than tilted forward as is seen in the CODA model. The kinematic thigh and shank segments were defined to be relative to the segments directly proximal to them. For the kinematic thigh, this meant it was defined relative to the pelvis; meaning, the proximal segment definitions (referring to what must be input to the Visual3D model type) were the iliac crest landmarks and the distal definitions were the hip joint centers. The kinematic shank was then defined relative to the thigh; meaning, the proximal segments were defined to be at the hip joint centers while the distal segments were defined as the lateral and medial epicondyles of the femur. Because these segments were tracked using their

respective clusters, this meant the hip and knee joint angles could be measured relative to the static posture (with static being zero). Finally, kinematic foot segments were created using the projected landmarks method. Briefly, to create these segments, new landmarks were created by projecting the malleoli, as well as 1st and 5th metatarsal markers onto the ground. The kinematic foot segments were then defined proximally by the floor-based malleoli landmarks, and distally by the floor-based metatarsal landmarks. This ensured that the foot segment was parallel to the floor during the static posture.

B.2.3 Kinematics and Kinetics Processing

Once gaps in the marker position data were filled and all markers were labeled in QTM, both the motion capture and force plate data were then exported to Visual3D (C-Motion Inc., Germantown, MD, US) for further processing. In Visual3D, skeletal models, which used the events from the pointer trials to place virtual markers, were built for both static trials (with and without the brace; see *Building the Model* for details). These models were applied to the dynamic walking trials. The height and weight of the participant were assigned to the models and tags were placed on each trial to allow us to process the trials individually. We ran a function to remove any offsets from the force plate data for each trial (FP_Auto_Baseline). Note this function also automatically sets the force plate minimum for calculating gait events (e.g., heel-strike). The marker position data and force plate data were then low-pass filtered using a zero phase-lag Butterworth digital filter (6 Hz) to remove motion artifacts and high frequency noise due to the treadmill motors, respectively. These filtered (processed) data were used to compute the kinematics and kinetics.

In order to see how the device performed when worn during walking, we calculated sagittal plane kinematics and kinetics (internal moments and powers) of the hip, knee, and ankle

joints of the right leg (the leg that was wearing the brace). These calculations were performed using the built-in functionality of Visual3D (Compute_Model_Based_Data). The hip joint angle was calculated as the angle between the kinematic thigh segment relative to the kinematic pelvis segment, the knee joint angle was calculated as the angle between the kinematic shank segment relative to the thigh segment, and the ankle joint angle was calculated as the angle between the kinematic foot segment and the shank segment. Using this same function, the hip moment and power were calculated for the thigh and resolved into the pelvis coordinate system, the knee joint moment and power were calculated for the shank and resolved in the thigh coordinate system, while the ankle joint moment and power were calculated for the foot and resolved into the foot coordinate system. Once the kinematics and kinetics were calculated, we ran the Visual3D automatic gait event detection function (Automatic_Gait_Events) to determine when heel-strike occurred based on the minimum force plate value determined by the FP_Auto_Baseline function. We then used these heel-strike events to segment the data based on strides and calculated the ensemble average across strides.

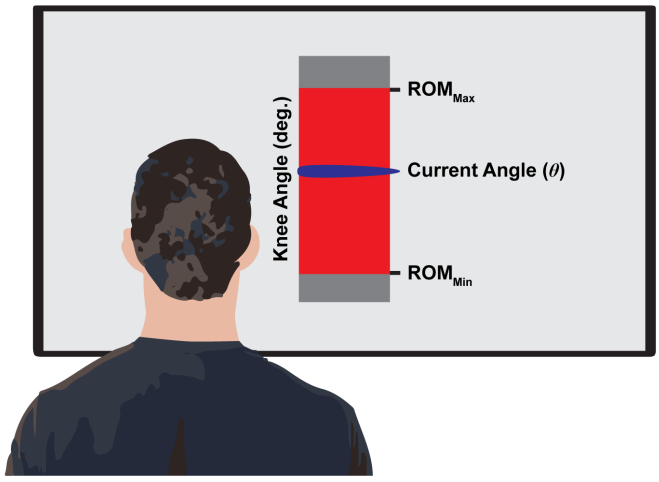

Figure B.2 Throughout the experiment, the participant was given visual feedback of his knee angle while walking. A red bar indicated the knee joint range of motion as measured while wearing the device without resistance, while a blue cursor indicated the real-time knee angle. This feedback was provided to ensure the subject did not reduce his movement excursions while walking with resistance.

B.3 Visual Feedback

Visual feedback was provided to the participant to encourage them to walk with their normal range of motion during trials with resistance. To create the visual feedback, we measured the participant's knee joint range of motion as they walked during the *No Resistance* trial, then projected these values onto a bar plot along with the real-time knee angle as measured with the encoder on the device. Hence, the max flexion angle was located at the top of the plot and the minimum angle (or max extension angle) was at the bottom of the plot, while a cursor indicated their real-time knee angle (Figure B.2). As he walked, the participant was encouraged to reach peak flexion during early swing, and peak extension as he approached heel-strike. This visual feedback was created using a custom LabVIEW vi (v2013, National Instruments Corp., Austin, TX, US) and displayed on a 177.8 cm (70 in) monitor located approximately 2.5 m in front of the treadmill.

We provided feedback in this validation experiment to ensure that the participant worked to overcome the resistance rather than just adapting a stiff knee walking strategy (Washabaugh et al., 2016). It has been found that, when walking under applied resistive loads, motor slacking occurs and individuals often reduce their movement excursions (Reinkensmeyer et al., 2009; Washabaugh et al., 2016). Hence, in these validation experiments, we chose to display the joint excursion using the participant's range of motion. In the past, other studies have used verbal coaching, metronomes, or obstacle avoidance protocols to achieve the same effect (Houldin et al., 2012; Reid & Prentice, 2001).

B.4 Repeatability of Benchtop Calibration

During the benchtop experiment, the software on the dynamometer was executed twice, which allowed us to perform repeatability analysis on the calibration curves. For this analysis,

we calculated Pearson's correlation coefficient (r), the slope of a line of best fit, and the coefficient of variation [CV(%)] between the two sets of torque data for each spring stiffness (Table B.2). Overall, we found the two trials were highly correlated ($r > 0.998$) and that the slope was approximately 1 for all springs, meaning that the two data sets were highly correlated and that an increase of 1 Nm for the first data set corresponds to a similar increase in the second data set (as is required for repeatability). The coefficient of variation between the two data sets was also very low [CV < 2.12%], indicating high precision between the two measurements. Ideally, this repeatability analysis would have been performed over hundreds of cycles of loading, as this is how the device would typically be used for rehabilitation. However, we anticipate that the resistive properties of the device should not change so long as the spring is not deformed beyond its elastic range, which would typically be the case with our device.

Table B.1 Benchtop testing analysis comparing our measured values of spring stiffness and resting position with theoretical values based on the governing principles of the device**.**

Theoretical Value	Measured Value	Difference (T-M)	Difference (%)
Spring Stiffness (k [N m deg^{-1}])			
0.178	0.215	-0.036	-20.4
0.356	0.362	-0.005	-1.4
0.497	0.501	-0.004	-0.8
0.675	0.605	0.071	10.5
0.788	0.663	0.125	15.9
Resting Position (Θ_r [deg])			
10.0	11.5	-1.5	-
20.0	19.0	1.0	-
30.0	28.1	1.9	-
35.0	35.3	-0.3	-
40.0	42.2	-2.2	-
50.0	48.8	1.2	-
60.0	54.9	5.1	-

Note: difference was calculated as the theoretical minus measured (T−M). The Percentage difference was calculated as (T−M)×100/T.

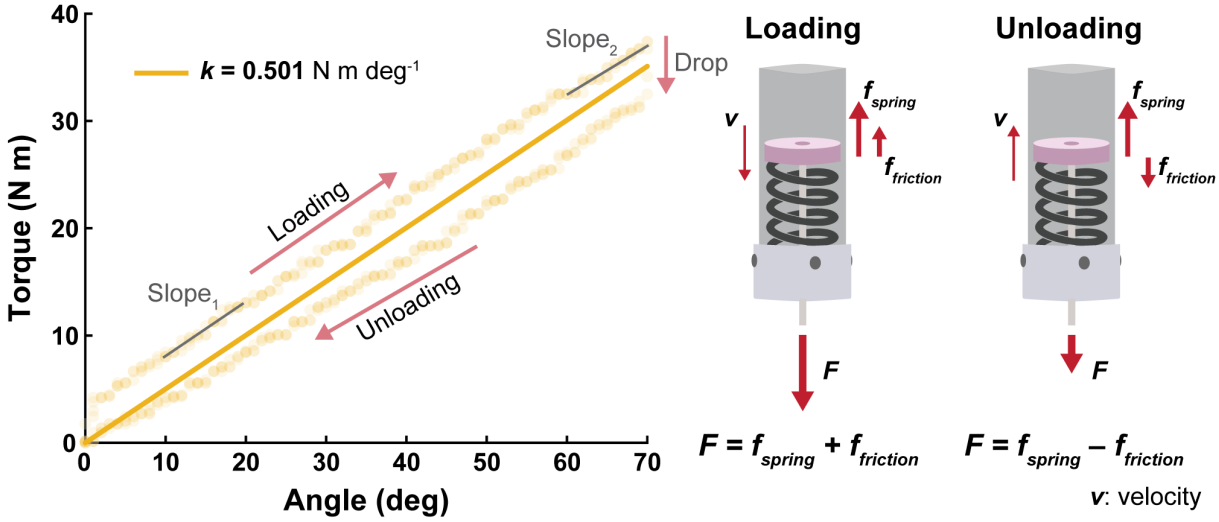

Spring	(N m deg^{-1})	k = 0.215	k = 0.362	k = 0.501	k = 0.605	k = 0.633
Slope$_1$	(N m deg^{-1})	0.334	0.479	0.784	0.832	0.801
Slope$_2$	(N m deg^{-1})	0.230	0.382	0.535	0.652	0.726
Drop	(N m)	2.99	4.08	4.90	5.58	6.94

Figure B.3 Differences between linear best-fit for spring stiffness and individual measurements. The stiffness traces in Figure 5.3 are linear best-fit lines for the spring calibration data. Plotting the data for an individual spring (Top Left), there are two distinct sources of error between best-fit lines and measured data: (1) hysteresis due to friction between the plunger and cylinder and (2) deformation of the device under high loads. The effects of (1) are evident by an overestimation of stiffness as the spring is loaded and an underestimation of stiffness as the spring is unloaded. Which occurs because the friction force acts in the same direction as the spring force during loading and in the opposite direction during recoil (Top Right). The change in friction during the transition between loading and unloading is represented by the drop in torque depicted in the graph. Notably, the friction is larger for stiffer springs (indicated by increasing drop), which could be caused by misalignments between the cable and the plunger or deformation of the cylinder causing the plunger to be pinched at higher resistances. The effects of (2) are evident in the change in measured stiffness ($Slope_1$ and $Slope_2$) as torque increases, indicating deformation of the surrounding system. $Slope_1$ and $Slope_2$ represent a linear best-fit for a subset of the data at the beginning and end of loading. (Bottom) Measured best-fit, slope, and drop for each of the springs used in this study.

Table B.2 Repeatability between two loading cycles of the spring calibration curves.

Spring (N m deg^{-1})	*r*	Slope	CV(%)
k=0.215	0.9985	0.9968	2.1125
k=0.362	0.9993	1.0034	1.8483
k=0.501	0.9991	0.9988	1.7380
k=0.605	0.9994	1.0045	1.6387
k=0.663	0.9997	0.9953	1.3295

r: Pearson's correlation coefficient, Slope: the slope of a linear fit, CV(%): the coefficient of variation

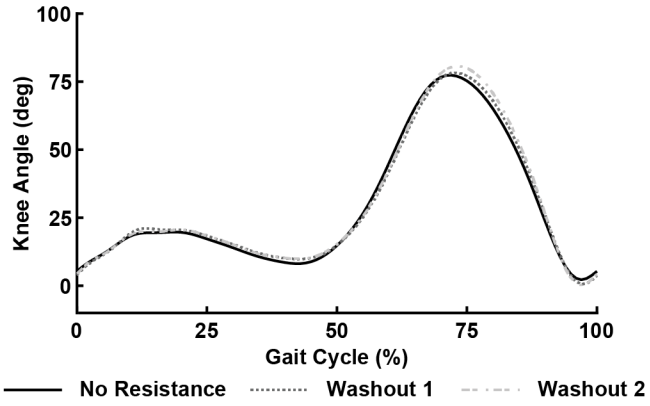

Figure B.4 Knee kinematics measured at the end of the washout periods. During experiment 2, we collected kinematics over the last 30 s of the 300 s washout trials that occurred between trainings. After training, the largest aftereffects occurred at the knee; however, the knee angle returned to the level seen during the no resistance trial following the washout trials. Washout 1 occurred between the conditions resisting flexion and extension; Washout 2 occurred between conditions resisting extension and bidirectionally.

Appendix C

Chapter 6 Supplemental Materials

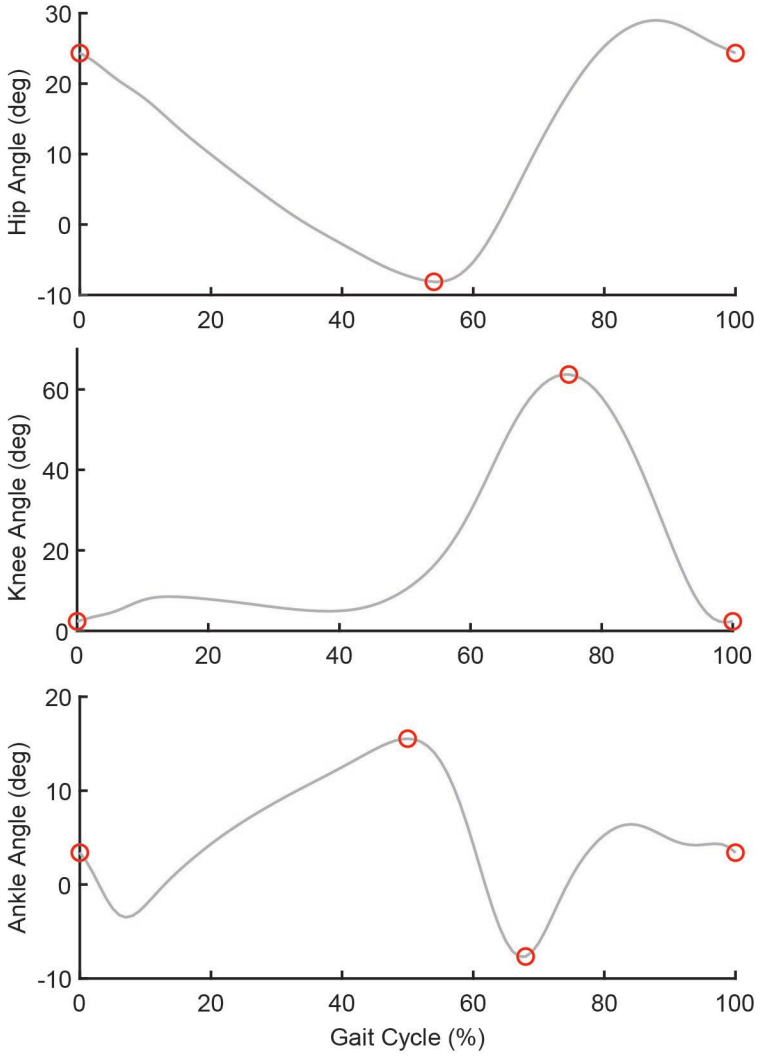

Figure C.1 Piecewise linear length normalization procedure. For all gait data, we identified several points of interest based on the baseline kinematics that data could be aligned to for statistical parametric mapping. Traces depict the average joint angle profiles during baseline walking. Red circles indicate the features that we identified as points of interest (POI) so that data could be resampled to have these POI align. Note, these same POI were used for the biomechanics and EMG data.

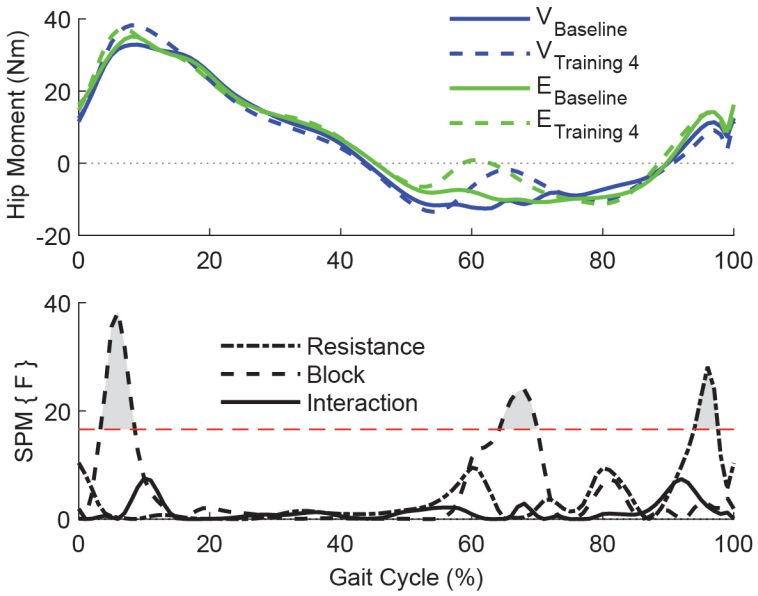

Effect	DoF	Range	Mean$_1$	Mean$_2$	*p*
Resistance	(1, 11)	94.0 – 97.6	8.9	13.1	**0.024**
Block	(1, 11)	3.3 – 8.6	31.2	34.9	**0.012**
		64.2 – 70.0	-10.6	-3.6	**0.008**

Figure C.2 Experiment 1: hip moment during training. (Top) Traces depict the hip moment profile over the gait cycle while walking with the elastic resistance (E) and the viscous resistance (V). (Middle) SPM{F} statistics plotted over the gait cycle. Traces that exceed the threshold (red dashed line) are considered significant and shaded gray. (Bottom) Table indicating the averages and significance of clusters that exceeded the threshold. For resistance main effects, mean 1 is the average for the viscous device over the cluster, and mean 2 is the average for the elastic device over the cluster. For block main effects, mean 1 is the average over the cluster for the baseline block, and mean 2 is the average over the cluster for the training 4 block. P-values are in bold if they are considered significant.

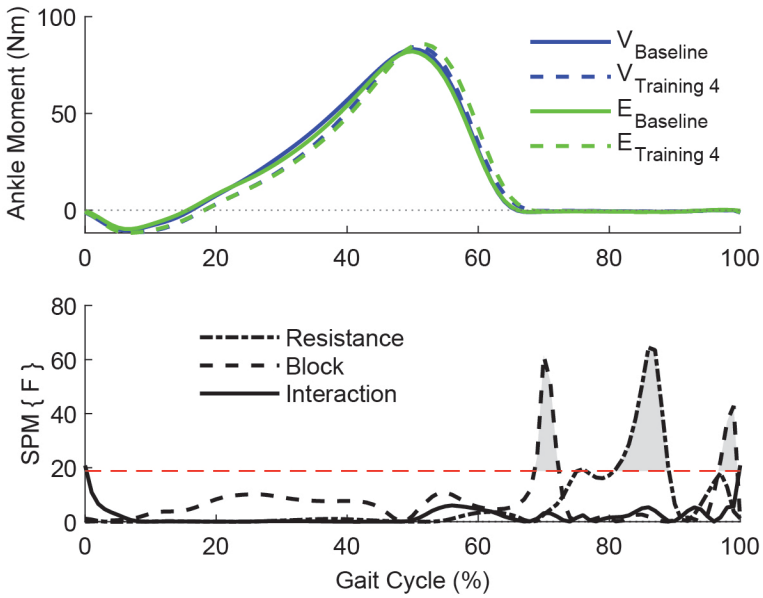

Effect	DoF	Range	Mean$_1$	Mean$_2$	*p*
Resistance	(1, 11)	75.2 – 76.4	-0.4	-0.6	**0.040**
		80.7 – 89.1	-0.7	-0.9	**< 0.001**
Block	(1, 11)	68.6 – 72.3	-0.7	-0.4	**0.007**
		96.7 – 99.6	0.0	-0.2	**0.016**
Interaction	(1, 11)	0.0 – 0.2			**0.050**
		99.9 – 100.0			**0.050**
Post hoc	$t_{V1\ E1}$	73.7 – 76.9	-0.4	-0.6	**0.004**
	$t_{V2\ E2}$	82.3 – 88.4	-0.7	-1.0	**< 0.001**
	$t_{V1\ V2}$	68.5 – 71.7	-0.8	-0.4	**0.003**
	$t_{E1\ E2}$	97.0 – 99.2	0.1	-0.1	0.019

Figure C.3 Experiment 1: ankle moment during training. (Top) Traces depict the ankle moment profile over the gait cycle while walking with the elastic resistance (E) and the viscous resistance (V). (Middle) SPM{F} statistics plotted over the gait cycle. Traces that exceed the threshold (red dashed line) are considered significant and are shaded gray. (Bottom) Table indicating the averages and significance of clusters that exceeded the threshold. For resistance main effects, mean 1 is the average for the viscous device over the cluster, and mean 2 is the average for the elastic device over the cluster. For block main effects, mean 1 is the average over the cluster for the baseline block, and mean 2 is the average over the cluster for the training 4 block. P-values are in bold if they are considered significant.

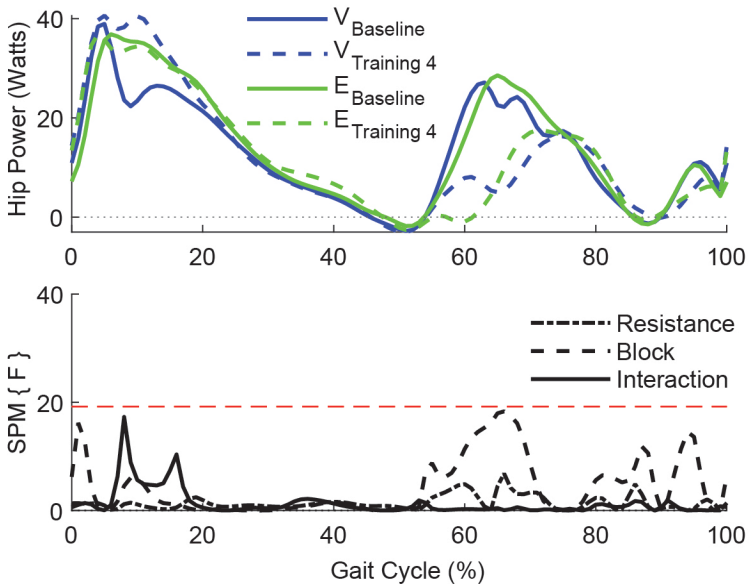

Figure C.4 Experiment 1: hip power during training. (Top) Traces depict the hip power profile over the gait cycle while walking with the elastic resistance (E) and the viscous resistance (V). (Bottom) SPM{F} statistics plotted over the gait cycle. Traces that exceed the threshold (red dashed line) are considered significant.

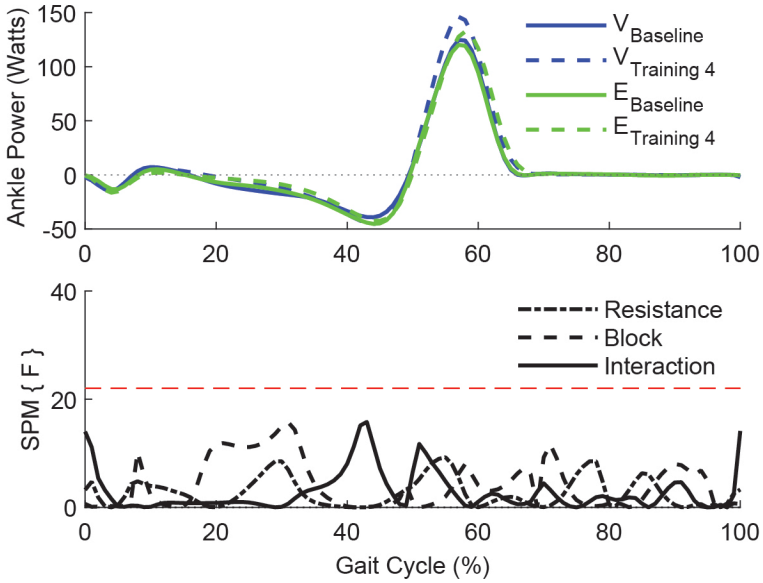

Figure C.5 Experiment 1: ankle power during training. (Top) Traces depict the ankle power profile over the gait cycle while walking with the elastic resistance (E) and the viscous resistance (V). (Bottom) SPM{F} statistics plotted over the gait cycle. Traces that exceed the threshold (red dashed line) are considered significant.

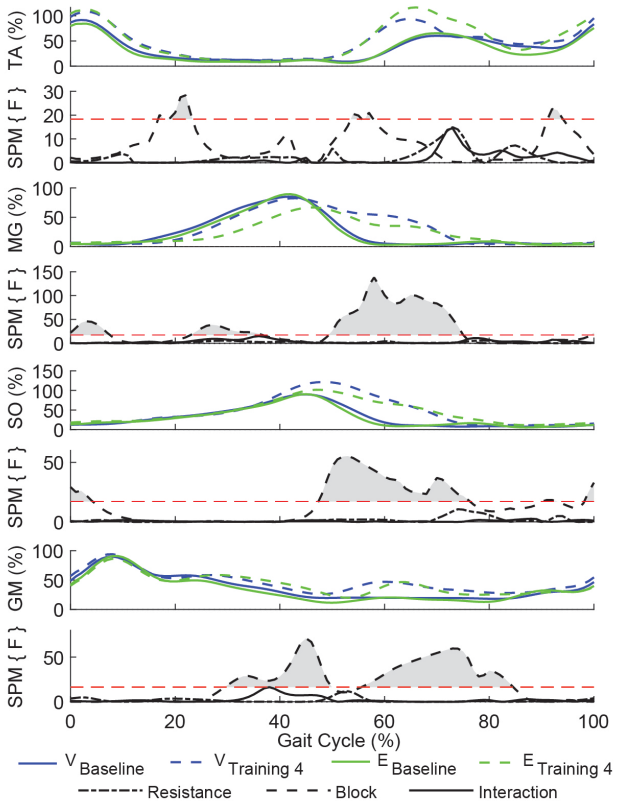

Effect	DoF	Range	Mean$_1$	Mean$_2$	p
TA					
Block	(1, 11)	16.7 – 17.8	17.6	29.6	**0.044**
		18.4 – 23.3	14.0	22.2	**0.003**
		53.6 – 55.6	9.0	36.9	**0.031**
		56.2 – 57.8	14.7	55.1	**0.037**
		91.1 – 94.1	33.5	53.4	**0.019**
MG					
Block	(1, 11)	0.0 – 7.5	4.2	6.6	**< 0.001**
		22.9 – 36.7	52.7	33.7	**< 0.001**
		49.3 – 75.0	10.2	40.2	**< 0.001**
		99.4 – 100.0	4.3	6.3	**0.049**
SO					
Block	(1, 11)	0.0 – 4.2	13.7	18.1	**0.014**
		47.4 – 76.3	27.0	68.1	**< 0.001**
		90.1 – 93.0	7.2	11.9	**0.027**
		98.2 – 100.0	11.2	15.5	**0.039**
GM					
Block	(1, 11)	29.5 – 49.9	27.6	41.6	**< 0.001**
		55.6 – 84.6	18.1	34.7	**< 0.001**

Figure C.6 Experiment 1: muscle activation of non-thigh muscles during training. (Left) Traces depict the muscle activation over the gait cycle while walking with the elastic resistance (E) and the viscous resistance (V) as well as SPM{F} statistics plotted over the gait cycle. SPM{F} traces that exceed the threshold (red dashed line) are considered significant and are shaded gray. (Right) Table indicating the averages and significance of clusters that exceeded the threshold. For resistance main effects, mean 1 is the average for the viscous device over the cluster, and mean 2 is the average for the elastic device over the cluster. For block main effects, mean 1 is the average over the cluster for the baseline block, and mean 2 is the average over the cluster for the training 4 block. P-values are in bold if they are considered significant. Muscle abbreviations: TA (tibialis anterior), MG (medial gastrocnemius), SO (soleus), GM (gluteus medius).

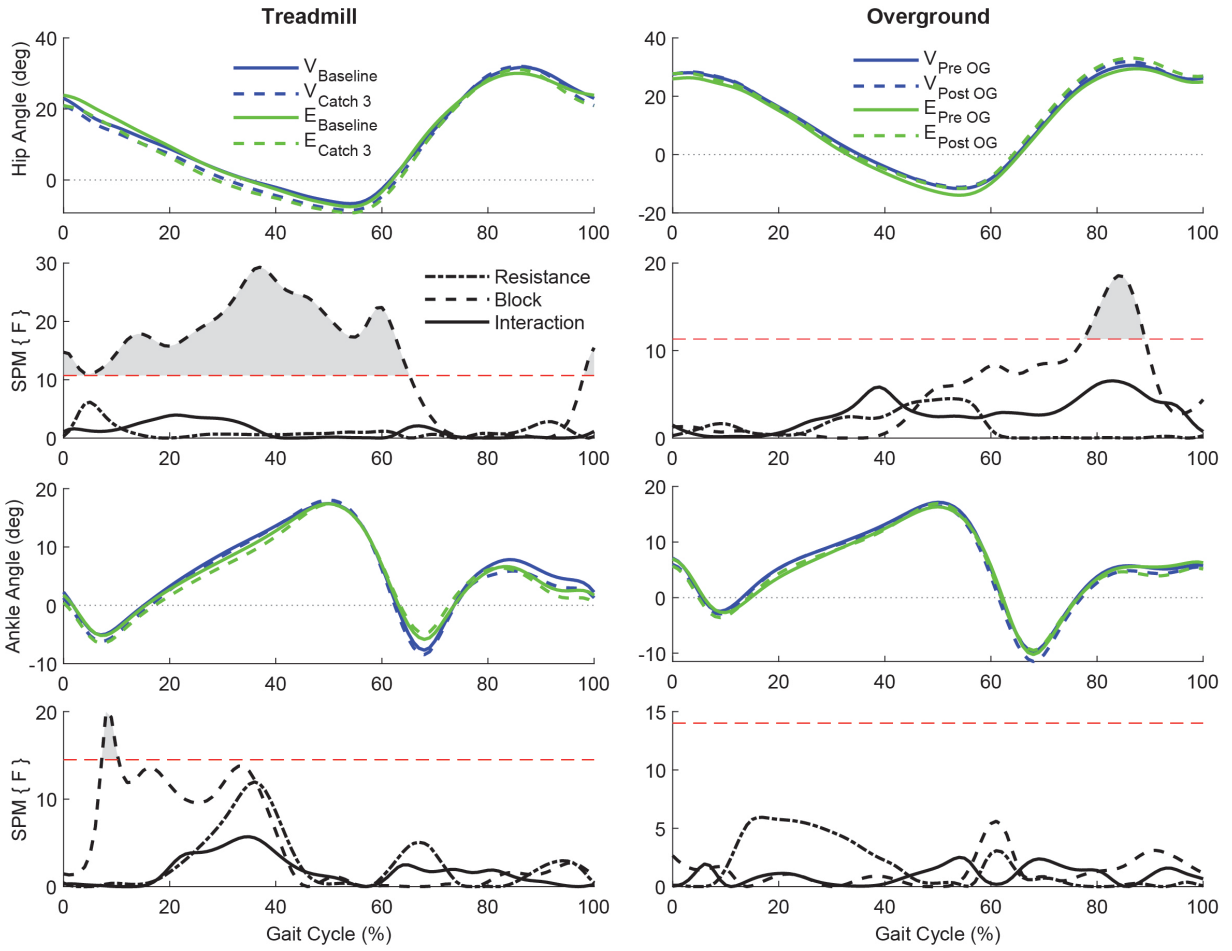

Effect	DoF	Range	Mean$_1$	Mean$_2$	*p*
Hip					
Block	(1, 11)	0.0 – 65.2	4.4	2.1	**< 0.001**
		98.1 – 100.0	23.9	21.5	**0.05**
Ankle					
Block	(1, 11)	7.2 – 10.4	-4.6	-5.8	**0.040**

Effect	DoF	Range	Mean$_1$	Mean$_2$	*p*
Hip					
Block	(1, 11)	77.5 – 89.1	28.2	30.8	**0.030**

Figure C.7 Experiment 1: hip and ankle angles during aftereffects. Plots indicate kinematics when walking on the treadmill (Left) and overground (Right). For each joint, (Top) traces depict the kinematic profile over the gait cycle while walking with the elastic resistance (E) and the viscous resistance (V). Below the kinematic traces, SPM{F} statistics are plotted over the gait cycle. Traces that exceed the threshold (red dashed line) are considered significant and are shaded gray. (Bottom) Tables indicating the averages and significance of clusters that exceeded the threshold. For block main effects over the treadmill, mean 1 is the marginal mean during Baseline block over the cluster, and mean 2 is the marginal mean during Catch 3 block over the cluster. For block main effects during overground walking, mean 1 is the average over the cluster for the Pre Overground block and mean 2 is the average over the cluster for the Post Overground block. P-values are in bold if they are considered significant.

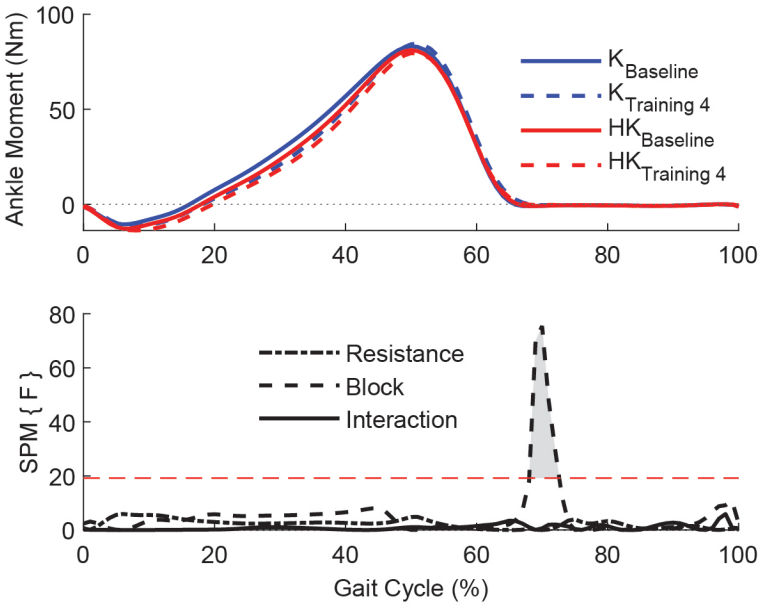

Effect	DoF	Range	Mean$_1$	Mean$_2$	*p*
Ankle					
Block	(1, 11)	68.0 – 72.6	-0.8	-0.3	**0.002**

Figure C.8 Experiment 2: ankle moment during training. (Top) Traces depict the ankle moment profile over the gait cycle while walking with the viscous device providing resistance to the knee (K) or to both the hip and knee (HK). (Middle) SPM{F} statistics plotted over the gait cycle. Traces that exceed the threshold (red dashed line) are considered significant and are shaded gray. (Bottom) Table indicating the averages and significance of clusters that exceeded the threshold. For block main effects, mean 1 is the average over the cluster for the baseline block, and mean 2 is the average over the cluster for the training 4 block. P-values are in bold if they are considered significant.

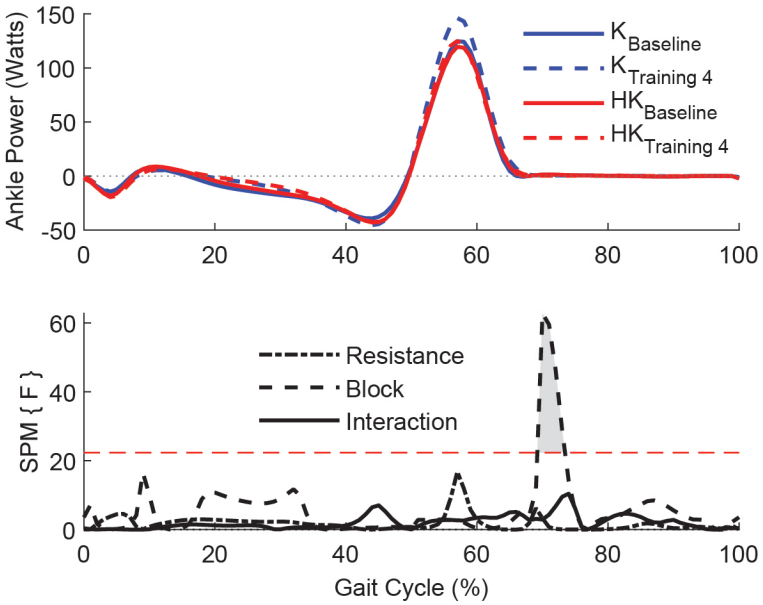

Effect	DoF	Range	Mean$_1$	Mean$_2$	*p*
Ankle					
Block	(1, 11)	69.2 – 73.4	1.2	0.4	**< 0.001**

Figure C.9 Experiment 2: ankle power during training. (Top) Traces depict the ankle power profile over the gait cycle while walking with the viscous device providing resistance to the knee (K) or to both the hip and knee (HK). (Middle) SPM{F} statistics plotted over the gait cycle. Traces that exceed the threshold (red dashed line) are considered significant and are shaded gray. (Bottom) Table indicating the averages and significance of clusters that exceeded the threshold. For block main effects, mean 1 is the average over the cluster for the baseline block, and mean 2 is the average over the cluster for the training 4 block. P-values are in bold if they are considered significant.

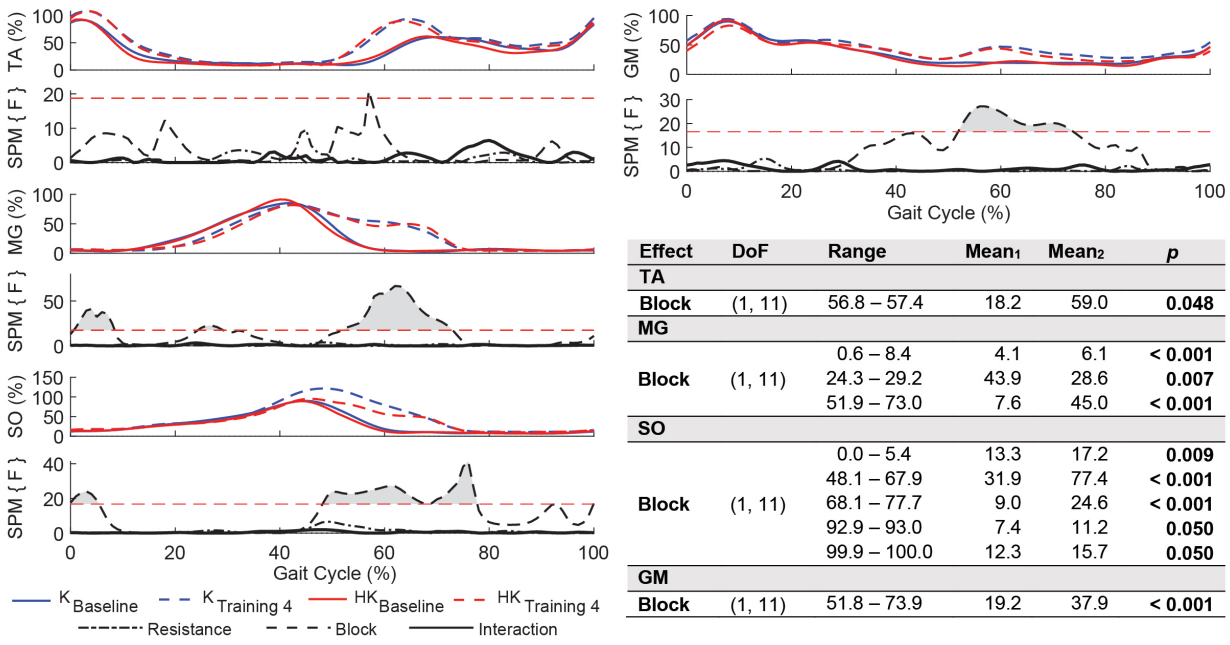

Effect	DoF	Range	Mean$_1$	Mean$_2$	*p*
TA					
Block	(1, 11)	56.8 – 57.4	18.2	59.0	**0.048**
MG					
Block	(1, 11)	0.6 – 8.4	4.1	6.1	**< 0.001**
		24.3 – 29.2	43.9	28.6	**0.007**
		51.9 – 73.0	7.6	45.0	**< 0.001**
SO					
Block	(1, 11)	0.0 – 5.4	13.3	17.2	**0.009**
		48.1 – 67.9	31.9	77.4	**< 0.001**
		68.1 – 77.7	9.0	24.6	**< 0.001**
		92.9 – 93.0	7.4	11.2	**0.050**
		99.9 – 100.0	12.3	15.7	**0.050**
GM					
Block	(1, 11)	51.8 – 73.9	19.2	37.9	**< 0.001**

Figure C.10 Experiment 2: muscle activation of non-thigh muscles during training. Traces depict muscle activation profiles over the gait cycle while walking with the viscous device providing resistance to the knee (K) or to both the hip and knee (HK) as well as SPM{F} statistics plotted over the gait cycle. SPM{F} traces that exceed the threshold (red dashed line) are considered significant and are shaded gray. (Bottom Right) Table indicating the averages and significance of clusters that exceeded the threshold. For Block main effects, mean 1 is the average over the cluster for the baseline block, and mean 2 is the average over the cluster for the training 4 block. P-values are in bold if they are considered significant. Muscle abbreviations: TA (tibialis anterior), MG (medial gastrocnemius), SO (soleus), GM (gluteus medius).

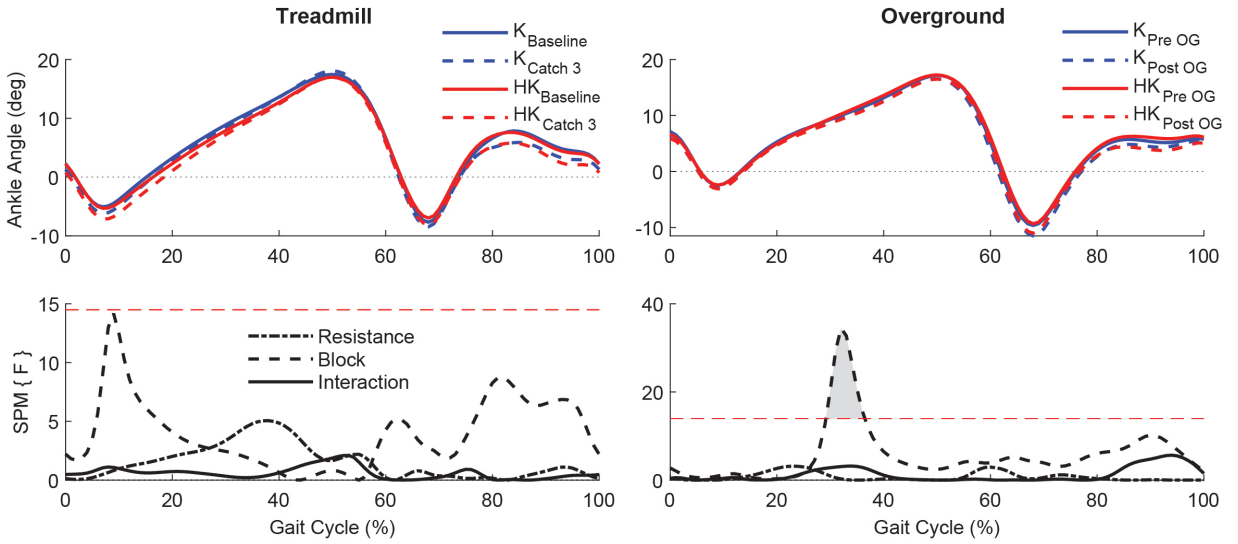

Effect	DoF	Range	Mean$_1$	Mean$_2$	*p*
Ankle					
Block	(1, 11)	29.2 – 36.5	10.4	9.8	**0.021**

Figure C.11 Experiment 2: ankle angles during aftereffects. Plots indicate kinematics when walking on the treadmill (Left) and overground (Right). (Top) Traces depict the kinematic profile over the gait cycle while walking with the viscous device providing resistance to the knee (K) or to both the hip and knee (HK). Below the kinematic traces, SPM{F} statistics are plotted over the gait cycle. Traces that exceed the threshold (red dashed line) are considered significant and are shaded gray. (Bottom) Tables indicate the averages and significance of clusters that exceeded the threshold. For block main effects during overground walking, mean 1 is the average over the cluster for the Pre Overground block and mean 2 is the average over the cluster for the Post Overground block. P-values are in bold if they are considered significant.

Appendix D

Chapter 7 Supplemental Materials

D.1 Computation of Time-varying Resistances Added to the Model

1. For the ankle weight, we tracked the acceleration of a point slightly proximal to the right ankle over the gait cycle and determined the force that would be felt by carrying a mass at that location. We modulated the mass coefficient (m = 2.36, 4.72, and 7.08 kg) and added the resulting resistance to the right tibia of the model at that location.
2. For the elastic band attached to the ankle, we tracked the position of a point slightly proximal to the right ankle over the gait cycle and used Hooke's Law to determine the force that would be felt at that location due to an elastic band (unstretched length l = 0.68 m with pretension = 5 N) anchored behind the model. We modulated the spring stiffness coefficient (k = 75, 165, and 255 N/m) and added the resulting resistance at the right tibia of the model.
3. For the viscous device, we tracked the angular velocities of the right hip and knee joints in the sagittal plane and modulated the damping coefficients (b_h = 0.17, 0.33, 0.5 and b_k = 0.04, 0.08, 0.12 N·m·s/degree). These coefficients were chosen such that the sum of the equivalent forces at the ankle caused by each joint torque was equivalent to the desired resistance level ($F_a = b_h(\omega_h/d_{ha})+b_k(\omega_k/d_{ka})$; such that $b_h(\omega_h/d_{ha}) = b_k(\omega_k/d_{ka}) = F_a/2$, where d represents the distance in the sagittal plane between the joints). Counteracting torques for the hip were added to the right pelvis and femur at the hip joint center;

counteracting torques for the knee were added to the right femur and tibia at the knee joint center of the model.

4. For the weight at the pelvis, we tracked the acceleration of the model's center of mass over the gait cycle and determined the force that would be felt by carrying a mass at that location. We modulated the mass coefficient (m = 3.04, 6.07, 9.12 kg) and added the resulting resistance to the pelvis at the center of mass of the model.
5. For the constant backwards pulling force at the pelvis, we tracked the position of the center of mass over the gait cycle and applied a constant force through a virtual cable (length l = 0.68 m) anchored behind the model. We modulated the force coefficient (f = 30, 60, and 90 N) and added the resulting resistance to the pelvis at the center of mass of the model.

Appendix E

IRB Protocol

Background

A growing body of evidence indicates that resistive gait training improves the locomotor ability of individuals with various neurological or orthopedic conditions (e.g., stroke, cerebral palsy, spinal cord injury, and knee joint trauma, etc.).[1–5] The basic premise underlying this approach is that the functional benefits of strength training (e.g., gait function) are augmented when combined with task-specific training, and the combination may facilitate motor learning and neural plasticity.[1,3,6,7] In clinic, therapists often apply resistance using ankle weights or resistance bands.[8] However, there are numerous ways in which resistance can be applied to motion (e.g., weights, resistance bands, springs, viscous dampers), and all of these methods are going to vary in how they engage the subject (i.e., elastic resistances are known to increase co-contraction during exercise when compared with weights or viscous resistances) (see Figure E.1).[9] Hence, it is important to understand the biomechanical and physiological mechanisms that mediate the acute adaptation to resisted walking before it is applied as an intervention. Therefore, with this study, we would like to examine these mechanisms while subjects walk with different resistance types by measuring biomechanical and physiological changes that occur due to the applied resistance. While these methods are applicable to a wide variety of patient population, our initial testing in this study will be performed on three testing populations: healthy individuals, stroke survivors, and individuals with ACL injury/surgery. Understanding of the biomechanical and physiological mechanisms will also help in the designing of future interventions.

Study Aims

Aim: Determine how different methods/resistance types for resisting walking (e.g., ankle weights, elastic bands, elastic/viscous passive braces) promote biomechanical and neurophysiological adaptations in healthy and clinical populations.

Hypothesis 1: Resisted walking with the various resistance types will significantly alter kinematics, muscle recruitment, and spatiotemporal gait parameters during and after the experiment, depending on the resistance type.

Hypothesis 2: The different resistance types will differ in the muscles they are able to target during resisted walking.

Hypothesis 3: Resisted walking will increase corticospinal excitability in the muscles to which the resistance is applied.

Methods

Types of resistance:

$$Weight: Force = mass * accelearation$$

$$Elastic/Spring: Force = Spring\ constant * displacement$$

$$Brakes: Force = Brake\ constant * velocity$$

Figure E.1 Examples of types of resistances and the equations that govern the resistive force. The force felt by the user will differ greatly based on the type of resistance, which could have an effect on physiological measures before during and after walking.

Subjects and Recruitment: We will recruit 120 participants who are either diagnosed with stroke (n = 30), ACL injury/surgery (n = 30), or uninjured controls (n = 60) to participate in this study. Subjects will be recruited via face-to-face contact, email, public advertisements, posting on UMClinicalStudies.org website, or through a stroke registry (IRB: HUM00099109). Additionally, subjects may be recruited from subject pools created through existing IRBs (HUM00073356, HUM00081480, HUM00080244, HUM00133860, HUM00130845, and HUM00087962). Subjects may be pre-screened to ensure their eligibility before coming to the lab.

Inclusion Criteria for Uninjured Controls:

- age ≥ 18 years

Exclusion Criteria for Uninjured Controls:

- Uncontrolled Diabetes or Hypertension;
- Any other medical condition that will significantly impact the study results

Inclusion Criteria for Stroke Survivors:

- age ≥ 18 years
- Ischemic or hemorrhagic stroke confirmed by CT, MRI, or clinical criteria
- No major deficits of sensation or proprioception

Exclusion Criteria for Stroke Survivors:

- Inability to provide written informed consent
- Unable to think clearly and remember (Mini-Mental State Exam score < 22 and miniMOCA < 8);
- Uncontrolled Diabetes or Hypertension;
- Acute Lower limb orthopedic conditions, such as recent fracture or surgery that limit mobility
- Severe limitations of joint range of motion
- Severe spasticity and joint contractures
- Severe aphasia
- Unable to walk independently with or without assistive devices;
- Any other medical condition that will significantly impact the study results

Inclusion Criteria for ACL injured/surgically repaired Subjects:

- age ≥ 18 years
- Suffered an ACL injury or have had an ACL surgery

Exclusion Criteria for ACL injured/surgically repaired Subjects:

- Inability to provide written informed consent
- Significant pain that limits their ability to walk or exercise
- History of recent significant knee injury (other than current ACL) or lower-extremity fracture
- Uncontrolled diabetes or hypertension

Exclusion Criteria for subjects exposed to Transcranial Magnetic Stimulation (TMS):

- Unable to obtain reliable motor evoked potentials
- Are pregnant or are actively trying to conceive
- Have unexplained recurrent headaches
- Have a recent history of seizure (epilepsy)
- Taking medications that can reduce the seizure threshold
- Have a history of repeated fainting spells or syncope
- Have a history of skull fracture/head injury
- Have metal implants in the skull
- Have cardiac pacemakers
- Have any other condition that could significantly affect the study results

We do not plan to exclude subjects based on stroke severity/impairment or stroke location as a post-hoc analysis would inform us on appropriate patient population selection for future interventional studies. We note that the risks of participating in the study do not change based on the severity or location of the stroke,[10,11] especially considering that the study involves only single or paired pulse TMS. There are no imaging requirements for the study subjects and interpretation (performed using chart reviews, medical records, or by the stroke physician) of the images (if available through medical records) will be used only to characterize the lesion location, severity, and type of injury for publication purposes. While magnetic fields rapidly attenuate with distance and there are no known short-term or long-term risks of TMS to the children of pregnant women,[12–14] we would still exclude individuals who are pregnant or are actively trying to conceive as there are no direct benefits to them from this study. Similar to our other TMS studies, we will use a self-reported questionnaire for identifying individuals who may be pregnant. An a priori power analysis indicated that 30 individuals in each group will yield > 80% power to detect statistically significant differences at $\alpha = 0.05$ for a conservative effect size estimation of 0.6. Additional uninjured controls are included so that controls are age matched between clinical populations.

Experimental Procedures

The experiment will consist of about 5 sessions/visits depending on subject's availability. Each session will last approximately 2 - 4 hours in duration. Subjects will be compensated $10 per hour for their time and effort. Additional compensation may be provided for subjects who may need travel assistance.

Screening and Informed Consent Visit: The subject will meet with authorized research personnel in the Neuromuscular and Rehabilitation Robotics Laboratory (NeuRRo Lab). During this visit, the participant will be provided with detailed information about the study, the risks and benefits of participation, and the nature of study procedures, including orientation to various testing devices used in this study. A study member will screen the subjects for the eligibility criteria using screening questionnaires and health related assessments. For safety purposes, stroke subject's eligibility to participate in the TMS experiment will be determined in consultation with the physician (Dr. Edward Claflin), particularly when the subject provides responses that could potentially increase the risk associated with the TMS procedure (e.g., prior history of seizure, medications that could reduce seizure threshold, etc.). A Folstein Mini-Mental State Examination (MMSE), which is a measure of individual's cognitive status and awareness and Montreal Cognitive Assessment Test (Mini version), will also be used to screen stroke individuals. Subjects need to score a minimum of 22 (on a scale of 30) in MMSE/8 (on a scale of 12) in mini MOCA to be considered eligible for the study. Both MMSE and MOCA have been shown to be sensitive in judging a patient's capacity to consent (e.g., http://www.ncbi.nlm.nih.gov/pmc/articles/PMC2717553/). We note that we will be doing a Mini MOCA as arm/hand impairments could affect their ability to perform the visuospatial and executive functions section of the questionnaire. The mini MOCA consists of selected subtests from the full MOCA, and includes a 5-word immediate and delayed memory test, a 6-item orientation task and a 1-letter phonemic fluency test (the letter F). The mini MOCA has been validated and recommended by NINDS and has been shown to be as sensitive as the full MOCA in individuals with cognitive impairment. (http://www.ncbi.nlm.nih.gov/pubmed/26713170). If the subject is found to be eligible to participate in the study and shows interest, an informed consent document will be provided. Subjects will then be familiarized to the testing procedures and instruments, and would be provided ample opportunity to ask questions regarding the study procedures, risks and benefits, and other study-related items. After consenting, the participant will then be scheduled for subsequent visits.

Functional Ability Testing

These tests are performed simply to gather clinical characteristics of the subjects participating in the study. Functional ability testing will be completed in approximately 1 to 1.5 hours and may be performed on the same day of the screening visit depending on subject's availability. If the subject does not have enough time to complete both screening and functional ability testing on a single day, we will have them visit the laboratory on a separate day. The battery of functional measures is listed in detail below, and include objective assessments of the individual's functional abilities including range of motion, balance, and strength. These tests may have to be performed on two different days to account for day-to-day variability. All the below tests have been validated in the testing populations and are commonly used, non-invasive functional/clinical measures. Subjects may complete the some or all of the following assessments:

1. Movement Kinematics: Kinematics of movement (limb position and joint angle) using a motion capture camera system or wearable encoders/goniometers.
2. Gait/balance assessment (e.g., gait speed, 2- or 6-minute walking test) using stopwatch, Mobility lab (APDM Inc.) – which measures temporal-spatial events and limb

accelerations. Additionally, we may use instrumented walkway/treadmill. To measure these parameters.

3. Lower-extremity impairment and functional measures, such as Fugl-Meyer score.
4. Modified Ashworth Scale: The modified Ashworth scale is a performance based body function test to measure muscle tone of subject.
5. Muscle Strength & Activation: Manual muscle testing or strength testing in an instrumented dynamometer can be performed to assess strength.
6. Self-reported questionnaires: Stroke impact scale, Tegner Activity Score, MARX activity score, Knee Injury and Osteoarthritis Outcome Score.

Paradigms and Assessments

The following tools will be used to quantify physiological effects of walking with resistance. <u>All assessment tools are noninvasive and are of minimal risk to the subject.</u>

1. <u>Muscle Activation and Coordination:</u> The magnitude of muscle activation and co-contraction of the antagonist muscles during testing will be measured using Electromyography (EMG) by means of noninvasive surface electrodes. Brands used in our lab include: (Trigno Wireless EMG, Delsys, Inc., Natick, MA, USA) and (Model MA-311, Motion Labs Systems, Inc., Baton Rouge, LA, USA). Previously accepted for use on human subjects in IRBs (HUM00081480, HUM00073356, HUM00130845, HUM00087962, and HUM00080244).
2. <u>Kinematics:</u> The subject's movement patterns during the experiment will be evaluated using motion capture camera system or instruments (i.e., angle encoders or goniometers) and monitored over time to see how the subject walks under resistance. We will compare the subjects gait kinematics before the resistance is applied, while resisted, and while resistance is removed. Previously accepted for use on human subjects in IRB (HUM00073356, HUM00087962, and HUM00133860).
3. <u>Spatiotemporal Gait Parameters:</u> Mobility lab (APDM Inc.) – which measures temporal-spatial events and limb accelerations, or instrumented walkway/treadmill will be used to measure the subject's spatiotemporal gait parameters (e.g., gait speed, cadence, stride length, stride duration, etc.) before, during, and after resisted walking. Previously accepted for use on human subjects in IRB (HUM00087962).
4. <u>Cortical Excitability:</u> The changes in motor cortical excitability that occur due to resisted walking will be measured using single or paired pulse transcranial magnetic stimulation (TMS). Stimulation using TMS allows us to monitor brain plasticity by measuring muscle activation due to stimulating of the motor cortex. For example, we could measure intracortical inhibition (paired pulse stimulation), or corticospinal excitability of the primary motor cortex (single pulse stimulation). *We will not be performing repetitive TMS* (rTMS). (Magstim-Bistim^2 magnetic stimulator, The Magstim Company Ltd, Whitland, Carmarthenshire, UK). Previously accepted for use on human subjects in IRB (HUM00081480, HUM00073356, HUM00087962, HUM00130845 and HUM00073356).

5. Changes in voluntary and electrically stimulated force output: Muscle strength (force output), voluntary activation (i.e., the ability to maximally activate a muscle during a contraction), and electrically evoked torque at different frequencies may be evaluated using isokinetic dynamometry and electrical stimulation techniques (Previously accepted for use on human subjects in IRB (HUM00080244, HUM00087962, HUM00130845, and HUM00133860).[15,16] These measures would provide information on central and peripheral contributions to changes in force generating capacity.

Experimental Paradigm

Once screening and functional ability testing have completed, we will begin recording baseline measurements of the subject's biomechanics and physiology.

Beginning of the Session

Using the methods and equipment noted above, we will measure the subject's spatiotemporal gait parameters. We will also measure the subject's baseline muscle strength and electrically evoked torque characteristics (i.e., muscle physiology) with electrical stimulation techniques, while the subject is seated on an instrumented dynamometer with their hips and knees flexed and their back supported. Self-adhesive or carbon impregnated rubber electrodes will be placed on the proximal and distal aspects of the quadriceps and hamstring muscles. We will also apply surface electromyography (EMG) sensors to many of the key muscles used in gait [e.g., vastus medialis (VM), rectus femoris (RF), medial hamstring (MH), lateral hamstring (LH), tibialis anterior (TA), medial gastrocnemius (MG), soleus (SO), and gluteus medius (GM)]. Typically, electrodes will be secured to the skin using self-adhesive tapes and cohesive flexible bandages. Electrode placement will be carried out according to the guidelines established by the international SENIAM initiative (www.seniam.org). Should electrode positions be occluded by the device, electrodes will be placed over non-occluded but similar synergist muscles. The quality of the EMG signals will be visually inspected to ensure that the electrodes were appropriately placed.

For subjects undergoing TMS, we will then measure their cortical excitability using single or paired pulse paradigms. TMS is a noninvasive brain stimulation technique known to be safe in both children and adults and it will be used to test corticospinal excitability of neural circuits.[17] Unlike the repetitive TMS paradigms, single or paired pulse protocols do not have any therapeutic benefits, but can provide meaningful information about changes in corticospinal excitability and brain physiology. However, they are substantially safer than rTMS protocols and have been in existence for more than two decades.[14] There is minimal risk of using these protocols even in individuals with neurological injury; further, single-pulse and paired-pulse TMS has been studied extensively in stroke survivors for more than 25 years with virtually no major or long-lasting side-effects.[18] We note that we have active IRB applications with an approved use of TMS in human subjects, including stroke survivors (HUM00081480; HUM00073356; no more than minimal risk). We note that MD supervision is not required during TMS for our study since we are only using single or paired pulse TMS in a class 3 study (i.e., for studying brain physiology in patients and normal subjects).[14]

TMS (1ms pulse width, ~100µs rise time – fixed by the manufacturer) will be performed over the primary motor area of the brain (M1), representing the muscles that will be under resistance. Stimulation will induce a muscle twitch and a motor evoked potential (MEP), which can be monitored using an EMG or force sensor. The site that produced the largest and most consistent MEPs will be marked and considered as the hotspot or target area for the stimulation.[19,20] We will perform a range of stimulation intensities surrounding the subjects depolarization/motor threshold (~60-140% of motor threshold) and collect the corresponding MEPs or force output.[20,21] The subject will be at rest or providing a background contraction during the stimulation. When determining changes in intracortical excitability, a subthreshold conditioning (i.e., < 100% of motor threshold) stimulus will precede (~1-30 ms) the test stimulus.[22] MEP EMG data will be normalized to background activity and expressed as a percentage of maximum. MEP torque data will be normalized to twitches elicited from peripheral stimulation.

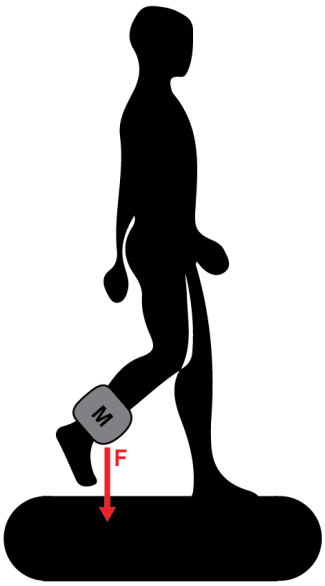

Figure E.2 Schematic of a subject walking while wearing an ankle weight

Treadmill Walking

First, subjects will walk on the treadmill without resistance so that we can measure their normal biomechanics for approximately 5 minutes. While walking, all subjects will be told to hold onto a hand-rail to minimize any risk of tripping and falling. A body-weight supporting harness will be used as an additional support in case the participant has substantial motor impairments or feels unsecure without the provision of supporting harness. Next, resistance will be added to the subject's leg. Resistance may be applied at the end-effector or at the joint levels involving one or more joints of the lower-extremity. Resistance forms include a mass attached to the subject's leg (e.g., ankle weights), a band attached to their ankle (e.g., theraband), or subjects will wear a resistive leg brace that uses passive springs (e.g., https://springloadedtechnology.com/) or passive brakes that has previously been approved for use on human subjects (HUM00133860) (see Figure E.2, Figure E.3, and Figure E.4). Because the leg brace is passive (i.e., does not add energy to the subject's movement, as a motor would) it is of minimal risk to the subject. Indeed,

this is safer than the elastic bands as it does not store energy. All of these methods for applying resistance would fall under a category of devices that are 510k exempt (21 CFR 890.5370, 890.5380, and 890.3475). We also note that we are not testing for safety or efficacy, but applying these resistive tools to measure the physiology of walking with different types of resistance (see Figure E.1). For resisted walking, the resistance level will be set to about 5-30% of the subject's MVC based on their comfort level.[3,4,23,24] Resistance level can be adjusted during the experiment manually or using computer controls. We will also perform trials where the resistance is removed (i.e., catch trials) in order to gauge how the subject is adapting to the resistance.[7,25,26] During the session, subjects will perform approximately seven trials, each lasting approximately five minutes. This will allow us to measure any instant and slow adaptations that occur when walking with resistance. While walking, subjects may be given feedback of their walking performance using kinematic measurement tools, such as we have done in: HUM00073356, HUM00087962, and HUM00133860.[27,28] Throughout treadmill walking, we may monitor gait biomechanics (e.g., EMG, kinematics, spatiotemporal gait parameters). Additionally, we may use load cells to monitor the force applied to the user (see Figure E.3).

End of the Session

Following resisted walking, we will then repeat the measurements and methods that were carried out at the beginning of the session. Subjects will be asked to return to the lab for the subsequent sessions.

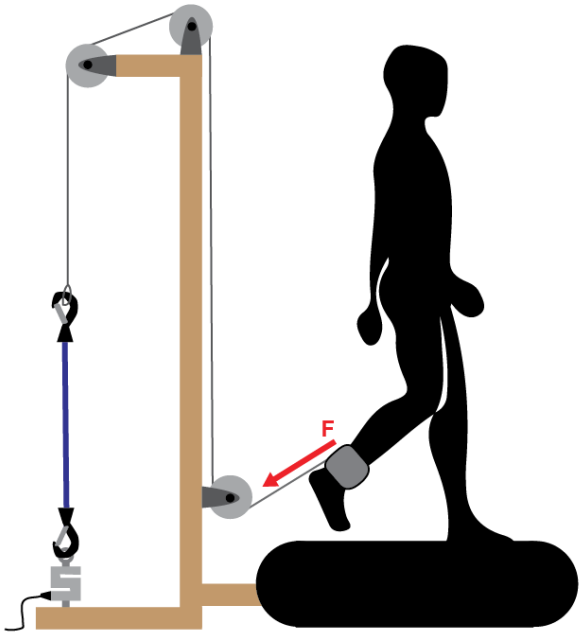

Figure E.3 Schematic of a subject walking while their leg is attached via a cuff to an elastic band. Note that a load cell is measuring the force applied by the elastic band.

Data Analyses

Kinematics

In order to evaluate how the participant's kinematics changed due to resisted walking, we will compute the subject's lower extremity kinematics during each trial. The kinematic data will be ensemble averaged across strides to compute average profiles for each trial. We may also calculate the derivative of the joint angles to measure the velocity and acceleration. From these averaged profiles, we could then extract variables such as the min and max joint angle and excursion. Additionally, the trials could be further broken up in order to indicate early and late adaptation to walking with resistance.

EMG Processing

To measure muscle activation during the study, we will compute the mean EMG activation of muscles during treadmill walking. The recorded raw EMG data from study will be band-pass filtered (e.g, 20-500 Hz), rectified, and smoothed using a zero phase-lag low pass Butterworth digital filter (e.g., 8th order, 6 Hz Cut-off).[29,30] The resulting EMG profiles for baseline and target-tracking trials will be normalized (using MVC contractions) and averaged across movement cycles and trials to compute mean EMG activity during these conditions.[31] We may also divide the movement cycle into discrete phases and compute the average EMG activity during each phase to determine the approximate temporal distributions of EMG activation (i.e. separate times of co-contraction due to acceleration and deceleration of the limb, abnormal synergies, or discrete motions within functional task). EMG will be compared between trials as well as between sessions.

TMS Processing

An MEP window will be established by finding the onset latencies of large MEPs recorded from the target muscles. A window of identical width will be set prior to the TMS trigger pulses to determine background activity. The rectified root mean square within the MEP window and pre-stimulus EMG/torque window will be used to calculate MEP amplitude and background activity, respectively. The mean MEP value will be expressed as a percentage of mean background activity and plotted against the corresponding stimulus intensity to obtain a subject-specific TMS input-output relationship. The slope of the TMS input-output relationship will be derived by fitting a Boltzmann curve. Additionally, we will monitor latency in the muscles response to TMS stimulus. Similarly, the MEPs obtained from the test pulses following the conditioning pulses will be ensemble averaged and normalized to the MEPs obtained without the conditioning pulses.

Statistical Analyses

The effect that resistance type has on kinematics, EMG, and spatiotemporal gait parameters during training will be evaluated using a two-way repeated measures ANOVA that includes the type of resistance applied to the subject (e.g., ankle weight, elastic band, and brace) and trials as within subject factors. Overground, TMS, and force output data will be analyzed using the same structural model, but instead of trials, we will compare before and after resisted walking. Significant main effects or interactions will be followed by post hoc analyses using paired t-tests with Bonferroni correction for multiple comparisons. A significance level of $\alpha = 0.05$ will be used for testing statistical significance.

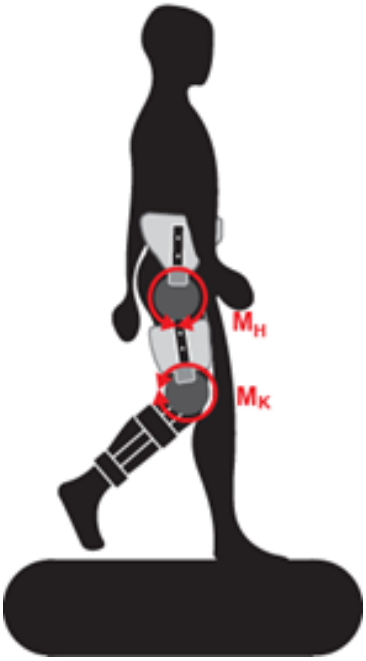

Figure E.4 Schematic of a subject walking while receiving resistance via a leg brace, where resistance is controlled using manual or controllable viscous brakes or springs.

Safety Considerations

The study procedures for this experiment are considered to be no greater than minimal risk. All procedures are noninvasive, the resistance methods are passive, and there are no children or vulnerable groups involved in this study. Almost all of the experimental testing procedures have been approved previously for use on human subjects (as a minimal risk procedure) in our other IRBs (HUM00133860, HUM00081480, HUM00073356, HUM00080244, HUM00130845, and HUM00087962). The potential risks for this study are described below:

Potential Risks

Surface EMG Related:

- *Allergic Reaction (infrequent):* Subjects may experience allergic reactions from the application of electrode paste and adhesive tapes necessary for surface EMG recordings. We will use hypoallergenic tapes to minimize allergic reactions. If redness or excessive itching occurs, the area will be monitored closely by study staff and testing will be ended at their discretion or in accordance with the subject's wishes.

  Walking Related:

- *Spasms (Infrequent):* If subjects suffer from spasticity, the initial movement while walking with resistance may trigger muscle spasms. This will gradually settle down with time. The resistance will be adjusted if this occurs to ease the spasms.
- *Skin irritation (Infrequent):* Subjects may experience some skin irritation from the cuffs due to bracing attached to the limbs. If subjects experience irritation, adequate padding

(coban or foam pads) will be provided between their skin and the cuffs to reduce the amount of irritation.

- *Tripping/Fall (Infrequent):* Subjects may trip if walking with resistance, especially if the subject has weak muscles. To minimize risk, subjects will be able to hold hand-rails, which increases stability while walking. We will also provide them with an option of wearing a body weight supporting harness to improve the feeling of safety during some activities. However, in our experience many people do not prefer wearing a harness, as the harness may produce some amount of discomfort while walking (a feeling of tight compression). Subjects may also experience tripping or falling during functional evaluation. However, these risks are no more than what they would encounter in their day-today activities. For safety purposes, the subject will always be under close supervision of a researcher while undergoing functional evaluation.
- *Muscle or joint pain (Infrequent):* During or following the experiment, subjects may feel temporary or persistent muscle aching or joint pain, or general fatigue. Any discomfort may be improved by adjusting the resistance, providing appropriate rest breaks at any time during the experiment, or using over-the-counter pain reliever.
- *Risk of fatigue (Likely):* There is a risk that subjects can become fatigued from walking with resistance for prolonged periods of time. Subjects will be allowed to rest and can also choose to end the test at their own will at any time. As with any research study, there may be additional risks that are unknown or unexpected. As described above, these risks will be minimized by allowing subjects to rest as needed and withdraw from the study voluntarily at any time. A research assistant will stand near subjects during the tests and will actively observe the subject for any distress. All devices will be built to eliminate risks of irritation or severe discomfort.
- *Patellar tendinitis or effusion (Rare):* It is possible that subjects could develop patellar tendonitis or an effusion during walking. While we believe these would be rare instances (other studies have not seen occurrences of these in an ACL repaired population even during high-intensity eccentric training), if a subject develops these issues, we would provide rest (~1 week) and then reschedule at a later time-point. If symptoms reoccur we will exclude the subject from the study.
- Strength & Activation Testing Related:
- *Muscle Fatigue or Soreness (Infrequent):* During measurement of muscle strength, subjects may experience temporary muscle fatigue and soreness. Although this soreness may persist for a period of several days following testing, this level of soreness is not greater than they would experience following a regular exercise session.
- *Discomfort from electrical pulses (Common):* Subjects may experience discomfort from the electrical pulses applied to the muscles. The electrical pulses are similar to those that are experienced commonly during treatment in rehabilitation. However, the discomfort should be momentary and should be tolerable as the pulse duration of the stimuli will be much smaller (200 μs) in comparison to the conventional therapeutic interventions (e.g.,

NMES or FES) in the clinic. An investigator will be present during all testing. Subjects will have the opportunity to inform the investigator regarding their discomfort any time during testing, and the electrical pulses can be stopped at the will of the subjects.

- *Fracture (Rare):* There is a rare chance of patellar fracture in ACL-reconstructed individuals with patellar-tendon graft during strong quadriceps contractions, especially when there is a delayed healing of the graft harvesting site in the case of orthopedic injury. We will restrict strength and activation testing in ACL-reconstructed individuals to ≤ 60° of knee flexion and will avoid forceful isometric contractions beyond 60° of knee flexion in order to minimize axial strain and harmful bending moments on the patella.

TMS Related:

- Single and paired pulse TMS protocols (which will be used in this study) are extremely safe in healthy/neurologically intact individuals as well as stroke survivors (Rossi et al. 2009, Krishnan et al. 2015, Groppa et al. 2012).[14,17,18] These techniques have been in existence for more than two decades and are known to have little serious side-effects, if any. TMS has been studied extensively in stroke survivors for more than 25 years with virtually no major or long-lasting side-effects. The contribution of TMS in understanding of mechanisms of functional recovery after stroke has been enormous (Dimyan MA and Cohen LG, 2010).[32] The TMS protocol used in this study are extremely safe as it is not known to alter the excitability of the brain. We would like to note that transcranial magnetic stimulation is considered as a nonsignificant risk by FDA as other devices with similar technology have been FDA approved for brain stimulation (e.g., http://www.eneura.com/tms.html, http://www.fda.gov/newsevents/newsroom/pressannouncements/ucm378608.htm, http://neurostar.com/ or http://www.brainsway.com/). Because single pulse and paired pulse protocols do not alter excitability and are not used as a medical/therapeutic interventions, there is paucity in the literature for studies with a direct aim of studying safety of these procedures in stroke. However, there is safety data on repetitive TMS (rTMS) protocols in individuals with stroke and pediatric neurological conditions (e.g. Krishnan et al. 2015 and Allen et al. 2017).[17,33] The existing data suggest that even rTMS paradigms (which are considered to have more risk than single or paired pulse protocols) are extremely safe when following the established guidelines (e.g., Rossi et al. 2009).[14] The known side-effects of TMS are as follows:

- *Clicking noise and muscle twitching (Common):* The subjects may feel twitches in their arms, face, and leg muscles. A loud clicking noise may be heard during the stimulus. They will have the opportunity to wear foam earplugs that can effectively prevent this discomfort.

- *Transient headache or scalp discomfort (Rare):* There is also a small risk of temporary headaches after TMS. However, these are momentary and typically goes away after the completion of the procedure.

- *Lightheadedness/dizziness (Rare):* Although not common, the subject may experience lightheadedness or dizziness. In the event of such symptoms, the experiment will be stopped. The subject will have the ability to stop the study at any time by asking the study team to either give them a rest or if necessary, remove the device. To minimize this risk, we will exclude subjects with a history of repeated fainting spells or syncope.
- *Seizure (Rare):* Rare cases have reported seizures during or immediately after magnetic brain stimulation, but these are particularly for repetitive TMS protocols that modulate cortical excitability and have not been reported for single or dual pulse stimulation procedures to our knowledge in the past 10 years. Indeed, single and paired pulse protocols have been known to be safe even in individuals with epilepsy (Hsu WY et al. 2015, Badawy RA et al. 2015).[34,35] To be extra-cautious, individuals who have a recent history of seizures (< 6 months) will be evaluated for their study participation in consultation with the physician (Dr. Edward Claflin) on this study and would be excluded from this research study if recommended. Dr. Claflin is a Board Certified Physician in PM&R and is an expert in neurorehabilitation, stroke, and electromyography and has a long history of collaboration with Dr. Krishnan. He has extensive clinical experience in rehabilitating individuals with Stroke and Traumatic Brain Injury. In addition, if the participant is taking certain types of medication known to substantially increase the risk of a seizure (as determined by the physician) they will not be allowed to participate in the study, unless approved by the physician. A screening questionnaire will be used to determine a subject's exposure to risk factors for TMS.[36] We are located in a building where there is an attending physician on call and reachable should there ever be an adverse event, which is consistent with the recommendations of Rossi for these protocols.[14] The PI of this study is also an expert in TMS with knowledge about the principles, physiology, and side effects of the technique, and has published numerous TMS papers, including a recent safety paper on TMS (and other noninvasive brain stimulation procedures) in children.[17] Indeed, this paper is used as a reference paper in several TMS courses that are conducted nationally. Further, any person performing TMS will be trained personally by Dr. Krishnan prior to their involvement in any study-related procedures. In the event that a subject has a serious adverse event (e.g., seizure), we would call the attending physician on call (via pager: 31380 or telephone: 3-4403, 6-7189) to seek immediate medical attention. Our lab is located in close vicinity to physician's offices and clinics; hence, we should not have any problem in receiving prompt medical care, if needed. If an attending physician is not available on call, we will call 911 for emergency care.
- Other side-effects may include lightheadedness, nausea, syncope, hearing problems, general fatigue or pain, which have been reported in rTMS studies. These symptoms generally subside with the cessation of stimulation and/or taking an over the counter analgesic
- As mentioned earlier, since there are no studies available to characterize the extent of single or paired pulse risk in stroke survivors, we are providing data from rTMS studies in individuals with stroke and pediatric neurological conditions for comparison purposes

only (please note that these are data from rTMS studies and not from single or dual pulse studies):

- Data from 322 Children with neurological disorders (Krishnan et al. 2015): mild/transient headache (11.5%), scalp discomfort (2.5%), Twitching (1.2%), mood changes (1.2%), Fatigue (0.9%), tinnitus (0.6%), seizure/syncope (0.6%).
- Data from 327 stroke survivors (Haoz et al. 2013): mild/transient headache (2.4%), anxiety (0.3%), syncope (0.6%), no reports of seizure.
- Unforeseeable Risks (Rare): As with any research study, there may be additional risks that are unknown or unexpected.

References:

1. Lam T, Pauhl K, Ferguson A, Malik RN, Krassioukov A, Eng JJ. Training with robot-applied resistance in people with motor-incomplete spinal cord injury : Pilot study. *J Rehabil Res Dev*. 2015;52(1):113-130. doi:10.1682/JRRD.2014.03.0090.
2. Wu M, Landry JM, Kim J, Schmit BD, Yen S-C, Macdonald J. Robotic resistance/assistance training improves locomotor function in individuals poststroke: a randomized controlled study. *Arch Phys Med Rehabil*. 2014;95(5):799-806. doi:10.1016/j.apmr.2013.12.021.
3. Wu M, Landry JM, Schmit BD, Hornby TG, Yen SC. Robotic resistance treadmill training improves locomotor function in human spinal cord injury: A pilot study. *Arch Phys Med Rehabil*. 2012;93(5):782-789. doi:10.1016/j.apmr.2011.12.018.
4. Wu M, Landry JM, Yen SC, Schmit BD, Hornby TG, Rafferty M. A novel cable-driven robotic training improves locomotor function in individuals post-stroke. In: *Proceedings of the Annual International Conference of the IEEE Engineering in Medicine and Biology Society, EMBS*. ; 2011:8539-8542. doi:10.1109/IEMBS.2011.6092107.
5. Matsuse H, Hashida R, Takano Y, et al. Walking Exercise Simultaneously Combined With Neuromuscular Electrical Stimulation of Antagonists Resistance Improved Muscle Strength, Physical Function, and Knee Pain in Symptomatic Knee Osteoarthritis. *J Strength Cond Res*. 2017;31(1):171-180. doi:10.1519/JSC.0000000000001463.
6. Kleim J a, Jones T a. Principles of experience-dependent neural plasticity: implications for rehabilitation after brain damage. *J Speech Lang Hear Res*. 2008;51(1):S225-39. doi:10.1044/1092-4388(2008/018).
7. Lam T, Anderschitz M, Dietz V. Contribution of Feedback and Feedforward Strategies to Locomotor Adaptations. *J Neurophysiol*. 2006;95:766-773. doi:10.1152/jn.00473.2005.
8. Lam T, Luttmann K, Houldin A, Chan C. Treadmill-based locomotor training with leg weights to enhance functional ambulation in people with chronic stroke: a pilot study. *J Neurol Phys Ther*. 2009;33(3):129-135. doi:10.1097/NPT.0b013e3181b57de5.
9. Stoeckmann TM, Sullivan KJ, Scheidt R a. Elastic, viscous, and mass load effects on

poststroke muscle recruitment and co-contraction during reaching: a pilot study. *Phys Ther*. 2009;89(7):665-678. doi:10.2522/ptj.20080128.

10. Demirtas-Tatlidede A, Alonso-Alonso M, Shetty RP, Ronen I, Pascual-Leone A, Fregni F. Long-term effects of contralesional rTMS in severe stroke: Safety, cortical excitability, and relationship with transcallosal motor fibers. *NeuroRehabilitation*. 2015;36(1):51-59. doi:10.3233/NRE-141191.

11. Kirton A, deVeber G, Gunraj C, Chen R. Cortical excitability and interhemispheric inhibition after subcortical pediatric stroke: Plastic organization and effects of rTMS. *Clin Neurophysiol*. 2010;121(11):1922-1929. doi:10.1016/j.clinph.2010.04.021.

12. Eryılmaz G, Sayar GH, Özten E, et al. Follow-up study of children whose mothers were treated with transcranial magnetic stimulation during pregnancy: preliminary results. *Neuromodulation*. 2015;18(4):255-260. doi:10.1111/ner.12231.

13. Hızlı Sayar G, Ozten E, Tufan E, et al. Transcranial magnetic stimulation during pregnancy. *Arch Womens Ment Health*. 2014;17(4):311-315. doi:10.1007/s00737-013-0397-0.

14. Rossi S, Hallett M, Rossini PM, Pascual-Leone A. Safety, ethical considerations, and application guidelines for the use of transcranial magnetic stimulation in clinical practice and research. *Clin Neurophysiol*. 2009;120(12):2008-2039. doi:10.1016/j.clinph.2009.08.016.

15. Krishnan C, Theuerkauf P. Effect of knee angle on quadriceps strength and activation after anterior cruciate ligament reconstruction. *J Appl Physiol*. 2015;119(3):223-231. doi:10.1152/japplphysiol.01044.2014.

16. Krishnan C, Williams GN. Quantification method affects estimates of voluntary quadriceps activation. *Muscle and Nerve*. 2010;41(6):868-874. doi:10.1002/mus.21613.

17. Krishnan C, Santos L, Peterson MD, Ehinger M. Safety of noninvasive brain stimulation in children and adolescents. *Brain Stimul*. 2015;8(1):76-87. doi:10.1016/j.brs.2014.10.012.

18. Groppa S, Oliviero A, Eisen A, et al. A practical guide to diagnostic transcranial magnetic stimulation: Report of an IFCN committee. *Clin Neurophysiol*. 2012;123(5):858-882. doi:10.1016/j.clinph.2012.01.010.

19. Krishnan C, Dhaher Y. Corticospinal responses of quadriceps are abnormally coupled with hip adductors in chronic stroke survivors. *Exp Neurol*. 2012;233(1):400-407. doi:10.1016/j.expneurol.2011.11.007.

20. Madhavan S, Krishnan C, Jayaraman A, Rymer WZ, Stinear JW. Corticospinal tract integrity correlates with knee extensor weakness in chronic stroke survivors. *Clin Neurophysiol*. 2011;122(8):1588-1594. doi:10.1016/j.clinph.2011.01.011.

21. Smith AE, Sale M V, Higgins RD, Wittert G a, Pitcher JB. Male human motor cortex stimulus-response characteristics are not altered by aging. *J Appl Physiol*. 2011;110(1):206-212. doi:10.1152/japplphysiol.00403.2010.

22. Pino G Di, Pellegrino G, Assenza G, et al. Modulation of brain plasticity in stroke: a novel

model for neurorehabilitation. *Nat Publ Gr*. 2014;10(10):597-608. doi:10.1038/nrneurol.2014.162.

23. Yen S-C, Schmit BD, Wu M. Using swing resistance and assistance to improve gait symmetry in individuals post-stroke. *Hum Mov Sci*. 2015;42:212-224. doi:10.1016/j.humov.2015.05.010.

24. Yen SC, Schmit BD, Landry JM, Roth H, Wu M. Locomotor adaptation to resistance during treadmill training transfers to overground walking in human SCI. *Exp Brain Res*. 2012;216(3):473-482. doi:10.1007/s00221-011-2950-2.

25. Emken JL, Reinkensmeyer DJ. Robot-enhanced motor learning: Accelerating internal model formation during locomotion by transient dynamic amplification. *IEEE Trans Neural Syst Rehabil Eng*. 2005;13(1):33-39. doi:10.1109/TNSRE.2004.843173.

26. Savin DN, Morton SM, Whitall J. Generalization of improved step length symmetry from treadmill to overground walking in persons with stroke and hemiparesis. *Clin Neurophysiol*. 2014;125(5):1012-1020. doi:10.1016/j.clinph.2013.10.044.

27. Saner RJ, Washabaugh EP, Krishnan C. Reliable sagittal plane kinematic gait assessments are feasible using low-cost webcam technology. *Gait Posture*. 2017;56(December 2016):19-23. doi:10.1016/j.gaitpost.2017.04.030.

28. Krishnan C, Washabaugh EP, Seetharaman Y. A low cost real-time motion tracking approach using webcam technology. *J Biomech*. 2015;48(3):544-548. doi:10.1016/j.jbiomech.2014.11.048.

29. Krishnan C, Allen EJ, Williams GN. Effect of knee position on quadriceps muscle force steadiness and activation strategies. *Muscle and Nerve*. 2011;43(4):563-573. doi:10.1002/mus.21981.

30. Krishnan C, Williams GN. Factors explaining chronic knee extensor strength deficits after ACL reconstruction. *J Orthop Res*. 2011;29(5):633-640. doi:10.1002/jor.21316.

31. Krishnan C, Ranganathan R, Dhaher YY, Rymer WZ. A Pilot Study on the Feasibility of Robot-Aided Leg Motor Training to Facilitate Active Participation. *PLoS One*. 2013;8(10). doi:10.1371/journal.pone.0077370.

32. Dimyan MA, Cohen LG. Contribution of Transcranial Magnetic Stimulation to the Understanding of Functional Recovery Mechanisms After Stroke. *Neurorehabil Neural Repair*. 2010;24(2):125-135. doi:10.1177/1545968309345270.

33. Allen CH, Kluger BM, Buard I. Safety of Transcranial Magnetic Stimulation in Children: A Systematic Review of the Literature. *Pediatr Neurol*. 2017;68:3-17. doi:10.1016/j.pediatrneurol.2016.12.009.

34. Hsu W-Y, Kuo Y-F, Liao K-K, Yu H-Y, Lin Y-Y. Widespread inter-ictal excitability changes in patients with temporal lobe epilepsy: A TMS/MEG study. *Epilepsy Res*. 2015;111(201):61-71. doi:10.1016/j.eplepsyres.2015.01.004.

35. Badawy RAB, Vogrin SJ, Lai A, Cook MJ. Does the region of epileptogenicity influence the pattern of change in cortical excitability? *Clin Neurophysiol*. 2015;126(2):249-256.

doi:10.1016/j.clinph.2014.05.029.

36. Rossi S, Hallett M, Rossini PM, Pascual-Leone A. Screening questionnaire before TMS: An update. *Clin Neurophysiol*. 2011;122(8):1686. doi:10.1016/j.clinph.2010.12.037.